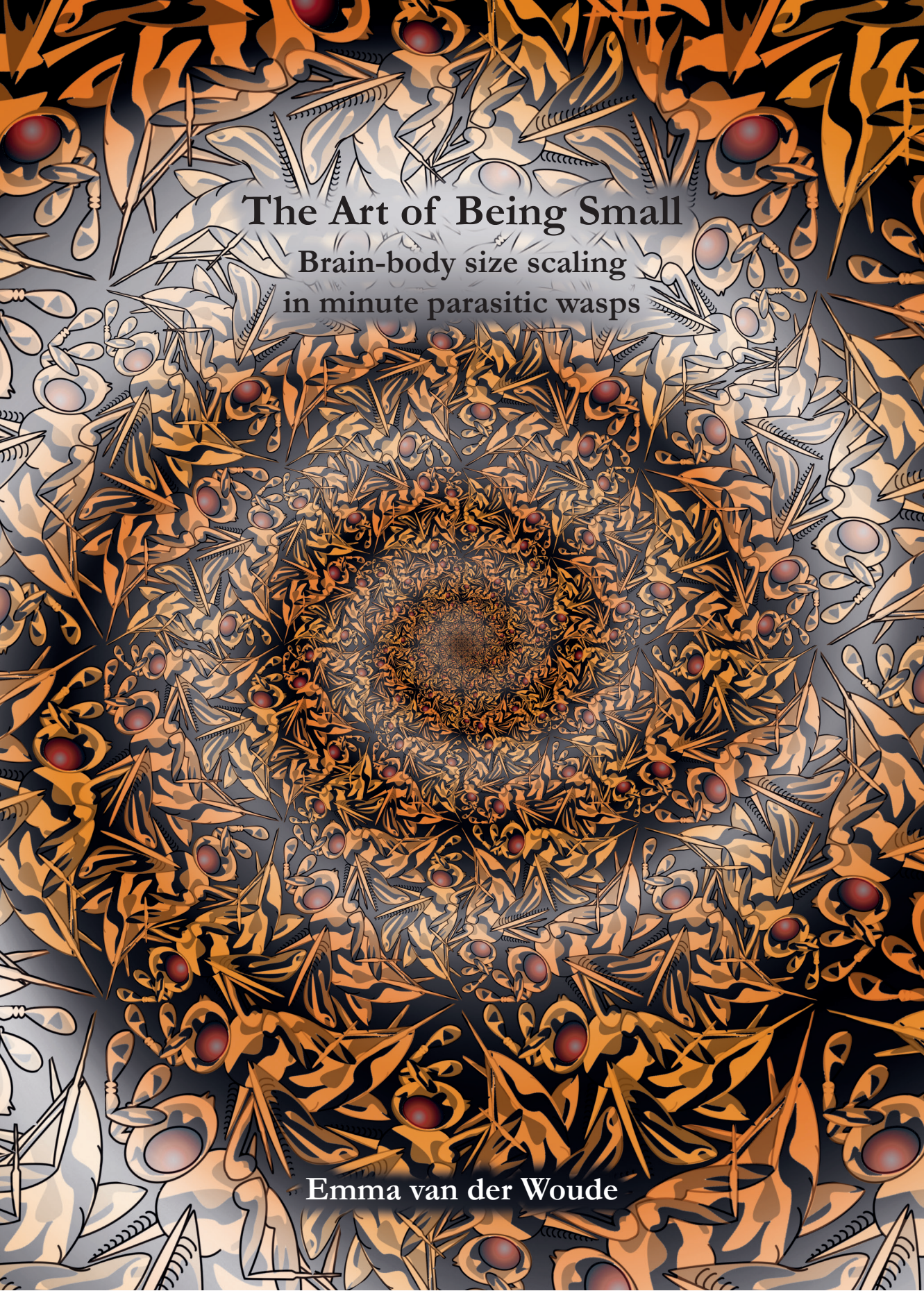

The Art of Being Small

Brain-body size scaling in minute parasitic wasps

Emma van der Woude

Propositions

1. Brain size is an unreliable predictor of cognitive capacity.
   (this thesis)

2. Evolutionary miniaturization of body size requires isometric brain scaling.
   (this thesis)

3. Object-oriented programming should focus on achieving simplicity in the code rather than complexity in the output.

4. The difficulty in accurately assessing intelligence is caused by lack of understanding what intelligence entails.

5. The focus of users of social media on convincing others that they live an interesting life, impedes living an interesting life.

6. The purpose of life is creating the illusion of a purpose of life.

Propositions belonging to the PhD thesis entitled

'The Art of Being Small:
Brain-body size scaling in minute parasitic wasps'

Emma van der Woude
Wageningen University & Research
October 27, 2017

The Art of Being Small

Brain-body size scaling in minute parasitic wasps

Emma van der Woude

Thesis committee

Promotor
Prof. Dr Marcel Dicke
Professor of Entomology
Wageningen University & Research

Co-promotor
Dr Hans M. Smid
Researcher, Laboratory of Entomology
Wageningen University & Research

Other members
Prof. Dr Marcel E. Visser, Netherlands Institute of Ecology, Wageningen
Dr Vera I. D. Ros, Wageningen University & Research
Dr Bart A. Pannebakker, Wageningen University & Research
Dr Peter Roessingh, University of Amsterdam

This research was conducted under the auspices of the C.T. de Wit Graduate School for Production Ecology & Resource Conservation.

The Art of Being Small

Brain-body size scaling in minute parasitic wasps

Emma van der Woude

Thesis
submitted in fulfilment of the requirements for the degree of doctor
at Wageningen University
by the authority of the Rector Magnificus,
Prof. Dr A.P.J. Mol,
in the presence of the
Thesis Committee appointed by the Academic Board
to be defended in public
on Friday 27 October 2017
at 1.30 p.m. in the Aula.

Emma van der Woude
The art of being small: Brain-body size scaling in minute parasitic wasps,
232 pages.

PhD thesis, Wageningen University, Wageningen, the Netherlands (2017).
With references, with summary in English.

ISBN: 978-94-6343-656-4
DOI: https://doi.org/10.18174/420849

Table of contents

Chapter 1. General introduction. **6**

Chapter 2. Breaking Haller's rule: brain-body size isometry in a minute parasitic wasp. **24**
Emma van der Woude, Hans M. Smid, Lars Chittka, Martinus E. Huigens.

Chapter 3. How to escape from Haller's rule: olfactory system complexity in small and large *Trichogramma evanescens* parasitic wasps. **36**
Emma van der Woude, Hans M. Smid.

Chapter 4. Maximized complexity in miniaturized brains: morphology and distribution of octopaminergic, dopaminergic and serotonergic neurons in *Trichogramma evanescens* parasitic wasps. **62**
Emma van der Woude, Hans M. Smid.

Chapter 5. Effects of isometric brain-body size scaling on the complexity of monoaminergic neuron networks in a minute parasitic wasp. **108**
Emma van der Woude, Hans M. Smid.

Chapter 6. Differential effects of brain scaling on memory performance in parasitic wasps. **126**
Emma van der Woude, Martinus E. Huigens, Hans M. Smid.

Chapter 7. No gains for bigger brains: Functional and neuroanatomical consequences of artificial selection on relative brain size in a parasitic wasp. **148**
Emma van der Woude, Jitte Groothuis, Hans M. Smid.

Chapter 8. General discussion. **178**

References **192**

Summary **212**

Curriculum vitae and list of publications **220**

Acknowledgements **226**

Chapter 1

General introduction

The art of being small

Body size varies enormously in the Animal Kingdom. Huge whales roam the deep sea, while the tiniest of insects crawl in miniature cavities. The smallest adult insects are parasitic wasps in the families Mymaridae and Trichogrammatidae (Polilov, 2015). Some of these wasps can reach body lengths even below 300 μm, which is similar in size as some unicellular protozoans (e.g. *Paramecium*) or large bacteria (e.g. *Thiomargarita*). The benefit of being so small is that it allows survival in micro-habitats and with a limited supply of nutrition (Niven and Farris, 2012). The disadvantage is that organs may have evolved morphological simplifications to achieve such small sizes. These simplifications can negatively affect physiology and behaviour, and may result in reduced longevity or fecundity. Despite the strong pressures to minimize the size of all organs, even the smallest wasps have fully functional brains that are similar in complexity to those of much larger animals (Strausfeld, 1976; Makarova and Polilov, 2013; Ito et al., 2014). These tiny, but elaborately-structured brains may facilitate the complex cognitive and behavioural abilities that are shown by some parasitic wasps, such as learning and hitch-hiking on potential hosts (Huigens et al., 2009). In this thesis, I focus on the secret tricks that allow insects to be fully functional at such tiny sizes. In other words: what is the art of being small?

Miniaturization of body size

Insects are among the smallest free-living animals, but even among fully developed insects there are exceptionally small individuals. Small insects can belong to species that have evolved miniaturized body sizes and exclusively consist of small individuals, or can be exceptionally small individuals of species with a wide range of sizes. Evolutionary miniaturization of body size is defined as the evolution of extremely small adults within a lineage, descending from a larger ancestor (Hanken and Wake, 1993). Examples of this evolutionary process can be found in both vertebrates and invertebrates (Hanken and Wake, 1993; Polilov, 2015). Miniaturization can evolve as an adaptation to various ecological challenges, such as the need to colonize miniature niches or to survive under a limited amount of resources (Niven and Farris, 2012). These evolutionary forces can act on the rate or duration of growth, resulting in fully developed but miniaturized adults (Hanken and Wake, 1993; Niven and Farris, 2012). Evolutionary miniaturization can therefore also be a by-product of selection for a reduction of growth, for example when earlier sexual maturation is advantageous in environments that rapidly change (Hanken and Wake, 1993).

In addition to the evolutionary process of a species becoming small, exceptionally small sizes can also occur within a species. Insect larvae can be extremely small, even when adults are not miniaturized (Hanken and Wake, 1993; Eberhard and Wcislo, 2011). Intraspecific "miniaturization" can also occur in adults, either through genetic variation or through phenotypic plasticity in adult body size. Genetic variation in traits that regulate growth can cause extremely small body sizes in part of a population (Kotrschal et al., 2013). Such genetic variability in body size is a requirement for evolutionary miniaturization. However, overall body size of the species will not change if there is no evolutionary benefit of being small. Phenotypic plasticity in body size is regulated by developmental programmes, which have evolved to regulate body size in response to environmental conditions during development, such as nutrient availability or ecological variation. In this way, developmental programmes can generate e.g. caste-specific phenotypes in social insects (Hölldobler and Wilson, 2009) and exceptionally small nutrient-deprived fruit flies (Lanet and Maurange, 2014).

As stated above, the smallest adult insects are parasitic wasps of the families Mymaridae and Trichogrammatidae (Polilov, 2015). These are egg parasitoids, which parasitise eggs of other insects and completely develop into adults inside these host eggs. It may be because of this particular parasitic lifestyle that these wasps are the smallest adult insects. The need to complete development inside another insect's egg, and the need to occupy the smallest of these host eggs, may select for smaller adults and therefore drive evolutionary miniaturization. This parasitic lifestyle may simultaneously allow for such miniaturized body sizes, because the development inside another insect's egg allows parasitoids to economize on the investment of yolk in their own eggs (Polilov, 2015). A parasitic lifestyle may therefore both drive and enable evolutionary miniaturization of body size. Further variation in body size of adult parasitoids may arise through phenotypic plasticity, in response to variation in the size or quality of host eggs, or in the number of parasitoid larvae that develop inside the same host egg. As a result, the absolutely smallest insects may be evolutionarily miniaturized parasitoids that emerge from small host eggs, or from eggs that host additional parasitoid larvae.

Evolutionary miniaturization of body size, genetic variation in body size, and phenotypic plasticity in body size are three different processes that may all result in extremely small insects, especially when these processes occur simultaneously. I will avoid the term "miniaturization" for the intraspecific processes (genetic variation and phenotypic plasticity) for two reasons. First, to avoid confusion with the more general evolutionary term. Second, because it is often difficult to

establish what the regular body size is of a species that shows a large variability in size. It is then not possible to state if the large individuals are normal and the small ones the exception, or if small individuals are normal and there is "gigantism" in large individuals. Instead, I will refer to phenotypic plasticity and genetic variation in body size for these intraspecific processes of body-size variation.

Costs of being small

The causes of evolutionary body size miniaturization and intraspecific small body sizes may be different, but both have the same result: exceptionally small individuals. Many of the trade-offs that have been studied or discussed for evolutionary miniaturization could also apply to the smallest individuals within a species. Exceptionally small individuals may experience similar costs and challenges, irrespective of whether they are regular-sized members of a miniaturized species or the smallest phenotypes in a generally larger-bodied species.

Being small comes with the challenge of fitting all vital tissues in an extremely small body. The modifications that underlie small body sizes can be very costly, because they may involve simplifications of shape, function, morphology, physiology or behaviour, which can result in reduced longevity and fecundity (Hanken and Wake, 1993; Bennett and Hoffmann, 1998; Polilov, 2015). Organs of small animals may seem underdeveloped, sometimes resembling those of earlier developmental stages of larger-bodied animals (Hanken and Wake, 1993). In miniature insects, the sensory systems consist of fewer and smaller components (i.e. sensilla on the antennae and ommatidia in the compound eyes) than in larger insects, which may affect sensory precision (Polilov, 2015). Furthermore, the reproductive systems of miniature insects contain smaller ovaries with fewer ovarioles, and therefore fewer eggs (Polilov, 2015). These fewer eggs are relatively larger to body size compared to those of larger insects. As a result, small insects may have reduced Darwinian fitness despite a relatively high investment in reproduction (Hanken and Wake, 1993). Another interesting functional reduction can be found in the circulatory systems of miniature insects, which contain no other components than a heart and aorta, and in some families (including Trichogrammatidae) even the heart is absent (Polilov, 2015). These reductions can only be vital in the smallest insects, in which diffusion may be a sufficient circulatory force (Polilov, 2008).

Small animals may also require novel morphological features to deal with the challenges of being small. Miniature insects from several different families independently evolved ciliated wings with many hair-like structures. These insects experience the air as very viscous due to their small size, which may have selected for wings with high porosity. Ciliated wings may be an adaptation that enables miniature insects to "paddle" rather than fly through viscous air (Sane, 2016). Miniaturized larvae of beetles and strepsipterans show another interesting morphological adaptation: the brain is partially shifted into the thorax, possibly due to lack of space in the head capsule (Beutel et al., 2005; Polilov and Beutel, 2009; Knauthe et al., 2016).

The most severe costs of being small may result from reductions in the size and complexity of the brain. The brain is the most important component of the central nervous system, and the organ that is involved in practically all aspects of an insect's life. Hence, reducing the size of the brain and adapting its structure may affect the performance of the brain, and therefore of the insect. Small insects may therefore "face a dilemma" (Eberhard and Wcislo, 2011), which may be solved by three not mutually exclusive strategies that may compensate for some of the costs of having small brains.

First, small insects may be adapted to occupy smaller niches that require fewer behavioural and cognitive abilities. Under this strategy, small insects may exploit more stable environments because they have a lower ability to respond to environmental variability than larger insects. There may also be selection for traits that compensate for reduced cognitive abilities, such as maintaining some traits at the expense of others, or evolving changes in lifestyle that are cognitively or behaviourally less demanding (Hanken and Wake, 1993; Eberhard and Wcislo, 2011; Polilov, 2015). Being extremely small has the additional benefit of a lower predation risk, so that survival may already be less dependent on cognitive abilities.

Second, small insects may have evolved modifications to neural architecture that optimize the performance of small brains (Eberhard and Wcislo, 2011). These adaptations may cause neural networks to operate more efficiently with minimal functional consequences. In this way, the repertoire of neural and cognitive abilities may be maintained, although accuracy may be lower. Reductions can be made to the number of functional components of the sensory systems, thereby maintaining sensory performance, but with a lower resolution (Chittka and Niven, 2009). Similar reductions can be made in the number of neural pathways that process similar information in parallel (Faisal et al., 2008; Niven and Farris, 2012). Such reductions can maintain the diversity of signalling pathways,

although reduced abilities to average neural signals may increase neural noise. Another adaptation that may increase efficiency in miniaturized brains is the use and reuse of the same neural networks for multiple different processing tasks (Anderson, 2010). One of the neurons that may operate in this way is VUMmx1, which is involved in various learning-related processes in honeybees (Niven and Chittka, 2010). Small insects also directly benefit from having a small brain, because distances between neurons are short. The length of neural connections can therefore be minimized, resulting in more efficient information processing than in larger insects (Striedter, 2005; Niven and Farris, 2012).

The third solution that may compensate for some of the cognitive costs of being small involves an increase in relative brain size. This strategy allows for maintained brain performance without the need for structural adaptations to optimize neural architecture. The trade-off of this strategy is that a relatively larger brain requires more energy, because brain tissue has a high metabolic rate and is therefore energetically expensive (Aiello and Wheeler, 1995; Niven and Laughlin, 2008). Despite these costs, however, this final solution appears to be a generally occurring phenomenon, and is described by Haller's rule.

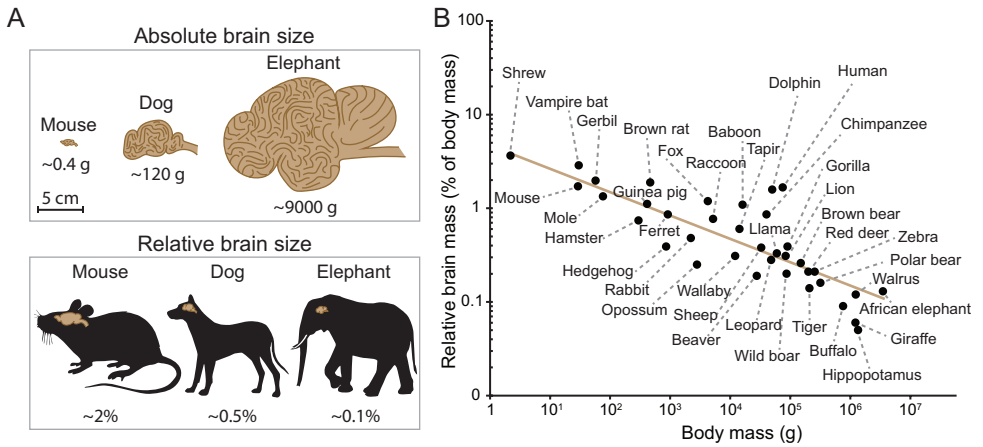

Figure 1. Brain size in some mammals. **(A)** Difference between absolute and relative brain size in mice, dogs and elephants. Absolute brain size (top panel) is larger in larger animals, but relative brain size (bottom panel) is smaller in larger animals. **(B)** Relative brain size decreases with increasing body size (brown trendline). Vertical distance from the trendline illustrates the deviation of brain size from its expected value for that body mass; e.g. humans and dolphins have exceptionally large brains. Data from Boddy et al. (2012).

Haller's rule

Brain size can be expressed by the absolute size of the brain (Figure 1A, top), and by the size of the brain relative to total body size (Figure 1A, bottom). Absolute brain size is determined by the size and number of neurons and glia cells in the brain. The size of neurons depends on the length and diameter of neurites, the number of connections with other neurons and on the volume of the cell body (which is in turn determined by the volume of the nucleus and cytoplasm). Absolute brain size largely depends on body size: small animals have small brains and large animals have large brains. A smaller body may simply require fewer and smaller neurons to operate it (Kaas, 2000; Roth and Dicke, 2005).

Relative brain size corrects for these body-size effects on absolute brain size, and can be expressed as a proportion of body mass or volume. In general, small animals have relatively larger brains than large animals. This phenomenon occurs throughout the animal kingdom; from mammals to insects (Kruska, 2005; Roth and Dicke, 2005; Striedter, 2005; Chittka and Niven, 2009; Eberhard and Wcislo, 2011). It implies that, for example, mice have relatively larger brains than elephants (Figure 1B). Not many relative brain sizes are known for insects, but some of the smallest insects have brains that are much larger in relative size than those of vertebrates (e.g. the brains of small *Brachymyrmex* ants constitute 15% of their total body mass; Seid et al., 2011).

The Swiss physiologist Albrecht von Haller (1708 – 1777) was the first to observe that small animals have relatively larger brains than large animals (Haller, 1757). This brain-body size scaling relationship became known as Haller's rule almost 200 years later (Rensch, 1948; Rensch, 1956). The relationship between brain size and body size follows a power law function. This function can be described as [brain size] = $a \times$ [body size]^b, using either mass or volume as a measure of brain and body size. The power law function becomes linear after logarithmic transformation, i.e. log[brain size]=$b \times$ log[body size] + log[a].

The intercept of the log-transformed function, described by the constant a in Haller's rule, provides information on relative brain size and the level of encephalization of the animals that are described by the allometric relationship. The slope of the log-transformed function, described by the coefficient b in Haller's rule, determines the shape of the relationship, i.e. the dependency of brain size on body size (Striedter, 2005; Eberhard and Wcislo, 2011). In the case of the situation that is described by Haller's rule, b is smaller than 1 and the brain-body function shows negative allometry. The smaller b is, the stronger the negative allometry and the larger the difference in relative brain size between

small and large animals. Larger scaling coefficients describe isometry when $b = 1$, which would result in a linear relationship between brain and body size, or positive allometry when $b > 1$, which would result in large animals having relatively larger brains than small animals. Scaling coefficients equal or larger than 1 have not (yet) been described for brain-body size scaling.

Brain-body size relationships can be studied at different levels within and between species (Figure 2A), and Haller's rule holds in all of these comparisons (Cheverud, 1982; Shingleton et al., 2007). Scaling coefficients are generally largest in comparisons between species (Kruska, 2005; Wehner et al., 2007; Figure 2A). These interspecific comparisons can reveal evolutionary patterns in brain-body size scaling, and have therefore been named "evolutionary allometry" (black line in Figure 2A). When combined with phylogenetic information, these comparisons can reveal how brain size evolved between species or taxa. The deviation of the average brain-body size value of a single species from the general allometric line is a measure for species-specific investment in brain tissue. An outlier above the allometric line has relatively large brains.

Intraspecific comparisons can focus on similarly-aged individuals ("static" allometry, thick coloured lines in Figure 2A), or on individuals of different ages during development ("ontogenetic" allometry, thin coloured lines in Figure 2A). Ontogenetic allometry can be used to study the growth of brain tissue during development, and to reveal at which time during development neural investment occurs. Such analyses can, for example, compare brain development in mammals that require much care after birth and those that are more independent, or determine the influence of different developmental conditions on the growth of the brain (Kruska, 2005). Ontogenetic allometry can be more complicated to study in insects, because growth rate can vary between larval and moulting stages, resulting in shifts in the allometric line (Tammaru and Esperk, 2007).

Static allometry can be used to compare relative brain size of adult individuals within a species. It can determine the effects of different selective environments on brain size, for example by comparing domesticated animals to their wild relatives (Kruska, 1996; Stuermer et al., 2003; Burns et al., 2009; Campi and Krubitzer, 2010). Such analysis revealed that wild and domesticated mink have the same allometric slope, but the intercept of the domesticated mink is lower (Kruska, 1996). A similar result was found in a comparison of a wild-caught and laboratory strains of Mongolian gerbils (Stuermer et al., 2003). These elevation displacements, also called "grade shifts" (Eberhard and Wcislo, 2011), suggest that domestication decreased relative brain size, without affecting the strength with which brain size scales with body size.

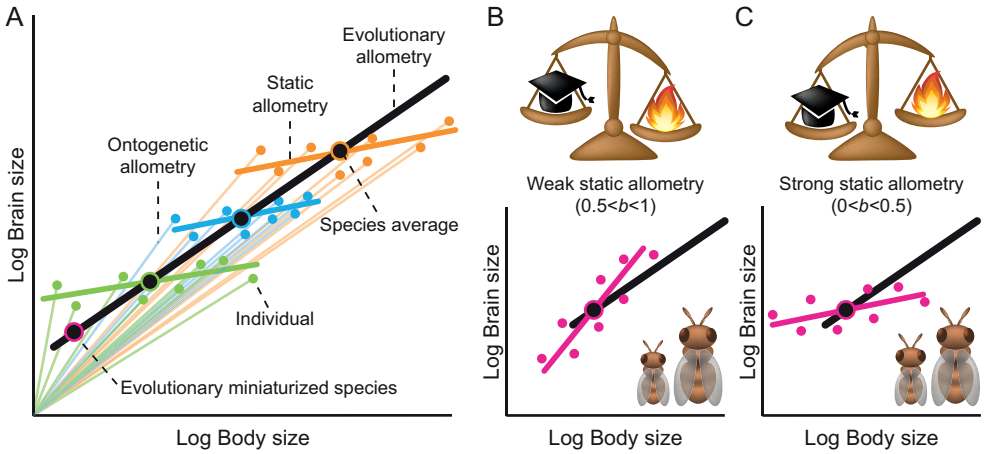

Figure 2. The concept of brain-body size allometry. **(A)** Theoretic distinction between ontogenetic, static and evolutionary allometry. Ontogenetic allometry entails the developmental growth of brain size of an individual (thin orange, blue and green lines). Intraspecific static allometry shows the brain-body size relationship of adult individuals (orange, blue and green dots) within a species (thick orange, blue and green lines). Average brain and body size of a species (black dots) can be used to determine the interspecific evolutionary allometric relationship of that group of species (black line). Evolutionarily miniaturized species (black dot with magenta stroke) have relatively large brains due to evolutionary allometry. **(B)** Due to their relatively large brains, evolutionarily miniaturized species experience strong energetic constraints on brain size. This may result in very weak allometry with a high static scaling coefficient and similar relative brain sizes in small and large conspecifics, at the cost of reduced brain performance. **(C)** When even the smallest individuals still require a high level of brain performance, cognitive constraints on brain size will result in relatively large brains in small conspecifics and there will be strong static allometry.

Mechanisms underlying Haller's rule

The phenomenon that is described by Haller's rule may result from the positive correlation between brain size and brain performance, and between brain size and metabolic costs. Larger brains can be capable of higher levels of cognitive performance, but also have higher metabolic costs, whereas small brains may be energetically cheaper, but also functionally inferior (Aiello and Wheeler, 1995; Chittka and Niven, 2009; Eberhard and Wcislo, 2011). This energy-performance trade-off of brain size can be one of the mechanisms that underlie static and evolutionary allometry. A specific amount and size of neurons, and therefore absolute brain size, may be required to achieve a specific level of brain performance (Chittka and Niven, 2009; Eberhard and Wcislo, 2011). To avoid loss of brain performance, smaller animals may develop with similar absolute brain sizes as larger animals. These brains are therefore larger relative to body

size than those of larger animals, resulting in a low scaling coefficient in Haller's rule.

Furthermore, small animals have a large body surface relative to body volume. As a result, they may need relatively larger numbers of sensory and motor neurons than larger animals. These neurons need to control and be distributed over an area rather than volume of body size, causing the number of sensory and motor neurons in a brain to depend more on body surface than body volume (Martin, 1981; Striedter, 2005). This implies that the fraction of brain volume that consists of sensory and motor neurons scales to body volume allometrically. The scaling coefficient of this fraction should approach ⅔, which is the relation between the scaling of surface area and volume of objects.

While the requirements for motoric, sensory, and cognitive brain performance can set lower limits on brain size in small animals, the high metabolic costs of brain tissue simultaneously force animals to economize on brain tissue (Aiello and Wheeler, 1995). This prevents brain size from being larger than necessary for the required level of brain performance, resulting in relatively smaller brains in larger animals. Through this combination of selective pressures, the energy-performance trade-off of brain size can cause allometric brain scaling. There may be additional developmental constraints that can influence the strength of allometric brain scaling. These developmental constraints can be morphological (e.g. constraints on head morphology), or energetic (e.g. maternal metabolic rate or restrictions that are set by development inside an egg; Martin, 1981; Harvey and Krebs, 1990). The balance between all of these constraints on brain size together determine the characteristics of brain-body size scaling.

Static allometry in evolutionarily miniaturized species

The presence of negative allometry in evolutionary brain-body size relationships implies that small-bodied species have relatively larger brains than species with larger body sizes. These small species spend an exceptionally large proportion of their available energy on the development and maintenance of relatively large brains. Small species may consequently experience the energetic constraints of brain tissue as a stronger evolutionary pressure than larger species. This can differentially shape the characteristics of intraspecific, static brain allometry of small and large species.

The high metabolic costs of the brains of small-bodied species may cause energetic costs to play a larger role in static brain scaling dynamics than benefits

for brain performance. The smallest individuals of these small species may form smaller brains than expected from the predictions of Haller's rule, because the need to reduce energetic costs outbalances the requirements for maintained brain performance (Figure 2B). This can have negative effects for their level of cognition, sensory perception and motor function. The larger conspecifics can allow the higher energetic costs and gain more from optimizing brain performance. This would result in weak allometry, with larger static scaling coefficients than in larger species. In this situation, small and large animals show large differences in absolute brain size, but small differences in relative brain size. Brain performance would be the most prominent constraint of being small, because the energetic constraints can drive brain size beyond the functional limits.

An example of weaker static allometry in smaller individuals is shown by *Atta colombica* ants. Workers of this species show very large differences in body size, which depend on developmental conditions. Small and large workers were found to show distinctly different static allometric lines, with differences in slope and intercept (Seid et al., 2011). Large *A. colombica* ants ($b = 0.29$) scale their brains stronger with body size than small *A. colombica* ($b = 0.60$). As a result, small workers have smaller and energetically cheaper brains than expected from the allometric relationship of large ants.

The other extreme could occur when evolutionarily miniaturized species experience strong cognitive constraints. The processes that underlie evolutionary allometry may have resulted in small species having an already compromised brain, which is minimized in all potentially available options. In this case, the constraints on brain performance may outbalance the (already strong) energetic constraints (Figure 2C). Small individuals need to heavily invest in brain tissue to maintain appropriate cognition, but suffer high energetic costs by doing so. This may have negative effects on their fitness, for example through reduced fecundity or longevity. Larger conspecifics could develop a much smaller relative brain size to achieve a more balanced energy expenditure and increase their fitness. As a result, static brain scaling would show strong negative allometry, described by a low static scaling coefficient. Small and large conspecifics then show very large differences in relative brain size, but can be more similar in brain performance. In the case of such strong brain allometry, the energetic costs of brain tissue would be the most prominent constraint of being small, because high energy expenditure compromises fitness of the smallest individuals.

Evolutionarily miniaturized species that still require high levels of cognition will experience the strongest constraints on energy expenditure and brain

performance. It is therefore especially interesting to study how the balance between energetic and cognitive constraints shaped the dynamics of static brain scaling in these species. The smallest insects on Earth are parasitic wasps from the families Mymaridae and Trichogrammatidae (Polilov, 2015), which develop inside the eggs of other insects. This developmental strategy strictly forces them to restrict body and brain size. This may drive static brain allometry towards large scaling coefficients. However, they simultaneously require a large behavioural and cognitive repertoire to find and use their hosts. These high cognitive demands may enforce relatively larger brain sizes in the smallest individuals, thereby driving brain scaling towards the other extreme.

In this thesis, I mainly focussed on the miniaturized parasitic wasp *Trichogramma evanescens* (Hymenoptera: Trichogrammatidae). The smallest members of this species can have body lengths of only 0.3 mm (Fischer et al., 2011). Despite these small sizes, these wasps are capable of olfaction, colour vision, flight, courtship behaviour, and determining the number and sex of offspring, but also more complex traits such as hitch-hiking behaviour, associative learning, and formation of long-term memory (Suzuki et al., 1984; Dutton and Bigler, 1995; Pompanon et al., 1997; Keasar et al., 2000; Huigens et al., 2004; Fatouros et al., 2005; Huigens et al., 2009; Huigens et al., 2010; Huigens et al., 2011; Kruidhof et al., 2012). Even the smallest *T. evanescens* need complex behaviour to locate and exploit their hosts, and this could require a relatively larger brain, as predicted by Haller's rule. However, such a large brain size may be energetically too costly. How do the smallest wasps deal with this trade-off? Do they compromise energetically, by developing into small adults with oversized brains that generate all required cognitive abilities at the cost of substantial energetic investments? Or do they compromise cognitively, by forming undersized, economical brains that are unable to generate the same level of brain performance as of their larger conspecifics?

Objective and hypotheses

The aim of this thesis was to find out how evolutionary pressures on cognition and energetic costs shaped the characteristics of static brain-body size scaling in evolutionarily miniaturized parasitic wasps. Specifically, I investigated intraspecifically if these wasps scale their brains in a way that optimizes performance or minimizes energy expenditure, as reflected by respectively a very low or very high scaling coefficient. For this first objective, I excluded genetic variation in relative brain size that may obscure the brain-body size relationship,

and focussed solely on phenotypic plasticity in body and brain size. I studied which adaptations in neural morphology underlie static brain scaling, and how static brain scaling affects cognitive performance of small and large individuals. Finally, I wanted to find out how the genetic component of brain size affects neural complexity and cognitive brain performance. For this final objective, I solely focussed on genetic variation in relative brain size, by limiting phenotypic plasticity in body size to exclude the effects of brain-body size scaling.

I expected that evolutionary pressures on cognition and energetic costs strongly affect brain-body size scaling in evolutionarily miniaturized parasitic wasps. The small size of both the wasps and their hosts restricts the investment in brain tissue, whereas the cognitive requirements to find and use their hosts restrict the compromises that can be made to the size and complexity of the brain. I hypothesized that requirements for brain performance, which are vital for host-finding and therefore reproduction, outbalance the need to reduce energetic costs in the smallest wasps. This should result in very strong negative allometry, i.e. brain sizes that are relatively large in the smallest individuals.

I also expected that both brain morphology and brain performance are affected by differences in brain size, both when these result from static brain-body size scaling (i.e. genetically identical small and large conspecifics), and from genetic variation in relative brain size (i.e. similarly-sized conspecifics with relatively large and relatively small brains). I hypothesized that differences in brain size affect the size and the number of neurons and functional neuropil components, and the relative size of neuropil areas. Differences in brain size can also affect neural and cognitive performance, as reflected for instance in their ability to learn and remember. I therefore hypothesized that wasps with larger brains have a better ability to learn odours and colours, and remember them for a longer period of time.

Approach

Throughout this thesis, I used two species of parasitic wasps: the miniaturized *Trichogramma evanescens* and the larger-sized *Nasonia vitripennis*. Body size of these parasitic wasps depends on the size of their host and the number of parasitoid larvae that develop inside the same host. This scramble competition results in a large variation in body size, even within genetically identical isofemale lines.

Trichogramma evanescens is extremely small: the smallest members of the species can have body lengths of only 0.3 mm (Fischer et al., 2011). This wasp develops

inside eggs of butterflies and moths. These eggs can be very small, which may have enforced the evolution of restricted body sizes in *T. evanescens*. There are some species of egg parasitoids that reach even smaller body lengths (Polilov, 2015), but the level of behavioural and cognitive complexity of these insects is unknown. *Trichogramma evanescens* is the smallest insect with a known complex behavioural and cognitive repertoire that includes hitch-hiking behaviour, associative learning, and formation of long-term memory after a single egg-laying experience (Huigens et al., 2004; Fatouros et al., 2005; Huigens et al., 2009; Huigens et al., 2010; Huigens et al., 2011; Kruidhof et al., 2012). These complex traits are performed by a miniaturized brain of approximately 37,000 neurons (Polilov, 2012).

Nasonia vitripennis parasitises fly pupae that are found in manure, carcasses and birds' nests (Darling and Werren, 1990). This species performs well in olfactory learning trials, and forms long-term memory after a single experience with a suitable host (Hoedjes et al., 2012; Schurmann et al., 2012). It is a well-studied genetic model organism with a sequenced genome (Werren and Loehlin, 2009; Werren et al., 2010), and available information on brain morphology (Haverkamp and Smid, 2014). A large advantage of this species for my study is the availability of a homozygous strain (Werren and Loehlin, 2009), and a genetically variable population (van de Zande et al., 2014). This enabled me to focus on the effects of both phenotypic plasticity and genetic variation in my study.

In this thesis, I exploited two complementary approaches, which enabled me to investigate the neuroanatomical and cognitive effects of both static brain-body size scaling and genetic variation in relative brain size. First, I induced phenotypic plasticity in body size, using isofemale strains of genotypically identical parasitic wasps. This approach allowed me to exclude genetic variation in brain size that may obscure the static brain-body size scaling relationship. I studied the characteristics of static allometry in the miniaturized wasp *T. evanescens,* and revealed how this brain-scaling strategy affects neuroanatomy. I also used this approach to study the effects of static brain-body size scaling on memory retention abilities. For this objective, I compared small and large conspecifics of evolutionarily miniaturized *T. evanescens* and of the larger parasitic wasp *N. vitripennis*.

Complementary to this approach, I used bidirectional artificial selection to create selection lines of parasitic wasps that show genetic variation in relative brain size. I minimized variation in body size, which allowed me to exclude the effects of phenotypic plasticity on the size, morphology and performance of the brain. I used this approach to study the effects of relative brain size on memory

retention, neuroanatomy and longevity in *N. vitripennis*. The combination of inducing phenotypic plasticity in body size in isofemale lines and inducing genetic variation in relative brain size in selection lines provided me with the required tools to distinguish between the effects of plastic variation in both brain size and body size, and genetic variation in brain size under maintained body size. This enabled me to find out what neural modifications underlie brain scaling (e.g. variation in neuron size, neural complexity or neuropil size), and what their consequences are for performance (e.g. memory retention, olfaction and longevity).

Thesis outline

In **Chapter 2**, I address how evolutionary pressures shaped the characteristics of brain scaling in *T. evanescens* wasps. Evolutionary pressures to maintain brain performance and host-finding abilities, may outbalance the need to reduce energetic expenditure of brain tissue in the smallest parasitic wasps. The miniaturized wasp *T. evanescens* may consequently show relatively large brains at the smallest body sizes. I created a large variation in body size in genotypically similar *T. evanescens,* and determined their brain and body size. Because the wasps are too light to weigh accurately, I measured brain and body volume using tissue clearing procedures, confocal laser scanning microscopy and 3-dimensional modelling software. These were used to determine the allometric strength of brain-body size scaling.

In the next four chapters, I studied how the results of Chapter 2 affect morphology and performance of small and large *T. evanescens*. In **Chapter 3,** I address this on neuropil level, by studying the neuroanatomical adaptations to the olfactory system that occur with brain scaling in *T. evanescens*. I used a combination of immunofluorescence staining and confocal laser scanning microscopy to visualize glomeruli in the antennal lobes, and compared the number and size of these glomeruli between small and large wasps. I used scanning electron microscopy to study olfactory sensilla on the antennae. I counted the sensilla of different types, measured them and mapped their location on the final antennal segment. These results revealed if plasticity in brain and body size required specific adaptations to the complexity of the olfactory system.

In Chapters 4 and 5, I studied the neural consequences of brain miniaturization and intraspecific variation in brain size on neuron level. In **Chapter 4**, I compared neural complexity in *T. evanescens* to other, larger insects. I aimed to find out if

miniaturization of the species *T. evanescens* required adaptations to the complexity of neural networks, or if the wasps only adapted neuron size. I focussed on a subset of neurons, i.e. those that produce octopamine, dopamine or serotonin. I used immunofluorescence staining in combination with confocal laser scanning microscopy to reveal neuron clusters in *T. evanescens*, and compared the number and size of cell bodies to those that have been described in other species. I further elaborate on this work in **Chapter 5**, by comparing adaptations to these same neuronal networks between small and large *T. evanescens*. This revealed if intraspecific brain scaling is facilitated by plasticity in neuron numbers, neuron size, or both.

I address the effects of static brain-body size scaling on cognition in **Chapter 6**. In this chapter, I studied both *T. evanescens*, and the larger parasitic wasp species *N. vitripennis*. I manipulated body size of genotypically similar wasps of both species by adapting the level of scramble competition in their hosts. I used single visual and olfactory conditioning trials to compare their memory retention over time. Differences in brain-scaling strategies and level of miniaturization between these two species could have resulted in differences in the body-size effects on memory retention. The results of this chapter revealed if having small brains compromises learning abilities.

In **Chapter 7**, I address the genetic component of relative brain size, which I excluded in the previous chapters. Relative brain size can determine the fraction of neurons that is assigned to different neural processing areas and tasks. A relatively large brain may show improved cognitive abilities, but may also be costly due to the large amount of energy that brain tissue requires. I created selection lines of *N. vitripennis* wasps that genetically differ in brain-body size ratio, and limited phenotypic plasticity in body size. This allowed me to study the effects of genetic variation in relative brain size on cognition, longevity and relative neuropil composition.

Finally, I integrate the findings of all previous chapters in a general discussion of my work in **Chapter 8**. I aimed to answer the main questions of my thesis in this final chapter. I focussed on the evolution of differences in brain-scaling strategies, on neuroanatomical and cognitive consequences of different brain-scaling strategies, the consequences of miniaturization of body and brain size, and compared the consequences of variation in brain size due to brain-scaling and due to genetic variation in relative brain size. I conclude with some future perspectives.


1

Chapter 2

Breaking Haller's rule: brain-body size isometry in a minute parasitic wasp

Emma van der Woude,
Hans M. Smid, Lars Chittka,
Martinus E. Huigens

Brain, Behavior and Evolution,
2013, 81(2):86-92

Abstract

Throughout the animal kingdom, Haller's rule holds that smaller individuals have larger brains relative to their body than larger-bodied individuals. Such brain-body size allometry is documented for all animals studied to date, ranging from small ants to the largest mammals. However, through experimental induction of natural variation in body size, and 3D reconstruction of brain and body volume, we here show an isometric brain-body size relationship in adults of one of the smallest insect species on Earth, the parasitic wasp *Trichogramma evanescens*. The relative brain volume constitutes on average 8.2% of the total body volume. Brain-body size isometry may be typical for the smallest species with a rich behavioural and cognitive repertoire: a further increase in expensive brain tissue relative to body size would be too costly in terms of energy expenditure. This novel brain scaling strategy suggests a hitherto unknown flexibility in neuronal architecture and brain modularity.

Introduction

Across and within all animal species investigated so far, Haller's rule holds that smaller animals have proportionally larger brains than larger-bodied forms (Rensch, 1948). In a double logarithmic plot, such an allometric brain-body size relationship is described by a straight line with a slope (the brain scaling coefficient *b*) smaller than 1. When *b* is smaller, the discrepancy in relative brain size between different-sized animals is larger. Brain-body size allometries that have been reported to date range from a within-species $b = 0.20$ for a tiny ant species to a between-species $b = 0.77$ for mammals, with a tendency of within-species coefficients to be smaller (Figure 1A; Martin, 1981; Wehner et al., 2007; Riveros and Gronenberg, 2010; Eberhard and Wcislo, 2011; Seid et al., 2011). In various species of ants, for example, intraspecific coefficients have been found to range between 0.20 – 0.40, whereas the interspecific coefficient based on mean brain and body mass of the same species is 0.57 (Wehner et al., 2007). In very small animals, brain-body size allometry implies that brain size becomes a limiting factor of body miniaturization because costs for development and maintenance of energetically expensive brain tissue (Aiello and Wheeler, 1995) will become an excessively high burden with increasing relative brain size (Kaas, 2000; Beutel et al., 2005; Grebennikov, 2008; Polilov and Beutel, 2009; Polilov, 2012).

In this study, we investigate the brain-body size relationship in minute (~0.3 – 0.7 mm long) parasitic *Trichogramma evanescens* wasps that complete their entire development inside eggs of butterflies and moths. Body volume can vary up to a factor 7 (see below) between genotypically identical wasps (Figure 1B and 2A), depending on the size of a host egg, and number of immatures developing inside it. Their brains are exquisitely miniaturized (Ø = 0.16 – 0.33 mm), and are thus only marginally larger than a single pyramidal motor neuron (Betz cell) in the human brain (Rivara et al., 2003). Nonetheless the wasps' brains constitute a large proportion of body volume (Table 1). The extreme small brain size in this species, however, does not seem to affect their behavioural performance. Female *Trichogramma w*asps, even the small phenotypes, display a rich behavioural and cognitive repertoire similar to much larger insects, including flight, walking, courtship, deciding over size and sex of their progeny, vision, olfaction, learning, and long- and short-term memory formation (Suzuki et al., 1984; Dutton and Bigler, 1995; Pompanon et al., 1997; Huigens et al., 2000; Keasar et al., 2000; Huigens et al., 2004; Fatouros et al., 2005; Fatouros et al., 2008; Huigens et al., 2009; Huigens et al., 2010; Huigens et al., 2011; Fatouros et al., 2012; Kruidhof et al., 2012). For example, to find suitable host eggs in nature, even small female

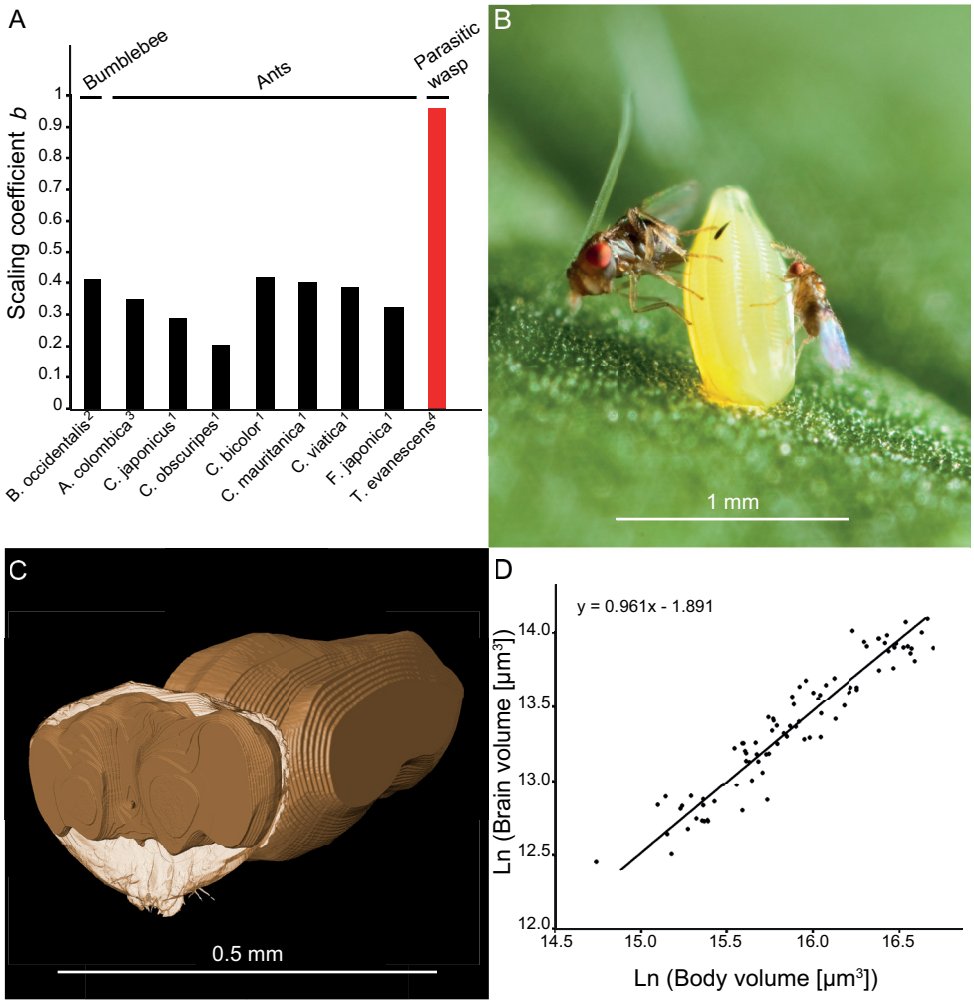

Figure 1. Brain-body size relationship in *T. evanescens* wasps. **(A)** Allometric within-species brain scaling coefficients *b* in the bumblebee *Bombus occidentalis*, the ants *Atta colombica, Camponotus japonicus, Camponotus obscuripes, Cataglyphis bicolor, Cataglyphis mauritanica, Cataglyphis viatica* and *Formica japonica,* compared to *T. evanescens*. **(B)** Two phenotypically very different sized, but genotypically almost identical, *T. evanescens* sisters (from iso-female strain GD011) parasitising an egg of the butterfly *Pieris rapae* (Photo N. E. Fatouros, www.bugsinthepicture.com). **(C)** 3D reconstruction of brain and body volume of a female wasp using AMIRA software. **(D)** Double logarithmic plot of brain versus body volume with the slope of the straight line representing the nearly isometric coefficient $b = 0.96$ (n = 87, $r^2 = 0.900$). [1] data from Wehner et al. (2007), [2] data from Riveros and Gronenberg (2010), [3] data from Seid et al. (2011), [4] data from this study.

T. evanescens wasps that developed in small host eggs can learn to respond to pheromones emitted by mated (and thus egg-laying) female butterflies. The wasps mount butterflies and when they hitch a single ride on a mated female butterfly that leads to an oviposition into freshly laid butterfly eggs, they learn to associate the butterfly's pheromones to the reward of fresh host eggs. After such a rewarding hitch-hiking experience, the wasps form either shorter or longer-lasting memory depending on the reward value constituted by the butterfly eggs (Huigens et al., 2009; Huigens et al., 2010; Kruidhof et al., 2012). These complex behavioural traits are essential to find and parasitise suitable host eggs in nature and might require a certain, minimal brain size.

We hypothesized that *T. evanescens* has reached the limits of brain scaling so that smaller wasps cannot further reduce brain size without compromising brain performance required for their complex parasitic lifestyle. In line with previous studies, we therefore expected to find a coefficient *b* within or even smaller than the 0.2 – 0.4 range documented for tiny insect species (Figure 1A; Wehner et al., 2007; Riveros and Gronenberg, 2010; Seid et al., 2011).

Materials and methods

Wasp size variation

To determine the relationship between brain and body volume, female *Trichogramma evanescens* Westwood wasps (Hymenoptera: Trichogrammatidae) of three iso-female strains (the genotypes GD011, GD025 and GD034) were used. The three females that were used to initiate the strains were collected in 2006 from a cabbage field close to the city of Wageningen, the Netherlands. Since then, the strains were cultured in small host eggs of the Mediterranean flour moth *Ephestia kuehniella* in a climate room (22 ± 1°C, 50 – 70% rh, L16:D8; developmental time from egg to adult wasp is ±11 days). Wasps of different sizes were reared by allowing female wasps to lay 1 – 2 eggs in *E. kuehniella* eggs (resulting in the smallest offspring) or to lay 1 – 4 eggs in larger host eggs of the cabbage moth *Mamestra brassicae* (Table 1, Figure 2). To obtain the largest offspring, female wasps were given the opportunity to lay only one fertilized (female) egg in a *M. brassicae* egg by observing their ovipositing behaviour as described previously (Suzuki et al., 1984; Huigens et al., 2000; Huigens et al., 2004). The obtained variation in body size was representative for the variation in body size found in nature.

Preparing wasps for confocal laser scanning microscopy

Wasps were fixed overnight in a mixture of 4% formaldehyde in 50% methanol in 0.1M phosphate buffer at neutral pH (Brandt et al., 2005). Fixation was followed by rinsing 3 times in 70% ethanol and subsequent dehydration in graded series of ethanol (5 minutes of 90%, 96% and twice in 100% ethanol). Wasps were cleared in pure xylene for approximately 20 minutes and antennae, legs and wings were removed. Heads and bodies were separated and mounted in DePeX (Fluka) on the same microscope glass, heads with the neck and bodies with the lateral part facing towards the coverslide (Brandt et al., 2005).

Volume measurements

Objects were scanned with a Zeiss LSM 510 confocal laser scanning microscope (CLSM) using a 488 nm wavelength argon laser (Smid et al., 2003; Bleeker et al., 2006). A Plan-Neofluar 40× oil-immersion objective was used for the heads and a Plan-Apochromat 10× lens for the bodies. To correct for refractive index mismatch between the oil-immersion lens and the dry lens, we used a correction factor of 1.6 for the z-axis of the body preparations (Brandt et al., 2005). Transparent properties of the cuticle allowed for complete scanning through the entire depth of the tissues. Digital image stacks were saved and analysed using AMIRA 5.3 software (Visage Imaging GmbH; Brandt et al., 2005). Brains and bodies were traced using the segmentation editor and converted to labelled datasets. Parts of the optic lobes were invisible because of eye pigments; the inner linings of the cuticle in these regions were used as boundaries. Microtome sections of *T. evanescens* heads observed by conventional light microscopy confirmed that optic lobes were indeed tightly connected to the head capsule (not shown). Labelled datasets were subsequently converted to 3D reconstructions (Figure 1C) and volumes were calculated by the material statistics option in the software. To calculate the entire body volume, head volume was taken together with the volume of thorax and abdomen. Body length was measured from the start of the thorax to the tip of the abdomen with the 3D line-measuring tool in AMIRA.

Statistical analysis

The natural logarithms of brain volume and body volume were used to obtain the brain-body size relationship. Model II type regressions, i.e. (standardized)

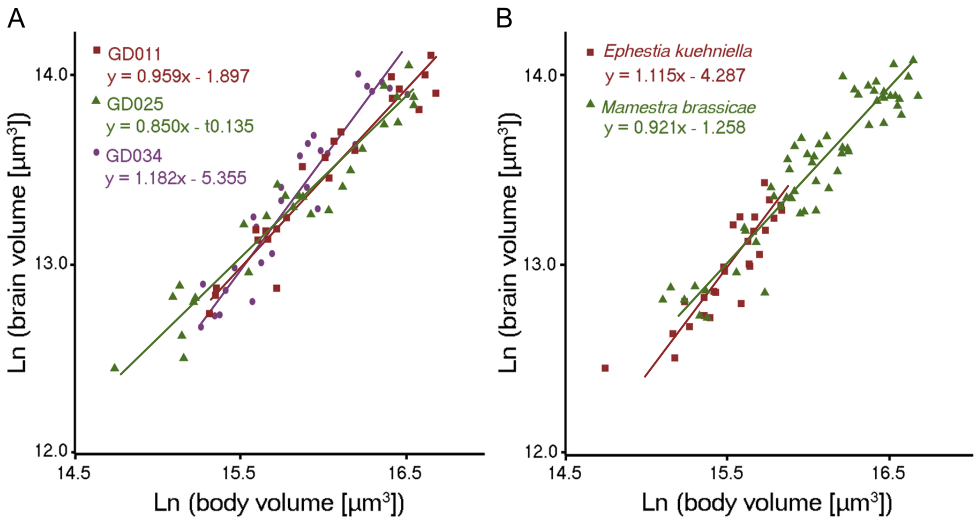

Figure 2. Effect of genotype and host species on the brain-body volume relationship in *T. evanescens* wasps. **(A)** Wasps belonging to the three iso-female *T. evanescens* strains (genotypes) GD011 (red; n = 29, r^2 = 0.929), GD025 (green; n = 29, r^2 = 0.930) and GD034 (purple; n = 29, r^2 = 0.894). **(B)** Wasps emerging from eggs of *E. kuehniella* (red; n = 29, r^2 = 0.797) or *M. brassicae* moths (green; n = 58, r^2 = 0.874). The slope of a straight line represents the brain scaling coefficient *b*.

major axis, are more appropriate than linear regression for determining allometric relationships, in which both X and Y values are measured with error. The aim of the model is to summarize the relationship instead of predicting values (Warton et al., 2006). We used standardized (reduced) major axis regression because it produces confidence intervals with a higher precision than major axis regression. All regression analyses were performed in the SMATR package for R (Falster et al., 2006). This software was used to calculate regression coefficients with confidence intervals, and to determine whether the slope of the regression line (the brain scaling component *b*) significantly deviated from 1 (isometric brain-body volume relationship) or not. Also, likelihood ratio analyses were performed to test for a common slope among regression lines of different genotypes and moth host species. When a common slope was found, SMATR was subsequently used to test for differences in elevation among the different regression lines. This determines the effect of genotype and host species on the brain-body volume relationship as ANCOVA does for linear regression (Warton et al., 2006). We used an independent-samples Kruskal-Wallis test to compare body length, brain volume, body volume, and relative brain volume between genotypes. An independent-samples Mann-Whitney U test was used to compare the same proxies for brain and body size between wasps developing from either

E. kuehniella eggs or *M. brassicae* eggs. All statistical tests were performed at $\alpha = 0.05$ in R 2.15.

Results

In our wasp sample, body length varied substantially (0.286 – 0.624 mm, Table 1). We found absolute body volume to vary by a factor of 7.01 (2,522,829 – 17,688,651 μm^3, corresponding in theory (based on water) to a weight of 0.0025 – 0.018 mg) whereas absolute brain volume varied by a factor of 5.14 (257,547 – 1,326,117 μm^3). Brain volume constituted on average 8.2% of body volume (Table 1), with a maximum of 10.9%, which is much greater than the 2.9% for another, even slightly smaller, trichogrammatid wasp species, *Megaphragma mymaripenne* (with a body length of ~0.2 mm; Polilov, 2012). Plotting brain volume against body volume after logarithmic transformation showed, in sharp contrast to what we expected, that *b* was on average 0.96 (Figure 1D). This is, to the best of our knowledge, the highest such coefficient ever found in any animal taxon. This scaling coefficient *b* is not significantly different

Table 1. Scaling coefficients *b* with confidence intervals and proxies for brain and body size in *T. evanescens* wasps depending on their genotype and the host species in which they developed.

	n	BodyL (μm)	BrainV (μm^3)	BodyV (μm^3)	Rel. BrainV (%)	*b*	CI for *b*
Genotype							
GD011	29	447 ± 76 ^{a}	7.2 ± 2.9 × 10^{5} ^{a}	9.3 ± 4.1 × 10^{6} ^{a}	7.9 ± 0.8 ^{a}	0.959 ^{a}	0.864 – 1.065***
GD025	29	448 ± 91 ^{a}	6.8 ± 2.9 × 10^{5} ^{a}	8.7 ± 4.2 × 10^{6} ^{a}	8.2 ± 1.2 ^{a}	0.850 ^{b}	0.766 – 0.943***
GD034	29	447 ± 65 ^{a}	6.8 ± 2.9 × 10^{5} ^{a}	7.9 ± 3.0 × 10^{6} ^{a}	8.5 ± 1.2 ^{a}	1.182 ^{c}	1.040 – 1.344***
Host							
E. kuehniella	29	390 ± 38 ^{a}	4.7 ± 1.2 × 10^{5} ^{a}	5.7 ± 1.3 × 10^{6} ^{a}	^{a}8.2 ± 1.0	1.115 ^{a}	0.934 – 1.331***
M. brassicae	58	458 ± 72 ^{b}	7.4 ± 2.7 × 10^{5} ^{b}	9.7 ± 4.0 × 10^{6} ^{b}	^{a}7.8 ± 1.1	0.921 ^{a}	0.838 – 1.013***
Total	87	448 ± 77	6.9 ± 2.9 × 10^{5}	8.6 ± 3.8 × 10^{6}	8.2 ± 1.2	0.961	0.897 – 1.029***

BodyL = body length, BrainV = brain volume, BodyV = body volume, Rel. BrainV = relative brain volume ((brain volume / body volume) × 100), CI = 95% confidence interval. Means are given ± SD. *a,b,c* indicate significant differences between genotypes or host species. *** $p < 0.001$.

from 1 (r_{85} = -0.126, p = 0.247), indicating an isometric relationship between brain and body size. Common slope tests revealed no significant deviations of the scaling coefficients of the different moth host species from the mean b of 0.96 (χ^2_1 = 3.516, p = 0.061, Figure 2B). This homogeneity of regression slopes allowed comparisons of elevations, which showed that moth host species did not significantly affect the brain-body volume relationship (χ^2_1 = 0.049, p = 0.825). There was a small, but significant difference in slopes between the three genotypes (χ^2_2 = 14.3, p < 0.001, Figure 2A). This implies that although the b values of the three genotypes all approach 1 (ranging between 0.85 and 1.18, Table 1), there is an effect of genotype on the brain-body size relationship.

Discussion

An isometric brain-body size relationship in extremely miniaturized animals with a rich sensory and behavioural repertoire, such as *T. evanescens,* is in contrast to what was expected from previous applications of Haller's rule. A trade-off between brain performance and energetic costs of having a large brain may explain this: a further increase in relative brain size may be too costly for this wasp species in terms of energy expenditure (Aiello and Wheeler, 1995; Chittka and Niven, 2009; Navarrete et al., 2011). Although very small beetles, strepsipterans and spiders can partially or completely relocate nervous tissue to other body parts to prevent the formation of an excessively large brain (Beutel et al., 2005; Polilov and Beutel, 2009; Eberhard and Wcislo, 2011; Quesada et al., 2011), this does not overcome the high energetic costs of maintaining a relatively large central nervous system (CNS). It therefore seems unlikely that *T. evanescens* displays a strong allometric relationship between whole CNS size and body size, even though such CNS – body size allometries were recently found for orb-weaving and cleptoparasitic spiders (Quesada et al., 2011).

We used iso-female strains to reduce genotypic variation that might obscure the brain-body size relationship. It is unlikely that the use of these iso-female strains caused the isometric relationship found in this study, because genes that affect the structure of the brain would be expected to determine numbers and morphology of all neurons in the brain, which ultimately would result in a brain of a certain absolute size. Thus, a fixed genotype would be expected to determine a more constant absolute brain size. The unique variation that we found in absolute, but not in relative brain size within a genotype can only be explained by a yet unknown flexibility in size, morphology and/or number of neurons, and potentially even in brain modularity (compartmentalisation; Kaas,

2000). This suggests the presence of specific plasticity genes that facilitate an unusually high level of plasticity in neuron numbers and/or neuron properties.

A recent estimate suggests that the adult brain of *T. evanescens* has 37,000 nucleated neurons (Polilov, 2012), 8 times more than the approximately 4600 neurons in the adult brain (and ~7400 in the whole CNS) of a related parasitic wasp species, *M. mymaripenne*. In that study by Polilov (2012), it was estimated that the brain volume of *M. mymaripenne* was on average ~13× smaller than in *T. evanescens* (corresponding body size of *T. evanescens* not known), suggesting that the average volume per neuron was higher in *T. evanescens*. Of these 4600 neurons in the brain of *M. mymaripenne*, however, approximately 95% were anucleate neurons, of which the somata were almost twice as small as those of the (< 300) nucleated neurons in the adult brain (Polilov, 2012). This suggests that nucleated neurons must be relatively small in *T. evanescens* when compared to nucleated neurons of other insects, including *M. mymaripenne*. A benefit of smaller neurons over larger ones is that they are energetically less expensive both at rest and whilst signaling (Niven and Laughlin, 2008), and may be packed more densely (Beutel et al., 2005). Biophysical theory and stochastic simulations indicate that neurite diameter can, however, not be reduced much below 0.1 μm because channel noise would disrupt communication (Faisal et al., 2005). The smallest diameters of neuron cell bodies documented for minute insects so far are 2 – 3 μm, possibly because neuron cell body diameter is restricted by the size of the nucleus (Grebennikov, 2008; Eberhard and Wcislo, 2011; Quesada et al., 2011). Interestingly, adult *M. mymaripenne* seem to have solved the latter problem by having anucleate neurons (Polilov, 2012). The question remains whether such anucleate neurons are as functional as nucleate neurons.

In conclusion, the isometric brain – body size relation found in *T. evanescens* suggests a strong constraint on the upper limit of relative brain size in extremely miniaturized insects. This is most likely an energetic limitation that determines a constant, relative brain size by preventing an increase of the brain – body size ratio in the smallest individuals. Since their complex behaviour sets a strong constraint on minimal cognitive performance as well, we expect that specific genes have evolved to facilitate extreme plasticity in absolute brain size by adjusting the number and/or properties of neurons. The use of tiny parasitic wasps that display brain isometry and a large variation in body size provides unique opportunities to study physical constraints on the smallest dimensions of neurons and adaptations in brain modularity, and the consequences on behaviour.

Acknowledgements

We thank Léon Westerd, Frans van Aggelen and André Gidding for insect rearing. This work was supported by the NWO/ALW open competition grant 820.01.012 (to H.M.S.) and NWO PE&RC Graduate Program grant 022.002.004 (to E.W.).

Chapter 3

How to escape from Haller's rule: olfactory system complexity in small and large *Trichogramma evanescens* parasitic wasps

Emma van der Woude,
Hans M. Smid

Journal of Comparative Neurology,
2016, 524(9):1876-1891

Abstract

While Haller's rule states that small animals have relatively larger brains, minute *Trichogramma evanescens* Westwood (Hymenoptera: Trichogrammatidae) parasitic wasps scale brain size linearly with body size. This linear brain scaling allows them to decrease brain size beyond the predictions of Haller's rule, and is facilitated by phenotypic plasticity in brain size. In the present study, we addressed whether this plasticity resulted in adaptations to the complexity of the morphology of the olfactory system of small and large *T. evanescens*. We used confocal laser scanning microscopy to compare size and number of glomeruli in the antennal lobe in the brain, and scanning electron microscopy to compare length and number of olfactory sensilla on the antennae. Results show a similar level of complexity of the olfactory system morphology of small and large wasps. Wasps with a similar genotype but very different brain and body size have similarly sized olfactory sensilla and most of them occur in equal numbers on the antennae. Small and large wasps also have a similar number of glomeruli in the antennal lobe. Glomeruli in small brains are, however, smaller in both absolute and relative volume. These similarities between small and large wasps may indicate that plasticity in brain size does not require plasticity in the gross morphology of the olfactory system. It may be vital for wasps of all sizes to have a large number of olfactory receptor types, to maintain olfactory precision in their search for suitable hosts, and consequently maintain their reproductive success and Darwinian fitness.

Introduction

Small animals have larger brains relative to their body size than large animals. This phenomenon is known as Haller's rule, and applies to vertebrate and invertebrate species (Rensch, 1948). The relationship between brain weight and body weight follows a power law, in which the exponent (the scaling coefficient) determines how brain size scales with body size. Scaling coefficients smaller than 1 result in the negative allometry that is described by Haller's rule. The closer a scaling coefficient is to 0, the stronger relative brain size increases in smaller animals.

Haller's rule generally holds for interspecific (Pagel and Harvey, 1989; Harvey and Krebs, 1990; Wehner et al., 2007; Isler et al., 2008) and intraspecific (Kruska, 1996; Stuermer et al., 2003; Wehner et al., 2007; Riveros and Gronenberg, 2010; Gonda et al., 2011; Seid et al., 2011) comparisons. Scaling coefficients, however, tend to be much smaller in intraspecific comparisons than in interspecific comparisons (Kruska, 2005; Wehner et al., 2007; Isler et al., 2008; Seid et al., 2011). This shows that small-bodied species have relatively larger brains than large-bodied species, but that relative brain size increases much stronger with decreasing body size within the same species.

The need for relatively larger brains in small animals may be caused by a requirement for a certain number and size of neurons and their projections for adequate brain performance (Chittka and Niven, 2009; Eberhard and Wcislo, 2011). If the size and complexity of a neural network are reduced below a threshold of functional network size, smaller brains could suffer from an unwanted loss of cognitive and behavioural complexity (Kaas, 2000; Faisal et al., 2005). The costs of maintaining a larger brain are mainly energetic, because brain tissue has a high metabolic activity (Aiello and Wheeler, 1995). Small animals consequently spend a larger proportion of their energy on maintaining their (relatively large) brains than large animals. These costs increase with increasing relative brain size, and may at some point outweigh the benefits of maintained brain performance. Unaffordable energetic costs of larger relative brain sizes may eventually limit the evolution towards smaller absolute body sizes (Eberhard and Wcislo, 2011).

So far, the only known species that does not scale brain size according to the predictions of Haller's rule is *Trichogramma evanescens* Westwood (Hymenoptera: Trichogrammatidae; Chapter 2). These are minute (~0.5 mm long) parasitic wasps that develop from egg to adult inside the eggs of butterflies and moths. The size of adult *Trichogramma* wasps depends on the size of the host eggs in which they developed, and on the number of conspecifics developing inside

these eggs. This developmental strategy can cause scramble competition that results in strong phenotypic plasticity in body size: body length of genetically identical adult females can range between 0.3 – 0.6 mm (Chapter 2). Interestingly, *T. evanescens* of very different body sizes show a unique, linear relationship between body and brain volume (Chapter 2). This indicates that, in contrast to the predictions of Haller's rule, wasps of all body sizes have the same relative brain volume. Brain volume in this species is on average 8.2% of body volume (Chapter 2), which is rather large compared to larger animals (Mares et al., 2005; Roth and Dicke, 2005). The energetic costs of this relatively large brain are expected to be very high, and may prevent small wasps from forming an even larger brain as would be expected from Haller's rule. Maintaining relative brain size may therefore be a strategy required for extreme body miniaturization.

Trichogramma evanescens wasps rely on cognitive and olfactory abilities to find and use suitable host eggs. As a result these abilities are vital for the wasps' reproductive success and Darwinian fitness. Female wasps have been shown to mount mated female butterflies and hitch-hike to the place where the butterflies will lay their eggs (Fatouros et al., 2005). The wasps can form short- and long-term memory of these events by associating butterfly pheromones that they experienced during the hitch-hiking phase with the reward of an oviposition in butterfly eggs (Huigens et al., 2009; Kruidhof et al., 2012). The wasps show more behaviours that require complex sensory and cognitive abilities, including vision, flight, and responding to sex pheromones of conspecifics and plant-cues induced by butterfly oviposition (Dutton and Bigler, 1995; Pompanon et al., 1997; Keasar et al., 2000; Pashalidou et al., 2010; Fatouros et al., 2014).

The wasps probably experience strong evolutionary pressures on cognition and miniaturization, which drive them to develop in small lepidopteran host eggs while maintaining the cognitive abilities to locate suitable hosts. The large relative brain size in large and small wasps suggests that a large investment in neural tissue is necessary to maintain their complex behavioural and cognitive repertoire. A reduction of sensory detection and neural processing abilities could have consequences for the wasps' behaviour, and ultimately their fitness.

An important implication of linear brain scaling is that it results in exceptionally small brains in the smallest individuals. Animals that scale their brains in accordance with Haller's rule form relatively larger brains at smaller body sizes, whereas linear brain scaling results in maintained relative brain size. This indicates that *T. evanescens* wasps display a level of brain size plasticity that is higher than in other species that have been investigated so far.

Linear brain scaling in *T. evanescens* is facilitated by plasticity in brain size: there can be a 5-fold difference in brain volume of genetically identical adult females (Chapter 2). There are two possible strategies through which the wasps could have accomplished this plasticity: through plasticity in neuron size while maintaining neural complexity, or through plasticity in the complexity of neural network structure by changing the number of neurons and their arborisations. Plasticity in neuron size, however, is limited by the minimum size neurons need to have to be functional. A reduction of axon diameter results in reduced neural firing rates because less space is available for energy-providing mitochondria (Perge et al., 2012). Axons with diameters below 0.1 μm malfunction because they cannot compensate for noise in the ionic membrane current, which is caused by random opening and closing of ion channels (Faisal et al., 2005). The smallest size of a neural cell body is determined by the size of its organelles. The majority of this volume is determined by the size of the nucleus, which in turn depends on genome size (Gregory, 2001). Cell body diameters as small as 1 – 2 μm have been recorded in insects (Beutel et al., 2005; Makarova and Polilov, 2013). It may be possible to form even smaller cell bodies by forming anucleate neurons; a strategy that is applied by the minute parasitic wasp *Megaphragma mymaripenne* (Polilov, 2012). In this insect 95% of the neural nuclei undergo lysis during the pupal stage, resulting in a functional nervous system consisting of mainly anucleate neurons.

The second strategy through which *T. evanescens* could have accomplished the observed plasticity in brain size, is through plasticity in the complexity of its neural networks. Specific plasticity genes could enable variation in neuron numbers, neuropil composition and complexity of neural arborisations. This neural plasticity could respond to the developmental conditions that cause variation in body size, i.e. the space and nutrition that is available inside the host egg (Lanet and Maurange, 2014). Such plasticity in neural complexity could result in simpler brain structures in small *T. evanescens*, and more complex ones in larger individuals.

The insect olfactory system is exceptionally well suited for studies of neural plasticity. On the olfactory antennal sensilla, odour molecules contact olfactory receptor proteins on dendrites of olfactory receptor neurons. These olfactory receptor neurons project to the antennal lobe in the brain, where neurons expressing similar receptor types synapse with projection- and interneurons in the same glomeruli, thereby forming functional morphological units (Gao et al., 2000; Vosshall et al., 2000; Luo and Flanagan, 2007). The number of glomeruli is consequently a measure of the number of genes that encode olfactory

receptor proteins, and the number of olfactory receptor types that are expressed (Couto et al., 2005, Robertson and Wanner, 2006). Comparisons of the number of glomeruli and olfactory sensilla thus allow analysis of neural plasticity in the complexity of the olfactory system, of which the results can be linked to olfactory performance.

In social insects, environmental signals affect the developmental process that eventually results in a caste-specific phenotype (Hölldobler and Wilson, 2009). Neural plasticity in the olfactory system can then result in genetically similar individuals having a different number of glomeruli and olfactory sensilla. In *Atta vollenweideri* ants, for example, workers can show three different phenotypes of the antennal lobe (Kelber et al., 2010). These have either a high or low number of glomeruli, and part of the workers with a high number of glomeruli form an additional macroglomerulus. These antennal lobe phenotypes correlate with behaviour and size of the worker, and result in the formation of clear sub-castes. This plasticity extends to the antennae, where the ants form fewer olfactory sensilla at smaller body sizes (Kelber et al., 2010). A similar relationship between olfactory sensilla and body size was found in bumblebees (Spaethe et al., 2007). Similarly, such plasticity may have allowed differences in the complexity of neuropil structures in *T. evanescens* of different sizes. This could have enabled very small body sizes, but at the potential cost of reduced behavioural complexity.

The aim of the present study was to find out if the plasticity in brain size that facilitates linear brain scaling in *T. evanescens* resulted in body size dependent adaptations to the complexity of olfactory system morphology. We focused on the antennal lobe in the brain, and on the sensory system on the antenna that projects towards the antennal lobe. Glomerular number and volume can be easily quantified, and the sensilla on the antenna can be measured in length and number. We assume that genetic variation between the wasps that we use in our study is virtually absent, because they are of an iso-female strain that has been subjected to 8 years of inbreeding. We can therefore study phenotypic plasticity in olfactory system morphology in response to variation in body size, without interference of genetic differences that could otherwise obscure this relationship. We expect that *T. evanescens* wasps facilitate the observed plasticity in brain size by adaptations in complexity of the olfactory system similar to those in other hymenopterans (Spaethe et al., 2007; Kelber et al., 2010), i.e. by reducing the number of glomeruli and antennal sensilla at smaller body sizes.

Materials and methods

Insects

We used two day old naive female *T. evanescens* Westwood (Hymenoptera: Trichogrammatidae) wasps of iso-female strain GD011, which have been reared since 2006 on eggs of the Mediterranean flour moth *Ephestia kuehniella* (Koppert Biological Systems, Berkel en Rodenrijs, the Netherlands) in a climate room (22 ± 1°C, 50 – 70% rh, L16:D8). *Manduca sexta* pupae were kindly provided by the Max Planck Institute for Chemical Ecology (Jena, Germany) and kept in a climate cabinet at 25 ± 1°C (L14:D10). Emerged moths of both sexes were placed in a flight cage with an approximately 20 cm tall tobacco plant (*Nicotiana tabacum* SR1) and a 30% sugar solution. Eggs were harvested daily from this cage.

Induction of body size variants

Body size variation was induced by rearing wasps on host eggs of different size, and by artificially manipulating the number of eggs laid into a host egg. Host eggs of two species were used: the Mediterranean flour moth *E. kuehniella*, and the tobacco hornworm *M. sexta*. Development times are similar on these two host species (approximately 11 days at 22 ± 1°C, 50 – 70% rh, L16:D8). Small wasps were reared in *E. kuehniella* eggs as described previously (Huigens et al., 2009; Chapter 2). These eggs are shaped as prolate spheroids of approximately 0.58 mm high, 0.38 mm in diameter and with a volume of 0.038 mm^3. Rearing *Trichogramma* in these eggs resulted in offspring with a length of 0.3 – 0.4 mm, measured from start of the thorax to the abdomen tip, thereby excluding the head (Chapter 2). The larger *M. sexta* eggs are spheroids of approximately 1.40 mm in diameter and 1.44 mm^3 in volume, and rearing in these hosts resulted in offspring with thorax-abdomen length of 0.4 – 0.8 mm (this study). To increase the proportion of large wasps emerging from *M. sexta* eggs, the number of eggs laid into this host was influenced by masking the surface of some host eggs. Female wasps can be manipulated to lay few eggs in *M. sexta* host eggs if the surface that can be perceived through antennal drumming appears smaller than it actually is (Schmidt and Smith, 1985; 1987). To achieve this, we distributed *M. sexta* eggs on top of 5 – 10 ml cooling 1% agarose (Sigma) in a petridish (Greiner Bio-One, 94 × 15 mm). This resulted in approximately half of the host egg surface being masked by agarose. As few as 6 wasps were observed to emerge from individual masked host eggs, which reached thorax-abdomen lengths of up to 0.8 mm. Up to 40 wasps per host egg were observed to emerge

from unmasked eggs, resulting in smaller wasps with thorax-abdomen lengths as small as 0.4 mm. A small proportion of unmasked host eggs also yielded large wasps, indicating that 0.4 – 0.8 mm is the natural body size range of *T. evanescens* wasps that emerge from *M. sexta* eggs.

Immunolabeling and confocal laser scanning microscopy for glomerular analysis

Female *T. evanescens* wasps reared on *M. sexta* or *E. kuehniella* eggs were used to ensure a large variation in body sizes. Approximately 60 wasps were cooled on ice, decapitated and the entire frontal cuticle of the head was removed with fine tweezers (Dumont no. 5, Sigma-Aldrich) in ice-cold phosphate buffered saline (PBS, Oxoid, Dulbecco `A' tablets). This allowed penetration of chemicals into the brain and exposed the antennal lobe for subsequent imaging procedures. Immediately after removal of the frontal cuticle, the head was transferred into ice-cold 4% formaldehyde in 0.1M phosphate buffer (pH = 7.2), freshly prepared from paraformaldehyde (Merck). When all opened heads were in the fixative, the dissection tray was moved to room temperature to allow fixation for 3 hours. The heads were then rinsed 6 times 30 minutes in PBS, incubated in 0.05% collagenase in PBS for 45 minutes at room temperature, and rinsed 4 times 5 minutes in PBS-T (0.5% Triton X-100 in PBS). A 1 hour pre-incubation in 10% normal goat serum (Dako Denmark) in PBS-T (PBS-T-NGS) was followed by incubation in a 1:125 final dilution of neuropil marker mouse mAb nc82 (NC82-c, Developmental Studies Hybridoma Bank, University of Iowa, Cat# nc82, RRID:AB_528108; Wagh et al., 2006) in PBS-T-NGS. This neuropil marker recognizes presynaptic active zone Bruchpilot (BRP) proteins, which form protein bands of 170 and 190 kDa in Western blots of homogenized *Drosophila* heads (Wagh et al., 2006). Immunolabeling was absent in *Drosophila* BRP null mutants (Kittel et al., 2006). Staining patterns in *T. evanescens* are similar to previous reports in *Drosophila* and ants (Lucas and Sokolowski, 2009; Wagh et al., 2006). After rinsing 6 times 30 minutes in PBS-T, a secondary antiserum of goat-anti-mouse antibodies linked to Alexa fluor 488 (Molecular Probes - Invitrogen Cat# A11008, RRID:AB_143165) was used at 1:200 dilution in PBS-T-NGS together with propidium iodide diluted 1:500 (Sigma-Aldrich) to visualize nuclei. Heads were then rinsed 4 times 30 minutes in PBS-T, and 4 times 30 minutes in PBS. Finally, the heads were mounted in Vectashield (Vector H-1000) with frontal side facing the coverslip.

A Zeiss LSM 510 confocal laser scanning microscope equipped with a 488-nm argon laser was used to scan the samples. A band pass emission filter was used at 505 – 550 nm to visualize Alexa fluor 488, and a long pass emission filter

was used at 560 nm to visualize propidium iode. Whole brains were scanned using a Plan-Neofluar 40× oil immersion objective (1.3 NA) and details of the antennal lobe using a Plan-Apochromat 63× oil immersion objective (1.4 NA). Resolution was kept at 1024 × 1024 pixels and 8 bit, and pixel area ranged between 0.06 × 0.06 and 0.49 × 0.49 μm^2. A z-section thickness of 0.8 μm was used for overview scans of whole brains, and 0.5 μm for detailed scans of the antennal lobe. We measured the volume of the brain and glomeruli in the antennal lobe by image segmentation, using the TrakEM2 plugin (Cardona et al., 2012) in the Fiji package of ImageJ 1.48s (RRID:SciRes_000137; Schindelin et al., 2012). We only segmented a single antennal lobe per brain, choosing the one with the clearest staining. Every glomerulus was segmented in a separate area list, which simplified counting of glomeruli per antennal lobe and allowed volume measurements of separate glomeruli. Brain volume measurements include the subesophageal ganglion. Measured brain volumes are slightly underestimated because the small size and the tight attachment to the eye pigments invariably caused damage to brain tissue after removal of frontal cuticle. When tracing the entire brain was not possible due to damaged tissue of one hemisphere, the volume of the undamaged hemisphere was duplicated. In total 15 antennal lobes and brains were analysed. Surface reconstructions of Figure 1 were smoothed in AMIRA 5.4 (Visage Imaging, Berlin, Germany).

Scanning electron microscopy for sensilla analysis

Approximately 100 female *T. evanescens* wasps that emerged from *M. sexta* eggs were CO2 sedated and sorted in order of ascending body length. The smallest 25 and largest 25 of the sedated wasps were transferred into a clean glass vial with ice-cold 2% glutaraldehyde (Sigma-Aldrich) in 0.5M sodium cacodylate buffer (pH = 7.4, Merck Schuchardt) and fixed for 2 hours, followed by rinsing 3x in 0.5M sodium cacodylate buffer and 1 hour postfixation in 1% OsO_4 (Agar Scientific) in 0.5M sodium cacodylate buffer. Wasps were subsequently 5x rinsed with water and stored overnight in CCl_4 at room temperature, followed by 3 short boiling steps in fresh CCl_4 (Bleeker et al., 2004). Wasps were transferred into 100% ethanol, critical point dried and sputtered with a 12 nm thick layer of iridium for observation with a FEI Magellan 400 scanning electron microscope at 2 kV. SEM pictures were analysed with the Fiji package of ImageJ 1.48s (Schindelin et al., 2012) using the cell counter plugin (De Vos, 2010) to count the number of sensilla of different types on the clava, and the measurement tool for body and sensillum lengths. In total 38 wasps were analysed for body and antennal length, and length and number of sensilla. Figure contrast of SEM

photographs was optimized in Adobe Photoshop CS6, which was also used to smooth the background for Figure 3.

Statistical analysis

To study the effects of body or brain size on the size and number of glomeruli and sensilla, we used linear regression models. Thorax-abdomen length and brain volume were used as independent variables. Length and number of antennal sensilla, and number and size of glomeruli (total volume, average volume, and volume and diameter of smallest and largest glomerulus) were used as dependent variables. Glomerular diameters were calculated from their volumes, assuming every glomerulus to be a perfect sphere. To test whether sensilla length and number, and glomerular volume and number depend on body or brain size, F-tests were used to test the slopes of the regression lines against zero.

If there is a difference in relative investment in glomeruli between large and small brained wasps, this would show as an allometric relationship between brain volume and glomerular volumes. To test for allometry, we used standardized major axis regression on the relationship between the natural logarithms of brain volume and glomerular volumes. The slope of the regression line was tested against 1 by analysing the correlation between fitted values and residuals as described by Warton et al. (2006). A slope (the scaling coefficient in allometric relationships) that is significantly smaller than 1 would be the result of negative allometry, whereas a slope larger than 1 is caused by positive allometry. All analyses were performed at $\alpha = 0.05$ with statistical software R version 3.0.2., in combination with packages smatr (Warton et al., 2012) and car (Fox, 2011). All values are shown as mean ± SD.

Results

Body and brain size

Wasps used for the analysis of the antennal sensilla ranged in thorax-abdomen length between 0.40 – 0.80 mm, and in total body length between 0.47 – 0.90 mm. We will continue to use thorax-abdomen length as proxy for total body length because variation in the orientation of the head makes measurements of total body length less accurate. These wasps were all reared on *M. sexta* eggs, which resulted in slightly larger wasps than those emerging from *Mamestra brassicae* and *E. kuehniella* eggs (thorax – abdomen length 0.3 – 0.6 mm), which were used in

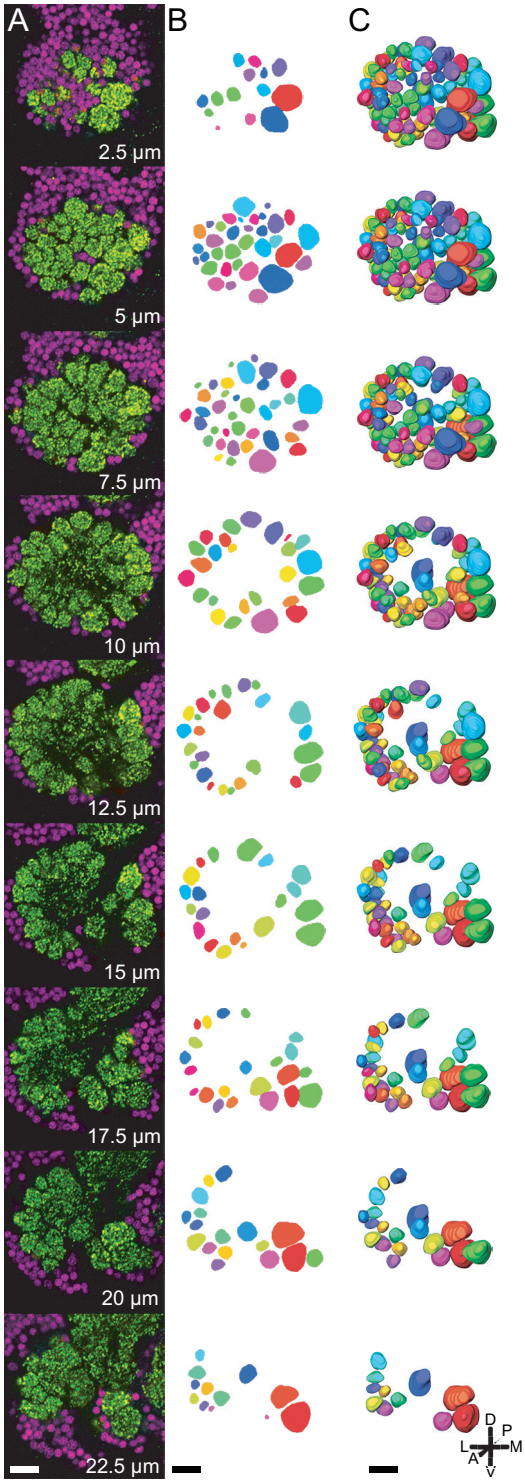

a previous study (Chapter 2). We did not measure body length of wasps used for the analysis of the glomeruli in the antennal lobe, because they were not processed individually after decapitation. Measured brain volumes of these wasps differed by a factor 2.8; ranging between $0.82 \times 10^6 - 2.32 \times 10^6\,\mu m^3$. Because brain – body size isometry found in *T. evanescens* results in a linear relationship between brain volume and body volume (Chapter 2), we assume that the level of variation in brain volume is similar to that in body volume.

◄ **Figure 1.** Morphology of glomeruli in the antennal lobe of *T. evanescens*. **(A)** Optical cross sections of an immunolabeled antennal lobe, shown from anterior to posterior with a 2.5 µm interval. Green areas show NC82-stained neuropil; magenta shows propidium iodide-stained cell bodies. **(B)** Segmentations of glomeruli shown in A. Glomeruli were randomly coloured. **(C)** Anterior view of the 3-dimensional surface reconstruction of segmentations shown in B. Glomeruli were hidden when they were in a more anterior position than the segmentations in the corresponding image in B. Surface reconstructions were smoothed in AMIRA 5.4 (Visage Imaging, Berlin, Germany). D: dorsal; M: medial; V: ventral; L: lateral; A: anterior; P: posterior. Bars equal 10 µm.

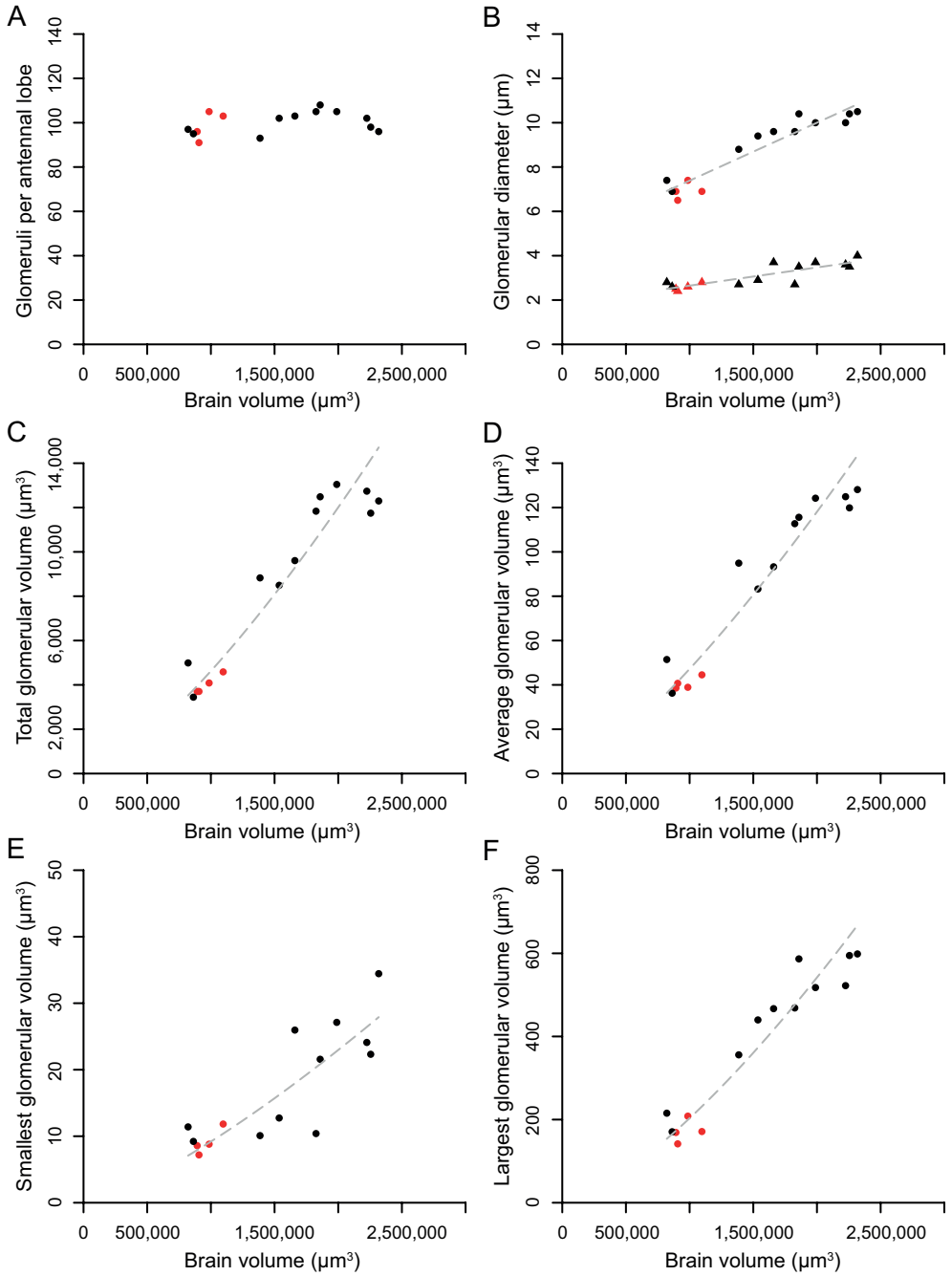

Figure 2. Number and size of antennal lobe glomeruli of wasps that differ in brain volume. Red markers indicate wasps that emerged from small *E. kuehniella* hosts, black markers indicate wasps that emerged from large *M. sexta* hosts. Dashed lines show regression lines of the relationships between brain volume and glomerular volumes and

diameters. **(A)** Number of glomeruli per antennal lobe for wasps with different brain volumes. On average 100 glomeruli are present inside the antennal lobe, which does not correlate with brain volume. **(B)** Diameter of smallest (triangles) and largest (circles) glomerulus in the antennal lobe of wasps with different brain volumes. Diameters increase with increasing brain volume (regression line smallest glomerulus: $y = 8.213 \times 10^{-7} x + 1.828$; largest glomerulus: $y = 2.613 \times 10^{-6} x + 4.773$). Total **(C)** and average **(D)** glomerular volume, and the volume of the smallest **(E)** and largest **(F)** glomerulus correlate with brain volume. Regression lines: total volume: $y = x^{1.377} - 10.579$; average volume $y = x^{1.323} - 14.421$; smallest volume $y = x^{1.320} - 16.022$; largest volume $y = x^{1.414} - 14.221$.

Analysis of the glomeruli in the antennal lobe

Counts of immunolabeled and segmented glomeruli (Figure 1) ranged between $91 - 10^8$ per antennal lobe, with an average of 99.9 ± 5.1 ($n = 15$). There was no significant effect of brain volume on the number of glomeruli in the antennal lobe ($F_{1,13} = 1.914$, $p = 0.190$; Figure 2A). Size of glomeruli, however, did increase with increasing brain size. This relationship was observed for total glomerular volume ($F_{1,13} = 138.670$, $p < 0.001$; Figure 2C), average glomerulus volume ($F_{1,13} = 173.070$, $p < 0.001$; Figure 2D), and the volume of the smallest ($F_{1,13} = 30.366$, $p < 0.001$; Figure 2E) and largest glomerulus ($F_{1,13} = 156.310$, $p < 0.001$; Figure 2F). Diameters of individual glomeruli ranged between 2.4 and 10.5 μm (Figure 2B), and volumes ranged between 7.2 and 598.5 μm^3 (Figure 2E,F). Standardized major axis regression analysis revealed a scaling coefficient of 1.38 in the relationship between brain volume and total glomerular volume, which significantly deviated from isometry ($r_{13} = 0.754$, $p = 0.001$). This shows that small wasps have a relatively smaller proportion of brain volume assigned to glomeruli than large wasps. Similar positively allometric relationships were found for average, smallest and largest glomerular volume, with scaling coefficients of 1.32, 1.32 and 1.41 respectively, all significantly different from 1 (average: $r_{13} = 0.698$, $p = 0.004$; smallest: $r_{13} = 0.459$, $p = 0.085$; largest: $r_{13} = 0.759$, $p = 0.001$). Relative volume of glomeruli ranged between 0.40% and 0.67% of brain volume (Table 1).

Antennal sensilla

Antennal length, measured from clava to radicle (Figure 3A), ranged between 165.6 – 380.2 μm, with an average length of 264.0 ± 53.8 μm. The length of the clava ranged between 64.2 – 112.9 μm, and was on average 92.7 ± 10.9 μm long. There was a significant relationship between these lengths and thorax-abdomen length (antenna: $F_{1,21} = 40.592$, $n = 23$, $p < 0.001$; clava: $F_{1,34} = 87.337$, $n = 36$, $p < 0.001$).

Table 1. Glomeruli and sensilla statistics.

Glomeruli	**Mean**	**SD**	**n**	**Range**	**Intercept**	**Slope**	*p*
Number	99.933	5.106	15	91 - 108	94.953	3.303E-06	0.190
Total volume (µm^3)	8372.050	3876.083	15	3445.11 - 13042.47	-1721.160	6.694E-03	<0.001
Average volume (µm^3)	83.147	37.230	15	36.26 - 128.09	-14.637	6.485E-05	<0.001
Relative volume (% of brain volume)	0.535	0.101	15	0.399 - 0.672	0.378	1.044E-07	0.026
Smallest glomerulus volume (µm^3)	16.384	8.632	15	7.19 - 34.44	-3.287	1.305E-05	<0.001
Largest glomerulus volume (µm^3)	375.137	177.336	15	141.61 - 598.53	-88.891	3.078E-04	<0.001
Smallest glomerulus diameter (µm)	3.067	0.533	15	2.395 - 4.037	1.828	8.213E-07	<0.001
Largest glomerulus diameter (µm)	8.713	1.523	15	6.467 - 10.456	4.773	2.613E-06	<0.001

Sensilla	**Mean**	**SD**	**n**	**Range**	**Intercept**	**Slope**	*p*
Number of MGS (ventral)	38.000	5.990	17	25 - 46	7.280	4.786E-02	<0.001
Density of MGS (ventral)	0.030	0.004	14	0.023 - 0.039	0.029	2.214E-06	0.834
Number of MTS (dorsal)	9.833	1.169	6	8 - 11	5.424	7.098E-03	0.031
Number of MTS (medial)	6.000	1.195	15	4 - 8	1.821	6.767E-03	0.006
Number of MTS (lateral)	4.700	1.174	20	2 - 7	3.152	2.564E-03	0.286
MGS length (µm)	16.050	1.409	32	11.570 - 18.252	15.849	3.327E-04	0.889
MPS length (µm)	46.971	5.349	34	35.775 - 58.794	40.348	1.069E-02	0.217
MTS length (µm)	37.260	4.616	28	26.784 - 43.505	30.946	1.018E-02	0.195
BS length (µm)	3.157	0.402	27	2.233 – 3.998	2.931	3.597E-04	0.646
BS diameter (µm)	1.644	0.173	28	1.265 - 1.929	1.620	3.953E-05	0.898

Shown are the mean, standard deviation (SD), number of measurements (n), measurement range, and intercept and slope of regression lines against brain volume (for glomeruli) or thorax-abdomen length (for sensilla). *P* values show if slope is significantly different from 0, showing if there is a relationship with brain volume or thorax-abdomen length.

An elaborate description of the different sensilla types of various *Trichogramma* species has been given before (Voegelé et al., 1975; Olson and Andow, 1993; Isidoro, 1996; Amornsak et al., 1998; Consoli et al., 1999; Ruschioni et al., 2012; Zhang et al., 2012). For our analysis of antennal sensilla, we followed the classification system previously used for several *Trichogramma* species (Olson and Andow, 1993; Consoli et al., 1999) for most sensilla types, but for clarity we applied Isidoro's (1996) nomenclature of the "multiporous gustatory sensilla" on the ventral side of the clava, which were previously described as multiporous trichoid sensilla type C (Olson and Andow, 1993) or falcate sensilla (Zhang et al., 2012).

We categorized the sensilla based on the suspected function derived from the number and location of pores on the surface (Olson and Andow, 1993; Isidoro, 1996; Consoli et al., 1999). Although our focus was on olfactory sensilla, we also briefly described other types. Aporous trichoid sensilla were classified as mechanosensilla, whereas uniporous trichoid sensilla contain both chemo- and mechanosensory neurons and are therefore likely to have a shared mechano- and gustatory function (Olson and Andow, 1993; Isidoro, 1996). Multiporous gustatory sensilla were present on the ventral clava side that touches the surface during host examination, i.e. the touch-and-taste area (Isidoro, 1996). These flattened sensilla contain pores on the outer margin where longitudinal grooves merge and contact the substrate. Although previously assumed to have a combined mechanosensory and gustatory function (Olson and Andow, 1993), they lack mechanosensory neurons and are consequently likely to be solely gustatory sensilla (Isidoro, 1996; Ruschioni et al., 2012). We classified all other multiporous sensilla (trichoid type A, placoid and basiconic) as olfactory. Coeloconic and campaniform sensilla were not present on the clava (Olson and Andow, 1993; Amornsak et al., 1998; Consoli et al., 1999; Zhang et al., 2012).

Olfactory sensilla

The multiporous trichoid sensilla type A (MTS) had an average length of 37.3 ± 4.6 μm (Figure 4B), which did not correlate with thorax-abdomen length ($F_{1,26} = 1.767$, $p = 0.195$, n = 28). Counts of MTS ranged between 8 and 11 on the dorsal clava side (mean 9.8 ± 1.2; Figure 5D), which showed a significant correlation with thorax-abdomen length ($F_{1,4} = 10.559$, $p = 0.0314$, n = 6). We analysed the number of MTS on the "lateral" (the outer clava side, i.e. the left half of the left antenna and the right half of the right antenna) and "medial" (the inner clava side, i.e. the right half of the left antenna and the left half of

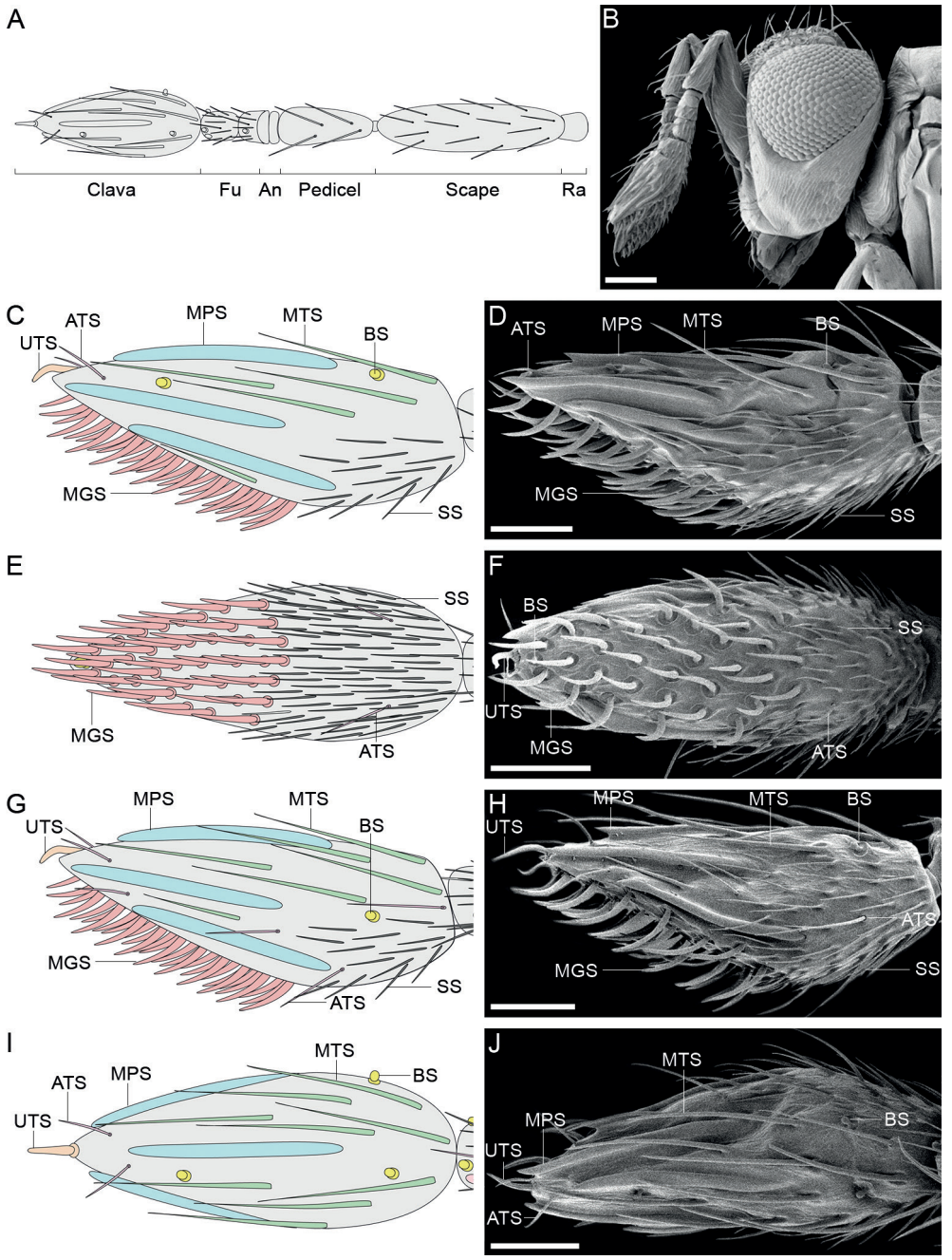

Figure 3. Position and morphology of sensilla on the antennae of *T. evanescens*. Left: Schematic overview showing the different segments on the antenna **(A)** and the different sensilla types on the clava **(C, E, G, I)**. Right: SEM photographs showing the natural orientation of the antennae on the head **(B)** and different sensilla types on the antennal

clava **(D, F, H, J)**. Schematic overviews and SEM photographs are shown for lateral **(C, D)**, ventral **(E, F)**, medial **(G, H)** and dorsal **(I, J)** view. Fu: funicles; An: anelli; Ra: radicle. Blue: multiporous placoid sensillum (MPS); green: multiporous trichoid sensillum (MTS); yellow: basiconic sensillum (BS); red: multiporous gustatory sensillum (MGS); pink: aporous trichoid sensillum (ATS); orange: uniporous trichoid sensillum (UTS). Also shown are setiform structures (SS); protective structures without a sensory function. Bars equal 50 μm in **(B)** and 20 μm in **(D,F,H,J)**. Figure contrast of SEM photographs was optimized and background was smoothed in Adobe Photoshop CS6.

the right antenna) antennal side, up to the dorsal clava median. Average MTS number was found to be 6.0 ± 1.2 on the medial side and 4.7 ± 1.2 on the lateral side. Only the number of MTS on the medial side showed a significant relationship with thorax-abdomen length (medial: $F_{1,13} = 10.500$, $p = 0.006$, n = 15; lateral: $F_{1,18} = 1.210$, $p = 0.290$, n = 20), indicating that the significant correlation for total MTS number on the dorsal views is caused by plasticity of the medial antennal side. The slope of the dorsal and medial regression lines were 0.008 ± 0.005 and 0.007 ± 0.008 respectively, suggesting that an extra MTS is formed for every 125 – 148 μm increase in thorax-abdomen length. The absolute range was 8 – 11 MTS on the dorsal side, and 4 – 8 on the medial side, with thorax-abdomen length ranging between 0.40 – 0.80 mm.

All wasps had 5 multiporous placoid sensilla (MPS) on the dorsal side of the clava. Average length of these sensilla was 46.8 ± 5.4 μm (Figure 4C), which did not correlate with thorax-abdomen length ($F_{1,32} = 1.584$, $p = 0.217$, n = 34). The small, bulb-shaped basiconic sensilla (BS) had an average length of 3.2 ± 0.4 μm, and average width of 1.6 ± 0.2 μm (Figure 4D). Both were unrelated to thorax – abdomen length (length: $F_{1,25} = 0.217$, $p = 0.646$, n = 27; diameter: $F_{1,26} = 0.017$, $p = 0.898$, n = 28). Location and number of BS did not vary between wasps of different sizes. All wasps had a total number of 4 BS on the clava; 1 located near the tip on the ventral side of the clava, 2 at the base of the dorsal side of the clava and 1 at the lateral side of the tip of the median MPS on the dorsal clava side.

Mechano- and gustatory sensilla

Length of multiporous gustatory sensilla (MGS) was on average 16.1 ± 1.4 μm, which did not significantly differ between wasps of different thorax-abdomen lengths ($F_{1,30} = 0.020$, $p = 0.889$, n = 32, Figure 4A). Small and large wasps had on average 38.0 ± 6.0 MGS per antenna, ranging between 25 in the smallest and 46 in the largest wasps (Figure 5A). There was a significant relationship between thorax-abdomen length and number of MGS ($F_{1,15} = 44.400$, $p < 0.001$, n = 17).

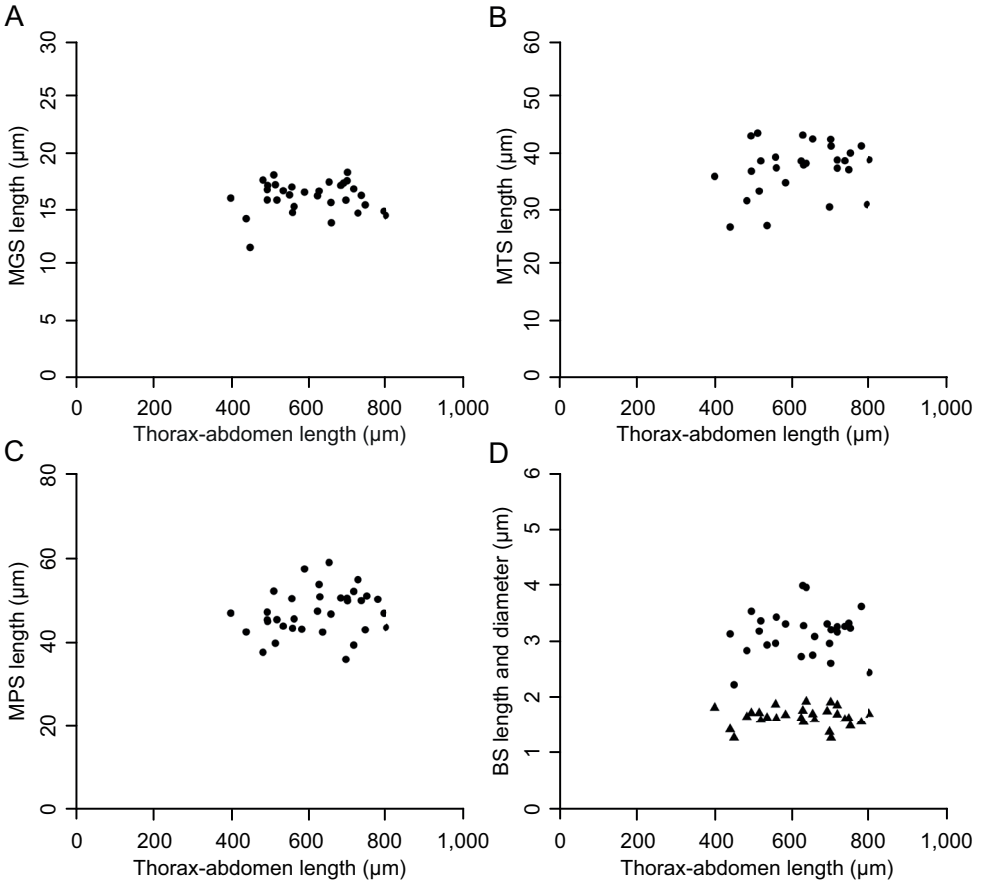

Figure 4. Measurements of sensillum lengths **(A-D)** and diameter **(D)** for wasps that differ in thorax-abdomen lengths. Length of multiporous gustatory sensilla (MGS; **A**), length of multiporous trichoid sensilla (MTS; **B**), length of multiporous placoid sensilla (MPS; **C**) and length (circles) and diameter (triangles) of basiconic sensilla (BS; b). None of these measurements correlate with thorax-abdomen length, which shows that sensillum size does not depend on the size of the wasps.

The number of MGS also significantly depends on the size of the ventral touch-and-taste area ($F_{1,12} = 18.837$, $p < 0.001$, n = 14, Figure 5B) with an average density of 0.030 ± 0.004 MGS per µm^2, which is similar for wasps of all sizes ($F_{1,12} = 0.050$, $p = 0.830$, n = 14, Figure 5C).

The number of aporous trichoid sensilla (ATS) did not vary between differently sized wasps. All wasps had 3 ATS on the dorsal side of the clava (2 at the tip, 1 at the base), 2 at the ventral side (among the setiform structures above the touch-and-taste area) and 2 at the medial side (located between the first and second MPS). Similarly, all wasps contain a single uniporous trichoid sensilla trichoidea

(UTS) at the tip of the clava. Upright orientation and the small number of these sensilla prevented analysis of the length.

Discussion

In this study, we addressed how the olfactory system of *T. evanescens* is adapted to enable the level of plasticity in brain size that facilitates linear brain scaling in these wasps. We expected that *T. evanescens* adapts the morphology of the olfactory system to variation in body size in a similar way as other hymenopterans (Spaethe et al., 2007; Kelber et al., 2010), i.e. by reducing the number of glomeruli and antennal sensilla at smaller body sizes. Our results show, however, a similar level of complexity of olfactory system morphology in small and large wasps. The olfactory sensilla of wasps with a similar genotype but very different brain and body size occur in equal numbers on the antennae, with the exception of MTS. Small and large wasps also have a similar number of glomeruli in the antennal lobe. This suggests that there is no difference in the number olfactory receptor types, and therefore in the dynamic range of odour molecules that can be perceived. Identification of complex odour blends may be an important host-finding trait for even the smallest wasps, and reduced olfactory precision might result in an unaffordable reduction of reproductive success and Darwinian fitness.

Glomeruli in small brains are, however, smaller in both absolute and relative volume. A relatively smaller size of glomeruli suggests that there are fewer olfactory receptors of each type, or that the number of synaptic contacts between olfactory receptor neurons, projection neurons and local interneurons are reduced. This could be related to the difference in MTS number between small and large wasps. The difference in relative glomerular volume could also be caused by a change in relative size of other neuropil areas. Overall, the results of our study may indicate that plasticity in brain size does not require plasticity in gross morphology of the olfactory system of *T. evanescens*. Still, plasticity in connectivity, for instance between olfactory receptor neurons and interneurons in the antennal lobe, may be involved in this process. The observed plasticity in brain size could, however, also be achieved through plasticity in neuron size and neuron number, which remains to be investigated.

Olfactory sensilla

Of all olfactory sensilla that we analysed, only the number of MTS was correlated to thorax-abdomen length. This resulted in wasps having an extra MTS for every

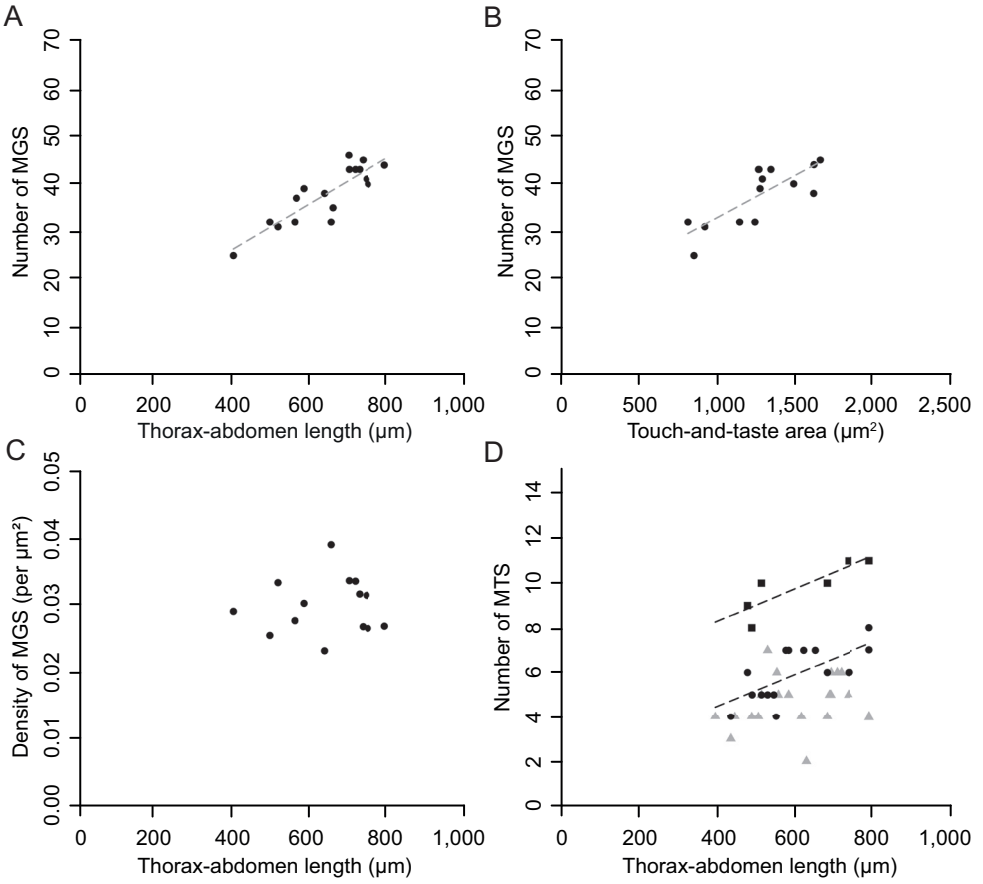

Figure 5. Number and density of multiporous gustatory sensilla (MGS; **A-C**) and multipouros trichoid sensilla (MTS; **D**) on the clava of differently sized *T. evanescens* wasps. **(A)** Relationship between the number of MGS and thorax-abdomen length shows that large wasps have more gustatory sensilla than small wasps (regression line formula y = 0.048x + 7.280). **(B)** The number of MGS increases with the size of the ventral touch-and-taste area that contains them (regression line formula y = 0.017x + 15.290). **(C)** Relationship between the density of MGS and thorax-abdomen length, which shows that all wasps form a similar number of MGS per µm² of touch-and-taste area. **(D)** Relationship between thorax-abdomen length and number of MTS on dorsal (squares, regression line formula y = 0.007x + 5.424), medial (circles, regression line formula y = 0.007x + 1.821) and lateral (grey triangles) side. The number of MTS only increases with increasing thorax-abdomen length on the dorsal and medial side of the clava.

125 – 148 µm increase in thorax-abdomen length (in total 8 – 11 MTS were counted on the dorsal clava side). Previous studies have reported fixed numbers of 8 MTS in *T. evanescens*, *T. nubilale* and *T. australicum* (Voegelé et al., 1975; Olson

and Andow, 1993; Amornsak et al., 1998), but body size of the wasps in these studies is unknown and may not have varied much between individuals.

The difference in MTS number between small and large wasps could be related to the difference in relative glomerular volume that we found in our study. Trichoid sensilla contain 1 – 3 olfactory receptor neurons in *Drosophila* (Shanbhag et al., 1999) and 2 – 3 in locusts (Cui et al., 2011), which project to a small subset of glomeruli. The number of olfactory receptor neurons per MTS in *T. evanescens* is unknown, but it is not likely that all different olfactory receptor types are present in individual MTS. The larger number of MTS that we found in larger wasps, could therefore result in a larger number of olfactory receptor neurons that provide additional input to a subset of glomeruli. This could increase the volume of these glomeruli, and consequently result in a relatively larger total glomerular volume in large brains.

Our results show an equal number of 5 MPS on the antennae of large and small wasps, consistent with findings in all *Trichogramma* species studied so far (Voegelé et al., 1975; Olson and Andow, 1993; Amornsak et al., 1998; Consoli et al., 1999; Zhang et al., 2012). The number of 4 BS found in our study confirms previous reports on *T. evanescens*, *T. nubilale*, *T. galloi* and *T. pretiosum* (Voegelé et al., 1975; Olson and Andow, 1993; Consoli et al., 1999), whereas only 3 BS were reported on the clava in *T. australicum* and *T. dendrolimi* (Amornsak et al., 1998; Zhang et al., 2012). Our findings of fixed numbers of MPS and BS on wasps with different body sizes are in contrast with findings in other hymenopterans. The number of BS correlates with body size in leaf-cutting ants, leading to an approximate 10× difference in sensillum number for ants with at 4.6× wider head (Kelber et al., 2010). In bumblebees the number of pore plate sensilla is 3.7× times larger with a 1.6× increase in head width (Spaethe et al., 2007). Brain scaling in these insects is most likely in accordance with Haller's rule, because brain allometry has been observed in related bumblebee and ant species (Riveros and Gronenberg, 2010; Seid et al., 2011). We expected that linear brain scaling led to an even stronger effect of body size on the number of olfactory sensilla in *T. evanescens* than in insects that scale their brains allometrically. It is therefore surprising that in *T. evanescens* the number of olfactory sensilla hardly changes with body size.

Gustatory sensilla

We found a large difference in gustatory sensilla numbers between large and small wasps: the largest wasp in our study had almost twice as many MGS as the smallest. It is remarkable that brain scaling affects gustatory sensillum number,

while olfactory sensillum number hardly changes. We did not analyse how this difference in MGS number relates to the complexity of the gustatory processing area that is present in the subesophageal ganglion. Studying this complexity is complicated by the lack of quantifiable gustatory substructures (Vosshall and Stocker, 2007). As a consequence, it is not possible to obtain information about gustatory system complexity in a similar way as from the antennal lobe glomeruli, that provide information about olfactory system complexity.

Female *Trichogramma* wasps determine sex ratio and number of eggs to be laid based on information they obtain while walking over the host egg and drumming on its surface with their antennae (Suzuki et al., 1984; Schmidt and Smith, 1985), and MGS have been suggested to be the main sensilla responsible for transferring this information (Olson and Andow, 1993). Having more MGS may, therefore, enable large wasps to measure host volume more precisely and allocate offspring in a more advantageous way.

Sensillum size

Sensillum length was independent of thorax-abdomen length. This corresponds to findings in other insects, where olfactory sensilla lengths appear to be independent of antennal length (Payne et al., 1973; Ramirez-Esquivel et al., 2014). If sensilla length is indeed similar in large and small *T. evanescens* wasps, the wasps should have an equal number of olfactory receptors. This could result in an equal ability to respond to low odour concentrations. Unfortunately, our sensilla length measurements show large variation, possibly caused by slight deviations from a horizontal orientation in the SEM pictures that increased errors in length measurements. For this reason, we cannot exclude that sensilla length depends on body size.

Glomeruli number

Antennal lobe glomeruli are considered as separate functional units because olfactory receptor neurons expressing a certain olfactory receptor protein type project to the same glomerulus (Gao et al., 2000; Vosshall et al., 2000; Luo and Flanagan, 2007). This suggests that the number of glomeruli is a measure of the diversity of olfactory receptor types, and therefore of the dynamic range of odour molecules that can be perceived. *Trichogramma evanescens* forms more glomeruli in the antennal lobe than recorded in much larger insects in other orders (e.g. 54 in *Drosophila melanogaster* flies (Grabe et al., 2015), 50 in *Anopheles gambiae* mosquitos (Ignell et al., 2005), and 62 in female *M. sexta* moths (Heinbockel et al., 2013)).

Within hymenopteran insects, however, the 100 glomeruli in *T. evanescens* is the lowest number found so far. Hymenopterans generally have large numbers of glomeruli, for example approximately 165 in honeybee workers (Arnold et al., 1985), and approximately 190 in parasitic wasps of the genus *Cotesia* (Smid et al., 2003; Das and Fadamiro, 2013). Even larger numbers of glomeruli are found in ants; e.g. up to 630 in *Apterostigma cf. mayri* (Nishikawa et al., 2008; Zube et al., 2008; Kelber et al., 2009; Kuebler et al., 2010; Stieb et al., 2011). All these insects are, however, several times larger than *T. evanescens*. The only similarly sized arthropod of which the glomeruli have been analysed is the 0.5 mm long predatory mite *Phytoseiulus persimilis* (van Wijk et al., 2006). The olfactory system of this mite consists of only 5 olfactory sensilla on the tarsi of the front leg pair, and only 14 – 21 glomeruli in the olfactory lobe. This suggests that a small number of olfactory receptor types is present in *P. persimilis*, and therefore that the olfactory range that can be perceived is much narrower than in *T. evanescens*.

The average of 100 glomeruli found both in small and large *T. evanescens* wasps consequently indicates that the diversity in the expressed types of olfactory receptors is not different, and thus that olfactory discrimination abilities may be comparable. The constant number of glomeruli in *T. evanescens* is in contrast with findings in *Atta vollenweideri* ants, where neural plasticity results in three distinct antennal lobe phenotypes (Kelber et al., 2010). Workers form either high or low numbers of glomeruli in their antennal lobes (around 443 and 383 respectively), and among the workers with high glomerular numbers there are phenotypes that do and do not form a macroglomerulus. These differences in antennal lobe phenotype correlate with worker size and behaviour, and result in the formation of sub-castes that may require different levels of olfactory performance. The lack of such antennal lobe plasticity in *T. evanescens* shows that brain size plasticity can occur without adaptations to the gross morphology of the olfactory system in these wasps. Large wasps already form the lowest number of glomeruli found so far in hymenopterans, and it is possible that the level of antennal lobe complexity cannot be further reduced in smaller wasps.

Glomerular size

Glomeruli in *T. evanescens* range in volume from 7.2 to 598.5 μm^3, and in diameter from 2.4 to 10.5 μm. Their glomeruli are very small compared to those of other (larger-sized) hymenopterans, where the smallest glomeruli in e.g. *Apterostigma* ants and *Cotesia* parasitic wasps are approximately 100 μm^3 (Smid et al., 2003; Kelber et al., 2009). The only glomeruli of similarly small size are found in *P. persimilis*, which is also of similar body size as *T. evanescens*. Glomerular

diameters range between 3 – 10 μm in this tiny predatory mite (van Wijk et al., 2006). This suggests that small glomeruli are associated with small bodies among arthropods.

Differences in glomerular volume relative to brain volume could provide additional information on the investment in olfactory processing centres in small and large wasps. Despite the isometric relationship between body volume and brain volume in *T. evanescens* (Chapter 2), we found a positively allometric relationship between brain volume and volume of glomeruli. This shows that small wasps have a relatively smaller proportion of the brain assigned to glomeruli than large wasps. Their antennal lobes might contain fewer synaptic contacts between olfactory receptor neurons, projection neurons and local interneurons. The difference in MTS number between small and large wasps suggests that large wasps have more olfactory receptor neurons than small wasps, which could cause a relatively larger total glomerular volume. Alternatively, a larger relative glomeruli size could also be caused by more arborisations of projection neurons and local interneurons, or by a decrease in relative size of other neuropil areas.

Conclusion

Our study is the first to compare olfactory structures in genetically similar individuals that show an exceptional plasticity in body size. While we expected that the linear brain scaling in *T. evanescens* resulted in body size dependent adaptations to the structure and complexity of the olfactory system, we found a similar size and number of most olfactory sensilla on the antennae, and number of glomeruli in the antennal lobe of small and large individuals. This remarkable similarity in olfactory perception and processing centres shows that plasticity in brain size might not affect olfactory precision. The wasps rely on the identification of complex odour blends for finding suitable hosts and maintaining reproductive success, and their olfactory abilities are therefore directly related to their Darwinian fitness. As a consequence, the morphology of the olfactory system may be fixed to ensure accurate olfactory discrimination in wasps of all sizes.

Additional brain morphology comparisons are required, however, to see if plasticity in brain size is achieved through plasticity in neuron size and neuron number, and if plasticity occurs in the complexity of other neuropil areas and sensory systems. Further TEM studies of the antennae are required to show how our findings are reflected in number and size of olfactory receptor neurons, and behavioural studies need to show if olfactory discrimination abilities are

indeed similar in small and large wasps. The question remains, however, how the wasps' escape from Haller's rule compromises their complex behavioural repertoire.

Acknowledgements

We thank Marcel Giesbers of the Wageningen Electron Microscopy Centre (WEMC) for help with our SEM study, and the Max Planck Institute for Chemical Ecology (Jena, Germany) for providing the *M. sexta* pupae. We also thank Marcel Dicke, Martinus E. Huigens, Jitte Groothuis and two anonymous reviewers for constructive comments on an earlier version of the manuscript. This work was supported by NWO PE&RC Graduate Program grant 022.002.004 (to EW).

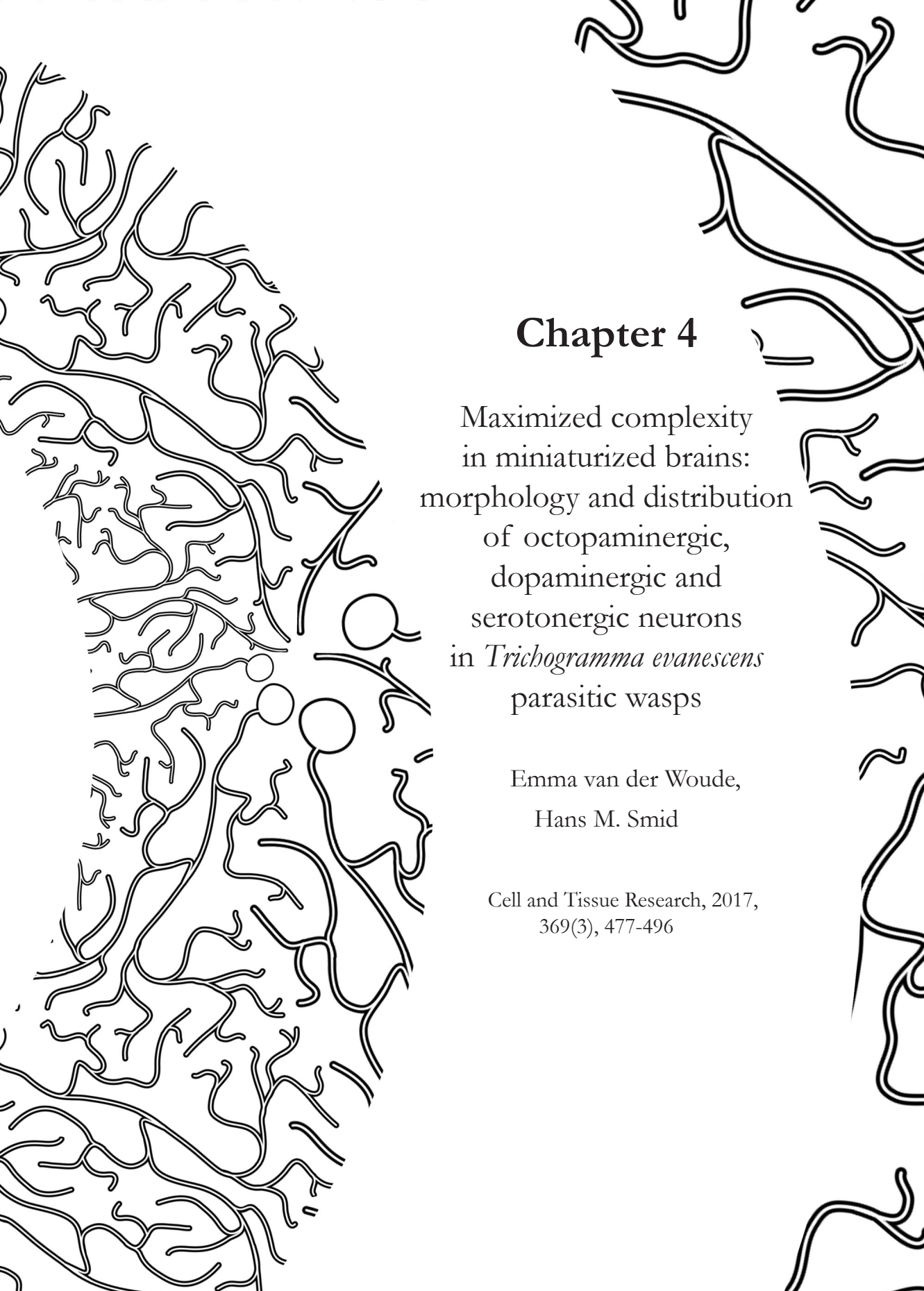

Chapter 4

Maximized complexity in miniaturized brains: morphology and distribution of octopaminergic, dopaminergic and serotonergic neurons in *Trichogramma evanescens* parasitic wasps

Emma van der Woude,
Hans M. Smid

Cell and Tissue Research, 2017,
369(3), 477-496

Abstract

Trichogramma evanescens parasitic wasps are extremely small insects, with body lengths as small as 0.3 mm. To facilitate this miniaturization, their brains may have evolved to contain smaller neural components and/or reduced neural complexity than larger insects. Here, we studied if the size and number of neurons are reduced in the miniaturized brain of *T. evanescens*, focussing on neurons that express serotonin (5HT), octopamine (OA), and dopamine (DA). We provide a first description of the distribution, projection patterns and number of 5HT-, OA-, and DA-like immunoreactive cell bodies in *T. evanescens*, and compare our observations to descriptions of much larger insects. Our results show that brains of *T. evanescens* contain comparable numbers of monoaminergic neurons as those of larger insects. The serotonergic neurons appear to be especially conserved; most of the clusters contain a similar number of neurons as described in *Apis mellifera* and *Drosophila melanogaster*. This maintained complexity may have been facilitated by miniaturization of neuron size. However, many dopaminergic and some octopaminergic neuron clusters in *T. evanescens* contain fewer neurons than in larger insects. Modification of the complexity of these monoaminergic systems may have been necessary to maintain neuron functionality during brain miniaturization in *T. evanescens*. The results of our study reveal some of the evolutionary adaptations that may enable behavioural and cognitive complexity with miniaturized brains.

Introduction

Trichogramma evanescens (Hymenoptera: Trichogrammatidae) parasitic wasps are extremely small gregarious parasitoids that lay their eggs inside the eggs of butterflies and moths. Adult body size of the wasps strongly depends, by means of phenotypic plasticity, on the level of nutrient availability inside the host egg. Genetically identical sister wasps reach body lengths as small as 0.3 mm when they develop in small host eggs or in competition with many developing larvae (Chapter 2), and as large as 0.9 mm when they develop in large hosts without competition from other wasp larvae (Chapter 3).

Trichogramma evanescens show isometric brain scaling, exhibiting a linear relationship between brain and body volume. This deviates from the situation that is described by Haller's rule, which states that small animals have relatively larger brains. As a result of brain isometry, the smallest *T. evanescens* have brains that are even smaller than predicted by Haller's rule. Their brain volume can be as small as $0.26 \times 10^6\ \mu m^3$ (Chapter 2), which is almost 2500× times smaller than the brain of a honeybee (Mares et al., 2005).

Despite these extremely small brains, *Trichogramma* wasps can walk, fly, discriminate between odours and colours, live for several weeks, and control the size, number and sex of their offspring (Suzuki et al., 1984; Waage and Ming, 1984; Dutton and Bigler, 1995; McDougall and Mills, 1997; Pompanon et al., 1997; Keasar et al., 2000; Fatouros et al., 2008). Furthermore, they detect their host eggs by hitch-hiking on butterflies that are ready to lay their eggs, and learn to associate odours and colours to the presence of suitable hosts (Fatouros et al., 2005; Huigens et al., 2009). This indicates that strongly miniaturized brains can still generate a level of behavioural complexity and modulation that is, even in the smallest individuals, comparable to much larger insects.

Evolution of miniaturized brains could have resulted in reductions in the size of neural components, reductions in neural complexity, or both. Indications of such modifications can be found through comparisons to larger species. For example, parasitic wasps of the genus *Cotesia* have body lengths that are a 10-fold larger than *T. evanescens*. Depending on the size of the wasps, there is a 10–100-fold difference in total volume of glomeruli inside the antennal lobes of the two wasps. However, there is only a 2-fold difference in antennal lobe complexity: *Cotesia* wasps have almost 200 glomeruli in the antennal lobe (Smid et al., 2003; Das and Fadamiro, 2013), whereas *T. evanescens* wasps have 100 glomeruli (Chapter 3).

Similar modifications may occur at neuron level: neuronal cell bodies and neurites are probably miniaturized as much as possible within physical limits, and further miniaturization can be achieved through modifications of neuron number and arborisation complexity. The physical limits of neuron size are determined by the minimum size that neurites need for adequate firing, and that cell bodies need to contain their cell organelles. A decrease beyond these limits may severely affect the physical performance of neurons. Thinner axons, for example, have reduced neural firing frequencies and are more sensitive to the effects of random opening and closing of ion channels (Faisal et al., 2005; Perge et al., 2012). A decrease of cell body volume affects the available space for cell organelles, of which the nucleus is the largest. Neuron performance may be affected when nucleus size is reduced, because it can require a reduction of genome size (Gregory, 2001) or even the formation of anucleate neurons (Polilov, 2012).

To further miniaturize brain size, while avoiding the compromised performance of undersized neurons, the number of neurons and neuronal connections may need to be reduced. A reduction of neuron numbers can occur through a proportional reduction of neurons in all neural pathways, or by removing some pathways entirely while maintaining others. For example, *Nasonia* parasitic wasps form fewer octopaminergic neurons in their brains than much larger honeybee workers (Sinakevitch et al., 2005; Haverkamp and Smid, 2014). This lower number of neurons is due to the formation of fewer octopaminergic neurons in the neuron clusters that are present in both honeybees and *Nasonia*, but also due to the complete absence of some other clusters. Even more severe modifications of neuronal complexity may have been required to achieve even smaller brain sizes in *T. evanescens*.

In the present study, we investigated how the size and number of neurons are affected in the miniaturized brain of *T. evanescens*. We studied quantifiable subpopulations of neurons that release serotonin (5HT), octopamine (OA) and dopamine (DA) as neurotransmitter. The morphology and distribution of these neurons are well defined in a variety of insect species. This allowed us to compare the number, size and location of monoaminergic neurons in *T. evanescens* to larger hymenopterans, such as *Nasonia* and *Cotesia* parasitic wasps (Bleeker et al., 2006; Haverkamp and Smid, 2014) and the even larger honeybee (Schürmann and Klemm, 1984; Schafer and Rehder, 1989; Schürmann et al., 1989; Kreissl et al., 1994; Sinakevitch et al., 2005). It also allowed comparisons to the more distantly related, but well-characterized, fruit fly (Monastirioti, 1999; Sinakevitch and Strausfeld, 2006; Busch et al., 2009; Mao and Davis, 2009; Blenau and Thamm, 2011). Serotonergic, octopaminergic, and dopaminergic

neurons are known to play critical roles in basic neural functioning. They are involved in a large variety of behavioural and physiological processes, including learning (Roeder, 2005; Blenau and Thamm, 2011; Burke et al., 2012; Yamamoto and Seto, 2014). With the present study, we provide a first description of the distribution, projection patterns and number of 5HT-like immunoreactive (5HT-L-IR), OA-like immunoreactive (OA-L-IR) and DA-like immunoreactive (DA-L-IR) neurons in the miniaturized brain of *T. evanescens*, and aimed to find out if the number of 5HT-L-IR, OA-L-IR and DA-L-IR neurons is smaller compared to larger insects.

Materials and methods

Insects

Trichogramma evanescens Westwood (Hymenoptera: Trichogrammatidae), inbred isofemale strain GD011, was reared in a climate room (22 ± 1°C, 50 – 70% rh, L16:D8) using differently-sized hosts, as described before (Chapter 2; Chapter 3). Body size of the wasps depends on the level of nutrient availability inside the host egg. Hence, using differently-sized hosts ensured that wasps with body sizes within the entire natural range emerged. We used host eggs of three species: small eggs of the Mediterranean flour moth *Ephestia kuehniella*, intermediate-sized eggs of the cabbage moth *Mamestra brassicae* and large eggs of the tobacco hornworm *Manduca sexta*. From the wasps that emerged from these hosts, we randomly selected individuals of a large variety of body sizes for our experiments, to ensure that the entire natural range of body sizes was represented by our study. Eggs of *E. kuehniella* were obtained as UV-irradiated eggs from Koppert Biological Systems (Berkel en Rodenrijs, the Netherlands). *Mamestra brassicae* were reared on cabbage plants (*Brassica oleracea*) in a climate room (21 ± 2°C, 50 – 70% rh, L16:D8). Adult moths oviposited on filter paper, and their eggs were used fresh for rearing procedures. *Manduca sexta* were obtained as pupae from the Max Planck Institute for Chemical Ecology (Jena, Germany) and kept in a flight cage with tobacco plants (*Nicotiana tabacum* SR1) inside a climate cabinet (25 ± 1°C, L16:D8). Eggs were collected from the plants and frozen until use in rearing procedures.

Analysis of 5HT-immunoreactivity

Two-day-old female *T. evanescens* (body lengths ranging between 0.3 and 0.9 mm) were immersed in ice-cold 4% formaldehyde in 0.1M phosphate buffer

(pH = 7.2), freshly prepared from paraformaldehyde (Merck, Darmstadt, Germany). The wasps were subsequently decapitated, antennae were removed and the eyes were carefully opened with fine tweezers (Dumont no. 5, Sigma-Aldrich) to allow optimal infiltration of the fixative. Heads were fixed either for four hours at room temperature or overnight at 4°C, and subsequently rinsed in four changes of phosphate-buffered saline (PBS; Oxoid, Dulbecco 'A' tablets). Access to the brain for further procedures and microscopic analysis was achieved by removing either the anterior or posterior cuticle with fine tweezers in PBS at room temperature. Permeability of the tissue was improved by incubating heads in 0.05% collagenase (Sigma-Aldrich) in PBS for 45 minutes at room temperature, followed by rinsing 4 × 10 minutes in 0.5% Triton X-100 in PBS (PBS-T). The heads were then pre-incubated for one hour in 10% normal goat serum (NGS; Dako, Denmark) in PBS-T (PBS-T-NGS), and subsequently incubated in a 1:200 dilution of rabbit anti-5HT antibodies (Millipore Cat# AB938, RRID:AB_92263) in PBS-T-NGS overnight at room temperature. After rinsing 6x30 minutes in PBS-T at room temperature, the heads were incubated in a secondary antiserum of goat-anti-rabbit antibodies linked to Alexa fluor 488 (Molecular Probes, Cat# A11008, RRID:AB_143165) at a 1:200 dilution and propidium iodide (Sigma-Aldrich) at 1:500 dilution in PBS-T-NGS, for four hours at room temperature. The heads were then rinsed 4 × 30 minutes in PBS-T, and 4 × 30 minutes in PBS, dehydrated in graded series of ethanol (30–50–70–90–96–100–100%, 2 minutes each) and cleared in xylene. Finally, the heads were mounted in DPX (Sigma-Aldrich) with the opened side of the head facing the cover slide.

Analysis of OA-immunoreactivity

Two-day-old female *T. evanescens* (body lengths ranging between 0.3 and 0.9 mm) were given an oviposition experience on fresh *M. brassicae* eggs 30 minutes before dissection. Such an oviposition experience has previously been shown to increase immunolabelling in *Nasonia* parasitic wasps (Haverkamp and Smid, 2014). Ovipositing wasps were removed from the host eggs by their wings, using fine tweezers. The wasps were directly placed in a dissection tray containing fixative at room temperature, which consisted of three parts saturated picric acid, one part 25% glutaraldehyde (Sigma-Aldrich) and 0.1% acetic acid. The head capsule was opened to allow infiltration of the fixative, and the heads were subsequently fixed at room temperature for four hours or overnight.

After fixation, heads were rinsed in several changes of 70% ethanol, after which

either the anterior or posterior cuticle was removed with fine tweezers. The heads were subsequently dehydrated using graded series of ethanol (30–50–70–90–96–100–100%, 2 minutes each), degreased in xylene for 20 seconds and rehydrated with the same graded series in reversed order to PBS. Oxidization of OA was reduced by a treatment of 0.1% or 1% sodium borohydride (Sigma-Aldrich) in PBS for 20 minutes, followed by four changes of PBS. A treatment of 0.05% collagenase in PBS (45 minutes at room temperature) was used to increase permeability of the tissue. This was followed by rinsing 4 × 5 minutes in PBS-T, and one hour pre-incubation in PBS-T-NGS. The heads were then incubated in a 1:200 dilution of rabbit anti-OA antibodies (MoBiTec Cat# 1003GE, RRID:AB_2314999) in PBS-T-NGS. After rinsing 6 × 30 minutes in PBS-T, a secondary antiserum of goat-anti-rabbit antibodies linked to Alexa fluor 488 (Molecular Probes, Cat# A11008, RRID:AB_143165) was used at 1:200 dilution in PBS-T-NGS together with 1:500 propidium iodide. Heads were then further processed as described above for mounting in DPX.

Analysis of DA-immunoreactivity

Immunohistochemical procedures for dopamine analysis were similar to those for octopamine analysis, except that the wasps did not receive an oviposition experience prior to dissection. The wasps were directly placed in the fixative, and after opening of the cuticle all heads were fixed for three hours at room temperature. Further processing was identical as described above, using as primary antibody mouse anti-DA (Millipore Cat# MAB5300, RRID:AB_94817) at a 1:200 dilution in PBS-T-NGS overnight at room temperature. After rinsing 6 × 30 minutes in PBS-T, a secondary antibody of rabbit-anti-mouse (Dako Cat# Z0259, RRID:AB_2532147) was applied at a 1:200 dilution for three hours at room temperature. Finally, a tertiary antiserum of goat-anti-rabbit antibodies linked to Alexa fluor 488 (Jackson ImmunoResearch Labs Cat# 115-545-003, RRID:AB_2338840) was used at a 1:200 dilution together with 1:500 propidium iodide overnight at 4°C. Heads were then further processed as described above for mounting in DPX.

Antisera specificity

Specificity of the rabbit anti-serotonin antibody was provided by the manufacturer (Mobitec, Germany). Evaluation of the antisera showed positive immunofluorescence staining in serotonin-containing human ileum structures.

Specificity of the rabbit anti-octopamine antibody was determined as specified by the manufacturer (Mobitec, Germany) using conjugate octopamine-glutaraldehyde-proteins: OA-G-BSA 1; Noradrenaline-G-BSA 1 : 90; Tyramine-G-BSA 1 : 142; L-DOPA-G-BSA 1 : 285; OA=G=BSA 1 : 442; DA-G-BSA 1 : 1120; Adrenaline-G-BSA 1 : >10,000; OA 1 : >10,000. Cross-reactivity of the mouse anti-dopamine antibody was determined as specified by the manufacturer (Mobitec, Germany): DA-G-BSA 1; L-DOPA-G-BSA 1 : 10,000; Tyrosine-G-BSA 1 : 36,000; Tyramine-G-BSA 1 / >50,000; Noradrenaline-G-BSA 1 : >50,000; OA-G-BSA 1 / >50,000; Adrenaline-G-BSA 1 / >50,000; DA 1 / >50,000. We performed additional control experiments using preparations without primary antisera. These did not reveal any immunolabelling.

Microscopy

A Zeiss LSM 510 confocal laser scanning microscope with a 488-nm argon laser was used with a band pass emission filter at 505 – 550 nm to visualize Alexa Fluor 488, and a long pass emission filter at 560 nm for propidium iodide. Heads were scanned using a Plan-Apochromat ×63 oil immersion objective (N.A. 1.4). The resolution was kept at 1024 × 1024 pixels and 8 bit, and voxel size ranged between 0.14 × 0.14 × 0.70 μm for overview scans of whole brains, and 0.07 × 0.07 × 0.20 μm for detailed scans of cell clusters. We did not correct for Z-axis refractive index mismatch because the refractive index of the used immersion oil matched the index of the mounting medium.

Orientation and nomenclature

The head of *T. evanescens* has a vertical orientation with ventral mouthparts. The orientations that were used in this study to indicate locations inside the brain, therefore, refer to the position along the anterior-posterior body axis. To identify clusters, we followed nomenclature as described for OA-L-IR neurons in *Nasonia vitripennis* and *Nasonia giraulti* parasitic wasps (Haverkamp and Smid, 2014). In this system, cell clusters are numbered from anterior to posterior. A similar nomenclature system was previously used for *Apis mellifera* (Schürmann and Klemm, 1984; Sinakevitch et al., 2005). We followed numbering of corresponding clusters in previous studies where possible, but deviated from these descriptions when clusters appeared in a different order.

We base our description of the location and projection of neurons on the general morphology of brain compartments that was described for *A. mellifera* (Brandt et

al., 2005) and *Nasonia* (Haverkamp and Smid, 2014). To identify corresponding areas in *T. evanescens*, we used the propidium iodide and background staining in preparations of the present study, in combination with previous preparations stained with neuropil marker mouse monoclonal antibody nc82 (Chapter 3). General morphology of brain compartments in *T. evanescens* corresponds to the descriptions of *Nasonia* (Haverkamp and Smid, 2014) and *A. mellifera* (Brandt et al., 2005) with three exceptions. First, only a single mushroom body calyx was visible in *T. evanescens*, whereas *Nasonia* and *A. mellifera* both have elaborate double calyces. The formation of single calyces is not uncommon among wasps of the superfamily Chalcidoidea (which includes *Trichogramma*, but also *Nasonia*), and has been suggested to be the consequence of miniaturization (Farris and Schulmeister, 2011). Second, there was no clear transition of the sub- into the supraoesophageal zone. Hence, we do not distinguish between these two and define 'brain' as the combination of the sub- and supraoesophageal zones. Third, we could not observe the distinction of the mandibular, maxillary and labial neuromeres in the suboesophageal zone of *T. evanescens*. This complicated the nomenclature of octopaminergic ventral unpaired median neurons (OA-VUM). These neurons are located in the midline of the suboesophageal zone in various insect species, and are usually named after the neuromere in which they occur (Schroter et al., 2007; Haverkamp and Smid, 2014). The OA-VUM cell bodies were located very close together in *T. evanescens*. We therefore combine them all into one cluster: OA-VUM.

Neuron analysis

We selected the 30 best-stained brains per monoamine analysis for cell body counts. Diameter and number of cell bodies were only analysed in brains in which the cluster of interest was clearly visible, and the best-stained hemisphere was selected for analysis of the cluster. To count cell bodies that were located close together, we used image segmentation to manually trace cell bodies. We used either the segmentation editor of Amira 5.4 (Visage Imaging GmbH, Berlin, Germany) or the TrakEM2 plugin (Cardona et al., 2012) in the Fiji package of ImageJ 1.50c (Schindelin et al., 2012). Cell body diameters were measured with the measuring tool in the Fiji package of ImageJ. Each cell was measured twice, and measurements of all cells within a cluster were averaged to obtain a single average value per cluster per brain. The measuring tool was also used to measure brain width, which was measured from medulla to medulla to avoid lamina areas that were damaged by the dissection procedures.

We included brains within the entire natural size range into our analysis. The size of the wasps did not affect the distribution and number of monoaminergic neurons in the brain, but there was an effect on neuron diameter (Chapter 5). Hence, we presently report the average diameter of cell bodies from the total body size range to cover the natural variation. Descriptions of neuron projection patterns were prepared from those preparations in which they were best visible, which were mostly large brains. We used the z-project function in the Fiji package of ImageJ 1.50c to create z-stack projections of cell bodies and neurites. Contrast of these images was enhanced in Adobe Photoshop CS6 (San Jose, CA).

Results

Overall quality of the immunolabelling

All antisera yielded good staining qualities in which many neuron clusters were visible, but the 5HT-L-IR staining was more intense than OA- and DA-L-IR staining. There were no visible differences in staining quality between brains of different sizes, nor in number or distribution of the monoaminergic neuronal cell bodies. However, neurites were better visible in large than in small brains due to their larger diameter and length. We will further compare the specific differences between small and large sister wasps in Chapter 5.

Average brain width (measured from medulla to medulla) was 136 ± 30 μm (n = 30) in wasps that were analysed for 5HT-like immunoreactivity, 123 ± 19 μm (n = 30) in wasps that were analysed for DA-like immunoreactivity, and 125 ± 18 μm (n = 30) in wasps that were analysed for OA-like immunoreactivity. Although dissecting brains of such small sizes was possible without severe damages to neuropil tissue, our methods induced some specific difficulties. Our method of dissecting the brains after tissue fixation made the brain less fragile and therefore easier to separate from the cuticle, but also reduced tissue elasticity. There were three specific areas that were rather vulnerable to consequent tissue damage during the dissection procedures. First, the ventral rim of the brain was sometimes damaged because of its tight attachment to the inflexible area close to the mouthparts. This may have influenced our analysis of the clusters that are located in the ventro-medial brain area, such as OA-VUM and DA-4. Second, the lamina was often damaged due to its close attachment to the retina, which had to be removed for laser penetration during imaging procedures. We therefore only included descriptions of lamina innervation from preparations in which this area was not damaged, and excluded the laminas in our estimations

of brain width. Third, the area around the oesophageal foramen was often damaged during decapitation, when the connection between the oesophagus and the remaining digestive tract was severed. This may have caused variation in our analysis of cluster OA-3 in this area.

Distribution of 5HT-L-IR neurons

The 5HT-L-IR staining was very intense and revealed many 5HT-L-IR neuron clusters and neurites (Figure 1). Average diameter of 5HT-L-IR cell bodies was 2.1 ± 0.44 μm (n = 175). Neurites were approximately 0.5 μm in diameter, and varicose terminals approximately 1 μm in diameter.

Cluster 5HT-0 (Figure 2A) is the most anterior serotonergic cell cluster in *T. evanescens*, located directly underneath the frontal cuticle and dorsal to the lobula. We indicate these cell bodies as 5HT-0 because they do not correspond to any of the clusters that are present in *A. mellifera*, and are located more anteriorly than 5HT-1 (Schürmann and Klemm, 1984). The close location to the cuticle resulted in damage of this cluster when the anterior head cuticle was removed. We therefore only analysed this cluster in heads of which the posterior cuticle had been removed. Cluster 5HT-0 invariably consists of two pairs of neurons, with an average diameter of 2.0 ± 0.33 μm (n = 6). The primary neurites of this cluster were not visible.

Cluster 5HT-1 (Figure 2C) is located ventro-lateral to the anterior side of the lobula, and innervates the optic lobes in the same hemisphere. This cluster contains up to six pairs of neurons, on average 4.5 ± 1.04 pairs, with an average diameter of 2.0 ± 0.38 μm (n = 30). Cluster 5HT-2 (Figure 2E) is located lateral to the mushroom body calyx, and contains only a single pair of serotonergic neurons in most preparations. In two preparations, however, respectively two and three pairs were found in this cluster. This results in an average count of 1.1 ± 0.40 neurons per cluster, with an average diameter of 2.1 ± 0.39 μm (n = 30).

Cluster 5HT-3 (Figure 2B) is the most pronounced group of serotonergic cell bodies in *T. evanescens*. These neurons are located posterior and medial to the calyx of the mushroom body and their position is lateral to the ocellar tract, close to the posterior cuticle. They are always well-stained and innervate a large part of the anterior neuropil. We counted up to 16 neuron pairs in this cluster, on average 12.1 ± 1.70 pairs (n = 21), with an average diameter of 2.1 ± 0.48 μm (n = 21). The cell clusters that have been described as 5HT-4 and 5HT-5 in *A. mellifera* (Schürmann and Klemm, 1984) were not observed in *T. evanescens*.

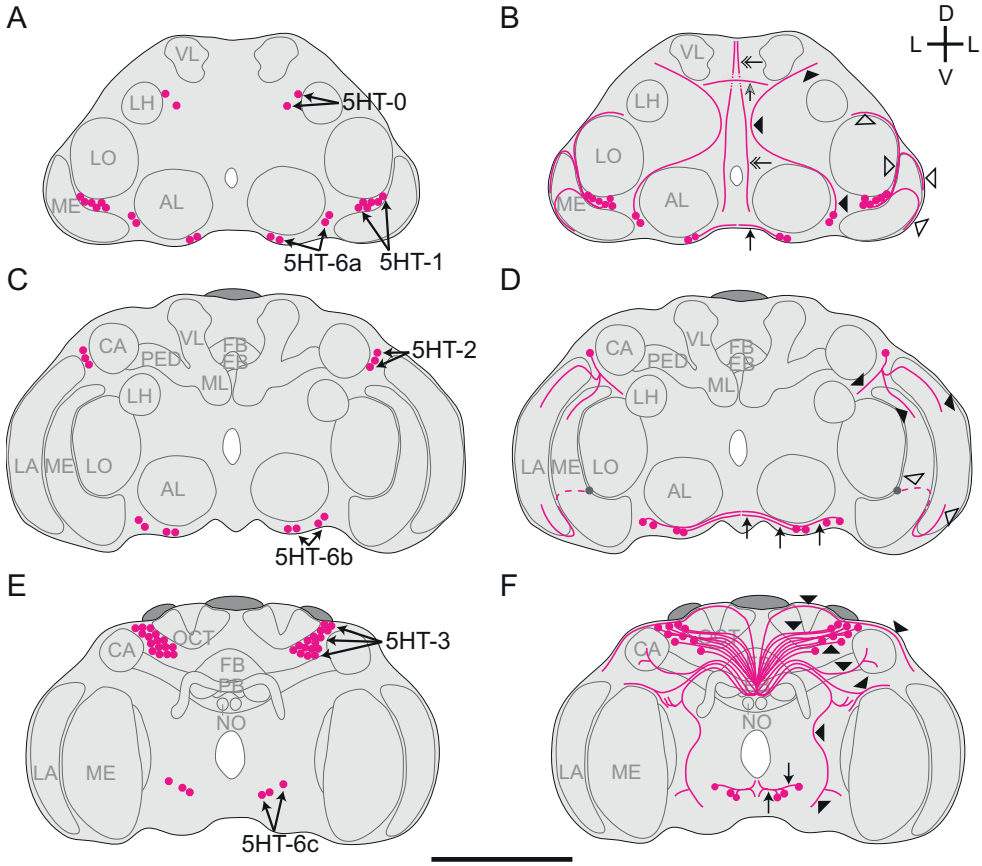

Figure 1. Schematic overview of the location of serotonin-like immunoreactive (5HT-L-IR) cell bodies **(A,C,E)** and projections **(B,D,F)** in the brain of *T. evanescens*, shown dorsal side up at three locations in depth of the brain. **(A-B)** Anterior view at approximately one quarter in depth of the brain. **(A)** Location of clusters 5HT-0, 5HT-1 and 5HT-6a. **(B)** The most anterior neurite (grey arrow) projects in lateral direction from the brain midline. Slightly more posteriorly, a neurite runs in a dorsal direction along the brain midline (feathered arrows). The neurites of the 5HT-1 cluster (open arrowheads) project along the lateral rims of the lobula and medulla. The 5HT-6a neurons on the lateral side of the antennal lobe project in a dorso-posterior direction (black arrowheads), following the brain midline before bending in a more lateral direction towards the dorso-lateral neuropil rim. Neurites of the medial 5HT-6a neurons (black arrow) form a network of fine bifurcations and varicose terminals in the ventro-posterior part of the brain. **(C-D)** Anterior view halfway in depth of the brain. **(C)** Location of clusters 5HT-2 and 5HT-6b. **(D)** The neurites of 5HT-2 (black arrowheads) innervate the medulla and dorso-posterior side of the lamina. The ventro-anterior side of the lamina is innervated by a bifurcation of 5HT-1 (open arrowheads) that projects from the cluster shown in B (grey cell body and dashed line show continuation from B). Neurites of 5HT-6b (black arrows) join the network of bifurcations and varicose

terminals formed by 5HT-6a. **(E-F)** Posterior view three quarters in depth of the brain. **(E)** Location of clusters 5HT-3 and 5HT-6c. **(F)** The projections from the 5HT-3 cell bodies (arrowheads) innervate most neuropil areas. Primary neurites project towards the brain midline and form a dense network. Neurites from this network project in lateral, dorso-anterior and ventro-anterior direction, innervating the mushroom body pedunculus and calyx and projecting towards the optic lobes and antennal lobes. Neurites of 5HT-6c (arrows) join the network of bifurcations and varicose terminals formed by 5HT-6a and 5HT-6b. Bifurcations also project anteriorly and posteriorly. (AL antennal lobe, LA lamina, ME medulla, LO lobula, LH lateral horn, CA calyx, PED pedunculus, VL vertical lobe, ML medial lobe, FB fan-shaped body, EB ellipsoid body, PB protocerebral bridge, NO noduli, OCT ocellar tract, D dorsal, V ventral, L lateral). Scale bar equals 50 μm for an average-sized brain.

Three clusters of 5HT-L-IR cell bodies are present at the ventral rim of the brain, directly ventro-posterior to the antennal lobe and further posteriorly. Their location corresponds to the location of 5HT-6 neurons in *A. mellifera* (Schürmann and Klemm, 1984), which are located in the labial, maxillary and mandibular neuromeres of the suboesophageal zone (Seidel and Bicker, 1996). We could distinguish between three subclusters and named them 5HT-6a, 5HT-6b and 5HT-6c, from anterior to posterior.

The 5HT-6a neurons (Figure 2H) lie directly ventro-posterior to the antennal lobes, where they can be found both on the lateral and medial side of the antennal lobe. We counted up to four pairs of neurons in this cluster, on average 2.3 ± 1.05 (n = 30), with an average diameter of 2.2 ± 0.48 μm. Cluster 5HT-6b (Figure 2H) lies in the ventral rim of the brain, approximately central in depth of the brain. We counted up to four pairs of neurons in this cluster, on average 2.1 ± 0.99 (n = 30), with an average diameter of 2.1 ± 0.41 μm. Cluster 5HT-6c (Figure 2I) is the most posterior cluster in the ventral rim of the brain. We counted up to three pairs of neurons in this cluster, on average 2.1 ± 0.89 (n = 28), with an average diameter of 2.2 ± 0.50 μm.

Projection patterns of 5HT-L-IR neurons

Although 5HT-L-IR neurites are thin (approximately 0.5 μm in diameter), the primary neurites of 5HT-L-IR cell bodies could be traced for all clusters, except 5HT-0. The most anterior neurite projects in lateral direction from the brain midline and gives off varicose terminals dorsal to 5HT-0 cell bodies (Figure 2A). Just posteriorly, a neurite runs in dorsal direction along the brain midline. These anterior neurites could not be traced further, so their origin and destination remain unknown.

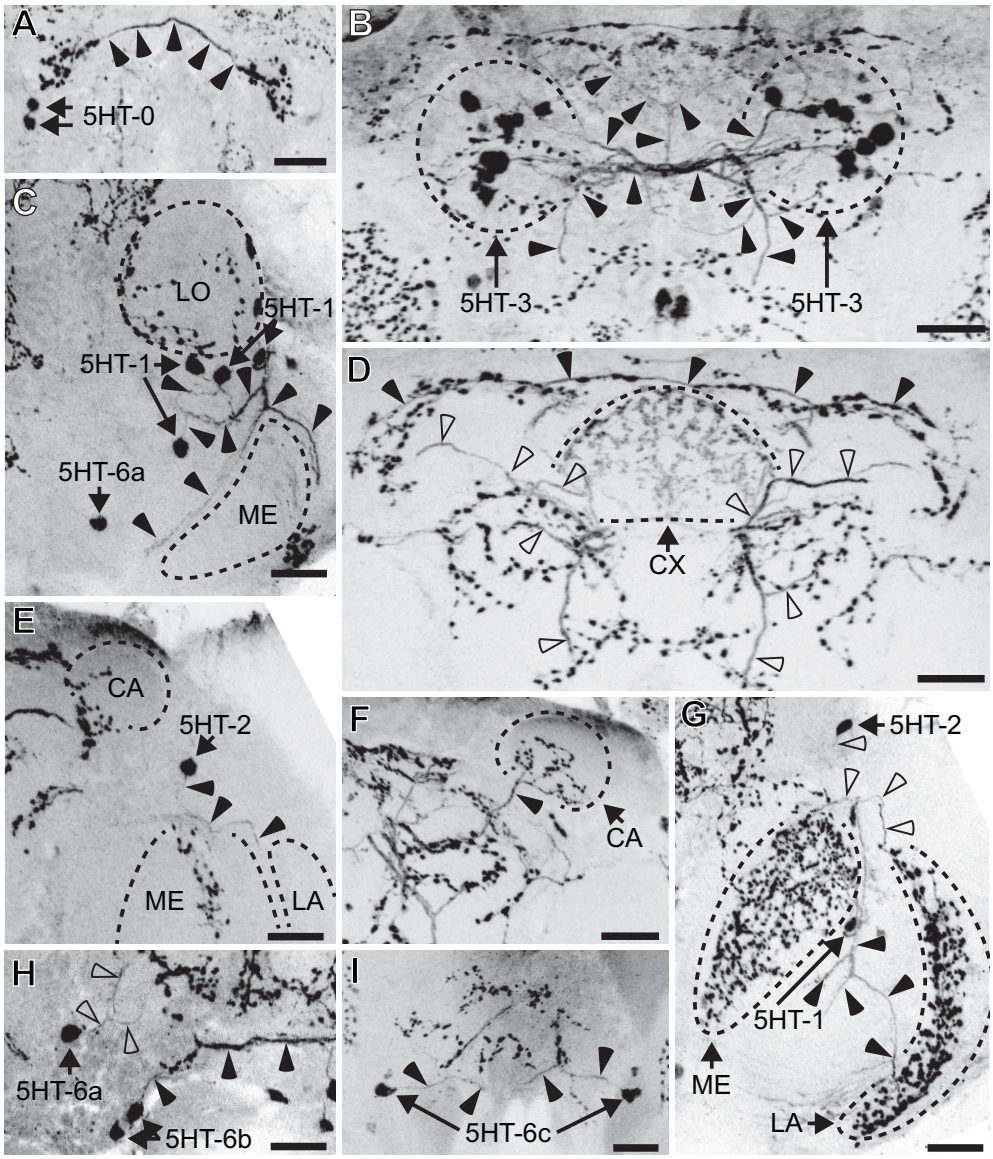

Figure 2. Z-stack projections of confocal images showing serotonin-like immunoreactive (5HT-L-IR) cell bodies and projection patterns in *T. evanescens*. **(A)** Cell cluster 5HT-0 is the most anterior cluster of two neuron pairs (arrows), located directly beneath the anterior cuticle. Arrowheads show the most anterior neurite that projects in lateral direction from the brain midline and gives off varicose terminals dorsal to 5HT-0 cell bodies. **(B)** The most prominent cell cluster in *T. evanescens* is 5HT-3, of up to 16 neuron pairs (arrows). The neurites (arrowheads) project medially and form a network of bifurcations (as indicated in Figure 1F) that project anteriorly and innervate most of the central brain. **(C)** Cell cluster 5HT-1 is located anterior between the lobula (LO) and

medulla (ME) and consists of up to six neuron pairs (arrows). Neurites (arrowheads) from this cluster bifurcate, project along the rim of the medulla and innervate the lamina. **(D)** Overview of the posterior central brain showing the innervation of the central complex (CX), neurites that run along the dorsal rim of the brain (black arrowheads) and neurites from the 5HT-3 network (open arrowheads, also shown in B). **(E)** The single neuron of the cell cluster 5HT-2 (arrow) is located on the lateral side of the mushroom body calyx (CA), and its neurites (arrowheads) innervate the optic lobes. **(F)** Innervation of the mushroom body calyx (CA) by a neurite of the 5HT-3 network (arrowhead). **(G)** Overview of the innervation of the medulla (ME) and lamina (LA), which contain a layered pattern of varicose terminals originating from bifurcations of 5HT-1 (black arrowheads, also shown in C) and 5HT-2 (open arrowheads, also shown in E). **(H)** Neurons of cluster 5HT-6b (up to four neuron pairs, arrows) in the ventral rim of the brain project towards the brain midline (black arrowheads). The lateral 5HT-6a neuron (up to four neuron pairs, arrow) projects in dorsal direction (open arrowheads). **(I)** The most posterior cell cluster is 5HT-6c, of up to three neuron pairs (arrow). Neurites (arrowheads) project medially and join the network of bifurcations of 5HT-6a and 5HT-6b neurons. (LA lamina, ME medulla, LO lobula, CA calyx, CX central complex, D dorsal, V ventral, A anterior, P posterior). Scale bars equal 10 μm, figures are oriented with dorsal side pointing upwards. Contrast of z-stack projections was enhanced in Adobe Photoshop CS6 (San Jose, CA).

The neurites that originate from neurons in clusters 5HT-1 and 5HT-2 innervate the optic lobes. The primary neurites of cluster 5HT-1 (Figure 2C, Figure 2G) project in dorso-posterior direction along the lateral rim of the lobula, and bifurcate at the edge of the medulla. One bifurcation continues along the lateral rim of the lobula in dorso-posterior direction. Two other bifurcations run along the lateral rim of the medulla: one in ventro-anterior direction, and one in ventro-posterior direction. The latter bifurcation innervates the ventro-anterior side of the lamina.

The primary neurite of cluster 5HT-2 (Figure 2E, Figure 2G) projects in ventral direction towards the optic lobes, where it bifurcates into three neurites. One of these continues in ventro-anterior direction along the lateral rim of the medulla. It gives off a dense network of varicose terminals on the posterior side of the medulla. Another bifurcation projects in ventro-posterior direction along the medial rim of the lobula, but could not be traced further. A third bifurcation continues in ventro-posterior direction along the lateral rim of the medulla, and innervates the dorso-posterior side of the lamina. Together with the 5HT-1 bifurcation that innervates the ventro-anterior side of the lamina, it forms a single layer of varicose terminals parallel to the surface of the eye. Compared to the lamina and medulla, the innervation of the lobula is sparse and consists of weakly labelled varicose terminals without a clear pattern. The origin of this innervation could not be traced.

The projections that originate from cluster 5HT-3 (Figure 2B, Figure 2D) are very prominent in *T. evanescens*. These neurites appear to innervate most neuropil areas. The primary 5HT-3 neurites project towards the brain midline, where they form a dense network. Neurites from this network project in lateral, dorso-anterior and ventro-anterior directions. The dorso-anteriorly projecting neurites follow the dorsal neuropil rim in the direction of the optic lobes. The neurite that projects laterally enters the mushroom bodies through the pedunculus and projects towards the calyx, where it bifurcates and gives off many varicose terminals (Figure 2F). The most pronounced neurite from the 5HT-3 neurite network runs in ventro-anterior direction (Figure 1F) and bifurcates close to the dorsal rim of the medulla. One bifurcation continues in the direction of the medulla, but could not be traced further. The other projects ventro-anteriorly in the direction of the posterior side of the antennal lobe, where it bifurcates again. These bifurcations could not be traced further. A second ventro-anteriorly projecting neurite from the 5HT-3 neurite network projects in the direction of the medulla, where it bifurcates on the dorsal side of the medulla. The bifurcations then run along the lateral and medial medulla rim, but could not be traced further.

The central brain contains many small varicose terminals, which appear to mainly originate at neurites of the 5HT-3 network. The only neuropil area that is completely devoid of any 5HT immunoreactivity, is the antennal lobe. Within the central complex, the ellipsoid body and fan-shaped body are clearly visible because they are richly innervated (Figure 2D), in contrast to the protocerebral bridge and noduli. The origin of innervation of the central complex could not be traced.

The 5HT-6a neurons on the lateral side of the antennal lobe project in dorso-posterior direction, following the brain midline before bending in a more lateral direction towards the dorso-lateral neuropil rim. Neurites of the medial 5HT-6a neurons join the neurites of 5HT-6b and 5HT-6c, and together form a network of fine bifurcations and varicose terminals in the ventro-posterior part of the brain (Figure 2H). Besides contributing to this network, the 5HT-6c neurons also bifurcate into a posteriorly and anteriorly projecting neurite. The posteriorly projecting neurite may descend to the thoracic ganglia, but we did not study this. The anteriorly projecting neurite could not be traced further.

Distribution of OA-L-IR neurons

The OA-L-IR staining was clear, but less intense than 5HT-L-IR staining. The

staining revealed many OA-L-IR neuron clusters, and several neurites (Figure 3). Average diameter of OA-L-IR cell bodies was 3.3 ± 0.75 μm (n = 88). Neurites and varicose terminals had average diameters of approximately 0.6 μm.

Cluster OA-1 (Figure 4A) is the most anterior cluster of OA-L-IR neurons. It consists of a single pair of cell bodies, located close to the anterior cuticle with an average diameter of 3.9 ± 0.91 μm (n = 9). Neurons of this pair are approximately 6 – 10 μm apart from each other.

Cluster OA-2 (Figure 4A) also consists of a single pair of OA-L-IR neurons, located directly posterior and ventral to cluster OA-1. Cell bodies of this pair are slightly closer together: approximately 3 – 7 μm. The average diameter of these cells was 3.9 ± 0.76 μm (n = 9).

Cluster OA-3 (Figure 4B) is the most pronounced OA-L-IR neuron cluster in *T. evanescens*. It is located ventro-posterior to cluster OA-2 and directly adjacent to the oesophageal foramen. We counted up to nine neuron pairs, on average 4.7 ± 1.61 (n = 22), with an average diameter of 3.1 ± 0.66 μm (n = 22).

The OA-L-IR cluster in the dorsal rim of the brain, which has been described as OA-4 in *A. mellifera* (Sinakevitch et al., 2005), *Drosophila melanogaster* (Sinakevitch and Strausfeld, 2006) and *N. vitripennis* (Haverkamp and Smid, 2014) was not observed in *T. evanescens*.

Cluster OA-5 (Figure 4C) is located latero-posterior to the antennal lobe. We found up to three pairs of OA-L-IR cell bodies in this cluster, on average 2.1 ± 0.83, with an average diameter of 3.1 ± 0.68 μm (n = 14).

Cluster OA-6 (Figure 4D) consists of a single neuron pair in the ventro-lateral rim of the brain, ventro-posterior to the antennal lobes and medial to the medulla. The average diameter of these cells was 3.5 ± 0.74 μm (n = 11).

Cluster OA-7 (Figure 4D) is the most posterior OA-L-IR neuron cluster, located ventro-lateral to the oesophageal foramen and close to the posterior cuticle. It consists of a single pair of neurons, which are also the smallest octopaminergic neurons with an average diameter of 2.8 ± 0.35 μm (n = 5).

The OA-VUM neurons (Figure 4E) in *T. evanescens* lie at the ventral base of the brain, very close to the mouthparts. This location is vulnerable to damage caused by the dissection procedure, as was described above. We counted up to 13 OA-VUM neurons in two exceptionally well-stained preparations, but on average only 4.4 ± 3.36 neurons were visible (n = 18) with an average diameter of 3.0 ± 0.58 μm (n = 18).

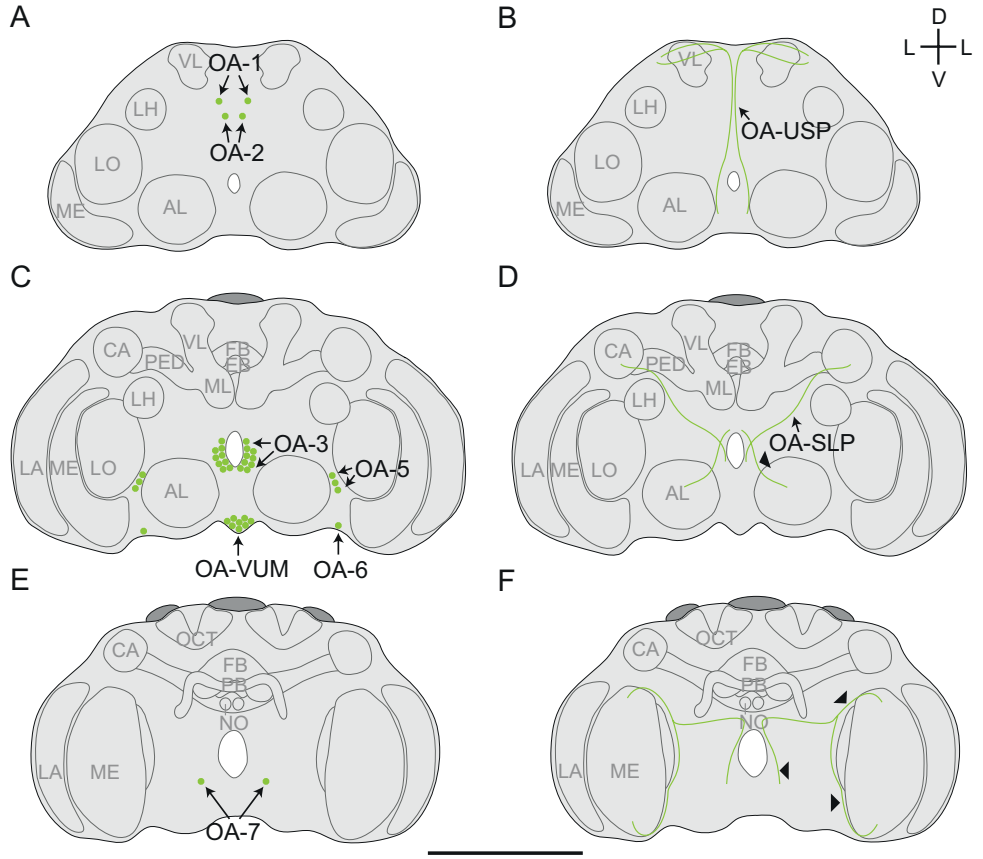

Figure 3. Schematic overview of the location of octopamine-like immunoreactive (OA-L-IR) **(A,C,E)** cell bodies and **(B,D,F)** projections in the brain of *T. evanescens*, shown dorsal side up at three locations in depth of the brain. **(A-B)** Anterior view at approximately one quarter in depth of the brain. **(A)** Location of clusters OA-1 and OA-2. **(B)** The umbrella-shaped projection (OA-USP, arrow) originates at the ventro-medial side of the brain, and runs in dorsal direction along the brain midline. It passes the posterior side of the OA-3 cluster and bifurcates at the dorso-posterior side of the brain. **(C-D)** Anterior view halfway in depth of the brain. **(C)** Location of clusters OA-3, OA-5, OA-6 and OA-VUM. **(D)** Several neurites form a network that surrounds the oesophageal foramen. The most anterior neurite from this network (arrowhead) projects laterally and innervates the antennal lobe. The stag-like projection (OA-SLP, arrow) projects in dorso-lateral direction and innervates the mushroom body calyx. **(E-F)** Posterior view three quarters in depth of the brain. **(E)** Location of cluster OA-7. **(F)** The optic lobes are innervated by a posterior neurite (arrowheads) that bifurcates into a neurite that innervates the dorso-posterior side of the medulla, and a neurite that projects anteriorly along the medial rim of the lobula and innervates the ventro-anterior side of the medulla. (AL antennal lobe, LA lamina, ME medulla, LO lobula, LH lateral horn, CA calyx, PED pedunculus, VL vertical lobe, ML medial lobe, FB fan-shaped body, EB ellipsoid body, PB protocerebral bridge, NO noduli, OCT ocellar tract, D dorsal, V ventral, L lateral). Scale bar equals 50 μm for an average-sized brain.

Projection patterns of OA-L-IR neurons

The connections of OA-L-IR neurites to their corresponding cell bodies were mostly invisible, but some projections into neuropil areas could be distinguished. The most pronounced neurite (Figure 4J) in our preparations was a projection that appears similar to the umbrella-shaped projection (OA-USP) that has previously been described for *Nasonia* (Haverkamp and Smid, 2014). This neurite originates at the ventro-medial side of the brain, but a connection with cell bodies was not visible. It passes very close to the posterior side of the OA-3 cluster, and then projects in dorsal direction along the brain midline, close to the oesophageal foramen. The neurite bends at the dorso-posterior side of the brain, and runs in ipsilateral direction where it bifurcates (Figure 4F) and continues in the direction of (but could not be observed to innervate) the mushroom bodies.

Several neurites form a network that surrounds the oesophageal foramen. The origin of these neurites could not be traced, but they are located close to clusters OA-3 and OA-VUM and may therefore originate at these clusters. Neurites from this network innervate the antennal lobe, the mushroom bodies and the optic lobes. The most anterior neurite from this network projects laterally and innervates the antennal lobe at its posterior side (Figure 4J). Another neurite from the anterior side of the network projects dorso-laterally and innervates the mushroom body calyx. This neurite resembles the stag-like projection (OA-SLP) that was described for *Nasonia* (Haverkamp and Smid, 2014). It is less pronounced than OA-USP and too faint to catch in z-stack projections.

The optic lobes are innervated by a neurite that projects from the ventro-anterior to the dorso-posterior side of the oesophageal foramen (Figure 3F). Close to the posterior cuticle, the neurite bends and projects laterally towards the optic lobes. It bifurcates into a neurite that innervates the dorso-posterior side of the medulla, and a neurite that follows the medial rim of the lobula in anterior direction and innervates the ventro-anterior side of the medulla. Two distinct layers of sparsely distributed varicose terminals are visible in the medulla (Figure 4G).

There is little variation in the density of OA-L-IR varicose terminals across the different neuropil areas. The overall density of these terminals is lower than the density of 5HT-L-IR varicose terminals, but not a single neuropil area is completely devoid of OA-like immunoreactivity. In the antennal lobes, the density of varicose terminals is higher in the centre than at the rim. Specific innervation of antennal lobe substructures, such as glomeruli, could not be analysed in these preparations.

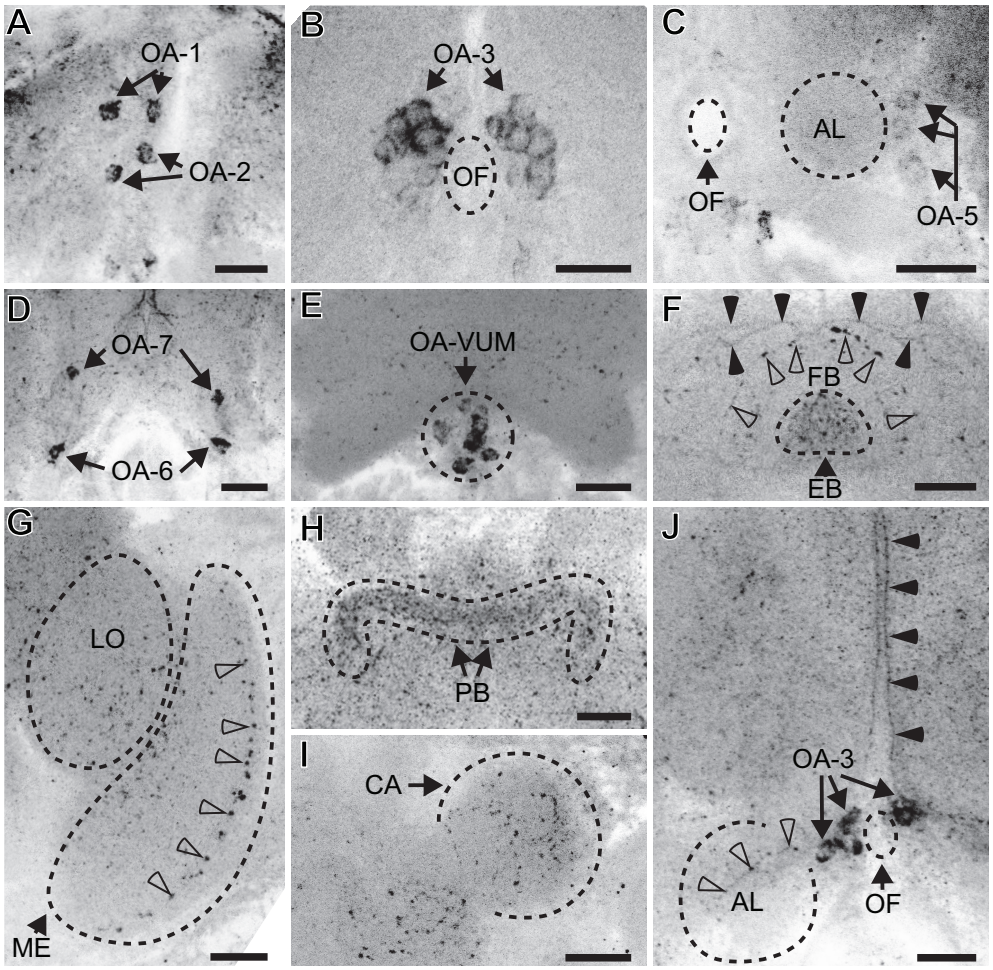

Figure 4. Z-stack projections of confocal images showing octopamine-like immunoreactive (OA-L-IR) cell bodies and projection patterns in *T. evanescens*. **(A)** OA-1 consists of a single pair of neurons (arrows), and is located directly beneath the anterior cuticle, close to the brain midline. Cluster OA-2 also consists of a single pair of neurons (arrows) and is located directly ventro-posterior to OA-1. **(B)** Cluster OA-3 (arrows, also shown in J) consists of up to nine neuron pairs and is located directly adjacent to the oesophageal foramen (OF). **(C)** Cluster OA-5 (arrows) consists of up to three neuron pairs and is located latero-posterior to the antennal lobe. **(D)** Cluster OA-6 (arrows) contains a single neuron pair at the lateral part of the ventral rim of the brain, and cluster OA-7 (arrows) is located more posteriorly ventro-lateral to the oesophageal foramen and also contains a single neuron pair. **(E)** Cluster OA-VUM (arrows) lies at the ventro-medial base of the brain and contains up to 13 unpaired neurons. **(F)** An arch of varicose terminals (open arrowheads) outlines the dorsal rim of the fan-shaped body (FB). The ellipsoid body (EB) contains a high density of varicose terminals. Dorsal to the fan-shaped body, the umbrella-shaped projection (OA-USP, black arrowheads)

bifurcates and projects laterally. **(G)** OA-like immunoreactivity in the lobula (LO) and medulla (LO). Arrowheads show a layer of varicose terminals in the medulla. **(H)** The protocerebral bridge (PB) is clearly visible due to a high density of varicose terminals. **(I)** The mushroom body calyx (CA) is contains several OA-L-IR varicose terminals. **(J)** Cluster OA-3 (arrows, also shown in B) may contribute neurites to the neurite network around the oesophageal foramen (OF). A neurite of this network projects towards the antennal lobes (AL, open arrowheads). The umbrella-shaped projection (OA-USP, black arrowheads) originates at the ventral side of the brain and projects in dorsal direction along the brain midline. (AL antennal lobe, LA lamina, ME medulla, LO lobula, CA calyx, OF oesophageal foramen, PB protocerebral bridge, FB fan-shaped body, EB ellipsoid body). Scale bars equal 10 μm, figures are oriented with dorsal side pointing upwards. Contrast of z-stack projections was enhanced in Adobe Photoshop CS6 (San Jose, CA).

The central complex shows pronounced varicose terminals, especially in the ellipsoid body (Figure 4F). This high density of varicose terminals makes the ellipsoid body stand out from the surrounding tissue. An arch of varicose terminals surrounds the central complex dorsal to the fan-shaped body (Figure 4F). The protocerebral bridge is also clearly visible due to a high density of varicose terminals (Figure 4H). There are several varicose terminals in the centre and rim of the mushroom body calyx (Figure 4I), whereas the mushroom body lobes cannot be distinguished from the surrounding neuropil tissue due to similarities in the intensity of background staining.

Distribution of DA-L-IR neurons

The DA-L-IR staining was less intense than the 5HT-L-IR staining. Many DA-L-IR neuron clusters were visible, but only few neurites (Figure 5). The average diameter of DA-L-IR cell bodies was 2.3 ± 0.38 μm (n = 160). Neurites and varicose terminals were approximately 0.5 μm in diameter. The orientation of dopaminergic neurons in *T. evanescens* differs from the descriptions in *A. mellifera* (Schafer and Rehder, 1989; Schürmann et al., 1989) and *D. melanogaster* (Nässel and Elekes, 1992; Monastirioti, 1999; Mao and Davis, 2009). Our numbering of cell clusters does, therefore, not correspond to the numbering that was used for those species.

Cluster DA-1 (Figure 6A) is the most anterior cell cluster, located latero-anteriorly in the central brain, directly underneath the frontal cuticle. We counted up to 5 pairs of neurons in this cluster. On average 2.6 ± 0.89 (n = 27) neurons were present, with an average diameter of 2.5 ± 0.33 μm (n = 27). Cell bodies of this cluster are somewhat scattered, located 3 – 16 μm apart from each other.

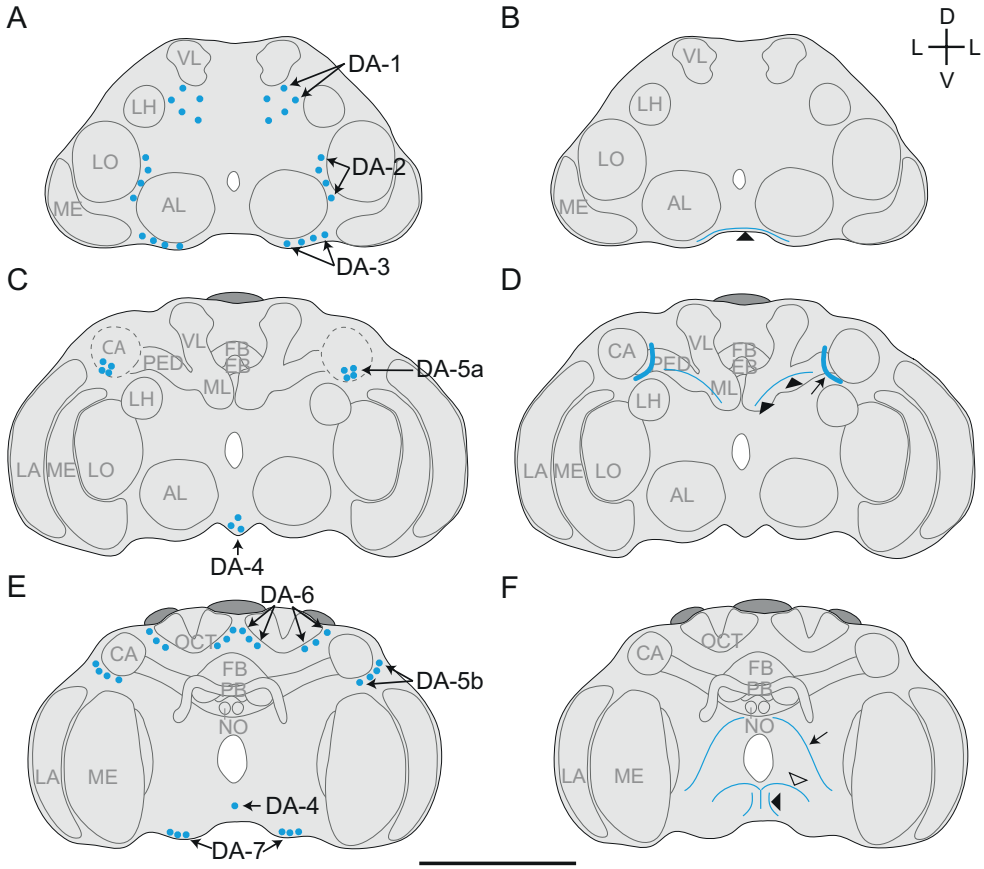

Figure 5. Schematic overview of the location of dopamine-like immunoreactive (DA-L-IR) **(A,C,E)** cell bodies and **(B,D,F)** projections in the brain of *T. evanescens*, shown dorsal side up at three locations in depth of the brain. **(A-B)** Anterior view at approximately one quarter in depth of the brain. **(A)** Location of clusters DA-1, DA-2 and DA-3. **(B)** A small network of neurites (arrowhead) project in medial direction along the ventral rim of the brain. **(C-D)** Anterior view halfway in depth of the brain. **(C)** Location of clusters DA-4 and DA-5a. Cluster DA-5a is located anterior to the calyx (CA, shown by dashed outline). **(D)** A thick bundle of DA-L-IR fibres (arrow) runs anteriorly to the mushroom body pedunculus and medially to the calyx. A single neurite (arrowheads) projects along the pedunculus in the direction of the calyx. **(E-F)** Posterior view three quarters in depth of the brain. **(E)** Location of clusters DA-4, DA-5b, DA-6 and DA-7. **(F)** A DA-L-IR neurite (arrow) projects ventro-laterally from the dorsal side of the oesophageal foramen to the ventral side of the oesophageal foramen. A single neurite (open arrowhead) projects dorsally along the brain midline and bifurcates just ventral to the oesophageal foramen. The most posterior neurite (black arrowhead) projects dorsally from the ventral rim of the brain, and may innervate the thoracic ganglia. (AL antennal lobe, LA lamina, ME medulla, LO lobula, LH lateral horn, CA calyx, PED pedunculus, VL vertical lobe, ML medial lobe, FB fan-shaped

body, EB ellipsoid body, PB protocerebral bridge, NO noduli, OCT ocellar tract, D dorsal, V ventral, L lateral). Scale bar equals 50 μm for an average-sized brain.

Cluster DA-2 (Figure 6A) lies posterior to cluster DA-1, medial to the lobula and dorso-lateral to the antennal lobes. It consists of up to four pairs of neurons, and on average 2.3 ± 0.86 (n = 28). Their average diameter was 2.3 ± 0.35 μm (n = 28).

Cluster DA-3 (Figure 6A) is located in the ventral rim of the brain, ventral to the antennal lobes. We counted up to four pairs of neurons in this cluster, and on average 2.7 ± 0.66 (n = 29). Their diameter was 2.0 ± 0.24 μm (n = 29).

Cluster DA-4 (Figure 6A) is located medially in the ventral rim of the brain, at an approximately similar location as OA-VUM. This cluster consists of up to four unpaired neurons. Sometimes one of these unpaired neurons is located more posteriorly, and we consider this part of the same cluster because this neuron is unpaired and occurs in the same ventro-medial location. On average 2.5 ± 0.82 (n = 25) neurons were present, with an average diameter of 2.5 ± 0.49 μm (n = 25).

Cluster DA-5 is located ventral and posterior to the lateral rim of the calyx, and dorsal to the lobula. It consists of up to eight pairs of neurons, and on average 3.9 ± 2.16 (n = 28). Average diameter of these neurons was 2.2 ± 0.33 μm (n = 28). This cluster appears to consist of two subclusters, indicated as DA-5a (Figure 6C) and DA-5b (Figure 6E). Cell bodies of DA-5a are oriented in a cluster ventro-anterior to the calyx. Slightly more posteriorly, cell bodies of cluster DA-5b are oriented in a dorso-ventral line at the lateral rim of the calyx. The two subclusters are located very close together, and we therefore do not distinguish between them in our analyses.

Cluster DA-6 (Figure 6D) is located posterior to the calyx and the central complex. Cell bodies of this cluster are positioned on the medial and lateral sides of the ocellar tract. We counted up to six pairs of neurons in this cluster, on average 3.2 ± 1.74 (n = 13), with an average diameter of 2.3 ± 0.32 μm (n = 13).

Cluster DA-7 (Figure 6F) is the most posterior dopaminergic cell cluster, located in the ventro-posterior rim of the brain. This cluster contained up to three pairs of neurons, on average 1.4 ± 0.70 (n = 10). Average diameter of these neurons was 2.4 ± 0.26 μm (n = 10).

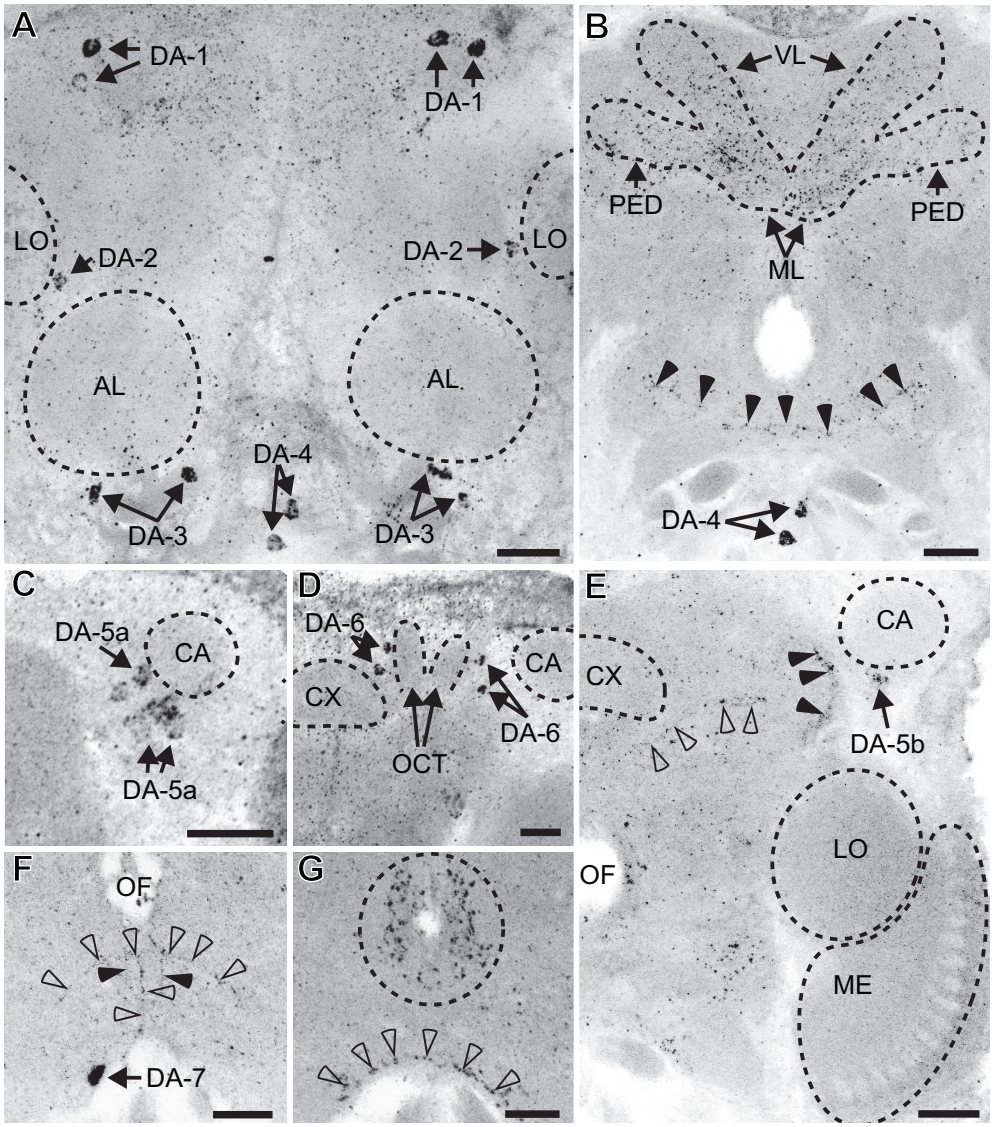

Figure 6. Z-stack projections of confocal images showing dopamine-like immunoreactive (DA-L-IR) cell bodies and projection patterns in *T. evanescens*. **(A)** Cluster DA-1 (up to five neuron pairs, arrows) is located in the latero-anterior central brain. Cluster DA-2 (up to four neuron pairs, arrows) is located medial to the lobula (LO) and dorso-laterally from the antennal lobe (AL). Cluster DA-3 (up to four neuron pairs, arrows) is located ventral to the AL. Cluster DA-4 (up to four unpaired neurons, arrows) is located medial in the ventral rim of the brain. **(B)** The pedunculus (PED), medial lobes (ML) and vertical lobes (VL) of the mushroom bodies show higher densities of varicose terminals than the surrounding neuropil. Arrowheads show a small anterior network of neurites that project in medial direction, dorsal to DA-4 (arrows). **(C)** Cluster DA-5 consists of up to eight neuron pairs (arrows), of which subcluster DA-5a is located on the ventro-

anterior side of the calyx (CA) and dorsal to the medulla (ME). **(D)** Cluster DA-6 (up to six neuron pairs, arrows) are located on the medial side of the CA, and surround the ocellar tract (OCT). **(E)** The calyx and optic lobes are the only neuropils that are devoid of DA-like immunoreactivity. Subcluster DA-5b (arrow) is located on the ventro-lateral side of the calyx. Black arrowhead shows the location of the neurite bundle that occurs on the ventro-medial side of the calyx, open arrowheads show the neurite that follows the pedunculus in the direction of the calyx. **(F)** Cluster DA-7 consists of up to three neuron pairs (arrow), located posterior in the ventral rim of the brain. The most posterior neurite runs parallel to the brain midline from the ventral rim of the brain in the direction of the oesophageal foramen (black arrowheads). Medial to this neurite, another neurite (open arrowheads) follows the brain midline and bifurcates just ventral to the oesophageal foramen. **(G)** Varicose terminals surround the oesophageal foramen (outlined area) and are present in the ventral rim of the brain (arrowheads). (AL antennal lobe, LA lamina, ME medulla, LO lobula, CA calyx, PED pedunculus, VL vertical lobe, ML medial lobe, CX central complex, OCT ocellar tract). Scale bars equal 10 μm, figures are oriented with dorsal side pointing upwards. Contrast of z-stack projections was enhanced in Adobe Photoshop CS6 (San Jose, CA).

Projection patterns of DA-L-IR neurons

Projections of DA-L-IR neurons were sparsely visible. The connections of the neurites to the corresponding cell bodies could not be traced in any of the clusters. The most pronounced DA-like immunoreactivity was found at the ventral base of the mushroom body calyx, where a bundle of DA-L-IR fibres (approximately 1.4 μm in diameter) is located anterior to the mushroom body pedunculus and medial to the calyx (Figure 6E). It is closely located to cluster DA-5, but we could not observe a connection. Close to this bundle, a single neurite appears to project dorso-laterally in the direction of the calyx (Figure 5D).

On the anterior side of the brain, there is a small network of neurites that project in medial direction through the ventral rim of the brain (Figure 6B). These neurites are located ventro-posterior to the antennal lobes and medial to the neurons of the DA-3 cluster. Although these neurites may originate from the DA-3 neurons, this could not be observed.

The most posterior neurite runs parallel to the brain midline, from the ventral rim of the brain in the direction of the oesophageal foramen (Figure 6F). This neurite may innervate the thoracic ganglia. Medial to this neurite, another neurite follows the brain midline and bifurcates just ventrally to the oesophageal foramen (Figure 6F). The bifurcations bend and project in ventro-lateral direction, where they could not be traced further. Another neurite projects ventro-laterally from the dorsal side of the oesophageal foramen (ventro-posterior to the medial

mushroom body lobe) to the ventral side of the oesophageal foramen (Figure 5F). This neurite could not be traced further. Neurites innervating other major neuropil areas (i.e. optic lobes, antennal lobes, lateral horn and central complex) were not visible.

The density of DA-L-IR varicose terminals is lower than the densities of 5HT- and OA-L-IR terminals. The entire brain appears equally innervated by similar, low levels of varicose terminals. Only the mushroom body calyces and optic lobes appear to be completely devoid of varicose terminals (Figure 6E). Higher densities of varicose terminals are visible in the pedunculus, and medial and vertical lobes of mushroom bodies (Figure 6B), and in the ventro-posterior part of the brain (in the ventral rim of the brain and surrounding the oesophageal foramen; Figure 6G).

Discussion

Our study provides a first description of the morphology of 5HT-, OA-, and DA-L-IR neurons in the brains of the minute parasitic wasp *T. evanescens*. In the sections below, we show that these miniaturized brains contain comparable numbers of monoaminergic neurons as much larger insects; i.e. *A. mellifera*, *D. melanogaster* and larger parasitic wasps of the genera *Nasonia* and *Cotesia*. Some neuron clusters in *T. evanescens* contain similar numbers of neurons as comparable clusters in larger insects, others contain fewer neurons and others are entirely absent. The 5HT-L-IR neuron clusters appear to be especially conserved in complexity. Some 5HT-L-IR clusters that are present in other insects are absent in *T. evanescens*, but most of the remaining clusters contain a similar number of neurons as in other species. There are more differences between the OA-L-IR neuron clusters of *T. evanescens* and larger insects, although the distribution and number of OA-L-IR neurons is very similar to descriptions of the related parasitic wasps of the genus *Nasonia*. The complexity of DA-L-IR neuron clusters appears to be severely reduced compared to other insects. We will elaborate on the differences in distribution, number and size of the neurons between *T. evanescens* and other insects in the following sections.

Immunohistochemistry

The OA-L-IR staining was less intense in *T. evanescens* than in a previous study of the larger parasitic wasps of the genus *Nasonia* (Haverkamp and Smid, 2014),

despite large similarities in methodologies of these two studies. The lower intensity in *T. evanescens* may relate to the small size of neuronal cell bodies and neurites in this wasp, and the thin optical sections that were required to accurately visualize these. This indicates that studying the smallest neurons in miniaturized species such as *T. evanescens* is technically challenging.

The 5HT-L-IR staining was more intense than OA- and DA-L-IR staining in our study. There may be more 5HT present in the brains than OA and DA, although titres of DA are much higher than titres of OA and 5HT in the brains of honeybees, bumblebees and ants (Harris and Woodring, 1992; Bloch et al., 2000; Cuvillier-Hot and Lenoir, 2006). Methodological differences could provide alternative explanations for the higher detectability of 5HT than OA and DA. The methods to visualize OA and DA used a glutaraldehyde-based fixative, which crosslinks proteins more strongly than the formaldehyde-based fixative used for 5HT-like immunoreactivity (Hopwood, 1967). Strong crosslinking could have reduced permeability of the tissues and partially masked antigens in a more severe way than occurred during the procedures to visualize 5HT. Furthermore, antibodies against OA and DA do not bind the oxidized form of their target amines, whereas this problem does not occur for antibodies against 5HT. Although we used sodium borohydride to reduce oxidized forms, it is not clear how effective this method is.

Antibodies against enzymes that are involved in the biosynthesis of OA and DA may provide complementary data to aid identification of OA- and DA-L-IR neurons. Antibodies against tyramine beta-hydroxylase have been used successfully to reveal OA-like immunoreactivity (Monastirioti et al., 1996; Koon et al., 2011; Wu et al., 2013), and antibodies against tyrosine hydroxylase have been used for DA-like immunoreactivity (Nässel and Elekes, 1992; Mao and Davis, 2009). Using these antibodies may enhance the detection of OA and DA in future studies in *T. evanescens*.

Distribution and projections of 5HT-L-IR neurons

We counted up to 38 5HT-L-IR neuron pairs in *T. evanescens* (Table 1). This is comparable to the number of 5HT-L-IR neuron pairs in *D. melanogaster*, where up to 41 neuron pairs were counted (Sitaraman et al., 2008). More neuron pairs were observed in *A. mellifera*: approximately 75 (Schürmann and Klemm, 1984). The difference in number of 5HT-L-IR neurons between *T. evanescens* and *A. mellifera* is partially caused by clusters 5HT-4 and 5HT-5. These were not visible in *T. evanescens*, but contain up to 24 neuron pairs in *A. mellifera*. Cluster

Table 1. Comparison of monoaminergic neurons between *T. evanescens* and larger insects. Shown are total number and diameter of serotonin-like immunoreactive (5HT-L-IR) cell bodies, octopamine-like immunoreactive (OA-L-IR) cell bodies and dopamine-like immunoreactive (DA-L-IR) cell bodies. Diameters are shown as average values or as reported total range.

	T. evanescens (this study)	*A. mellifera*	*D. melanogaster*	*N. vitripennis* and *N. giraulti*
5HT-L-IR	38 pairs	75 pairs [a]	41 pairs [e]	-
	2.1 ± 0.4 µm	8 – 30 µm [a]		-
OA-L-IR	16 pairs 13 unpaired	80 pairs [b] 14 unpaired [c]	41 pairs 26 unpaired [f]	24 pairs 12 – 14 unpaired [i]
	3.3 ± 0.8 µm	8 – 45 µm [b]	5 – 10 µm [f]	6 – 11 µm [i]
DA-L-IR	30 pairs 4 unpaired	119 pairs [d]	282 pairs [g] 2 unpaired [h]	-
	2.3 ± 0.4 µm	8 – 30 µm [d]	-	-

Data from: [a] Schürmann and Klemm, 1984; [b] Sinakevitch et al., 2005; [c] Schroter et al., 2007; [d] Schürmann et al., 1989; [e] Sitaraman et al., 2008; [f] Sinakevitch and Strausfeld, 2006; [g] Mao and Davis, 2009; [h] Budnik and White, 1988; [i] Haverkamp and Smid, 2014.

5HT-1 explains the remaining difference; this cluster contains up to 30 neuron pairs in *A. mellifera*, but only up to six in *T. evanescens*. In *D. melanogaster*, this cluster contains up to twice as many neurons as in *T. evanescens*. All other clusters contain an approximately equal number of neuron pairs in *T. evanescens*, *A. mellifera* and *D. melanogaster*. These striking similarities in neuron numbers indicate that the 5HT-L-IR neuron clusters in *T. evanescens* are very conserved compared to other insects.

The distribution pattern of 5HT-L-IR neuron clusters in *T. evanescens* largely corresponds to the pattern in *A. mellifera* and *D. melanogaster* (Schürmann and Klemm, 1984; Monastirioti, 1999; Blenau and Thamm, 2011), but there were some differences, which we describe in detail in the Supplementary Information.

Distribution and projections of OA-L-IR neurons

We counted up to 16 OA-L-IR neuron pairs, and up to 13 unpaired OA-L-IR neurons in the brain of *T. evanescens*. The number of paired OA-L-IR neurons is larger in other insects (Table 1). On average 24 OA-L-IR neuron pairs were

present in the *Nasonia* brain (Haverkamp and Smid, 2014), 41 in *D. melanogaster* (Sinakevitch and Strausfeld, 2006), and up to 80 in *A. mellifera* (Sinakevitch et al., 2005). This difference in number of neurons between *T. evanescens* and other insects is partially caused by differences in the number of neurons per cluster, and partially by differences in the number of clusters that are present in these species. The clusters that were observed in both *T. evanescens* and *Nasonia* contained equal numbers of neurons in both species. In contrast, almost all paired clusters in *A. mellifera* and *D. melanogaster* contain more neurons than in *T. evanescens*. However, there was a remarkable similarity in the number of OA-VUM neurons in *T. evanescens* and other hymenopterans. We counted up to 13 OA-VUM neurons in two well-stained *T. evanescens* brains, which is comparable to *A. mellifera* (14 neurons; Schroter et al., 2007), *Nasonia* wasps (12 – 14 neurons; Haverkamp and Smid, 2014) and *Cotesia* wasps (14 – 20 neurons; Bleeker et al., 2006).

The distribution pattern of OA-L-IR neuron clusters in *T. evanescens* largely corresponds to previous findings in the parasitic wasps *Nasonia vitripennis* and *Nasonia giraulti* (Haverkamp and Smid, 2014). These similarities could be explained by the close relation of these parasitic wasps; they both belong to the superfamily Chalcidoidea. The distribution of OA-L-IR neuron clusters in *T. evanescens* is also very similar to the distribution in *A. mellifera* (Kreissl et al., 1994; Sinakevitch et al., 2005) and *D. melanogaster* (Sinakevitch and Strausfeld, 2006; Busch et al., 2009). Mostly the same clusters are present in the three species, but they occur at slightly different locations, in more subclusters and with more neurons per cluster in *A. mellifera* and *D. melanogaster*. A full comparison of the distribution of OA-L-IR neurons between *T. evanescens* and other insects can be found in the Supplementary Information.

Distribution and projections of DA-L-IR neurons

The most striking difference in DA-like immunoreactivity between *T. evanescens* and other insects is the difference in the total number of DA-L-IR neurons. We counted up to 30 paired and four unpaired DA-L-IR neuron pairs in *T. evanescens*, whereas much higher numbers were observed in other insects (Table 1). *Apis mellifera* has up to 119 DA-L-IR neuron pairs (Schürmann et al., 1989), and *Calliphora erythrocephala* and *Phormia terraenovae* blowflies up to 152 DA-L-IR neuron pairs (Nässel and Elekes, 1992). An antibody against tyrosine hydroxylase, a precursor of dopamine, revealed 282 immunoreactive neuron pairs in the protocerebrum of *D. melanogaster* (Mao and Davis, 2009). Most DA-

L-IR neurons were observed in the locust *Schistocerca gregaria*: up to 127 neurons in the midbrain, and more than 3000 in the optic lobes (Wendt and Homberg, 1992).

We expected that the distribution of DA-L-IR neuron clusters in *T. evanescens* would be similar to the distribution of DA-L-IR clusters in other insects, especially those of other hymenopterans. However, the distribution of dopaminergic neurons in *T. evanescens* differs much from the distribution in *A. mellifera* (Schafer and Rehder, 1989; Schürmann et al., 1989), *C. erythrocephala* and *P. terraenovae* blowflies (Nässel and Elekes, 1992), *D. melanogaster* (Budnik and White, 1988; Monastirioti, 1999; Mao and Davis, 2009) and locusts (Wendt and Homberg, 1992). Comparison to other insects is further complicated by the lack of connections of DA-L-IR neurites to cell bodies in *T. evanescens*. This obstructed the identification of similarities in neuron clusters across insects based on similarities in the areas they innervate. A different antibody, for example against tyrosine hydroxylase, might reveal more DA-like immunoreactivity and aid the comparison with other species. A full comparison of the distribution of DA-L-IR neurons between *T. evanescens* and other insects can be found in the Supplementary Information.

Neuron numbers in comparison with other insects

Overall, our study shows that miniaturized *T. evanescens* brains contain comparable numbers of monoaminergic neurons as much larger insects (Table 1). This is surprising, given the difference in total number of neurons between *T. evanescens* and larger insects. For example, the total number of neurons in the brains of *A. mellifera* has been estimated to be around 960,000 (Menzel and Giurfa, 2001). This is approximately 26 times more than the 37,000 neurons that were estimated to be present in the brains of *T. evanescens* (Makarova and Polilov, 2013). However, when comparing the number of monoaminergic neurons of *T. evanescens* to *A. mellifera*, much smaller differences are found. *Apis mellifera* have only approximately twice as many 5HT-L-IR neurons (Schürmann and Klemm, 1984), 3.5 times as many DA-L-IR neurons (Schürmann et al., 1989) and five times as many OA-L-IR neurons (Sinakevitch et al., 2005). This indicates that a certain level of neural complexity is required to preserve the performance of the monoaminergic neurons. Maintaining such a high level of complexity may have been enabled by more extreme reductions in numbers of other types of neurons, and by miniaturization of neuron size (on which we elaborate in the section below).

Of the three types of monoaminergic neurons that we studied, the 5HT-L-

IR neuron clusters appear to be most conserved. The comparison of 5HT-L-IR neuron counts shows a striking similarity in number of neurons in all clusters that are present in *T. evanescens* and other insects, except for 5HT-1. This conserved distribution of 5HT-L-IR neurons indicates that modifications to these clusters could compromise vital physiological functions. Differences in total cell count of 5HT-L-IR neurons between *T. evanescens* and other insects are mostly caused by clusters that are lacking in *T. evanescens* and present in other insects, and a difference in neuron number of the cluster that innervates the optic lobes; 5HT-1. In *A. mellifera*, this cluster contains approximately five-fold more neuron pairs than in *T. evanescens*, and in *D. melanogaster* this cluster contains approximately two-fold more neuron pairs than in *T. evanescens*. The optic lobes have a strong columnar structure, which relates to the organization of ommatidia in the compound eyes (Paulk et al., 2013). The number of 5HT-L-IR neurons that modulate functioning of the optic lobes may directly relate to the size of the eye and number of ommatidia. Hence, the differences in numbers of ommatidia between *T. evanescens* (approximately 128; Fischer et al., 2011), *D. melanogaster* (approximately 750; Paulk et al., 2013) and *A. mellifera* (approximately 4500; Srinivasan, 2010), may underlie the difference in numbers of 5HT-1 neurons between these insects.

The OA-L-IR neuron clusters appear to be less conserved than the 5HT-L-IR clusters, although there were large similarities in the number of neurons in those OA-L-IR neuron clusters that were present in both *T. evanescens* and the related parasitic wasp *Nasonia*. Only two clusters that were visible in *Nasonia* were absent in *T. evanescens*: OA-0 and OA-4. Almost all paired OA-L-IR clusters in *A. mellifera* and *D. melanogaster* contain more neurons than in *T. evanescens* and *Nasonia*, except clusters OA-3 and OA-VUM. Cluster OA-3 was the only paired OA-L-IR neuron cluster that consists of an approximately equal number of neurons in *T. evanescens*, *Nasonia* (Haverkamp and Smid, 2014), *Cotesia* (Bleeker et al., 2006), *A. mellifera* (Sinakevitch et al., 2005), and *D. melanogaster* (Busch et al., 2009). The number of OA-VUM neurons in *T. evanescens* is similar to the number of OA-VUM neurons that were described in other hymenopterans: i.e. *A. mellifera* (Schroter et al., 2007), *Nasonia* (Haverkamp and Smid, 2014) and *Cotesia* (Bleeker et al., 2006).

The large similarity in numbers of neurons in OA-3 and OA-VUM in *T. evanescens* and other insects indicates that adequate functioning requires a conserved number of neurons, despite large differences in brain size. Neurites of cluster OA-3 and OA-VUM could contribute to the network of neurites around the oesophageal foramen, and they may have vital functions for the neuropil areas that they

innervate (i.e. optic lobes, mushroom bodies and antennal lobes). Furthermore, OA-VUM neurons are important in the neural processing pathways that lead to memory formation in insects (Hammer and Menzel, 1995; Schroter et al., 2007). The conservation of OA-VUM neuron numbers among hymenopterans has been hypothesized to be related to the complex learning abilities that are required for a parasitic life style (Haverkamp and Smid, 2014), which evolved at the base of the Euhymenoptera (Whitfield, 2003; Farris and Schulmeister, 2011). The conserved number of OA-VUM neurons in bees and wasps, including the miniaturized *T. evanescens* with a ~2500× smaller brain volume than *A. mellifera* (Mares et al., 2005; Chapter 2), supports this hypothesis.

The DA-L-IR neuron clusters appear to be least conserved of the three monoaminergic systems that we studied. There was a large difference in distribution of DA-L-IR neurons between *T. evanescens* and other insects, and most clusters can therefore not be directly compared. Furthermore, the total number of DA-L-IR neurons is much higher in other insects. This may indicate that a severe modification of the dopaminergic neuron clusters facilitated the evolution of small brain sizes, and that these modifications were possible without compromising vital physiological functions.

Neuron size in comparison with other insects

As expected, monoaminergic neurons are smaller in *T. evanescens* than in larger insects (Table 1). For example, the diameter of OA-L-IR cell bodies was on average 3.3 μm in *T. evanescens*, 6 – 11 μm in *Nasonia* wasps (Haverkamp and Smid, 2014), 5 – 10 μm in *Cotesia* wasps (Bleeker et al., 2006), 5 – 10 μm in *D. melanogaster* (Sinakevitch and Strausfeld, 2006) and 8 – 45 μm in *A. mellifera* (Sinakevitch et al., 2005). Diameters of DA- and 5HT-L-IR cell bodies are even smaller; on average 2.3 μm and 2.1 μm respectively in *T. evanescens* and 8 – 30 μm in *A. mellifera* (Schürmann and Klemm, 1984; Schafer and Rehder, 1989; Schürmann et al., 1989). More accurate comparisons of neuron size between species would require volumetric data on cell body and brain volumes. Such comparisons could reveal if neuronal cell bodies are more or less miniaturized than would be expected from the difference in brain size between *T. evanescens* and larger insects.

Neuronal cell bodies have previously been reported to range between 1.2 and 2.8 μm in diameter in *T. evanescens* (Makarova and Polilov, 2013). The monoaminergic cell bodies that we measured in our study were larger, ranging in diameter between 1.4 and 5.7 μm (Chapter 5). This could indicate that monoaminergic cell bodies are larger than those of other types of neurons. However, cell body

diameters in our study may also be larger because we included wasps of up to 0.9 mm in body length.

Neuronal cell body diameters in *T. evanescens* are among the smallest that have been described in insects, which may be a consequence of brain miniaturization (Niven and Farris, 2012; Makarova and Polilov, 2013). The smallest insects show a strongly reduced volume of cytoplasm in their neurons (Makarova and Polilov, 2013). As a result, the nucleus can occupy up to 90% of neuronal cell body volume (Polilov, 2005). This indicates that the size of the nucleus limits neuronal cell body size. The volume of the nucleus in turn relates to the size of the genome (Gregory, 2001). Genome size has, to our knowledge, not been established for *T. evanescens*. However, genome sizes of related species are surprisingly similar to those of larger insects. For example, *Trichogramma platneri* has a similar genome size (i.e. ~176 Mb; Ardila-Garcia et al., 2010) as *D. melanogaster* (i.e. ~180 Mb; Adams et al., 2000), and the genome of *Trichogramma brassicae* was found to be similar in size (i.e. ~246 Mb; Johnston et al., 2004) as the genome of *A. mellifera* (i.e. ~235 Mb; Ardila-Garcia et al., 2010). Hence, the smaller size of cell bodies in *T. evanescens* compared to those of *A. mellifera* and *D. melanogaster* (as outlined above) may not be caused by a difference in genome size. The evolutionary process of miniaturization of neuron size may instead have resulted in densely packed chromatin inside the nucleus (Makarova and Polilov, 2013; Polilov, 2015). Further miniaturization of cell body size may require modifications that also negatively affect the functionality of the neurons, such as lysis of neuronal nuclei (Polilov, 2012). Lower numbers of neurons or neuron clusters, such as we observed in this study, may have been a necessary modification that prevented the loss of functionality of neurons during the evolutionary process of brain miniaturization in *T. evanescens*.

The average diameter of OA-L-IR cell bodies is considerably larger than 5HT- and DA-L-IR cell bodies: approximately 53% and 42% larger respectively. There appears to be a similar trend in *A. mellifera*: OA-L-IR cell bodies can reach diameters of up to 45 μm (Sinakevitch et al., 2005), whereas the largest 5HT- and DA-L-IR cell bodies have a diameter of 30 μm (Schürmann and Klemm, 1984; Schafer and Rehder, 1989). This difference in neuron size is not reflected by the size of the varicose terminals. The 5HT-L-IR varicose terminals are almost twice as large (approximately 1 μm in diameter) as OA- and DA-L-IR terminals (0.6 and 0.5 μm respectively), indicating that release sites of 5HT-L-IR neurons are larger.

Conclusion

Our study shows that the monoaminergic neuron systems in the minute brain of *T. evanescens* are highly comparable in complexity to those in much larger insects. However, reductions of complexity do occur in the neuronal systems that we studied, possibly as a consequence of the miniaturized brain sizes in these wasps. Monoaminergic cell body diameters are smaller in *T. evanescens* than in larger insects. Miniaturization of neuron size may have enabled maximized complexity of neuronal systems; the monoaminergic neuron clusters contain more neurons than expected from the differences in total number of neurons in the brains of *T. evanescens* and larger insects. We observed that these reductions in neuron numbers are not proportional, but vary for the different monoaminergic systems.

Some neuron clusters are similar in complexity as in larger insects, other clusters are partially reduced, and others are entirely absent in *T. evanescens*. The neuron clusters of which the complexity was maintained were mostly serotonergic and some octopaminergic clusters. The complexity of these clusters may have been maintained because they play key roles in brain performance. The clusters that were partially reduced or completely absent were mostly dopaminergic and some octopaminergic clusters. Modifications of these clusters may have facilitated brain miniaturization, and appear to have been possible without compromises to vital brain functions.

The results of our study reveal some of the evolutionary adaptations that may facilitate optimal behavioural and cognitive complexity with miniaturized brains. These results are especially interesting in comparison with the modification of monoamine neuron clusters that arise as a result of intraspecific differences in body size between small and large sister wasps (Chapter 5). Further research should unravel what the functional consequences are of the absence of some neuron clusters and innervation patterns in *T. evanescens* compared to larger insects, such as the unique absence of 5HT-like innervation of the antennal lobe. Furthermore, it would be interesting to compare the numbers of 5HT- and DA-L-IR neurons between *T. evanescens* and the related but larger *Nasonia* parasitic wasps, which show a large similarity in OA-L-IR neuron distribution. This could reveal if the numbers of different monoaminergic neurons are similarly conserved between these two species.

Acknowledgements

We thank the Max Planck Institute for Chemical Ecology (Jena, Germany) for providing *Manduca sexta* pupae; Léon Westerd, Frans van Aggelen and André Gidding for culturing *Mamestra brassicae*; the experimental farm of Wageningen University (Unifarm) for growing the tobacco plants; and Norbert de Ruijter (Wageningen University, Laboratory of Cell Biology) and Henk Schipper (Wageningen University, Experimental Zoology) for use of the confocal laser scanning microscopes. This work was supported by NWO PE&RC Graduate Program grant 022.002.004 (to EW) and by NWO Open Competition grant 820.01.012 (to HS).

Supplementary Information

Distribution and projections of 5HT-L-IR neurons in comparison to other insects

The distribution pattern of 5HT-L-IR neuron clusters in *T. evanescens* largely corresponds to the pattern in *A. mellifera* and *D. melanogaster* (Schürmann and Klemm, 1984; Monastirioti, 1999; Blenau and Thamm, 2011), but there were some differences. Cluster 5HT-0 in *T. evanescens* has not been described for *A. mellifera* (Schürmann and Klemm, 1984), but the location of this cluster appears similar to the most anterior cell cluster in *D. melanogaster* in the anterior lateral protocerebrum (Blenau and Thamm, 2011). Furthermore, we did not observe the deutocerebral giant cell that was described for *A. mellifera* (Rehder et al., 1987), nor the clusters in the anterior medial and posterior lateral protocerebrum that were described for *D. melanogaster* (Blenau and Thamm, 2011).

The deutocerebral giant cell innervates the antennal lobes in *A. mellifera* (Rehder et al., 1987; Seidel and Bicker, 1996). Interestingly, the absence of this neuron in *T. evanescens* co-occurs with an absence of 5HT-L-IR neurites and varicose terminals in the antennal lobes. The cell body of the neuron that innervates the antennal lobes could also not be found in *Harpegnathos saltator* ants, but serotonergic innervation of the antennal lobe was present in this species (Hoyer et al., 2005) and all other insects species studied so far (Dacks et al., 2006). Serotonergic antennal lobe innervation was found to be sparse and incomplete in various families of parasitic wasps, but never completely absent (Dacks et al., 2006). Our study suggests that chemical modulation of antennal lobe neurons may not be serotonergic in *T. evanescens*.

Cluster 5HT-1 is located anteriorly between the lobula and medulla in *T. evanescens*. This cluster has previously been described in *A. mellifera*, where it occurs in two

subclusters: one located directly between the lobula and medulla, and one that is located more ventrally at the rim of the brain (Schürmann and Klemm, 1984). In *D. melanogaster*, a single 5HT-L-IR neuron cluster has been described at a similar location, located in the lateral protocerebrum between the medulla and central neuropil (Blenau and Thamm, 2011).

The innervation pattern of the optic lobes shows a single layer of varicose terminals in both the medulla and lamina of *T. evanescens*, which corresponds to observations in *A. mellifera* (Schürmann and Klemm, 1984; Nässel, 1988). However, the origin of innervation of the medulla and lamina in *T. evanescens* differs from the descriptions for *A. mellifera* and *D. melanogaster*. In *A. mellifera* and *D. melanogaster*, the optic lobes are only innervated by neurites of the clusters that correspond with 5HT-1 (Schürmann and Klemm, 1984; Nässel, 1988), whereas cluster 5HT-2 also contributes to optic lobe innervation in *T. evanescens*. The neurites of cluster 5HT-2 could not be traced in *A. mellifera* (Schürmann and Klemm, 1984), and a similar cluster has not been described for *D. melanogaster* (Blenau and Thamm, 2011). The involvement of cluster 5HT-2 in the innervation of the optic lobes of *T. evanescens* suggests that this cluster has similar functions as cluster 5HT-1, which has been hypothesized to modulate optic lobe neurons, visual processing and diurnal activity (Nässel et al., 1985; Nässel, 1988).

Cluster 5HT-3 had most cell bodies in *T. evanescens*, and neurites that innervated many neuropil areas by projecting in lateral, dorso-anterior and ventro-anterior direction. A similar cluster is described in *A. mellifera*, which innervates anterior neuropil areas (Schürmann and Klemm, 1984). Cluster 5HT-3 could be similar to the cluster described in the posterior medial protocerebrum in *D. melanogaster*, which is located in the posterior cell body rind, medial to the calyx (Blenau and Thamm, 2011).

The mushroom bodies are among the neuropil areas that are innervated by 5HT-3 neurites. A single neurite enters the mushroom bodies through the pedunculus and bifurcates inside the calyx. The other components of the mushroom bodies lack serotonergic innervation. This is in contrast to the mushroom body innervation pattern that was described for *A. mellifera* (Schürmann and Klemm, 1984). Here, the calyces completely lack 5HT-like immunoreactivity, whereas the pedunculus, medial-, and vertical lobes contain a pronounced pattern of layered 5HT-like immunoreactivity. Similar mushroom body innervation patterns were shown in ants, but here the calyx is innervated by a few neurites (Hoyer et al., 2005). These differences could suggest that modulation of mushroom body functioning differs between hymenopterans.

We did not observe the 5HT-4 and 5HT-5 clusters that were described for *A. mellifera* (Schürmann and Klemm, 1984). Cluster 5HT-4 is located in the pars intercerebralis in *A. mellifera*, at the posterior medial rim of the medial calyx. Cluster 5HT-5 is located more posteriorly in the pars intercerebralis in *A. mellifera*, ventral to 5HT-4. These clusters may be completely lacking in *T. evanescens*. Alternatively, the 5HT-4 and 5HT-5 clusters could be located too close to the cluster of 5HT-3 neurons to distinguish between them, because the second calyx that is present in *A. mellifera* is absent in *T. evanescens*. In *A. mellifera*, the 5HT-4 cluster causes the layered innervation pattern of the mushroom bodies (Schürmann and Klemm, 1984), and innervates the central complex (Seidel and Bicker, 1996). This layered mushroom body innervation was absent in *T. evanescens*. The central complex did show 5HT-L-IR innervation, but the origin could not be traced.

We observed three clusters of 5HT-L-IR cell bodies in the ventral rim of the brain of *T. evanescens*, and grouped these as 5HT-6. This corresponds to findings in *A. mellifera*, where the labial, maxillary and mandibular neuromeres of the suboesophageal zone each contain a cluster of 5HT-L-IR cell bodies (Rehder et al., 1987; Seidel and Bicker, 1996). There are also three clusters at similar locations in *D. melanogaster* (Monastirioti, 1999; Blenau and Thamm, 2011). There was a difference in the number of cell bodies per cluster between *A. mellifera* and *T. evanescens*. In *A. mellifera* there are only two cell body pairs per cluster (Blenau and Thamm, 2011), whereas we counted up to four pairs per cluster in *T. evanescens*. There may be some variability in our neuron counts that is caused by different clusters lying too close together to distinguish between in some of the samples. However, many brains have more than six 5HT-6 neurons in total. This indicates that cluster 5HT-6 does contain more neurons in *T. evanescens* than in *A. mellifera*.

The lateral 5HT-6a neuron projects dorsally towards the brain midline. This projection pattern is in contrast to that of the other 5HT-6 neurons, which project medially and form a network of bifurcations in the ventral rim of the brain, similar as in *A. mellifera* (Rehder et al., 1987). We cannot exclude that the lateral 5HT-6a neuron is part of a different cell cluster. The location of the lateral 5HT-6a neuron resembles the location of the ventral 5HT-1 cluster in *A. mellifera* (Schürmann and Klemm, 1984) and the deutocerebral giant interneuron (Rehder et al., 1987). However, the projection patterns of both clusters differ from the projection that was observed for the lateral 5HT-6a neuron: the ventral 5HT-1 neurons project towards the optic lobes (Schürmann and Klemm, 1984), and the deutocerebral giant interneuron innervates the antennal lobe (Rehder et al.,

1987). We decided to consider the lateral 5HT-6a neuron as part of the 5HT-6a cell cluster, because it is located very close to the medial 5HT-6a neuron and cannot be distinguished from it when its neurites are not visible.

Distribution and projections of OA-L-IR neurons in comparison to other insects

The distribution pattern of OA-L-IR neuron clusters in *T. evanescens* largely corresponds to previous findings in the parasitic wasps *Nasonia vitripennis* and *Nasonia giraulti* (Haverkamp and Smid, 2014). These similarities could be explained by the close relation of these parasitic wasps; they both belong to the superfamily Chalcidoidea. Only the clusters that were described in *Nasonia* as OA-0 and OA-4 were not found in *T. evanescens*. Cluster OA-0 was found in only a single preparation of *N. giraulti* (n = 20) and not at all in *N. vitripennis* (n = 24) (Haverkamp and Smid, 2014). This low detection frequency may explain why we did not find this cluster in *T. evanescens*.

We observed more OA-L-IR clusters in *T. evanescens* than were described for the parasitic wasps *Cotesia glomerata* and *Cotesia rubecula* (Bleeker et al., 2006). Only the clusters that correspond to OA-3 and OA-VUM were described for *Cotesia* wasps, and an additional OA-L-IR cluster in the pars intercerebralis that we did not observe in *T. evanescens*. However, the staining intensity in *Cotesia* was low compared to the intensity in *Nasonia* (Haverkamp and Smid, 2014). The low numbers of neurons that were detected in *Cotesia* may therefore not reflect a difference in OA-like immunoreactivity, but instead relate to methodological differences.

The distribution of OA-L-IR neuron clusters in *T. evanescens* is also very similar to the distribution in *A. mellifera* (Kreissl et al., 1994; Sinakevitch et al., 2005) and *D. melanogaster* (Sinakevitch and Strausfeld, 2006; Busch et al., 2009). Mostly the same clusters are present in the three species, but they occur at slightly different locations, in more subclusters and with more neurons per cluster in *A. mellifera* and *D. melanogaster*. There were some OA-L-IR clusters that were present in *D. melanogaster* and *A. mellifera*, but that we did not observe in *T. evanescens*. These were the dorso-medial OA-4 neuron clusters, the cluster between the lobula and calyx, some of the subclusters, and the ventral paired median neuron cluster in *A. mellifera*.

The most anterior OA-L-IR neuron clusters in *T. evanescens* were OA-1 and OA-2. They appear at similar locations as the equivalent clusters that were described for *Nasonia* wasps, and consist of a single neuron pair per cluster in both *T. evanescens*

and *Nasonia* (Haverkamp and Smid, 2014). Similar clusters were described for *A. mellifera*, but cluster OA-2 occurs at a more ventral location in *A. mellifera* than in *T. evanescens* (Kreissl et al., 1994; Sinakevitch et al., 2005). In *D. melanogaster*, OA-1 occurs at a similar location as in *T. evanescens*, but OA-2 is located more laterally: between the ventro-medial and lateral protocerebrum (Sinakevitch and Strausfeld, 2006). Clusters OA-1 and OA-2 were not observed in *Cotesia* wasps (Bleeker et al., 2006).

The most pronounced OA-L-IR neuron cluster in *T. evanescens* was OA-3, in the area around the oesophageal foramen. This cluster was also the cluster with the most pronounced OA-like immunoreactivity in *Nasonia* (Haverkamp and Smid, 2014) and *Cotesia* wasps (Bleeker et al., 2006). A similar cluster is located around the oesophageal foramen in *A. mellifera* and *D. melanogaster*, and is divided into anterior and posterior subclusters (Sinakevitch et al., 2005; Sinakevitch and Strausfeld, 2006). Cluster OA-3 was the only paired OA-L-IR neuron cluster that consists of an approximately equal number of neurons in *T. evanescens* and in other insects. We counted up to nine neuron pairs in *T. evanescens*, whereas 11 neuron pairs were counted in *Nasonia* (Haverkamp and Smid, 2014) and *A. mellifera* (Sinakevitch et al., 2005), and up to eight in *Cotesia* (Bleeker et al., 2006) and *D. melanogaster* (Busch et al., 2009).

Cluster OA-5 consists of up to three neuron pairs in *T. evanescens*. A similar cluster with a three neuron pairs has been described for *Nasonia* wasps (Haverkamp and Smid, 2014), but not for *Cotesia* (Bleeker et al., 2006). Cluster OA-5 consists of two subclusters in *A. mellifera* (Sinakevitch et al., 2005). Subcluster OA-5a is located at a similar location as OA-5 in *T. evanescens*, and consists of only a single neuron pair. Subcluster OA-5b is located at a more posterior location, but we did not observe an equivalent neuron cluster in *T. evanescens*. Three subclusters of OA-5 have been described for *D. melanogaster*, of which OA-5a resembles the location of OA-5 in *T. evanescens* most (Sinakevitch and Strausfeld, 2006).

The location of cluster OA-6 in *T. evanescens* (latero-posterior to OA-VUM in the ventral rim of the brain) corresponds to the location of the posterior subcluster of OA-6 in *A. mellifera* (Sinakevitch et al., 2005), and a similar cluster was also found in *D. melanogaster* (Sinakevitch and Strausfeld, 2006). Cluster OA-6 has not been described for *Nasonia* wasps. There are two clusters lateral to the OA-VUM neurons in *Nasonia*: the ventral median paired neuron cluster in the anterior suboesophageal zone and the posterior median paired neuron cluster in the posterior suboesophageal zone (Haverkamp and Smid, 2014). However, these are located ventro-medially, close to the midline, whereas OA-6 is located ventro-laterally in *T. evanescens*.

The location of the most posterior OA-L-IR neuron cluster (OA-7) corresponds to the location of the dorsal median paired neuron cluster in the dorso-posterior suboesophageal zone of *Nasonia* wasps (Haverkamp and Smid, 2014). This cluster has not been described for *A. mellifera* (Kreissl et al., 1994; Sinakevitch et al., 2005), nor for *D. melanogaster* (Sinakevitch and Strausfeld, 2006; Busch et al., 2009).

The OA-VUM neurons in *T. evanescens* lie at the ventral rim of the brain, very close to the mouthparts. The OA-VUM cluster has been described for many insects, for instance in *A. mellifera* (Sinakevitch et al., 2005; Schroter et al., 2007), *Nasonia* (Haverkamp and Smid, 2014), *Cotesia* (Bleeker et al., 2006), *D. melanogaster* (Sinakevitch and Strausfeld, 2006; Busch et al., 2009), *Phaenicia sericata* blowflies (Sinakevitch and Strausfeld, 2006), and *Manduca sexta* hawk-moths (Dacks et al., 2005). The OA-VUM cluster is usually divided into subclusters named after the neuromere in which they occur; either the mandibular, maxillary or labial neuromere of the suboesophageal ganglion. We could not distinguish between different subclusters in *T. evanescens*, because the neurons are too close together. The average count of approximately four OA-VUM neurons in *T. evanescens* was rather low because the area around the mouthparts is fragile and was often damaged in our preparations, but we counted up to 13 OA-VUM neurons in two well-stained brains. This is remarkably similar to the number of OA-VUM neurons that are present in other hymenopterans: i.e. 14 in *A. mellifera* (Schroter et al., 2007), 12 – 14 in *Nasonia* wasps (Haverkamp and Smid, 2014) and 14 – 20 in *Cotesia* wasps (Bleeker et al., 2006).

The neurites of OA-L-IR neurons were less intensely stained than those of 5HT-L-IR neurons. They could not be traced throughout their entire length, and their connections to cell bodies could not be observed at all. However, most of the neurites that were described for *Nasonia* wasps (Haverkamp and Smid, 2014) were also visible in *T. evanescens*. Only the neurite tracts that project from the OA-VUM in the direction of the oesophageal foramen were not found in *T. evanescens*.

The OA-USP was the most pronounced neurite in *T. evanescens*. Its projection pattern is largely similar to the pattern of OA-USP in *Nasonia*, but differs in one aspect: in *T. evanescens* it does not bifurcate into an ipsilateral and contralateral projecting neurite. Only one hemisphere is innervated by a neurite that bends in ipsilateral direction at the dorsal rim of the brain. In this aspect, the projection pattern of OA-USP in *T. evanescens* seems identical to the projection of OA-VUMmd4 in *A. mellifera* (Schroter et al., 2007). This neurite runs along the brain midline and bends in ipsilateral direction at the dorsal rim of the brain. We did

not observe a connection of OA-VUM cell bodies to neurites in *T. evanescens*, and the OA-USP could not be traced further ventrally from the oesophageal foramen. We can therefore only speculate about the equivalence of OA-USP in *T. evanescens* and the OA-VUMmd4 projection in *A. mellifera*.

The network of neurites around the oesophageal foramen was also described for *Nasonia* (Haverkamp and Smid, 2014). Neurites from this network innervate the optic lobes, mushroom bodies and antennal lobes in *T. evanescens*. The neurites that innervate the optic lobes show a generally similar projection pattern in both *Nasonia* and *T. evanescens*, but the projections differ in two points. First, in *T. evanescens* there appears to be only a single neurite that innervates the optic lobes, whereas five neurites are responsible for this in *Nasonia*. Second, only the medulla appears to be innervated in *T. evanescens* by this network, whereas both the lobula and medulla are innervated in *Nasonia*.

The mushroom body calyx of *T. evanescens* is innervated by another neurite of the network around the oesophageal foramen. Its projection pattern resembles the pattern of the stag-like projection (OA-SLP) that was described for *Nasonia* (Haverkamp and Smid, 2014), and the projections from OA-VUMmx1 and OA-VUMmd1 in *A. mellifera* (Schroter et al., 2007). Innervation of the mushroom body calyx by OA-SLP has not been described for *Nasonia*. Instead, this neurite innervates the mushroom body pedunculus. In *A. mellifera*, OA-VUMmx1 and OA-VUMmd1 do innervate the mushroom body calyces. Furthermore, OA-SLP in *Nasonia* and OA-VUMmx1 and OA-VUMmd1 in *A. mellifera* innervate the antennal lobe and lateral horn. We observed a neurite that projects laterally from the network around the oesophageal foramen in *T. evanescens* and innervates the antennal lobe, but we could not distinguish a connection between this neurite and OA-SLP. The neurites that innervate the lateral horn were not visible in *T. evanescens*.

Distribution and projections of DA-L-IR neurons in comparison to other insects

The most anterior cell clusters that we observed in *T. evanescens* were not described for *A. mellifera* (Schafer and Rehder, 1989; Schürmann et al., 1989). These are the dorsal DA-1 cluster, and cluster DA-2 medial to the lobula and dorso-lateral to the antennal lobes. These two clusters may be equivalent to the two clusters in the anterior protocerebrum in *D. melanogaster*: the protocerebral anterior medial (PAM) or protocerebral anterior lateral (PAL) cluster (Budnik and White, 1988; Mao and Davis, 2009). The PAM cluster has been shown to be important for both aversive and appetitive learning in *D. melanogaster* (Aso et al., 2010; Burke

et al., 2012; Liu et al., 2012; Waddell, 2013). However, cluster DA-2 is located more ventro-laterally than both of these clusters in *D. melanogaster*. Cluster DA-2 may also be equivalent to the protocerebral posterior lateral cluster 2 (PPL2) in *D. melanogaster*, which is located more posteriorly than cluster DA-2 in *T. evanescens*, but resembles DA-2 in its location on the lateral rim of the central brain, medial to the optic lobes (Mao and Davis, 2009).

Cluster DA-3 is located in the ventral rim of the brain, ventral to the antennal lobes. The close location to the antennal lobes suggests that these neurons may be similar to the neurons that were described in the suboesophageal zone of *A. mellifera*, which project in anterior direction and innervate the antennal lobes (Schafer and Rehder, 1989; Schürmann et al., 1989). Although we did not observe any neurites that innervate the antennal lobes in *T. evanescens*, the immunoreactivity that we did observe in the antennal lobes may originate at DA-3. In *D. melanogaster*, two clusters are located ventro-posterior to the antennal lobe. These are the protocerebral posterior medial 3 (PPM3) and protocerebral posterior lateral 3 (PPL3) clusters (Mao and Davis, 2009). The location of these clusters is slightly more posterior than the location of DA-3 in *T. evanescens*, although the more ventral location of the antennal lobe in *T. evanescens* makes it difficult to compare clusters between the two species.

Cluster DA-4 is located medially in the ventral rim of the brain, and consists of up to four unpaired neurons in *T. evanescens*. Three of these neurons are located in the ventro-anterior rim of the brain and another unpaired neuron occurs more posteriorly. A similar situation occurs in *D. melanogaster* and blowflies (Budnik and White, 1988; Nässel and Elekes, 1992). Here, two DA-L-IR neurons are located right next to a ventral unpaired median neuron in the anterior part of the suboesophageal zone, and a second ventral unpaired median neuron is located at a more posterior location. No clusters of ventral unpaired median neurons were described in *A. mellifera* (Schafer and Rehder, 1989; Schürmann et al., 1989).

Cluster DA-5 consists of two adjacent subclusters that are located ventro-anterior and lateral to the calyx and dorsal to the optic lobes. Clusters of DA-L-IR neurons occur at similar locations on the lateral side of the calyces in *A. mellifera* and *D. melanogaster* (Schafer and Rehder, 1989; Schürmann et al., 1989; Mao and Davis, 2009). In *A. mellifera*, cluster C3 is located ventral to the lateral calyx (Schafer and Rehder, 1989), and an additional DA-L-IR cluster was observed lateral to the medial calyx (Schürmann et al., 1989). In *D. melanogaster*, the cluster on the lateral side of calyx is indicated as protocerebral posterior lateral 1 (PPL1; Mao and Davis, 2009). The PPL1 cluster functions together with PAM in the regulation of appetitive and aversive learning in flies (Aso et al.,

2010; Burke et al., 2012; Liu et al., 2012; Waddell, 2013). The DA-5 cluster may perform similar functions in *T. evanescens*.

Cluster DA-6 is located in the neural tissue that surrounds the ocellar tracts, dorso-posterior to the mushroom bodies and the central complex. This cluster could be similar to the DA-L-IR neuron cluster that is located dorso-posterior to the central complex in *A. mellifera* (Schafer and Rehder, 1989; Schürmann et al., 1989), and to two protocerebral posterior medial clusters (PPM 1 and 2) in *D. melanogaster* (Mao and Davis, 2009).

Cluster DA-7 is the most posterior dopaminergic cell cluster, located in the most posterior part of the ventral rim of the brain. This cluster could be similar to the posterior DA-IR-L neuron clusters in the suboesophageal zone of *A. mellifera* (Schafer and Rehder, 1989; Schürmann et al., 1989). Most of these clusters in *A. mellifera* project anteriorly towards the antennal lobes, although the most posterior cluster (that was described as S7 by Schafer and Rehder (1989)) projects laterally and towards the thoracic ganglia. We observed similar lateral projections in the ventral rim of the brain and two neurites that appear to innervate the thoracic ganglia in *T. evanescens*. In blowflies, two pairs of DA-L-IR neurons occur in the lateral rim of the posterior suboesophageal zone (Nässel and Elekes, 1992). They have not been described for *D. melanogaster* (Budnik and White, 1988; Monastirioti, 1999; Mao and Davis, 2009).

Innervation of neuropil areas was sparse: low densities of varicose terminals occur throughout the brain, and only the mushroom body lobes and ventral rim of the brain show higher levels of DA-like immunoreactivity. We did not observe any DA-like immunoreactivity in the optic lobes of *T. evanescens*, similar to *A. mellifera* (Schafer and Rehder, 1989; Schürmann et al., 1989). The mushroom body calyx was also devoid of DA-like immunoreactivity. Similar mushroom body innervation patterns were reported for locusts and blowflies, where all mushroom body areas show DA-like immunoreactivity except the calyces (Nässel and Elekes, 1992; Wendt and Homberg, 1992). Initial reports on DA-like immunoreactivity in *D. melanogaster* only showed innervation of the mushroom body lobes (Zhang et al., 2007), but later studies also discovered DA-L-IR neurites innervating the calyx (Mao and Davis, 2009). *Apis mellifera* show a more pronounced innervation of the mushroom bodies, which consists of many varicose terminals in the calyces and layers of DA-like immunoreactivity in the lobes and pedunculus (Schürmann et al., 1989).

We observed a single DA-L-IR neurite that followed the pedunculus in the direction of the calyx in *T. evanescens*. This neurite resembles the projection of

the DA-L-IR neuron cluster lateral to the lateral calyx in *A. mellifera* (Schafer and Rehder, 1989). This projection runs to the medial side of the pedunculus, innervates the vertical lobe, and projects medioventrally along the dorsal side of the medial lobe towards the brain midline. The neurite does not resemble any of the DA-L-IR neurites described in *D. melanogaster* (Claridge-Chang et al., 2009; Krashes et al., 2009; Mao and Davis, 2009; Aso et al., 2010; Aso et al., 2012; Burke et al., 2012).

The most pronounced DA-like immunoreactivity was found at the base of the mushroom body calyx, where a bundle of DA-L-IR fibres follows the lateral rim of the brain, anterior to the mushroom body pedunculus and medial to the calyx. It does not resemble the layered pattern of DA-like immunoreactivity that has been described for the mushroom body pedunculus and lobes of *A. mellifera* (Schürmann et al., 1989), because the bundle projects in the direction of (but could not be observed to innervate) the lobula instead of being restricted to the mushroom bodies. Despite the close location to cluster DA-5, we could not observe a connection between the bundle of DA-L-IR fibres and cluster DA-5, nor with the neurite that projects along the pedunculus. The origin, function or resemblance to other insects is therefore unknown.

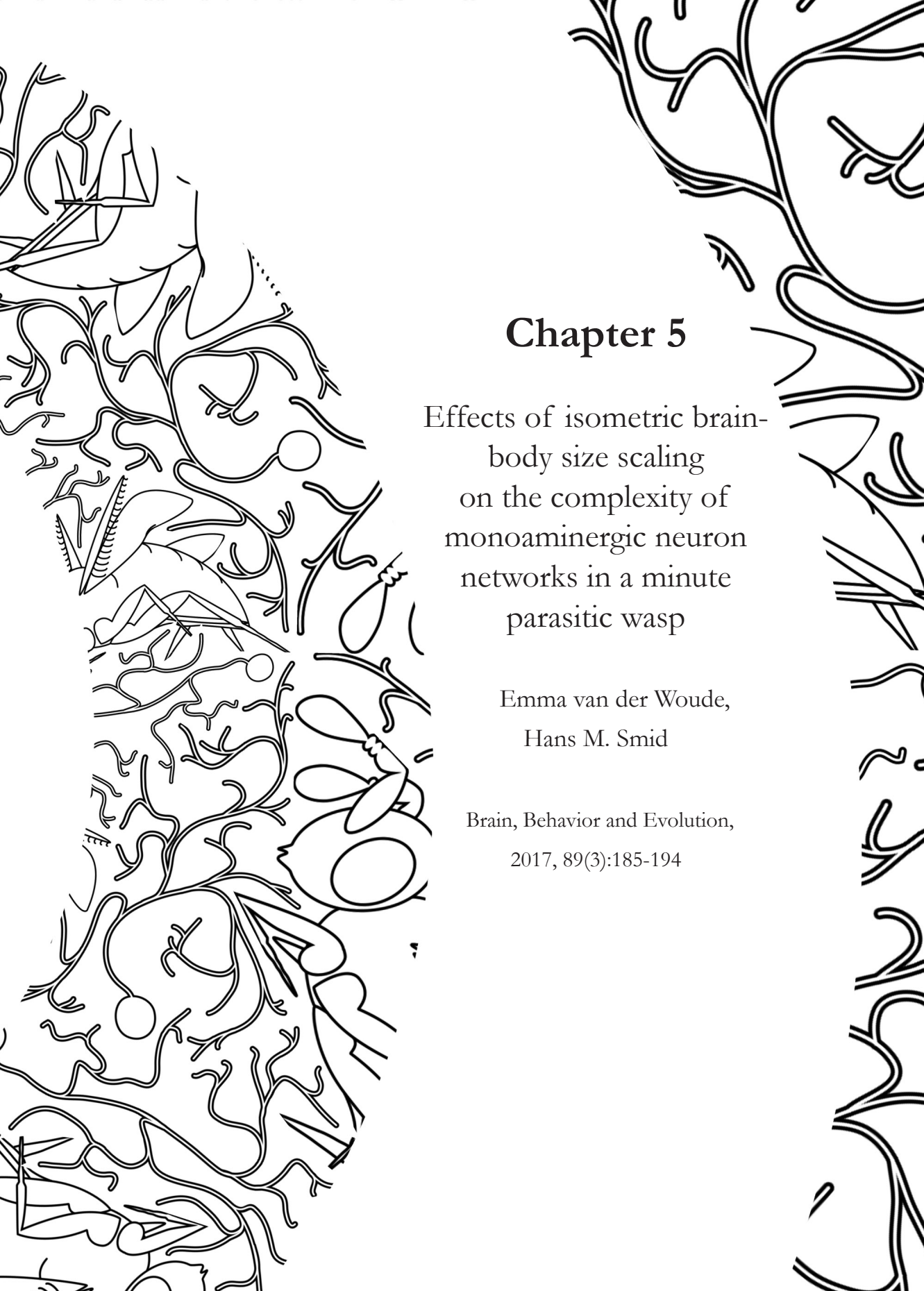

Chapter 5

Effects of isometric brain-body size scaling on the complexity of monoaminergic neuron networks in a minute parasitic wasp

Emma van der Woude,
Hans M. Smid

Brain, Behavior and Evolution,
2017, 89(3):185-194

Abstract

Trichogramma evanescens parasitic wasps show large phenotypic plasticity in brain and body size, resulting in a 5-fold difference in brain volume between genetically identical sister wasps. Brain volume scales linearly with body volume in these wasps. This isometric brain scaling forms an exception to Haller's rule, which states that small animals have relatively larger brains than large animals. The large plasticity in brain size may be facilitated by plasticity in neuron size, in the number of neurons, or both. Here, we investigated whether brain isometry requires plasticity in the number and size of monoaminergic neurons that express serotonin (5HT), octopamine (OA), and dopamine (DA). Genetically identical small and large *T. evanescens* appear to have the same number of 5HT-, OA-, and DA-like immunoreactive cell bodies in their brains, but these cell bodies differ in diameter. This indicates that brain isometry can be facilitated by plasticity in the size of monoaminergic neurons, rather than plasticity in numbers of monoaminergic neurons. Selection pressures on body miniaturization may have resulted in the evolution of miniaturized neural pathways that allow even the smallest wasps to find suitable hosts. Plasticity in the size of neural components may be among the mechanisms that underlie isometric brain scaling while maintaining cognitive abilities in the smallest individuals.

Introduction

According to Haller's rule, small animals have relatively larger brains than large animals. This negative allometric brain-body size relationship follows a power law function in which the exponent (the scaling coefficient) describes how mass or volume of the brain scales with mass or volume of the body. This scaling coefficient is smaller than 1 in the case of negative allometry. Haller's rule applies to most animal species studied so far, both in comparisons between species and within species (Wehner et al., 2007; Isler et al., 2008; Seid et al., 2011). The computational power of a brain may depend more on the absolute number of neurons and connections than on relative brain size (Chittka and Niven, 2009). Hence, the relatively larger brains in small animals may be the consequence of a need to maintain cognitive abilities, and therefore absolute brain size, in smaller-bodied animals.

Because brain tissue has a high metabolic rate (Aiello and Wheeler, 1995), smaller animals suffer relatively higher energetic costs of maintaining a relatively large brain. These increasing energetic demands eventually limit evolutionary miniaturization of a species (Eberhard and Wcislo, 2011), and may similarly limit the variation in body size within a species. Interestingly, some of the smallest animals on Earth appear to 'evade' Haller's rule (Chapter 2; Groothuis and Smid, 2017). Among these are *Trichogramma evanescens*, minute parasitoid wasps that develop inside the eggs of butterflies and moths. Adult body size depends on the size of the lepidopteran host egg, and on the number of competing parasitoid larvae that develop inside the same egg. This results in phenotypic plasticity in body size; body length can range between 0.3 and 0.9 mm in genetically identical sister wasps (Chapter 3). *Trichogramma evanescens* parasitic wasps do not show negative brain-body size allometry, but scale their brains in a linear way with body size (Chapter 2). Such isometric brain scaling, with scaling coefficients equal to 1, results in the same relative brain size in small and large wasps. This brain-scaling strategy may be an adaptation that allows body miniaturization beyond the limits that are imposed by the energetic trade-offs of allometric brain scaling.

As a consequence of isometric brain scaling, small *T. evanescens* have brains that are smaller than predicted by Haller's rule, and large *T. evanescens* have brains that are larger than predicted by Haller's rule. Brain size plasticity may therefore be more extreme in *T. evanescens* than in species that scale their brains allometrically. We have previously found a 5-fold difference in brain volume between genetically similar small and large sister wasps (Chapter 2). This indicates that there is extreme phenotypic plasticity in brain size in this species, which is solely determined by

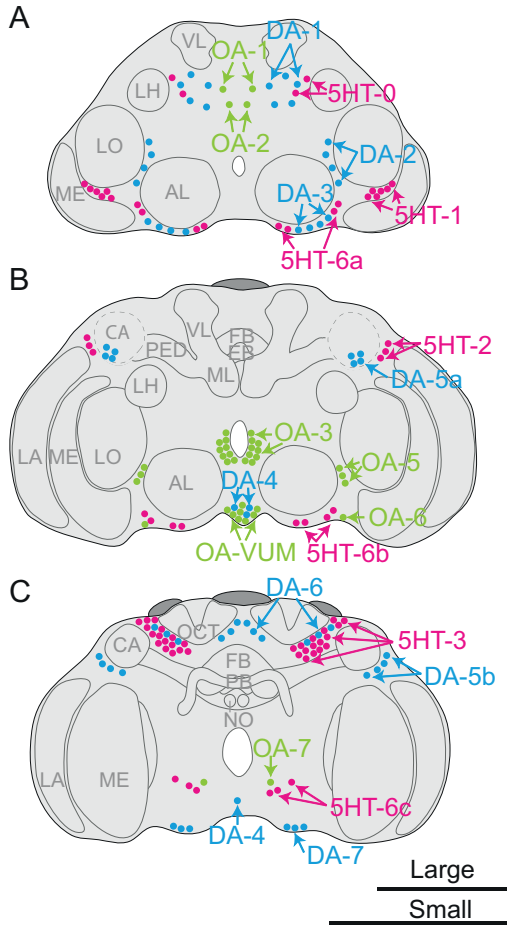

Figure 1. Overview of distribution of serotonin-, octopamine- and dopamine-like immunoreactive (5HT-L-IR, OA-L-IR and DA-L-IR) neuron clusters in the brain of *T. evanescens*. **(A)** Anterior view with dorsal side up at approximately one quarter in depth of the brain. **(B)** Anterior view halfway in depth of the brain. Dashed lines indicate the outline of the calyx, which is located posterior to cluster DA-5a. **(C)** Posterior view three quarters in depth of the brain. Shown cell body distributions are combined from separate experiments for the three monoamines (Chapter 4), hence the relative locations of different monoaminergic clusters may differ from this schematic representation. (AL antennal lobe, LA lamina, ME medulla, LO lobula, LH lateral horn, CA calyx, PED pedunculus, VL vertical lobe, ML medial lobe, FB fan-shaped body, EB ellipsoid body, PB protocerebral bridge, NO noduli, OCT ocellar tract). Scale bars indicate 50 µm, top scale bar for an average large brain, bottom scale bar for an average small brain.

the amount of nutrition that was available during development. Such extreme plasticity in brain size could be regulated by plasticity in the morphology of neuronal pathways. This may show as differences between small and large wasps in neuron size, in the number of neurons and arborisations, or both. These differences may have functional consequences, because cell bodies (Gregory, 2001) and axons (Faisal et al., 2005; Perge et al., 2012) need a minimum size for adequate functioning, and neural pathways with lower numbers of neurons and connections may have reduced computational power (Chittka and Niven, 2009; Niven and Farris, 2012). Hence, a trade-off of isometric brain scaling may be that neuron size or number fall beyond functional limits in the smallest brains.

We have previously shown that small and large *T. evanescens* show a similar level of complexity in the gross morphology of their olfactory system (Chapter 3).

Small and large wasps form the same number of glomeruli in the antennal lobe, and the same number of most types of olfactory sensilla on the antennae. The wasps do adapt the size of glomeruli; absolute and relative glomerular volumes were smaller in small wasps. Interestingly, there were no differences between small and large wasps on a cognitive level, shown by similar levels of olfactory and visual memory retention (Chapter 6). These findings suggest that despite their isometric brain scaling, *T. evanescens* are adapted to small body sizes, without apparent compromises to neural functioning. This could be achieved through maintained numbers of neurons, which are not reduced beyond their minimum size for adequate functioning.

Here, we studied how isometric brain scaling affects the number and size of neuronal cell bodies, in three quantifiable subsets that express serotonin (5HT), octopamine (OA), and dopamine (DA), respectively. These monoamines are derivatives of amino acids that act as neurotransmitters, neuromodulators, and neurohormones in the insect brain (Roeder, 1994; Libersat and Pflueger, 2004). They play critical roles in basic neural functioning, and are involved in many vital behavioural, cognitive and physiological processes (Roeder, 1994; Blenau and Thamm, 2011; Burke et al., 2012; Yamamoto and Seto, 2014). Although the monoaminergic systems may be highly conserved to maintain vital functions, plasticity in neuron numbers could to some extent be possible. This has been shown in *Pheidole dentata* ants, where the number of serotonergic cell bodies in the optic lobe differs with age and subcaste (Seid et al., 2008). Similar plasticity in number of neurons could also underlie isometric brain scaling in *T. evanescens*.

We have previously described the general morphology of 5HT-, DA- and OA-like immunoreactive (5HT-L-IR, OA-L-IR and DA-L-IR) neurons in the species *T. evanescens* (Figure 1), and compared our descriptions to those of larger insects (Chapter 4). The aim of the present study was to unravel whether brain isometry requires plasticity in the size and number of 5HT-L-IR, OA-L-IR and DA-L-IR neurons in small and large *T. evanescens*. We focus on phenotypic plasticity in body size in the context of adult body size variation that results from differences in scramble competition during larval development. Hence, we studied genetically identical wasps of similar age and experience, but with large differences in body and brain size. We expected that neuron size is reduced to a functional limit in small wasps, while neurons are larger in large wasps. Furthermore, we expected that small wasps show a lower number of monoaminergic neurons in their brains compared to large wasps, to facilitate isometric brain scaling.

Materials and Methods

Insects

Female *Trichogramma evanescens* Westwood (Hymenoptera: Trichogrammatidae) of inbred isofemale strain GD011 were reared in a climate room (22 ± 1°C, 50 – 70% rh, L16:D8) in eggs of three host species: the Mediterranean flour moth *Ephestia kuehniella*, the cabbage moth *Mamestra brassicae* and the tobacco hornworm *Manduca sexta*. Eggs of *E. kuehniella* were obtained as UV-irradiated eggs from Koppert Biological Systems (Berkel en Rodenrijs, the Netherlands). *Mamestra brassicae* were reared on cabbage plants (*Brassica oleracea*) in a climate room (21 ± 2°C, 50 – 70% rh, L16:D8). Adult moths oviposited on sheets of filter paper, and their eggs were used fresh for rearing procedures. *Manduca sexta* were obtained as pupae from the Max Planck Institute for Chemical Ecology (Jena, Germany). Adults were kept in a flight cage with a tobacco plant (*Nicotiana tabacum* SR1) inside a climate cabinet (25 ± 1°C, L16:D8). Eggs were collected from the tobacco plants and frozen until use in rearing procedures.

Generating body size variation

We used three species of differently sized host eggs to generate body size variation in *T. evanescens*. Adult body size depends on the amount of nutrition that was available during larval development, and therefore on the size of the host egg and the number of developing larvae inside it (Chapter 2; Chapter 3). *Ephestia kuehniella* eggs are shaped as prolate spheroids of ~0.52 mm long and ~0.38 mm in diameter, and with a volume of ~0.038 mm^3. These eggs can only host a single (occasionally two) developing *T. evanescens* larvae. Wasps that emerge from these eggs are always small: 0.3 – 0.4 mm measured from thorax to the tip of the abdomen (Chapter 2). *Mamestra brassicae* eggs are spheroids, with a diameter of ~0.60 mm and a volume of ~0.11 mm^3. These eggs can support the development of 1 – 5 wasps, resulting in adults with thorax-abdomen length ranging between 0.3 – 0.6 mm (Chapter 2). *Manduca sexta* eggs are spheroids of approx. 1.40 mm in diameter and ~1.44 mm^3 in volume. These eggs can host 6 – 40 developing wasps, and adults that emerge from these eggs reach thorax-abdomen lengths of 0.4 – 0.8 mm respectively (Chapter 3).

To increase the proportion of large wasps that emerged from *M. brassicae* eggs, we observed oviposition behaviour on these hosts and removed the wasp after laying her first egg as described previously (Suzuki et al., 1984; Chapter 2). Host eggs on which oviposition behaviour was observed were combined with eggs to

which the wasps had unlimited access for 4 hours, to ensure that both large and small offspring emerged.

To increase the proportion of large wasps that emerged from *M. sexta* eggs, we manipulated female wasps to lay fewer eggs in these hosts. Drilling through the larger *M. sexta* eggs takes the wasps a long time, and is generally followed by a period of host feeding. This makes these eggs unsuitable for observation of oviposition behaviour. We instead exploited the wasps' host examination behaviour to generate body size variation on *M. sexta*. Wasps of the genus *Trichogramma* assess host egg size through antennal drumming of its surface, and adapt the number of eggs they lay inside this perceived volume. When the egg appears smaller due to a partially inaccessible surface, *Trichogramma* wasps lay fewer eggs inside (Schmidt and Smith, 1985; 1987). Hence, we partially masked the surface of *M. sexta* eggs by distributing them on 5 – 10 ml cooling 1% agarose (Sigma) in a petridish (Greiner Bio-One, 94 × 15 mm) as described before (Chapter 3). This resulted in some eggs being fully exposed for antennal drumming, and some eggs being partially covered by agarose. The wasps had access to these eggs for 4 hours. This combination of partially masked and fully exposed *M. sexta* eggs ensured that both small and large wasps emerged.

Analysis of immunoreactivity

We prepared the samples as described in Chapter 4. In brief, heads of two-day-old female *T. evanescens* wasps were partially opened and fixed. Either the anterior or posterior cuticle was removed with fine tweezers to allow imaging of the brain. These heads were stained with either rabbit anti-5HT antibodies (Millipore Cat# AB938, RRID:AB_92263), rabbit anti-OA antibodies (MoBiTec Cat# 1003GE, RRID:AB_2314999) or mouse anti-DA (Millipore Cat# MAB5300, RRID:AB_94817), all at a 1:200 dilution. For analysis of OA and 5HT, a secondary antiserum of goat-anti-rabbit antibodies linked to Alexa fluor 488 (Molecular Probes, Cat# A11008, RRID:AB_143165) was applied at a 1:200 dilution together with 1:500 propidium iodide (Sigma-Aldrich). For analysis of DA, a secondary antibody of rabbit-anti-mouse (Dako Cat# Z0259, RRID:AB_2532147) was applied at a 1:200 dilution, followed by a tertiary antiserum of goat-anti-rabbit antibodies linked to Alexa fluor 488 (Jackson ImmunoResearch Labs Cat# 115-545-003, RRID:AB_2338840) at a 1:200 dilution together with 1:500 propidium iodide. Heads were scanned with a Zeiss LSM 510 confocal laser scanning microscope, using a 488-nm argon laser and a Plan-Apochromat ×63 oil immersion objective (N.A. 1.4). A band pass emission

filter at 505 – 550 nm was used to visualize Alexa Fluor 488, and a long pass emission filter at 560 nm for propidium iodide.

Classification of brain size

We measured brain width and brain height from optical sections to differentiate between small and large wasps. The tight attachment of the lamina to the compound eye caused damage to this area when the reflective layer had to be removed for imaging. We therefore used the lateral boundaries of the medullas as proxy for brain width. The distance between the dorsal and ventral rim of the brain was used to estimate brain height. Measurements were performed in optical cross sections using the measurement tool in the Fiji package of ImageJ 1.48s (Schindelin et al., 2012). These distances were ranked and used to select the 15 largest and 15 smallest well-stained brains of each antibody treatment.

Neuron analysis

Image segmentation was used to accurately determine the number of neurons in clusters that contained many cells close together. Cell bodies of paired neuron clusters (all clusters except OA-VUM and DA-4) were analysed in the best stained hemisphere of each selected brain. We used either the segmentation editor of Amira 5.4 (Visage Imaging GmbH, Berlin, Germany) or the TrakEM2 plugin (Cardona et al., 2012) in the Fiji package of ImageJ 1.48s (Schindelin et al., 2012). Cell diameters were measured with the measuring tool in the Fiji

Table 1. Average brain width and height (± SD) of small and large wasps that were used to analyse serotonin-, octopamine- and dopamine-like immunoreactive (5HT-L-IR, OA-L-IR and DA-L-IR) neurons. Differences in brain width and height between small and large wasps are based on independent samples t-tests.

	Brain width ± SD (µm)				**Brain height ± SD (µm)**		
	Small	Large	Difference		Small	Large	Difference
5HT	107 ± 5.29 (n = 15)	164 ± 7.75 (n = 15)	$p < 0.001$	**5HT**	81 ± 7.13 (n = 15)	110 ± 5.79 (n = 15)	$p < 0.001$
OA	112 ± 9.45 (n = 15)	145 ± 6.45 (n = 15)	$p < 0.001$	**OA**	85 ± 4.49 (n = 15)	111 ± 6.43 (n = 15)	$p < 0.001$
DA	107 ± 6.85 (n = 15)	140 ± 10.54 (n = 15)	$p < 0.001$	**DA**	70 ± 5.78 (n = 15)	89 ± 10.18 (n = 15)	$p < 0.001$

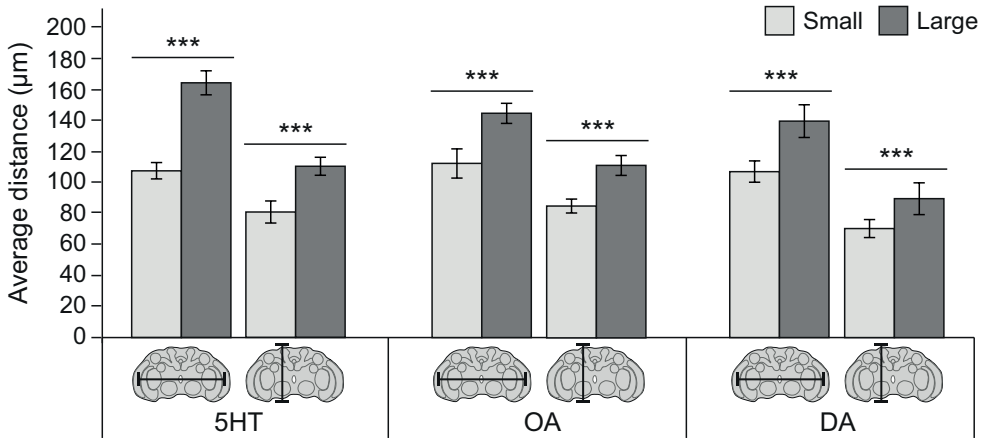

Figure 2. Difference in brain size between the small and large wasps that were used to analyse serotonin-, octopamine- and dopamine-like immunoreactive (5HT-L-IR, OA-L-IR and DA-L-IR) neurons, showing the average distance (± SD) measured from left to right medullas and from dorsal to ventral rim of the brain, as indicated in the corresponding graphs below the bars. Brain size was measured of 15 wasps per size class and monoamine treatment. Asterisks indicate significant differences in brain width or height between small and large wasps based on independent samples t-tests; *** $p < 0.001$.

package of ImageJ 1.48s. Each cell body was measured twice, and measurements of all cells within a cluster were averaged to obtain a single average value per cluster per brain.

Statistical analysis

Differences in brain width and height between small and large wasps were analysed with independent samples t-tests. Generalized linear models with Poisson distribution and log-link function were used to analyse the number of cell bodies in neuron clusters, using size class and neuron cluster as fixed factors. Type III Wald χ^2 analysis of deviance was used to test for significance of main effects. Cell body diameter was analysed with linear models, using log-transformed diameters to obtain normally distributed residuals. Analysis of variance was used to test for significance of main effects, followed by Tukey HSD post-hoc tests. In all cases, separate models were run for the separate monoamine experiments. All analyses were performed in R version 3.1.0 at $\alpha = 0.05$. Values are shown as mean ± SD.

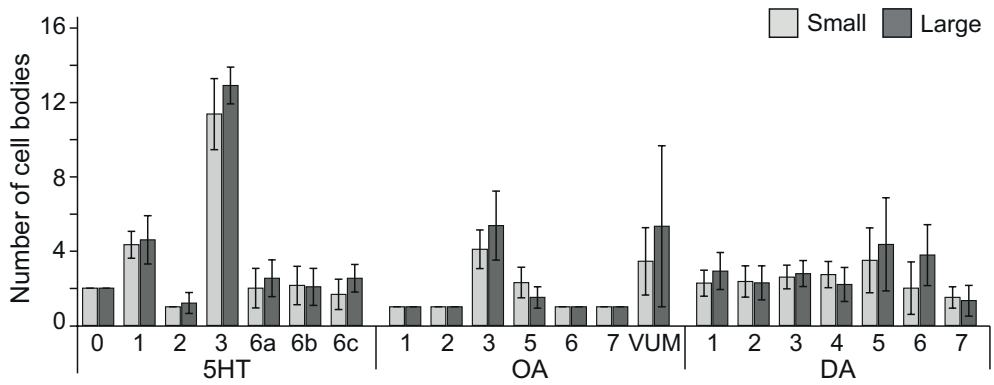

Figure 3. Average number of cell bodies (± SD) per cluster of serotonin-, octopamine- and dopamine-like immunoreactive (5HT-L-IR, OA-L-IR and DA-L-IR) neurons in small and large brains of *T. evanescens*. There was no effect of brain size on the number of cell bodies. N-values are shown in Table 2.

Results

Immunolabelling

The antisera that we used provided clear immunolabelling results, but there was a difference in the intensity of staining between the three antisera. The 5HT-L-IR staining was more intense than OA- and DA-L-IR staining. There appeared to be no differences in intensity of the immunoreactive staining between differentially sized brains. All detected neuron clusters were visible in wasps of all sizes (Figure 1). An elaborate description of the precise morphology and location of neuron clusters, also in comparison to other insects, can be found in Chapter 4.

Brain size variation

We measured the size of the brains in the small and large size classes for each of the three separate monoamine immunolabelling treatments (n = 15 for each combination of size class and monoamine treatment). Brain size was measured from left to right medulla, and from dorsal to ventral rim of the brain (Table 1, Figure 2). Small wasps had significantly smaller brain widths (5HT: $t_{25} = 23.390$, $p < 0.001$; OA: $t_{23} = 10.156$ $p < 0.001$; DA: $t_{24} = 10.028$, $p < 0.001$) and brain heights (5HT: $t_{27} = 12.572$, $p < 0.001$; OA: $t_{23} = 12.632$, $p < 0.001$; DA: $t_{22} = 6.354$, $p < 0.001$) than large wasps.

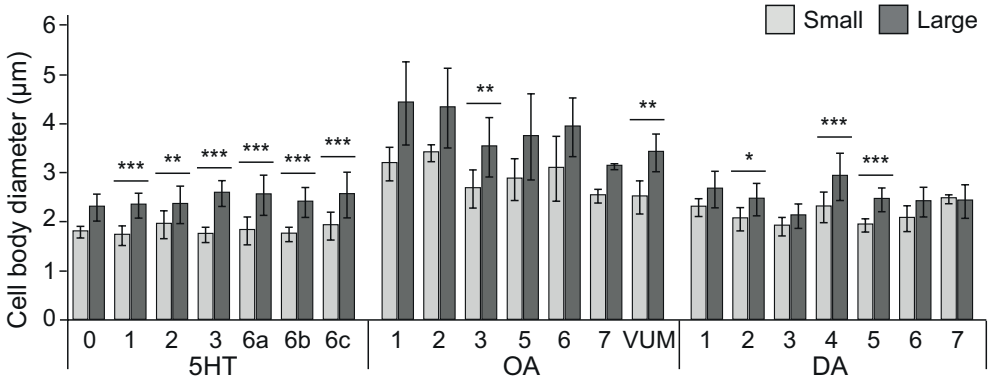

Figure 4. Average diameter (± SD) of cell bodies per cluster of serotonin-, octopamine- and dopamine-like immunoreactive (5HT-L-IR, OA-L-IR and DA-L-IR) neurons in small and large brains of *T. evanescens*. N-values are shown in Table 2. Asterisks indicate significant differences in cell body diameter between small and large wasps based on linear models and TukeyHSD post-hoc tests; * $p < 0.05$, ** $p < 0.01$, *** $p < 0.001$.

Effects of body size on number of cell bodies

Generalized linear models revealed that there was no difference in number of monoaminergic cell bodies between small and large wasps (5HT: $\chi^2_1 = 2.979$, $p = 0.084$; OA: $\chi^2_1 = 2.897$, $p = 0.089$; DA: $\chi^2_1 = 1.450$, $p = 0.229$; Figure 3, Table 2). We counted on average 20.8 ± 5.24 (n = 30) 5HT-L-IR cell bodies per brain, 9.03 ± 4.52 (n = 30) OA-L-IR cell bodies, and 14.7 ± 5.31 (n = 30) DA-L-IR cell bodies. There was a difference in the number of cell bodies between the different clusters (5HT: $\chi^2_6 = 420.791$, $p < 0.001$; OA: $\chi^2_6 = 73.034$, $p < 0.001$; DA: $\chi^2_6 = 23.553$, $p < 0.001$). Most cell bodies were observed in cluster 5HT-3, which contained up to 16 cell bodies (on average 12.1 ± 1.70). Many OA-L-IR neuron clusters contained only a single pair of cell bodies in all preparations, but cluster OA-VUM contained up to 13 cell bodies. However, the close location of this cluster to the mouthparts was vulnerable to damage during the dissection procedure, which resulted in an average count of 4.4 ± 3.36 OA-VUM neurons per brain. Table 2 shows details of the cell body counts for each neuron cluster, separately for small and large wasps, and for small and large wasps combined. The interactions between size class and neuron cluster were not significant (5HT: $\chi^2_6 = 2.073$, $p = 0.913$; OA: $\chi^2_6 = 3.351$, $p = 0.764$; DA: $\chi^2_6 = 4.527$, $p = 0.606$).

Table 2. Number and diameter of cell bodies of serotonin-, octopamine- and dopamine-like immunoreactive (5HT-L-IR, OA-L-IR and DA-L-IR) neurons in the brains of small and large *T. evanescens*.

Number of 5HT-L-IR cell bodies				
	Max.	Small	Large	Average
5HT-0	2	2.0 (n = 3)	2.0 (n = 3)	2.0
5HT-1	6	4.3 ± 0.72 (n = 15)	4.6 ± 1.30 (n = 15)	4.5 ± 1.04
5HT-2	3	1.0 (n = 15)	1.2 ± 0.56 (n = 15)	1.1 ± 0.40
5HT-3	16	11.4 ± 1.91 (n = 10)	12.9 ± 0.99 (n = 11)	12.1 ± 1.70
5HT-6a	4	2.0 ± 1.07 (n = 15)	2.5 ± 0.99 (n = 15)	2.3 ± 1.05
5HT-6b	4	2.1 ± 1.03 (n = 15)	2.1 ± 1.00 (n = 15)	2.1 ± 0.99
5HT-6c	3	1.7 ± 0.82 (n = 14)	2.5 ± 0.74 (n = 14)	2.1 ± 0.89
Number of OA-L-IR cell bodies				
	Max.	Small	Large	Average
OA-1	1	1.0 (n = 4)	1.0 (n = 5)	1.0
OA-2	1	1.0 (n = 4)	1.0 (n = 5)	1.0
OA-3	9	4.1 ± 1.04 (n = 11)	5.4 ± 1.86 (n = 11)	4.7 ± 1.61
OA-5	3	2.3 ± 0.82 (n = 10)	1.5 ± 0.58 (n = 4)	2.1 ± 0.83
OA-6	1	1.0 (n = 6)	1.0 (n = 5)	1.0
OA-7	1	1.0 (n = 3)	1.0 (n = 2)	1.0
OA-VUM	13	3.4 ± 1.81 (n = 9)	5.3 ± 4.33 (n = 9)	4.4 ± 3.36
Number of DA-L-IR cell bodies				
	Max.	Small	Large	Average
DA-1	5	2.3 ± 0.70 (n = 15)	2.9 ± 1.10 (n = 12)	2.6 ± 0.89
DA-2	4	2.4 ± 0.84 (n = 14)	2.3 ± 0.91 (n = 14)	2.3 ± 0.86
DA-3	4	2.6 ± 0.63 (n = 15)	2.8 ± 0.70 (n = 14)	2.7 ± 0.66
DA-4	4	2.7 ± 0.70 (n = 15)	2.2 ± 0.92 (n = 10)	2.5 ± 0.82
DA-5	8	3.5 ± 1.74 (n = 14)	4.4 ± 2.50 (n = 14)	3.9 ± 2.16
DA-6	6	2.0 ± 1.41 (n = 4)	3.8 ± 1.64 (n = 9)	3.2 ± 1.74
DA-7	3	1.5 ± 0.58 (n = 4)	1.3 ± 0.82 (n = 6)	1.4 ± 0.70

Cell body counts show the maximum number of cell bodies per cluster, and the average number (± SD) in small, large and all measured wasps. There was no difference in number of cell bodies per clusters between small and large wasps.

Effects of body size on size of cell bodies

Average diameters of the cell bodies in the different clusters ranged between 1.7 – 4.4 μm (Table 2). Linear models showed that cell body diameter was larger in large wasps than in small wasps (5HT: $F_{1,161} = 221.537$, $p < 0.001$; OA: $F_{1,74} = 73.495$, $p < 0.001$; DA: $F_{1,146} = 65.662$, $p < 0.001$; Figure 4). Average diameter of 5HT-L-IR cell bodies was 1.8 ± 0.23 μm (n = 88) for small wasps and 2.4 ± 0.36 μm (n = 87) for large wasps. Average diameter of OA-L-IR cell

Table 2. (cont.)

Diameter of 5HT-L-IR cell bodies				
	Small	Large	Difference	Average
5HT-0	1.8 ± 0.12 (n = 3)	2.3 ± 0.27 (n = 3)	$p = 0.581$	2.0 ± 0.33
5HT-1	1.7 ± 0.20 (n = 15)	2.3 ± 0.25 (n = 15)	$p < 0.001$	2.0 ± 0.38
5HT-2	1.9 ± 0.28 (n = 15)	2.3 ± 0.38 (n = 15)	$p = 0.007$	2.1 ± 0.39
5HT-3	1.7 ± 0.16 (n = 10)	2.6 ± 0.26 (n = 11)	$p < 0.001$	2.1 ± 0.48
5HT-6a	1.8 ± 0.28 (n = 15)	2.5 ± 0.41 (n = 15)	$p < 0.001$	2.2 ± 0.48
5HT-6b	1.7 ± 0.15 (n = 15)	2.4 ± 0.30 (n = 15)	$p < 0.001$	2.1 ± 0.41
5HT-6c	1.9 ± 0.29 (n = 14)	2.5 ± 0.46 (n = 14)	$p < 0.001$	2.2 ± 0.50
Diameter of OA-L-IR cell bodies				
	Small	Large	Difference	Average
OA-1	3.2 ± 0.34 (n = 4)	4.4 ± 0.85 (n = 5)	$p = 0.101$	3.9 ± 0.91
OA-2	3.4 ± 0.17 (n = 4)	4.3 ± 0.81 (n = 5)	$p = 0.576$	3.9 ± 0.76
OA-3	2.7 ± 0.39 (n = 11)	3.5 ± 0.60 (n = 11)	$p = 0.006$	3.1 ± 0.66
OA-5	2.9 ± 0.42 (n = 10)	3.7 ± 0.87 (n = 4)	$p = 0.200$	3.1 ± 0.68
OA-6	3.1 ± 0.66 (n = 6)	3.9 ± 0.60 (n = 5)	$p = 0.264$	3.5 ± 0.74
OA-7	2.5 ± 0.14 (n = 3)	3.1 ± 0.06 (n = 2)	$p = 0.949$	2.8 ± 0.35
OA-VUM	2.5 ± 0.34 (n = 9)	3.4 ± 0.38 (n = 9)	$p = 0.003$	3.0 ± 0.58
Number of DA-L-IR cell bodies				
	Small	Large	Difference	Average
DA-1	2.3 ± 0.18 (n = 15)	2.7 ± 0.37 (n = 12)	$p = 0.134$	2.5 ± 0.33
DA-2	2.1 ± 0.24 (n = 14)	2.5 ± 0.33 (n = 14)	$p = 0.011$	2.3 ± 0.35
DA-3	1.9 ± 0.19 (n = 15)	2.1 ± 0.25 (n = 14)	$p = 0.527$	2.0 ± 0.24
DA-4	2.3 ± 0.31 (n = 15)	2.9 ± 0.48 (n = 10)	$p < 0.001$	2.5 ± 0.49
DA-5	1.9 ± 0.13 (n = 14)	2.5 ± 0.24 (n = 14)	$p < 0.001$	2.2 ± 0.33
DA-6	2.1 ± 0.26 (n = 4)	2.4 ± 0.30 (n = 9)	$p = 0.704$	2.3 ± 0.32
DA-7	2.5 ± 0.09 (n = 4)	2.4 ± 0.34 (n = 6)	$p = 1.000$	2.4 ± 0.26

Average cell body diameters (± SD) are shown for small, large and all measured wasps. Differences in cell body diameter between small and large wasps are based on linear models and TukeyHSD post-hoc tests.

bodies was 2.8 ± 0.48 μm (n = 47) for small wasps and 3.8 ± 0.71 μm (n = 41) for large wasps. The average diameter of DA-L-IR cell bodies was 2.1 ± 0.28 μm (n = 81) for small wasps and 2.5 ± 0.39 μm (n = 79) for large wasps. Tukey HSD post-hoc tests (Table 2) revealed that cell body diameters differed between small and large wasps for all 5HT-L-IR clusters except cluster 5HT-0. In contrast, the only OA-L-IR and DA-L-IR clusters that differed in diameter between small and large wasps were cluster OA-3, OA-VUM, DA-4 and DA-5.

Serotonergic cell bodies are similarly sized in all clusters ($F_{6,161} = 1.652$, $p = 0.136$), whereas the diameters of octopaminergic ($F_{6,74} = 6.065$, $p < 0.001$) and dopaminergic ($F_{6,146} = 12.266$, $p < 0.001$) cell bodies vary between different clusters. The interactions between size class and cell body diameter were not significant (5HT: $F_{6,161} = 1.554$, $p = 0.164$; OA: $F_{6,74} = 0.164$, $p = 0.986$; DA: $F_{6,146} = 2.166$, $p = 0.050$).

Discussion

Our results show that isometric brain scaling in *T. evanescens* may be facilitated by plasticity in the size of the cell bodies, rather than in the numbers of monoaminergic neurons. Small and large wasps show no differences in the number of serotonergic, dopaminergic and octopaminergic cell bodies in their brains, but they do show differences in the size of these cell bodies. This suggests that monoaminergic neurons support neural and behavioural functions that are vital for even the smallest wasps. Maintaining the number of monoaminergic neurons may maintain cognitive and behavioural complexity, and allow even the smallest wasps to find suitable hosts.

Isometric brain scaling results in brains that are smaller than predicted by Haller's rule in small *T. evanescens*, and in brains that are larger than predicted in large *T. evanescens*. We expected that this extreme brain size plasticity required modifications to the number and size of neurons. Specifically, we hypothesized that plasticity in cell body size alone would not be sufficient to achieve isometric brain scaling, because cell body size may approach functional limits in small wasps. We expected that an additional decrease of neuron number would be required to achieve the smallest brains. Our results show a difference in neuronal cell body size between small and large wasps, but no difference in the number of monoaminergic neurons. This indicates that plasticity in cell-body size, at least in these specific sets of neurons, can be sufficient to achieve isometric brain scaling.

Similar modifications are shown on neuropil level in the antennal lobe. The antennal lobe consists of several spherical glomeruli, which are functional units that contain the synapses of olfactory receptor neurons, projection neurons and interneurons (Hansson and Anton, 2000). We have previously shown that the number of antennal lobe glomeruli is similar in small and large *T. evanescens*, but there is plasticity in glomerular volume (Chapter 3). The combined results of the present and previous studies indicate that neural complexity can be similar

in small and large wasps, at least on the level of neuropil structures and of individual neurons. However, differences in neural complexity may occur on other levels, such as those of synaptic connections.

The number of neurons inside a brain is an important component of its computational power (Chittka and Niven, 2009). Hence, the similarities in the numbers of monoaminergic cell bodies and antennal lobe glomeruli in small and large wasps could imply that the function of neuropil structures and neural pathways is also maintained. We have previously investigated memory retention capacities of small and large wasps after a single olfactory or visual conditioning experience (Chapter 6). We indeed found that small and large wasps show similar memory retention levels and duration of memory retention. Plasticity in the size of neuronal cell bodies and neuropil structures may be one of the mechanisms that underlie isometric brain scaling and simultaneously maintains cognitive abilities.

Maintained numbers of neurons may be specific for these monoaminergic clusters, or a general effect of isometric brain scaling that is also shown in other neuronal systems. If neuron numbers are only maintained in these specific monoaminergic neuron clusters, this may mean that modifications of these clusters are too costly, for example because they facilitate the high level of behavioural and cognitive complexity that is required to locate suitable host eggs. If neuron numbers are generally maintained in all neuronal systems, this may have evolved as a consequence of selection pressures on body miniaturization. *Trichogramma* wasps can parasitise and develop inside very small host eggs. Some of the smallest hosts can only support a single developing *T. evanescens* that will develop into a small adult (Salt, 1940). The limited availability of nutrients in such small hosts may severely constrain development, especially the investment in metabolically expensive tissues such as the brain (Aiello and Wheeler, 1995). These selection pressures may have resulted in the evolution of miniaturized neural pathways that support the behavioural and cognitive requirements of even the smallest *T. evanescens* wasps. The larger size of neuronal cell bodies of large wasps indicates that there may be costs associated with having small neurons, which outweigh the benefits of increased numbers of neurons. These costs may not be associated with memory retention (Chapter 6), but can be present in other neural, behavioural or physiological traits.

Although smaller neurons are more energy-efficient than larger neurons (Niven, 2016), there are costs associated with reducing neuron size. The reduction of neural membrane area results in less space for ion channels, which increases neural noise (Niven and Farris, 2012). Smaller neurons can also have thinner neurites

with reduced neural firing rates (Niven, 2016). They may also have a reduced number of arborisations and a lower level of connectivity between neurons. Reduction of cytoplasm volume may reduce the available space for mitochondria, and may therefore negatively affect the generation of energy (Niven and Farris, 2012). A reduction of cell body volume may also affect the volume of the cell organelles, of which the nucleus is the largest. A reduction of nucleus size may involve modifications of genome size or chromatin compaction (Gregory, 2001; Polilov, 2015). These modifications may compromise neural functioning, because they affect transcription dynamics. Even more extreme reductions of cell body size are shown by another minute member of the family Trichogrammatidae, the 0.2 mm long *Megaphragma mymaripenne* (Polilov, 2012). Approximately 95% of the neural nuclei lyse during pupal development, resulting in an adult brain with mostly anucleate neurons. Lysis of neural nuclei has not been observed in *T. evanescens* (Polilov, 2016). The lack of nuclei implies that anucleate neurons are incapable of genetic transcription, which may severely impair neural functioning in adult *M. mymaripenne*. This may cause reduced longevity of *M. mymaripenne* compared to other wasps of the family Trichogrammatidae, and could explain why honey-fed *M. mymaripenne* live on average five days at a temperature of 25°C (Bernardo and Viggiani, 2000), whereas e.g. *Trichogramma minutum* live on average 25 days at the same temperature (Yu et al., 1984).

The costs of having small cell bodies may be similar for small *T. evanescens* as described above. Small wasps may have cell bodies with a higher level of chromatin compaction, which may hinder transcription, and less space for mitochondria, which may negatively affect the available amount of energy. Although we could not accurately establish this with the present methodology, neurites of small *T. evanescens* may also be reduced in size and in arborisation complexity. This can result in lower information processing rates and increased neural noise (Niven, 2016). These neural modifications could negatively affect fitness, for example by contributing to the reduced longevity of small *T. evanescens* compared to larger conspecifics (Waage and Ming, 1984; Doyon and Boivin, 2005). Having larger neurons may be a factor that contributes to higher longevity of large wasps. Whether the ratio between nucleus and cell body size was different in small and large *T. evanescens* could not be observed in this study, because the separation between the antibody- and propidium iodide-stained channels was not clear enough to accurately measure nucleus size. More detailed TEM studies are required to show if neuronal cell body size is modified through changes to the volume of cytoplasm, the nucleus, or both, and if the size and connectivity of neurites is similarly affected. This may reveal if the lower limit to neuron size is reached in the smallest *T. evanescens*.

In conclusion, the results of this study shed light on how the smallest insects manage to evade Haller's rule. In the monoaminergic systems that we studied, isometric brain scaling appears to be facilitated by modification of neuronal cell body size, whereas neuron numbers are maintained. These modifications resemble those on neuropil level in the antennal lobe, where glomerular volumes differ in small and large wasps, but numbers of glomeruli are maintained (Chapter 3). The absence of changes in the numbers of monoaminergic cell bodies and antennal lobe glomeruli suggests that the performance of neural pathways may be similar in small and large *T. evanescens*, which corresponds to our previous findings of similar olfactory and visual memory retention in small and large wasps (Chapter 6). Plasticity in the size of neuronal cell bodies may be one of the 'tricks' to evade Haller's rule and simultaneously maintain cognitive abilities in the smallest wasps. However, differences in neural complexity between small and large wasps may occur on levels outside the scope of the present study, such as those of synapses, which should be identified in further research.

Acknowledgements

We thank the Max Planck Institute for Chemical Ecology (Jena, Germany) for providing *Manduca sexta* pupae; Léon Westerd, Frans van Aggelen and André Gidding for culturing *Mamestra brassicae*; the experimental farm of Wageningen University (Unifarm) for growing the tobacco plants; Norbert de Ruijter (Wageningen University, Laboratory of Cell Biology) and Henk Schipper (Wageningen University, Experimental Zoology) for use of the confocal laser scanning microscopes; and Marcel Dicke for constructive comments on a previous version of this article. This work was supported by NWO PE&RC Graduate Program grant 022.002.004 (to EW) and by NWO Open Competition grant 820.01.012 (to HS).

Chapter 6

Differential effects of brain scaling on memory performance in parasitic wasps

Emma van der Woude,
Martinus E. Huigens,
Hans M. Smid

Abstract

Small animals usually have relatively larger brains than large animals. This allometric brain scaling is described by Haller's rule. However, some of the smallest insects on Earth scale their brains beyond the predictions of Haller's rule. *Trichogramma evanescens* parasitic wasps show brain isometry, leading to similar relative brain sizes in small and large conspecifics. Somewhat larger *Nasonia vitripennis* parasitic wasps display diphasic brain scaling with isometry in small individuals and allometry in large individuals. These brain-scaling strategies may cause undersized brains in small wasps, with reduced cognitive abilities. Here, we induced intraspecific body-size variation in genetically identical *T. evanescens* and *N. vitripennis*, and examined cognitive trade-offs of brain scaling. We compared visual and olfactory memory retention between small and large conspecifics. Results show that diphasic brain scaling affects memory retention levels in *N. vitripennis*, whereas isometric brain scaling does not affect memory retention in *T. evanescens*. The two species may experience different evolutionary pressures that shaped the cognitive consequences of brain scaling. A possible trade-off of brain isometry in *T. evanescens* could be present in brain properties different from memory performance. In contrast, it may be more adaptive for *N. vitripennis* to invest in other aspects of brain performance, at the cost of memory retention.

Introduction

An individual's ability to learn and memorize has been related to the size of the brain, both absolute brain size and the size of the brain relative to total body size (Kotrschal et al., 2013; Roth and Dicke, 2005; Striedter, 2005). However, relative brain size also directly depends on body size: small animals have relatively larger brains than large animals. This is known as Haller's rule, and generally applies within and between animal species in all taxa (Gonda et al., 2011; Harvey and Krebs, 1990; Isler et al., 2008; Kruska, 1996; Pagel and Harvey, 1989; Rensch, 1948; Riveros and Gronenberg, 2010; Seid et al., 2011; Stuermer et al., 2003; Wehner et al., 2007). Haller's rule follows a power-law function in which the exponent, the scaling coefficient, determines the shape of the relationship. The more the scaling coefficient approaches 0, the stronger the negative allometry that Haller's rule describes. A scaling coefficient that equals 1 describes a linear relationship, known as isometry.

The brain scaling phenomenon described by Haller's rule may be a consequence of mechanisms through which neural architecture determines behavioural output. It is the absolute, not relative, number and size of neurons and connections that determines neural processing power (Chittka and Niven, 2009). Small animals may thus need to form relatively larger brains to achieve similar levels of neural processing abilities as large animals (Eberhard and Wcislo, 2011). This directly implies that small animals suffer high energetic costs, because brain tissue has a high metabolic rate (Aiello and Wheeler, 1995). These energetic costs can become too high to be overcome by the smallest animals, which limits body miniaturization (Eberhard and Wcislo, 2011). Interestingly, some of the smallest insects appear to have evolved unique brain scaling solutions that deviate from the predictions of Haller's rule, possibly to avoid the energetic costs of having a relatively large brain (see Groothuis and Smid (2017) for a recent overview of brain scaling in differently-sized insects). An example is shown by polymorphic leaf-cutter ants (*Atta colombica*), which vary in body length between 5 – 10 mm (Feener et al., 1988). Workers show an allometric relationship between brain and body size (Seid et al., 2011). However, a break point splits the allometry into two separate functions. Larger ants show a scaling coefficient of 0.29, which is comparable to scaling coefficients found for other ant species (Wehner et al., 2007). Haller's rule is less strong in smaller ants, which have a much larger scaling coefficient of 0.60. The brains of small ants are, therefore, smaller than is expected from the predictions of Haller's rule.

Another example is shown by smaller *Nasonia vitripennis* parasitic wasps (Figure 1A). These wasps parasitise and develop inside fly puparia. Adult body size

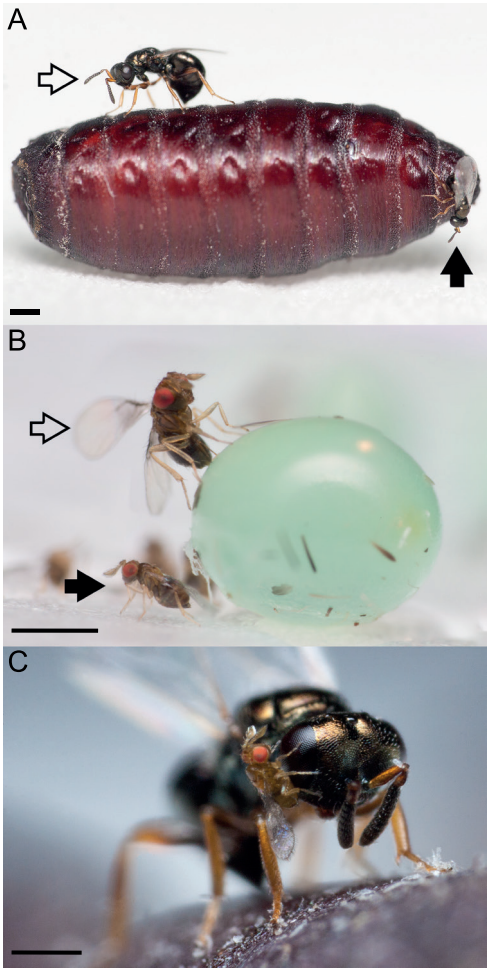

Figure 1. Phenotypic plasticity in body size, showing large (open arrows) and small (black arrows) wasps of the species used in this study. **(A)** *N. vitripennis* on a *C. vomitoria* host pupa. **(B)** *T. evanescens* on an *M. sexta* host egg. **(C)** A small *T. evanescens* on the head of a large *N. vitripennis*, illustrating the difference in body size between the two species. Scale bars indicate 0.5 mm. Pictures: Jitte Groothuis.

depends on the number of developing larvae inside the same host pupa through scramble competition, resulting in body lengths ranging between 1.2 – 2.4 mm measured from thorax to abdomen tip (Groothuis and Smid, 2017). Again, a break point divides the wasps into two groups with distinct brain scaling strategies. Interestingly, larger wasps follow Haller's rule, whereas the smallest wasps show isometric brain scaling (Figure 2A).

The most extreme brain scaling solution is shown by some of the smallest insects on Earth, *Trichogramma evanescens* parasitic wasps (Figure 1B). These minute wasps parasitise and develop inside lepidopteran eggs. Adult body size depends on scramble competition in a similar way as in *N. vitripennis*, resulting in body lengths ranging between 0.3 – 0.9 mm (Chapter 2; Chapter 3). *Trichogramma evanescens* wasps scale their brains isometrically with body size (Chapter 2; Figure 2A). A consequence of this brain isometry is that small and large individuals have the same relative brain size, with brains that are much smaller in the smallest *T. evanescens* and much larger in the largest *T. evanescens* than is predicted by Haller's rule.

The abovementioned examples show that Haller's rule does not apply to the smallest insects, possibly because small invertebrates avoid the excessive energetic costs that are associated with a relatively larger brain. Isometric brain scaling may enable smaller body sizes than would have been possible under allometric brain

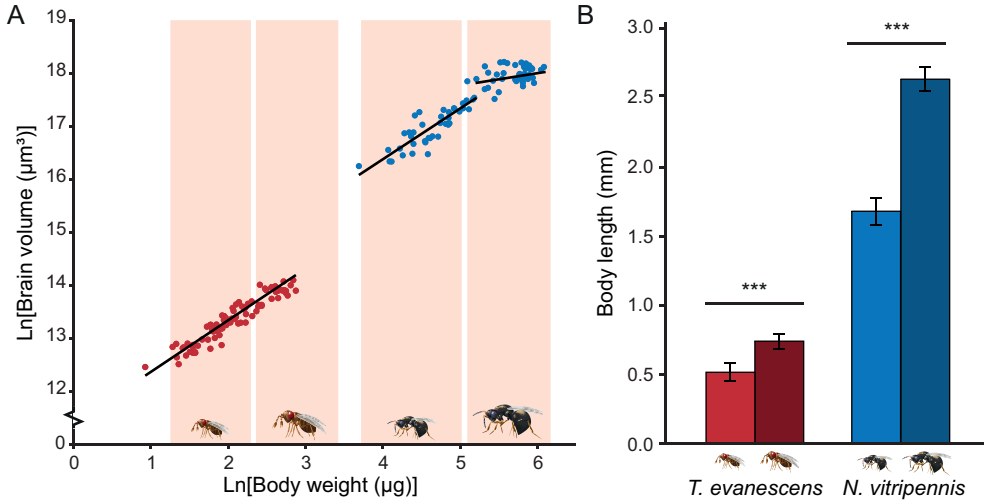

Figure 2. Brain- and body-size scaling in *T. evanescens* and *N. vitripennis*. **(A)** Brain-body size scaling is isometric in *T. evanescens* (red dots, data from Chapter 2), and diphasic in *N. vitripennis* with isometry in small individuals and negatively allometric in large individuals (blue dots, data from Groothuis and Smid, 2017). Red blocks indicate the estimated correspondence to the size classes in the present study, based on body length measurements in Chapter 2 and Groothuis and Smid (2017). Note that the largest body lengths of *T. evanescens* in the present study exceed the measured body lengths in Chapter 2, due to the use of larger host species. Body volume data from Chapter 2 were converted to body weights under the assumption of a similar density as water. **(B)** Body length measurements (mean ± SD) of the large and small size classes of *T. evanescens* (red bars) and *N. vitripennis* (blue bars) in the present study. Body length was measured from the head to the tip of the abdomen. Asterisks indicate significant differences based on Welch two-sample t-tests (*** $p < 0.001$).

scaling. However, brain isometry may simultaneously cause trade-offs with brain performance. Brains that are miniaturized beyond the predictions of Haller's rule may become too small to maintain neural processing abilities. The smallest invertebrates could consequently show impaired learning abilities and reduced memory retention, and suffer more from the metabolic costs that are associated with forming and retaining long-term memory (Hoedjes et al., 2011; Margulies et al., 2005; Mery and Kawecki, 2005; Snell-Rood et al., 2009).

In the present study, we examined cognitive trade-offs of isometric brain scaling. We compared memory performance (level and duration of memory retention) of small and large conspecifics of *T. evanescens* and *N. vitripennis* (Figure 1C), both after visual and olfactory conditioning. *Nasonia vitripennis* can form long-term memory of olfactory cues after a single experience of drilling a hole in the host pupa and feeding from its contents (Hoedjes and Smid, 2014; Schurmann et al.,

2012). *Trichogramma evanescens* naturally hitch-hike on mated female butterflies, which enables them to parasitise freshly laid eggs and form long-term memory of the butterfly's anti-aphrodisiac pheromone (Huigens et al., 2009; Kruidhof et al., 2012). Associative learning of colours is less frequently studied in these species, but has been described in both (Keasar et al., 2000; Oliai & King, 2000).

We hypothesize that isometric brain scaling compromises memory performance in small wasps of both species, because brain isometry might reduce brain size beyond the size that is required to maintain brain performance. We expect that these effects are more pronounced in *T. evanescens* than in *N. vitripennis*, because brain isometry in *T. evanescens* causes more strongly miniaturized brains in small individuals than does isometric – allometric brain scaling in *N. vitripennis*.

Materials and methods

Insects

Trichogramma evanescens Westwood (Hymenoptera: Trichogrammatidae) of inbred strain GD011 were reared on UV-irradiated host eggs of Mediterranean flour moth *Ephestia kuehniella* (Lepidoptera: Pyralidae; obtained from Koppert Biological Systems, Berkel en Roderijs, The Netherlands; Huigens et al., 2009; Chapter 2). The wasps were kept in a climate room (22 ± 1°C, 50 – 70% rh, L16:D8), and used to create body-size variants as described below.

Nasonia vitripennis Walker (Hymenoptera: Pteromalidae) of inbred strain AsymCx were reared on *Calliphora vomitoria* pupae (obtained as maggots from Kreikamp, Hoevelaken, The Netherlands) in a climate cabinet (25 ± 1°C, L16:D8; Hoedjes et al., 2012). These pupae were also used as unconditioned stimulus in the conditioning assays of *N. vitripennis*.

Cabbage moths *Mamestra brassicae* (Lepidoptera: Noctuidae) were reared on cabbage plants (*Brassica oleracea*) in a climate room (21 ± 2°C, 50 – 70% rh, L16:D8). Adult moths oviposited on sheets of filter paper, which were used as unconditioned stimulus in conditioning assays of *T. evanescens*. *Manduca sexta* hawkmoths (Lepidoptera: Sphingidae; obtained as pupae from the Max Planck Institute for Chemical Ecology, Jena, Germany) were kept in a flight cage with tobacco plants (*Nicotiana tabacum* SR1) inside a climate cabinet (25 ± 1°C, L16:D8; Chapter 3). Eggs were harvested daily from this cage, stored at -20°C and used to rear small and large *T. evanescens*.

Induction of body size variation

We manipulated wasps to lay either large or small numbers of eggs inside their hosts (Figure 3A). This results in different levels of scramble competition inside the host egg or pupa, leading to a large variation in body size. Body-size variants of *N. vitripennis* were induced with adapted wasp-to-host ratios (Groothuis & Smid, 2017). The smallest offspring emerged after parasitism of 5 *C. vomitoria* pupae by 50 *N. vitripennis*, and the largest offspring after parasitism of 20 pupae by 10 females. Wasps were removed from the pupae after 24 hours.

Wasps of the genus *Trichogramma* assess host-egg size through antennal drumming of the host surface (Schmidt & Smith, 1985). To induce body-size variation in *T. evanescens*, we therefore partially masked the surface of some *M. sexta* eggs by placing them on 5 – 10 ml cooling 1% agarose (Sigma) in Petri dishes (Greiner Bio-One, 94 × 15 mm) as described before (Chapter 3). This partial masking of host eggs resulted in smaller host-egg surfaces available for size assessment by the wasps. Fewer eggs were laid inside these masked hosts, which developed into larger offspring than generally emerged from unmasked host eggs. To ensure that large and small wasps were both available, we used a combination of masked and unmasked eggs.

For both species we created small and large size classes by visually inspecting body sizes. To determine body size of these classes, we sampled 100 large and 100 small *T. evanescens* and *N. vitripennis* wasps from 2 separate generations. These wasps were CO_2-sedated and their body length was measured from head to abdomen tip, and from thorax to abdomen tip, using a microscope ocular with an internal reticle scale (Table 1). Wasps of both species had unlimited access to honey and water until use in the conditioning trials.

Conditioning procedures

Females of both wasp species were trained to remember an odour or colour as illustrated in Figure 3B. We used single classical conditioning trials as described before (Hoedjes et al., 2014b; Hoedjes et al., 2012). Wasps obtained a rewarding experience with a host (the unconditioned stimulus, US) while perceiving a conditioned stimulus (CS+); either a colour or odour. Next, the wasps received an unrewarding experience (absence of hosts) on a different conditioned stimulus (CS-); another colour or odour. Conditioning procedures were carried out reciprocally, using either two odours or two colours as conditioned stimuli. Half of the groups were conditioned using the first of the two conditioned

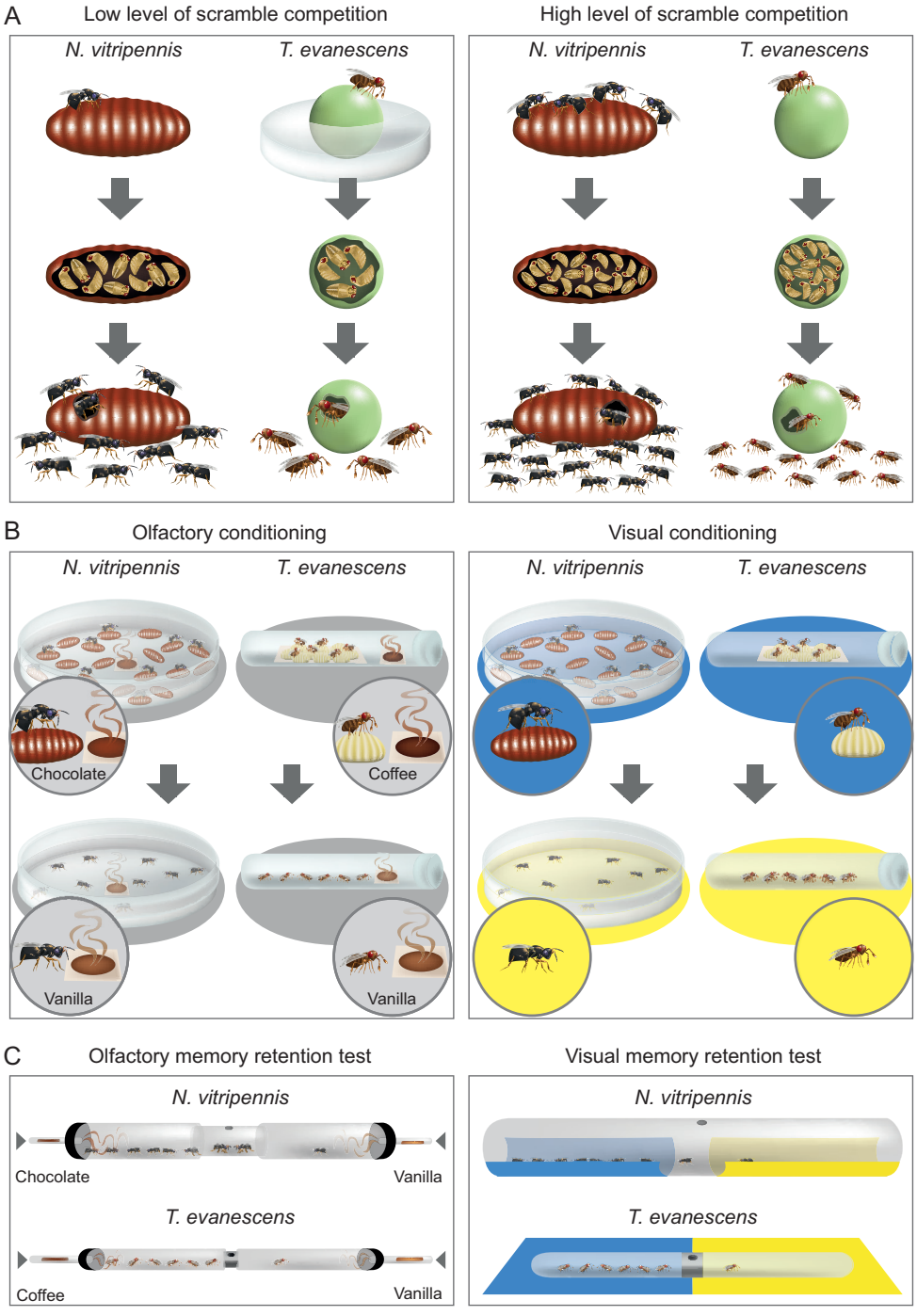
A
Low level of scramble competition
High level of scramble competition
N. vitripennis
T. evanescens
N. vitripennis
T. evanescens
B
Olfactory conditioning
Visual conditioning
N. vitripennis
T. evanescens
N. vitripennis
T. evanescens
Chocolate
Coffee
Vanilla
Vanilla
C
Olfactory memory retention test
Visual memory retention test
N. vitripennis
N. vitripennis
Chocolate
Vanilla
T. evanescens
T. evanescens
Coffee
Vanilla

◄ **Figure 3.** Experimental set-up as used in this study. **(A)** Variation in body size was created by inducing either low (left) or high (right) levels of scramble competition inside the hosts of *N. vitripennis* and *T. evanescens*. For *N. vitripennis*, we varied the ratio between ovipositing females and their *C. vomitoria* host pupae. For *T. evanescens*, we adapted the perceivable host egg surface by partially masking the host eggs with agarose. Females will lay fewer eggs if they perceive a smaller area when drumming on the egg surface with their antennae. **(B)** During conditioning, the wasps experience either an odour (left) or a colour (right) (CS+), while parasitising a host egg or pupa (US). This is followed by a resting phase in a clean Petri dish or vial on a neutral background (not shown in the figure). Next, the wasps experience the second odour or colour without the presence of the rewarding hosts (CS-). The conditioning procedures are done in a reciprocal manner: half of the groups receive the first odour or colour as CS+ and the other half of the groups receive the second odour or colour as CS+. Small and large wasps are trained simultaneously in separate groups. **(C)** To test memory retention, the wasps are placed in the centre of T-mazes that contain the CS+ and CS- on opposite sides. The number of wasps that make a choice for the CS+ and CS- is recorded. Arrowheads at the olfactory T-mazes indicate an incoming flow of humidified air.

stimuli as CS+ and the second as CS-, and the other half of the groups received the second of the two conditioned stimuli as CS+ and the first as CS-. In total, we conditioned 151 reciprocal groups of *N. vitripennis* and 198 reciprocal groups of *T. evanescens*.

Female *T. evanescens* (2 days old) were conditioned inside glass vials (7.5 cm long, 1.2 cm diameter) in groups of approximately 50 wasps. Pieces of filter paper (~1 cm^2) with a clutch of approximately 30 *M. brassicae* eggs were used as US. Female *N. vitripennis* (2 days old) were conditioned in Petri dishes (8.5 cm diameter) in groups of approximately 50 wasps. These dishes contained approximately 40 *C. vomitoria* pupae as US and were covered with filter paper.

The duration of the CS+ phase was 15 minutes for *T. evanescens* and 1 hour for *N. vitripennis*. The difference in duration of the CS+ phase relates to the difference in time it takes the two species to start laying eggs in these particular host species. For *T. evanescens*, drilling in *M. brassicae* takes a short time and the wasps start oviposition within minutes after finding the host. They were removed after 15 minutes to ensure that they had sufficient time to start oviposition, but also remain motivated to find hosts during the subsequent memory retention tests. Initiating oviposition takes a longer time for *N. vitripennis*. During an hour-long experience on a *C. vomitoria* host, the wasps will drill into the pupa and start feeding from its contents (Hoedjes et al., 2014a).

After the CS+ phase, the wasps were removed from their hosts with an aspirator (with additional aid of fine tweezers for *T. evanescens*) and placed in clean vials

or dishes on neutral backgrounds for a resting period of 15 minutes. This was followed by the CS- phase, which lasted for 15 minutes for both species.

Olfactory conditioning trials were performed using Royal Brand Bourbon Vanilla extract and Natural Chocolate extract as CS for *N. vitripennis*, and Royal Brand Bourbon Vanilla extract and Natural Coffee extract for *T. evanescens* (Nielsen-Massey Vanillas Intl., Leeuwarden, the Netherlands). These artificial odours were chosen because they represent neutral stimuli for the wasps, for which they do not show innate preferences. Chocolate and vanilla have previously been found to be most suitable for olfactory conditioning in *N. vitripennis* (Hoedjes et al., 2012). For *T. evanescens*, pilot experiments revealed that using coffee extract instead of chocolate induced higher memory retention levels (not shown). The extracts were placed on pieces of filter paper (~1 cm^2) in drops of 1 µl for *T. evanescens* and 5 µl for *N. vitripennis*, and placed inside the conditioning vial or dish during the CS+ and CS- phases.

Visual conditioning trials were performed with the colours blue and yellow as CS for both species (Clairefontaine Trophée 120 g/m^2 hues 1291 and 1292 for *T. evanescens* and hues 1247 and 1292 for *N. vitripennis*). Blue and yellow have previously been used as visual stimuli in conditioning experiments with *N. vitripennis* (Oliai & King, 2000). Using a slightly brighter shade of blue for *N. vitripennis* and a slightly darker shade for *T. evanescens* improved memory retention levels for both species during pilot experiments (not shown). For *T. evanescens*, the conditioning vials were placed in boxes (10.5 × 15.5 cm) that were lined with blue or yellow paper. For *N. vitripennis* the conditioning dishes were placed on blue or yellow paper. The conditioning procedures took place in areas that were shielded from environmental light, and lit by 4 fluorescent tubes (Philips Master TL5 H0 39W/865 for *T. evanescens* and Philips Master TL5 H0 39W/840 for *N. vitripennis*).

Memory retention tests

Memory retention (Figure 3C) was tested 1, 4 and 24 hours after conditioning. Olfactory memory was retained longer than 24 hours in *N. vitripennis*, and was therefore tested 1, 3 and 5 days after conditioning. A third of each group of 50 wasps was tested at each time point, ensuring that each individual wasp was tested only once.

Olfactory memory of *N. vitripennis* was tested in the T-maze described by Hoedjes et al. (2012). An adapted version of this T-maze was used for *T. evanescens*,

consisting of two transparent, polycarbonate tubes (1.6 cm diameter, 11 cm long) that connected smoothly to a 3 cm-long central aluminium tube. Both types of T-mazes contained a small opening to insert wasps and fine mesh to allow air flow to leave the T-maze. The distal ends were connected to Teflon tubes that contained a single glass capillary (ID 1.3 mm, Stuart SMP1/4, Bibby Scientific, Staffordshire, UK) for odour transmission on each side of the T-maze. One side contained a capillary filled with vanilla extract, and the other side contained chocolate extract in the T-maze for *N. vitripennis* and coffee extract in the T-maze for *T. evanescens*. Charcoal filtered, moisturized air (60 – 70% relative humidity) flowed past odour capillaries at 100 ml/min per side for *N. vitripennis* and 30 mL/min per side for *T. evanescens*.

Visual memory retention in *N. vitripennis* was tested in 40-cm-long polycarbonate tubes (3.6 cm diameter; Kunststofshop, Zevenaar, the Netherlands). The lower half of the tubes was covered with blue paper on one side, and yellow paper on the other side. The central 5 cm were left transparent and contained a small hole for insertion of wasps.

Visual memory retention in *T. evanescens* was tested in a T-maze that was constructed from two glass vials (15 cm long, 1.8 cm diameter). The vials were connected by aluminium tubes similar to those that connected the olfactory T-maze. The setup was placed in a box (10.5 × 40 × 5 cm) lined with blue paper on one side and yellow paper on the other side.

All memory retention tests took place in areas that were shielded from environmental light. The olfactory T-maze for *N. vitripennis* was illuminated by a LED strip (Grandi 'white' 6000-6500K, 170 lm/m with 30 leds/m mounted against a white shelf 40 cm above the T-maze), the other T-mazes were lit by the same TL tubes that were used during conditioning. Wasps were inserted into the T-mazes with an aspirator. After 10 minutes, the number of wasps on each side of the T-maze was counted. Wasps in the central areas were considered as non-responding. The orientation of the T-mazes was reversed after two tests to prevent any bias from environmental influences.

Statistical analysis

Differences in body length between size classes were analysed with Welch two sample t-tests. Memory retention was expressed as performance index (PI; Hoedjes et al., 2012). The PI was calculated by taking the fraction of wasps that made a choice for the odour or colour of their CS+, and subtracting the fraction

of wasps from the other reciprocal group that made a choice for the odour or colour that they experienced as CS-. A PI for visual memory retention, for example, is calculated by subtracting the fraction of wasps that received yellow as CS+ and chose blue, from the fraction of wasps that received blue as CS+ and chose blue.

The fractions that were used to calculate PIs were obtained as estimated response means of generalized linear mixed models (GLMMs) with logit link function and binomial distribution. The models' dependent variables were the number of wasps on one side of the T-maze (on blue for visual memory retention tests, on coffee for olfactory memory retention tests with *T. evanescens*, and on chocolate for olfactory memory retention tests with *N. vitripennis*), with the total number of wasps making a choice as denominator. The model response of visual memory retention tests, for example, is therefore the fraction of wasps that chose blue over yellow. Including CS+ as fixed effect allowed to test for the effect of conditioning on the preference for the two odours or colours that were used as conditioned stimuli. Other fixed effects that were included in the model were time after conditioning, body size class and the interactions between fixed effects. Random effects were included to correct for conditioning date and the reciprocal conditioning pair the wasps belonged to.

To test if memory was formed, Bonferroni-corrected χ^2 pairwise comparisons were used to test the effect of CS+ on the preference for conditioned stimuli. In case of a significant main effect of body size on memory retention, post-hoc χ^2 pairwise comparisons tested if memory retention differed between the size classes within the different time points after conditioning. Response rates of wasps were determined by defining another GLMM using the fraction of wasps making a choice out of the total number of wasps inserted as dependent variable. Fixed factors were size and time after conditioning. Differences in response rate of small and large wasps were determined using Bonferroni-corrected χ^2 pairwise comparisons. Statistical analyses were performed in R 3.0.2 with packages lme4 (Bates et al., 2014), phia (De Rosario-Martinez) and lsmeans (Lenth, 2014).

Results

Body size variation

Body length ranged between 0.367 – 0.967 mm in *T. evanescens* and 1.375 – 2.825 mm in *N. vitripennis* (Table 1, Figure 2B). When body length was measured from

the thorax to abdomen tip (thereby excluding the head), this length ranged between 0.311 – 0.856 mm in *T. evanescens* and 1.175 – 2.475 mm in *N. vitripennis*. Average body length (±SD) in *T. evanescens* was larger (0.745 ± 0.054 mm) in the large size class than in the small size class (0.521 ± 0.064 mm; $t_{192.51} = 26.766$, $p < 0.001$). In *N. vitripennis*, average body length was 2.634 ± 0.085 mm in the large size class and 1.681 ± 0.099 mm in the small size class, and significantly different between the size classes ($t_{193.44} = 72.929$, $p < 0.001$). Average thorax – abdomen length in *T. evanescens* was 0.654 ± 0.052 mm in the large size class, and 0.444 ± 0.058 mm in the small size class, and also differed between the size classes ($t_{192.26} = 26.880$, $p < 0.001$). In *N. vitripennis*, average thorax-abdomen length was 2.330 ± 0.078 mm in the large size class and 1.450 ± 0.094 mm in the small size class, also significantly different ($t_{191.71} = 71.889$, $p < 0.001$).

Olfactory memory retention in N. vitripennis

In total, 2025 *N. vitripennis* responded in the olfactory memory retention tests (79 reciprocal groups). A single olfactory conditioning trial resulted in memory retention in *N. vitripennis* ($\chi^2_1 = 150.075$, $p < 0.001$; Figure 4A), which did not decrease over time after conditioning ($\chi^2_2 = 4.789$, $p = 0.091$). Small wasps had a lower level of memory retention than large wasps ($\chi^2_1 = 15.473$, $p < 0.001$). There were no differences in duration of memory retention between wasps of different sizes ($\chi^2_1 = 0.981$, $p = 0.612$).

Small and large *N. vitripennis* retained olfactory memory up to 5 days after conditioning. One day after conditioning, small wasps showed a PI (±SE) of 23.90 ± 6.44% ($\chi^2_1 = 19.536$, $p < 0.001$) and large wasps of 46.39 ± 6.00%

Table 1. Body length values of large and small body size classes of *T. evanescens* and *N. vitripennis* (n = 100 in each group). Shown are mean ± SD and total range of body lengths measured from head to abdomen tip, and from thorax to abdomen tip.

	T. evanescens		*N. vitripennis*	
	Large	Small	Large	Small
Body length				
Average	0.745 ± 0.054 mm	0.521 ± 0.064 mm	2.634 ± 0.085 mm	1.681 ± 0.099 mm
Range	0.644 – 0.967 mm	0.367 – 0.633 mm	2.400 – 2.825 mm	1.375 – 1.900 mm
Thorax-abdomen length				
Average	0.654 ± 0.052 mm	0.444 ± 0.058 mm	2.330 ± 0.078 mm	1.450 ± 0.094 mm
Range	0.556 – 0.856 mm	0.311 – 0.556 mm	2.150 – 2.475 mm	1.175 – 1.650 mm

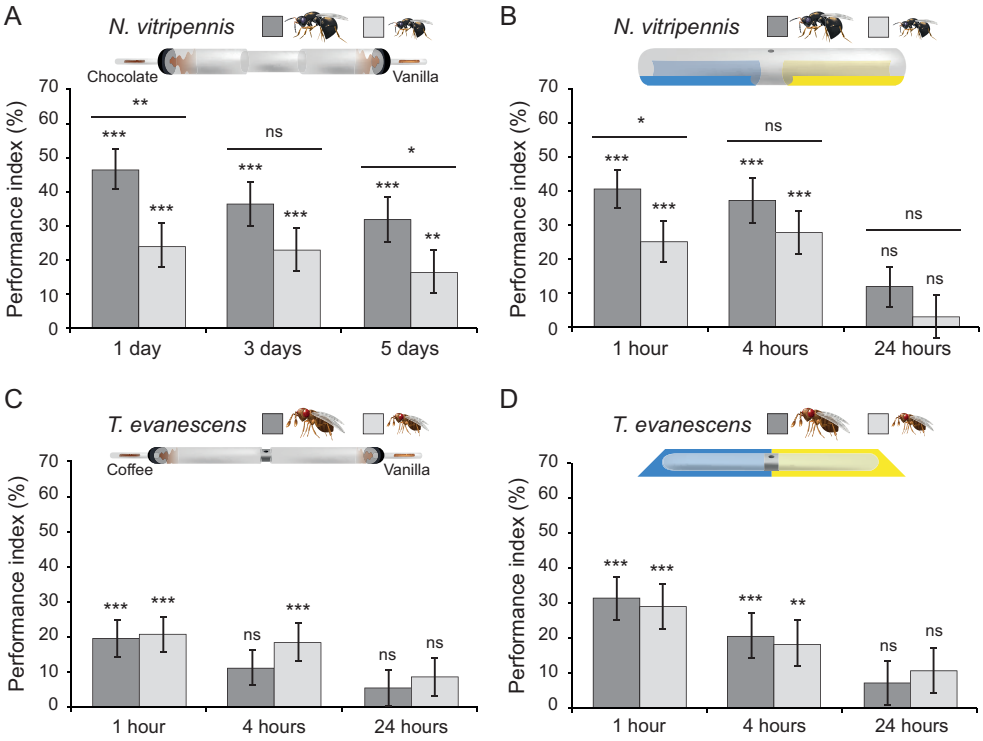

Figure 4. Memory retention over time for small (light bars) and large (dark bars) *T. evanescens* and *N. vitripennis*. Performance index (PI ± SE) shows difference in percentage of preference between reciprocally trained groups. **(A)** Olfactory memory in *N. vitripennis*; **(B)** visual memory in *N. vitripennis*; **(C)** olfactory memory in *T. evanescens*; **(D)** visual memory in *T. evanescens*. GLMM showed an overall effect of body size on memory retention for *N. vitripennis*, whereas memory retention is equal for small and large *T. evanescens*. Asterisks indicate significant memory retention and differences in memory retention between small and large wasps (Bonferroni-corrected χ^2 pairwise comparisons of GLMM response); * $p < 0.05$; ** $p < 0.01$; *** $p < 0.001$; ns not significant.

($\chi^2_1 = 60.356$, $p < 0.001$). Three days after conditioning, small wasps showed a PI of 22.88 ± 6.54% ($\chi^2_1 = 18.201$, $p < 0.001$) and large wasps of 36.41 ± 6.57% ($\chi^2_1 = 36.694$, $p < 0.001$). Five days after conditioning, small wasps showed a PI of 16.25 ± 6.50% ($\chi^2_1 = 10.349$, $p = 0.008$) and large wasps of 31.79 ± 6.75% ($\chi^2_1 = 28.189$, $p < 0.001$). The PI was significantly lower for small wasps than for large wasps one day after conditioning ($\chi^2_1 = 8.998$, $p = 0.003$) and five days after conditioning ($\chi^2_1 = 4.258$, $p = 0.040$), but did not differ between small and large wasps three days after conditioning ($\chi^2_1 = 3.192$, $p = 0.074$).

Visual memory retention in N. vitripennis

In total, 1964 *N. vitripennis* responded in the visual memory retention tests (72 reciprocal groups). A single visual conditioning trial resulted in memory retention in *N. vitripennis* ($\chi^2_1 = 105.495$, $p < 0.001$; Figure 4B), which decreased over time after conditioning ($\chi^2_2 = 31.116$, $p < 0.001$). Small wasps had a lower level of memory retention than large wasps ($\chi^2_1 = 7.731$, $p = 0.005$). There were no differences in the duration of memory retention between wasps of different sizes ($\chi^2_1 = 0.831$, $p = 0.660$).

Small and large *N. vitripennis* retained visual memory up to 4 hours after conditioning. One hour after conditioning, small wasps showed a PI (±SE) of 24.97 ± 6.16% ($\chi^2_1 = 20.724$, $p < 0.001$) and large wasps of 40.51 ± 5.67% ($\chi^2_1 = 53.577$, $p < 0.001$). Four hours after conditioning, small wasps showed a PI of 27.70 ± 6.51% ($\chi^2_1 = 23.621$, $p < 0.001$) and large wasps of 37.16 ± 6.62% ($\chi^2_1 = 43.449$, $p < 0.001$). Twenty-four hours after conditioning, small wasps showed a PI of 2.94 ± 6.39% ($\chi^2_1 = 0.296$, $p = 1.000$) and large wasps of 11.82 ± 5.94% ($\chi^2_1 = 4.402$, $p = 0.215$). The PI was significantly lower for small wasps than for large wasps one hour after conditioning ($\chi^2_1 = 5.122$, $p = 0.024$), but did not differ between small and large wasps four hours after conditioning ($\chi^2_1 = 2.132$, $p = 0.144$) and twenty-four hours after conditioning ($\chi^2_1 = 1.309$, $p = 0.253$).

Olfactory memory retention in T. evanescens

In total, 2733 *T. evanescens* responded in the olfactory memory retention tests (107 reciprocal groups). A single olfactory conditioning trial resulted in memory retention in *T. evanescens* ($\chi^2_1 = 52.213$, $p < 0.001$; Figure 4C), which decreased over time after conditioning ($\chi^2_2 = 7.381$, $p = 0.025$). Small and large wasps form the same level of memory retention ($\chi^2_1 = 0.922$, $p = 0.337$). There were no differences in the duration of memory retention between wasps of different sizes ($\chi^2_1 = 0.509$, $p = 0.775$).

Small *T. evanescens* retained olfactory memory up to 4 hours after conditioning, while 4-hour memory was no longer significantly different from 0 in large wasps. One hour after conditioning, small wasps showed a PI (±SE) of 20.83 ± 5.10% ($\chi^2_1 = 20.195$, $p < 0.001$) and large wasps of 19.64 ± 5.42% ($\chi^2_1 = 16.140$, $p < 0.001$). Four hours after conditioning, small wasps showed a PI of 18.44 ± 5.41% ($\chi^2_1 = 14.422$, $p < 0.001$) and large wasps of 11.16 ± 5.14% ($\chi^2_1 = 6.199$, $p = 0.077$). Twenty-four hours after conditioning, small wasps

showed a PI of 8.68 ± 5.57% (χ^2_1 = 2.996, p = 0.501) and large wasps of 5.53 ± 5.28% (χ^2_1 = 1.385, p = 1.000).

Visual memory retention in T. evanescens

In total, 3002 *T. evanescens* responded in the visual memory retention tests (91 reciprocal groups). A single visual conditioning trial resulted in memory retention in *T. evanescens* (χ^2_1 = 94.529, p < 0.001; Figure 4D), which decreased over time after conditioning (χ^2_2 = 23.717, p < 0.001). Small and large wasps form the same level of memory retention (χ^2_1 = 0.006, p = 0.937). There were no differences in the duration of memory retention between wasps of different sizes (χ^2_1 = 0.509, p = 0.776).

Small and large *T. evanescens* retained visual memory up to 4 hours after conditioning. One hour after conditioning, small wasps showed a PI (±SE) of 29.05 ± 6.60% (χ^2_1 = 29.301, p < 0.001) and large wasps of 31.48 ± 6.16% (χ^2_1 = 46.351, p < 0.001). Four hours after conditioning, small wasps showed a PI of 18.22 ± 6.66% (χ^2_1 = 13.845, p = 0.001) and large wasps of 20.51 ± 6.41% (χ^2_1 = 20.761, p < 0.001). Twenty-four hours after conditioning, small wasps showed a PI of 10.71 ± 6.54% (χ^2_1 = 5.322, p = 0.126) and large wasps of 7.20 ± 6.39% (χ^2_1 = 3.281, p = 0.420).

Response rate

Response rate was defined as the percentage of wasps making a choice, out of the total number of wasps that were introduced into the T-maze. Response rate was lower in small than in large *T. evanescens* (visual: χ^2_1 = 15.840, p < 0.001; olfactory: χ^2_1 = 25.800, p < 0.001). Small *T. evanescens* showed a response rate (±SE) of 78.63 ± 2.51% during visual memory retention tests and 76.64 ± 1.85% during olfactory memory retention tests. Large *T. evanescens* showed a response rate of 84.42 ± 1.98% during visual memory retention tests and 84.30 ± 1.45% during olfactory memory retention tests. In *N. vitripennis*, small wasps showed a lower response rate than large wasps during visual retention tests (χ^2_1 = 4.339, p = 0.037), and a higher response rate than large wasps during olfactory memory retention tests (χ^2_1 = 18.315, p < 0.001). Small *N. vitripennis* showed a response rate (±SE) of 91.67 ± 0.95% during visual memory retention tests and 85.49 ± 1.12% during olfactory memory retention tests. Large *N. vitripennis* showed a response rate of 94.20 ± 0.81% during visual memory retention tests and 78.49 ± 1.41% during olfactory memory retention tests.

Discussion

We expected that the extreme brain-scaling strategies of miniaturized parasitic wasp species, i.e. isometry in *T. evanescens* and a combination of isometry and allometry in *N. vitripennis*, would result in small individuals with brains that are too small to equal memory performance of large conspecifics. We found that such a cognitive cost of isometric brain scaling was apparent in *N. vitripennis*, but that it was absent in the smaller wasp species *T. evanescens*. For both species, we used inbred iso-female strains to exclude inter-individual genetic effects. The results of the present study therefore suggest that developmental plasticity in brain and body size differentially affects brain performance in *N. vitripennis* and *T. evanescens*.

In *N. vitripennis*, the level of visual and olfactory memory retention was significantly lower in small wasps than in large conspecifics. This could not be explained by a difference in host-searching activity; small *N. vitripennis* showed a lower response rate than large wasps during visual memory tests, but a higher response rate than large wasps during the olfactory memory tests. The duration of memory retention did not differ between small and large *N. vitripennis*. The cognitive costs of brain scaling in *N. vitripennis* may therefore mainly be reflected in the level of memory retention, rather than in the type of memory or its retention over time.

The present study shows that body size does not affect memory performance in *T. evanescens*, despite the isometric brain scaling that occurs in this species (Chapter 2). Hence, that small *T. evanescens* showed similar levels and duration of memory retention as large conspecifics is surprising. These results may suggest that for this species, the costs of the extreme developmental size plasticity of the brains are not reflected in this aspect of cognitive performance. The different effect of body size on memory performance between *T. evanescens* and *N. vitripennis* could relate to ecological differences between the two species, and to differences in developmental plasticity in neural architecture, on which we elaborate below.

Ecological importance of learning

The results of the present study show that *N. vitripennis* and *T. evanescens* are capable of forming both visual and olfactory memory, which can be of ecological importance for these wasps. Both *N. vitripennis* and *T. evanescens* continue to produce and mature eggs throughout their life, and will therefore need to continue searching for suitable hosts (Jacob and Boivin, 2005; Rivero and West, 2002).

The two species are also both gregarious generalists that exploit a large variety of host species (Huigens et al., 2009; Hoedjes et al., 2012). Learning can allow them to focus their searching activities on the particular host species that are present in their current environment (Hoedjes et al., 2011). Our study revealed that *N. vitripennis* retained olfactory memory longer than visual memory, which suggests that olfactory cues play a larger role during host searching than visual ones. In contrast, the similarity in memory retention of visual and olfactory cues in *T. evanescens* could suggest that these wasps use both visual and olfactory cues to find suitable hosts.

Trichogramma evanescens wasps differ from *N. vitripennis* in the strategy that they apply to find their hosts. Female *T. evanescens* have been shown to mount mated female butterflies and use them as means of transportation to the butterflies' egg-laying sites (Huigens et al., 2009). This phoresy behaviour enables wasps of the genus *Trichogramma* to find and parasitise freshly-laid host eggs, despite the limited control these tiny wasps have over the direction of their flight (Fatouros et al., 2005). Phoresy may reduce the amount of energy and neural capacity that needs to be allocated to navigation and flight, and allow increased investment in the cognitive and sensory abilities that are required to locate lepidopteran host species. This could underlie the similarities in memory performance of small and large *T. evanescens*. In contrast, it may be more adaptive for small *N. vitripennis* to economize on memory performance, and maintain energy, motor capacities and navigational functions to actively search for hosts.

Memory performance could have been affected by the ecology of the host species that we used as unconditioned stimuli. There are various characteristics that determine how rewarding a particular host is, such as clutch size, host size, nutritional quality, and whether the host has already been parasitised (Kruidhof et al., 2012). For *T. evanescens*, the reward value of the host determines how long memory is retained (Kruidhof et al., 2012). Long-term memory is formed after an oviposition experience on a clutch of *Pieris brassicae* eggs, but memory is retained shorter after an oviposition experience on *Pieris rapae* eggs, which are somewhat smaller and deposited as single eggs on multiple plant species (Kruidhof et al., 2012). The reward value of the host does not affect memory performance of *N. vitripennis* (Hoedjes et al., 2014a). Oviposition into three differently-sized host species results in the emergence of different numbers and sizes of offspring, but using these differently-sized hosts as unconditioned stimuli does not result in differences in memory retention. Hence, *T. evanescens* and *N. vitripennis* appear to have evolved different strategies of dealing with ecological variation in quality or suitability of their host species. Oviposition learning may be less dependent on

ecological conditions for *N. vitripennis* than for *T. evanescens*. It is interesting that the opposite is the case for body-size variation.

Plasticity in brain morphology

The lower memory retention levels in small *N. vitripennis* could indicate that small and large adults differentially invest in specific brain areas. Groothuis and Smid (2017) compared relative neuropil volumes for *N. vitripennis* females that were similar in size range and obtained in the same way as individuals in the present study. Indeed, they found that the mushroom bodies are relatively smaller in small than in large wasps, whereas relative volume of other neuropils remains the same or becomes relatively larger. The mushroom bodies are the location where different types of sensory pathways converge that convey the US and CS, and there is overwhelming evidence that they are essential for learning and memory formation (Perry & Barron, 2012). The finding that scramble competition induces developmental programmes that lead to smaller wasps with smaller relative mushroom body volumes (Groothuis & Smid, 2017) supports our results of small individuals having lower memory performance. Similar data for mushroom-body volume in *T. evanescens* are currently not available, but the results of the present study could indicate that relative mushroom-body volume is maintained in small and large *T. evanescens*.

First explorations of the neural architecture of *T. evanescens* revealed striking similarities in neural complexity of small and large individuals, whereas the size of these neural components does relate to body size. In the antennal lobe, olfactory glomeruli were found to be larger in wasps with larger brain volumes, but differently-sized wasps had the same number of glomeruli in their antennal lobes (Chapter 3). Similarly, small and large *T. evanescens* differed in the diameter of neuronal cell bodies that express serotonin, dopamine and octopamine, but did not differ in the number of these neurons (Chapter 5). These first explorations suggest that the complexity of the brains of small and large *T. evanescens* is similar, which supports the similarities in memory retention levels of these wasps. In *N. vitripennis*, the number and size of octopaminergic neurons has been studied but only in large individuals of this species (Haverkamp and Smid, 2014). Future studies should reveal if *N. vitripennis* evolved a different strategy than *T. evanescens*, which could involve reduced numbers of neurons and olfactory glomeruli in smaller individuals.

Our results do not necessarily imply that *T. evanescens* is better adapted to being small than *N. vitripennis*. Although memory performance appears to be

maintained in *T. evanescens*, there can still be other trade-offs in isometric brain scaling. Isometric brain scaling implies that large individuals have brains that are much larger than expected from Haller's rule. There must be benefits of having these large brains that outweigh the high energetic costs of deviating from Haller's rule. The results of the present study indicate that these benefits may not be cognitive in *T. evanescens*: large brains do not provide higher memory retention levels. Instead, the trade-offs of isometric brain scaling must be sought in other aspects of brain performance or fitness. These could relate, for example, to the smaller size of neuronal cell bodies in the smallest *T. evanescens* (Chapter 5). The limited volume of these cell bodies may restrict the number of energy-generating mitochondria and could enforce chromatin to be tightly packed, which may obstruct transcription and neural processing. These modifications may affect the longevity of the smallest *T. evanescens*, and larger conspecifics could avoid these costs by investing more in brain tissue.

Conclusion

The results of our study indicate that different evolutionary pressures shaped the cognitive consequences of extreme brain-scaling strategies. The smallest *T. evanescens* maintain memory performance under isometric brain scaling, which may be facilitated by a developmental strategy that reduces the size of neural components, while neural complexity is maintained. A possible trade-off of brain isometry in *T. evanescens* must be sought in brain properties different from memory retention (this chapter) and olfaction (Chapter 3), and could relate to neuronal cell body size. The larger parasitic wasp species *N. vitripennis* is unable to maintain memory retention levels at small body sizes, which may relate to previous findings of relatively smaller mushroom bodies in small *N. vitripennis* (Groothuis & Smid, 2017). It may be more adaptive for small *N. vitripennis* to invest in other aspects of brain performance, at the cost of memory performance. Future studies will need to reveal if the similarities in memory retention level in small and large *T. evanescens* can be explained by maintained relative mushroom body size, and if isometric brain scaling causes costs and benefits in other traits. A comparison of neural complexity in small and large *N. vitripennis* and *T. evanescens* may reveal which mechanisms enable their brain-scaling strategies, and explain the cognitive consequences for the smallest insects.

Acknowledgements

We thank Jessica de Bruijn, Lucía Martín de Bernardo Gisbert, Clara Galves-Orjol and Alexandra Roux for help with designing and conducting experiments; Marcel Dicke and Jitte Groothuis for constructive comments on a previous version of this article; Maartje Liefting (Free University of Amsterdam) for sharing the visual conditioning and memory retention procedure for *N. vitripennis*; Marjolein Kruidhof (Wageningen Plant Research) for statistical advice; the Max Planck Institute for Chemical Ecology (Jena, Germany) for providing *M. sexta* pupae; Léon Westerd, Frans van Aggelen and André Gidding for culturing *M. brassicae*; and the experimental farm of Wageningen University (Unifarm) for growing the tobacco plants. This work was supported by NWO PE&RC Graduate Program grant 022.002.004 (to EW) and by NWO Open Competition grant 820.01.012 (to HS).

Chapter 7

No gains for bigger brains: Functional and neuroanatomical consequences of artificial selection on relative brain size in a parasitic wasp

Emma van der Woude*,
Jitte Groothuis*,
Hans M. Smid

* These authors contributed equally to this work.

Abstract

Cognitive constraints are shaped by ecological conditions, (1) by determining resources available for development and maintenance of brain tissue and (2) by requiring adaptive behaviour to optimize an animal's fitness. As brain performance relates to relative brain size, there may be heritable genetic variation in relative brain size. Here, we used bidirectional artificial selection to study the consequences of genetic variation in relative brain size on brain morphology, cognition and longevity in *Nasonia vitripennis* Walker parasitoid wasps. Our results show a robust change in relative brain size after 26 generations of selection and 6 generations of relaxation, which indicates that there is heritable genetic variation in relative brain size. Total average neuropil volume of the brain was 16% larger in wasps selected for relatively large brains than in wasps selected for relatively small brains. This difference in brain volume differentially affected relative neuropil volumes, because the relative volume of the antennal lobes was larger in wasps with relatively large brains. We show that having a relatively small or large brain did not influence olfactory memory retention, whereas wasps with a larger relative brain size had a shorter longevity, which was even further reduced after a learning experience. In conclusion, having relatively large brains is costly for *N. vitripennis*, whereas no cognitive benefits were recorded. These effects of genetic variation on neuropil composition and memory retention are different from previously described effects of phenotypic plasticity in absolute brain size.

Introduction

Brain size is linked to brain performance through the number of neurons and their connectivity (Striedter, 2005; Chittka and Niven, 2009). Variation in brain size, both in absolute size and relative to body size, can therefore underlie differences in cognitive abilities (Dicke and Roth, 2016). Brain size variation can be caused by genetic variation, but also by phenotypic plasticity. Phenotypic plasticity can be regulated by genetically encoded developmental programmes (e.g. Lanet and Maurange, 2014). These determine how a single genotype morphologically responds to different developmental conditions, such as differences in nutritional levels, caste differentiation and sex determination. Natural genetic variation in the plasticity genes that facilitate these differential development programmes may predispose animals to optimize their development to match specific ecological circumstances, such as low food availability. Interestingly, animals that develop into differentially-sized individuals, for example due to differences in food availability during embryonic or larval development, do not scale their entire body size isometrically. One striking example of tissue-specific scaling is known for the brain, a phenomenon described by Haller's rule (Rensch, 1948; Rensch, 1956). This rule states that small animals require relatively larger brains than large animals. The relationship between brain size and body size follows a power law function. In the case of a negative allometry that is described by Haller's rule, the scaling coefficient of this power law function is smaller than 1. Haller's rule holds both for interspecific (e.g. Pagel and Harvey, 1989; Harvey and Krebs, 1990; Wehner et al., 2007; Isler et al., 2008), and intraspecific (e.g. Wehner et al., 2007; Riveros and Gronenberg, 2010; Seid et al., 2011) comparisons.

Development and maintenance of relatively larger brains is more costly for smaller animals, because brain tissue has high metabolic costs (Aiello and Wheeler, 1995). This may present strong constraints on the evolution of extremely small animals. In this context, it is intriguing that one of the smallest animals on Earth, the parasitic wasp *Trichogramma evanescens*, shows a different brain scaling strategy than predicted by Haller's rule (Chapter 2). These wasps are gregarious parasitic wasps that develop from egg to adult inside eggs of butterflies and moths. Body size depends on the level of scramble competition between larvae that develop inside the same host egg. This can lead to large phenotypic variation in absolute brain and body size, even between genetically identical individuals (Chapter 2). Although body volume can vary with a factor 7 between sister wasps of the same inbred isofemale line, this does not affect their relative brain size; the wasps show isometric brain scaling.

This isometric brain scaling results in small wasps having brains that are smaller than predicted by Haller's rule. Interestingly, this does not affect their memory performance (Chapter 6). Small and large *T. evanescens* show similar memory retention levels. Furthermore, the complexity of the olfactory pathway remains remarkably unaffected by its size: small wasps have the same number of antennal lobe glomeruli and most types of olfactory sensilla as large wasps (Chapter 3). This indicates that *T. evanescens* is well adapted to develop as small adults.

The larger parasitoid wasp *Nasonia vitripennis* parasitises and develops inside fly pupae, and body size depends on scramble competition in a similar way as in *T. evanescens*, scaling their dry body weight with a factor of 10. Brain-body size scaling in this parasitoid also deviates from Haller's rule, but applies a different brain scaling rule than *T. evanescens* (Groothuis and Smid, 2017). The wasps show diphasic brain scaling with isometry in small and negative allometry in large *N. vitripennis*, possibly because they switch to a different developmental programme.

The isometric phase causes relatively smaller brains in small wasps than is predicted by Haller's rule. In contrast to *T. evanescens*, this does affect their memory performance: large *N. vitripennis* show higher levels of olfactory and visual memory retention than small *N. vitripennis* (Chapter 6). This may be related to differences in relative neuropil volumes. Among other neuropils, the mushroom bodies (known to be important for memory formation in other insects) were relatively smaller in the smallest wasps; on the other hand, the relative volume of the lateral horn (known to be involved in naive responses to olfactory cues (Parnas et al., 2013; Strutz et al., 2014)) had not changed. This may indicate that, when challenged with restricted resources, isogenic *N. vitripennis* are able to utilize different developmental programmes and develop differentially structured brains. In this example, the decrease in absolute and relative mushroom body volume may underlie their aforementioned lower memory performance. These studies indicate that *T. evanescens* and *N. vitripennis* are differentially adapted to dealing with the stringent dietary conditions that arise from larval scramble competition.

Ecological conditions may require adaptive behaviour to optimize an animal's fitness. This may be realized by a relatively larger brain. However, higher developmental and operating costs of brain tissue, associated with a relatively larger brain, may incur negative effects on fitness and longevity (Aiello and Wheeler, 1995; Mery and Kawecki, 2005). Furthermore, populations that evolve under more stringent dietary conditions may experience different selection pressures on genes that determine brain size than populations that evolve

under more permissible dietary conditions. In the case of a parasitic wasp, such differences may exist by adapting to different host species. Different host species may require different cognitive abilities because host oviposition behaviour may require different foraging strategies of the parasitic wasps (Smid et al., 2007; Kruidhof et al., 2012; Smid and Vet, 2016), while also requiring adaptations to differences in host quality or size.

To be able to adapt to such different ecological circumstances, heritable genetic variation in relative brain size must be present. For instance, our previous work on brain scaling in *T. evanescens* showed that the precise scaling coefficients differed for different isogenic lines, indicating genetic variation in the plasticity genes that determine brain size in this species (Chapter 2). Recent studies show that relative brain size can be selected for in guppies (Kotrschal et al., 2013), and that this has correlated effects on learning abilities (Kotrschal et al., 2013; Kotrschal et al., 2015b), gut mass (Kotrschal et al., 2013), survival (Kotrschal et al., 2015a), proactiveness (Kotrschal et al., 2014), sexual traits (Kotrschal et al., 2015c), and the immune system (Kotrschal et al., 2016). The differences in relative brain size between large- and small-brained guppies are caused by differences in the expression of only a single gene: Angiopoietin-1 (Chen et al., 2015).

Our previous research showed that phenotypic differences in absolute brain and body size that are induced by differences in scramble competition affect neuropil composition and memory retention abilities in an isogenic strain of *N. vitripennis*. Here, we studied the consequences of genetic variation in relative brain size using constant, low levels of scramble competition to minimize such phenotypic effects of body size. This was done by means of a bidirectional artificial selection regime, using the ratio between head width and body length as proxy for relative brain size (Groothuis and Smid, 2017) in a population of *N. vitripennis* that was specifically collected and maintained to preserve natural genetic variation (van de Zande et al., 2014). Furthermore, we studied the effects of this selection regime on brain structure, cognition and longevity. We expected that there is heritable variation in relative brain size under constant nutritional levels. We expected that (A) there is a positive correlation between relative brain size and memory performance, (B) relative neuropil volumes are affected by selection for relative brain size, and (C) there is a negative correlation between relative brain size and longevity.

Materials and methods

Insects

We used female *N. vitripennis* Walker (Hymenoptera: Pteromalidae) of strain HVRx, which was specifically collected and maintained to preserve natural genetic variation (van de Zande et al., 2014). The wasps were reared on *Calliphora vomitoria* pupae (obtained as maggots from Kreikamp B.V., Hoevelaken, The Netherlands) and kept in a climate cabinet at 20 ± 1 °C with a 16:8 L:D cycle. The generation time was ca. 3 weeks.

Selection regime

To initiate the selection lines, 200 mated female *N. vitripennis* were sedated with CO_2. Body length and head width of these wasps were measured using a dissection microscope with ocular micrometre. The ratio between head width and body length was calculated and used as proxy for relative head size. The 30 wasps with the largest ratio were randomly distributed over 3 rearing vials in groups of 10 wasps, to initiate 3 selection lines for large heads (defined as Large (L)). Similar procedures were used to initiate 3 selection lines for small heads (defined as Small (S)), using the 30 wasps with the smallest ratio.

Another 30 wasps were randomly selected from the starting population and used to initiate 3 control lines (defined as Control (C)) to control for the effect of selection on inbreeding. This resulted in three replicate lines per selection regime: large L1, L2, L3, small, S1, S2, S3 and control C1, C2, C3. Each rearing vial contained 20 *C. vomitoria* pupae and a drop of honey.

In every subsequent generation, 50 mated female wasps per S and L line were sedated and measured as described above. The 10 wasps with the largest (for L) and smallest (for S) ratios between head width and body length were used to initiate the next generation. For the C lines, 10 randomly chosen females were used, without measurements. These selection procedures were repeated for 25 generations. After the 25th generation, selection was relaxed, with the exception of generations 30, 33 and 40.

Neuropil staining and relative neuropil measurements

Per replicate line, 12 female wasps were randomly selected from generation 33 (resulting in a total of 108 wasps). The wasps were sedated on ice, after which they were decapitated in ice-cold phosphate buffered saline (PBS, Oxoid, Dulbecco

'A' tablets). The brains were removed using sharpened tweezers (Dumont #5, Sigma), placed in phosphate buffered (0.1M) 4% formaldehyde solution (pH 7.2) and fixed for 2.5 hours at room temperature. After fixation, the brains were rinsed in PBS 6 × 5 minutes and treated with 5 mg/ml collagenase (Sigma) in PBS for 1 hour at RT. Following rinsing in PBS containing 0.5% Triton-X-100 (PBS-T) 4 × 5 minutes, brains were incubated for 1 hour in blocking buffer, PBS-T containing 10% normal goat serum (PBS-T-NGS, Dako, Glostrup, Denmark). Incubation in primary antibody, 1:250 nc82 (mouse-anti-Bruchpilot concentrate, NC82-c, Developmental Studies Hybridoma Bank, University of Iowa, Iowa City, IA; Cat. no. nc82, RRID:AB_528108) in PBS-T-NGS was overnight at RT, followed by 6 × 20 minutes rinsing in PBS-T and 4 hours incubation at RT in secondary antibody, 1:100 rabbit-anti-mouse (Dako) in PBS-T-NGS. After another 6 × 20 minutes rinse in PBS-T the brains were incubated overnight at 4 °C in tertiary antibody, 1:200 Alexa Fluor® 488-conjugated goat-anti-rabbit (Invitrogen) and 1:250 propidium iodide (Sigma-Aldrich) in PBS-T-NGS. Subsequent steps were performed in the dark as much as possible. Brains were dehydrated through a series of increasing EtOH dilutions (30–50–70–80–90–96–2×100%), degreased via a 50/50 EtOH/xylene step, and kept in xylene until mounting. Brains were mounted in DPX (Sigma) between a glass microscope slide, fitted with two stacked strips of double-sided adhesive tape (Henzo, Roermond, The Netherland) as spacer, and a 18 mm × 18 mm #1 cover slip. All incubations were performed with brains grouped per replicate.

Whole mount Z-stacks were acquired using a Zeiss LSM 510 confocal microscope equipped with a Plan-Neofluar 25×/0.8 oil immersion objective. Alexa Fluor® 488 and PI were excited using the Ar-488 nm line and captured with 505 – 550 nm BP and 560 nm LP filters, respectively. Images were obtained at 512 × 512 px with a 0.7× digital zoom and a step size of 2 μm, resulting in a final voxel calibration of 1.018 × 1.018 × 2 μm. As the refractive indices of immersion and mounting medium match, no z-correction was required. Depending on the size and orientation of a scanned brain, 1 to 3 stacks were acquired and later combined with the Stitching plugin (Preibisch et al., 2009) in FIJI (Schindelin et al., 2012). Due to the fragile nature of *Nasonia* brains (Haverkamp and Smid, 2014), we inspected the obtained stacks for integrity of all neuropils and selected the 3 best-stained brains per replicate line (resulting in 9 brains per treatment, and 27 brains for the entire experiment).

Neuropil segmentation was performed in Amira 5.4.2 (Visage Imaging). Due to its tight connection with the eye, the optic lobe lamina is often damaged during dissection. Therefore, it was not included in this analysis. The nc82 channel was

used to assign 11 unique labels to the neuropil in the Segmentation Editor, see Figure 3 in the main text. Each neuropil was manually labelled each 1-3 slices, after which the Interpolate option was used. Manual correction was performed to ensure correct labelling of each slice. Neuropil volumes were calculated by the MaterialStatistics module and saved as .csv file for collection and calculation of relative volume in an MS Excel spreadsheet. Relative neuropil volume was calculated as the percentage of the total neuropil volume.

Memory retention

Olfactory memory retention of the selection lines was tested in generation 33. We used single classical olfactory conditioning trials, as described before (Hoedjes and Smid, 2014; Chapter 6). The wasps were 1 – 2 days old and kept on water and honey until use in the conditioning trials. Groups of approximately 60 wasps were distributed over a Petri dish (8.5 cm diameter). Here, the wasps obtained an oviposition experience (unconditioned stimulus, US) while experiencing an odour (conditioned stimulus, CS): the CS+ phase. The rewarding unconditioned stimulus consisted of 40 *C. vomitoria* pupae. The conditioned stimulus was 5 µl of either Royal Brand Bourbon Vanilla extract or Natural Chocolate extract (Nielsen-Massey Vanillas Intl., Leeuwarden, the Netherlands), pipetted on small squares of filter paper. The wasps were allowed to drill and oviposit inside the pupae for 1 hour, while experiencing the odour of the CS+. Wasps that were not drilling in the pupae were removed after 15 minutes. After 1 hour, the wasps were removed from the pupae with an aspirator and placed in a clean petri dish for a neutral resting phase of 15 minutes. Next, the wasps experienced 5 µl of the second of the two odours in absence of hosts: the CS- phase. This phase lasted for another 15 minutes. After this phase, the wasps were collected in clean vials and stored with water and honey until use in the memory retention tests. The conditioning trials were performed in a reciprocal manner: one group of every line was conditioned using vanilla as CS+ and chocolate as CS-, another group was conditioned using chocolate as CS+ and vanilla as CS-. Four groups per replicate line were conditioned on chocolate and four groups per replicate line were conditioned on vanilla.

Memory retention was tested in the T-maze as described before (Hoedjes and Smid, 2014). One side of the T-maze contained a glass capillary (ID 1.3 mm, Stuart SMP1/4, Bibby Scientific, Staffordshire, UK) filled with vanilla extract, and the other side contained chocolate extract. Charcoal filtered, moisturized air (60 – 70% relative humidity) flowed past the odour capillaries at 100 ml/min per side. Wasps were inserted in the T-maze in groups of approximately 15 wasps,

resulting in 3 measurements per conditioned group. Memory of each wasp was tested 1, 3 and 5 days after the conditioning trials. After 5 minutes the number of wasps on the vanilla and chocolate side was recorded.

Longevity

Longevity was studied in generation 40. Wasps of each replicate selection line were used either naively or after an olfactory conditioning trial (as described above). Each replicate line was analysed with 2 groups of naive and 2 groups of conditioned wasps, each group containing 30 wasps. These groups were placed in clean rearing tubes with unlimited access to water and honey and kept in a climate cabinet at 25 °C. The tubes were refreshed weekly. Every 2 days the number of dead wasps was counted.

Statistical analyses

Response to selection was analysed using a linear mixed model with the ratio between head width and body length as dependent variable. Selection regime (L or S), generation and the interaction between these two were used as fixed factors. Replicate number was used as a random factor. Deviance of model terms was analysed using type II Wald χ^2 tests. Similar linear mixed models were used to test the selection's effect on body length and head width, using respectively the natural logarithm of body length or head width as dependent variable. Ordinary linear regression on head width and mean-centred body length was used to study if the difference in head-body size ratio between the selected lines can be explained by allometric brain scaling in combination with differences in body size. Head width was used as dependent variable, and body length and selection regime (L, C or S) as fixed factors. Body lengths were mean-centred by subtraction of the average body length of all wasps in that generation. This ensured that differences in the intercept reflect differences in head-body ratio between the selected lines, as head width is compared at mean-centred body length (Egset et al., 2011; Tsuboi et al., 2016). If there are still differences in head-body ratio at mean-centred body length, these are not caused by allometric brain scaling resulting from the difference in body size between the lines. ANOVA comparisons were used to test for differences in slope and intercept between the lines. We used this method to analyse wasps separately for generation 26, 33 and 40.

We calculated realized heritability after 25 generations of selection. We used the ratio between the cumulative selection response and the cumulative selection

differential, following the method for divergent selection described by Walsh & Lynch (Walsh and Lynch, 2009). The cumulative selection response was defined as the difference in mean head-body ratio between L and S in generation 26. The cumulative selection differential was defined as the cumulative difference in selection differentials (mean head-body ratio of the selected group subtracted from the mean of that whole population) between L and S of 25 generations. The value for realized heritability was duplicated to correct for selection on only females, instead of on both parents.

Differences in neuropil volumes were analysed in generation 33 with a linear mixed model. We used the absolute total neuropil volume or relative volume per neuropil as dependent variables, with selection regime as fixed factor and line as random factor. As we compared multiple relative neuropil volumes, we corrected the *p*-values for multiple comparisons with the Holm-Bonferroni method (m = 11; Holm, 1979) in MS Excel. Neuropils with significant effects of selection regime on relative volume were further analysed with χ^2 pairwise comparisons to test for significant differences between the selection regimes.

Differences in memory retention abilities were analysed in generation 33. Memory retention was expressed as a performance index (PI): the difference in preference between reciprocally trained groups. This PI is calculated by subtracting the fraction of wasps that chose the odour of their CS- from the fraction of wasps in the reciprocal group, which chose that same odour but received it as their CS+. Values of PIs were calculated from estimated response means that were obtained from generalized linear mixed models (GLMMs) with logit link function and binomial distribution. The dependent variable was the number of wasps that chose chocolate with the total number of wasps making a choice as denominator. Fixed effects included the odour of CS+, time after conditioning, selection line and the interactions between these effects. Random effects were included to correct for date of conditioning, selection line repeat and reciprocal conditioning pair. Presence of memory was tested with χ^2 pairwise comparisons, which test for the effect of CS+ on the preference for the conditioned stimuli. Similar tests were used to analyse differences in memory retention between the different lines. Response rates of the memory retention tests were determined by a GLMM that used the fraction of wasps making a choice out of the total number of wasps inserted as dependent variable, and selection regime and time after conditioning as fixed factors. Differences in response rate between the lines and times were determined with χ^2 pairwise comparisons.

Longevity was analysed in generation 40. We used a two-way ANOVA that tested for the effect of selection regime, conditioning and the interaction between

these terms using time till death as dependent variable. This was followed by TukeyHSD post-hoc tests to analyse differences in longevity between selected lines and to test for an effect of conditioning on longevity within selected lines. Statistical analyses were performed in R version 3.1.0 in combination with packages lme4 (Bates et al., 2014), phia (De Rosario-Martinez), lsmeans (Lenth, 2014).

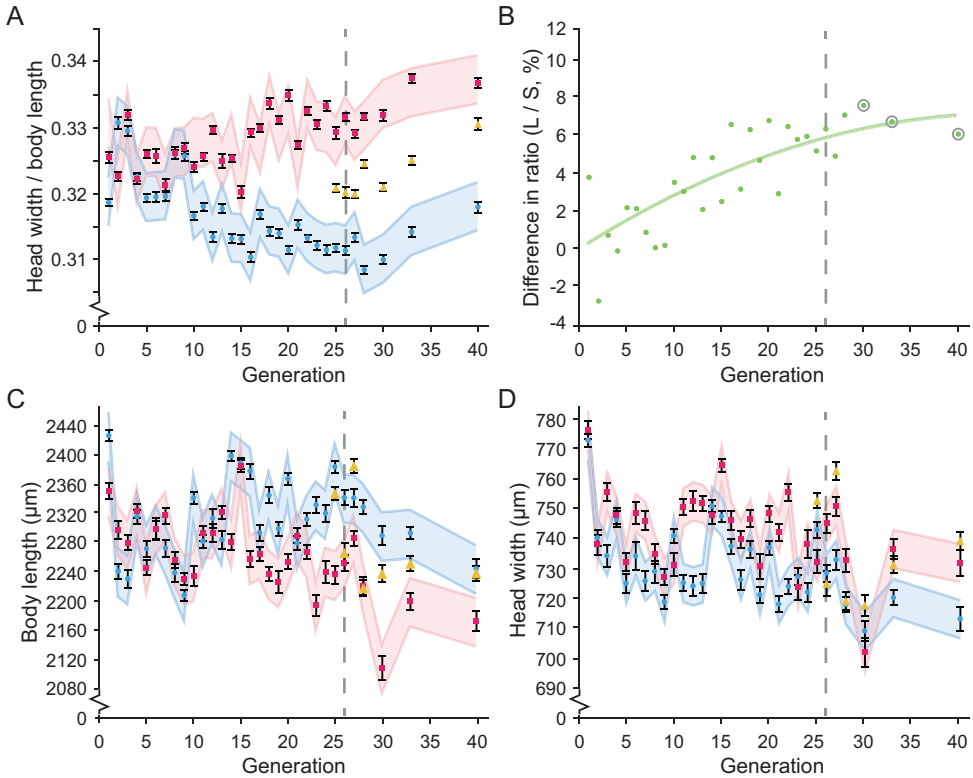

Figure 1. Relative brain size responds to bidirectional selection. Data points depict means over all individuals of all lines in a selection regime. Magenta squares: wasps selected for relatively large brains (L lines); blue circles: wasps selected for relatively small brains (S lines); yellow triangles: wasps of the control treatment (C lines). Dashed vertical lines in panels A-D show the start of relaxation of the selection regime, grey circles in panel B show generations used for additional selection. Linear mixed model predictions were used to calculate confidence intervals. **(A)** Relative brain size is shown as the mean ± SE of the head-body size ratio for all wasps of a certain selection regime. **(B)** Difference in the head-body size ratio between the L and S lines increases with each selected generation. Regression formula: $y = -0.0035\ x^2 + 0.317x$, $R^2 = 0.651$. **(C)** Absolute body length (mean ± SE) and **(D)** absolute head width (mean ± SE) both respond to selection. Note that L wasps have shorter bodies than S (panel C), but wider heads (panel D).

Results

Selection regime

There was a significant effect of the selection regime on the head-body size ratio (χ^2_1 = 4496.16, p < 0.001; Figure 1A). After generation 25 (the last generation undergoing selection), the difference in head-body size ratio was 6.30% (Figure 1B). In generation 33 we assessed brain morphology and memory retention (discussed below); in this generation the difference in head-body size ratio was 6.67%. We assessed longevity in generation 40, here the difference in ratio was 6.03%. On average, the final differences in ratio between wasps of the large (L) and small (S) lines were 6.41% in generations 26 to 40 (Figure 1B). Generation number significantly affected head-body size ratio (χ^2_{30} = 898.47, p < 0.001), as did the interactions between selection regime and generation (χ^2_{30} = 1996.18, p < 0.001). Realized heritability (h^2) of the ratio was 0.067 in generation 26.

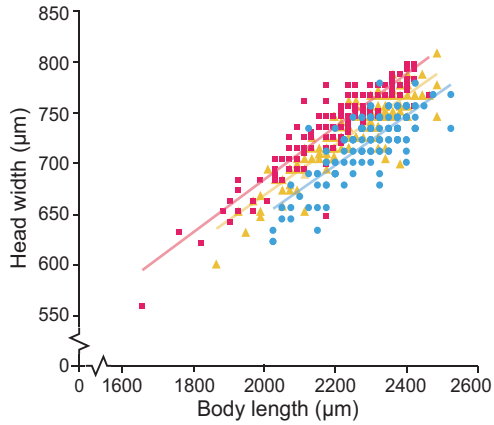

Figure 2. Head width and body length of individual wasps selected for relatively large (magenta squares) and small (blue circles) head-body ratio, and unselected control lines (yellow triangles). Data are shown for generation 33, which is the same generation used to study neuropil composition and memory performance. Regression analysis was performed on mean-centred body lengths, which ensured that differences in the intercept reflected differences in head-body ratio. This revealed differences in the intercepts, but not in the slopes. Similar results for generation 26 and 40 are shown in Figure S1.

Selection regime (for small versus large head-body size ratio) had a significant effect on body length (χ^2_1 = 322.437, p < 0.001; Figure 1C). Body length was also affected by generation (χ^2_{30} = 888.169, p < 0.001) and the interaction between selection and generation was significant (χ^2_{30} = 537.050, p < 0.001). Selection regime also affected head width (χ^2_1 = 202.113, p < 0.001; Figure 1D), as did generation (χ^2_{30} = 864.363, p < 0.001) and the interaction between selection and generation was significant (χ^2_{30} = 191.226, p < 0.001).

Figure 2 shows the relationship between head width and body length in wasps of the three lines in generation 33. Linear regression on head width and mean-centred body length revealed significant differences between the lines in generation 33 in intercept (L: 749.048, C: 730.396, S: 709.134; $F_{2,444}$ = 36.466,

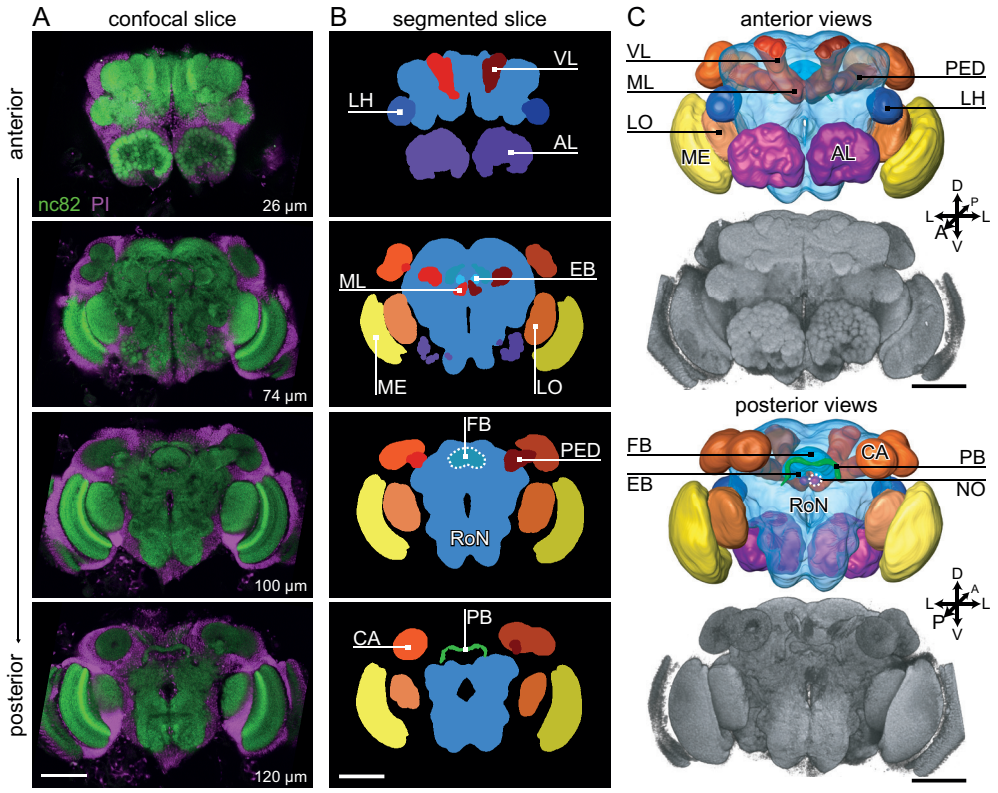

Figure 3. Overview of neuropils measured. Scale bars depict 100 µm in all panels. **(A)** Selected slices through a single *N. vitripennis* brain from line L3, fluorescently labelled with nc82 (green) and PI (magenta). Bottom-right insets indicate slice depth in µm from the anterior direction. Image contrast was increased in FIJI. **(B)** Schematic representation of segmented neuropils in the corresponding slices of panel A. Optic lobes (OL) consisting of lobula (LO) and medulla (ME); mushroom body (MB), consisting of the calyx (CA), pedunculus (PED), vertical lobe (VL), and medial lobe (ML). PED, VL, and ML were segmented as one label, the ventral mushroom body (MB-V); central complex (CX), consisting of fan-shaped body (FB), ellipsoid body (EB), protocerebral bridge (PB), and noduli (NO); lateral horn (LH); antennal lobe (AL) (the AL hub and glomeruli were segmented as a whole); and the remainder of the neuropil (RoN). The lamina, visible in panel A and the volume renderings of panel C, was not segmented. **(C)** Anterior and posterior views of a surface model based on the segmentations shown in panel B, accompanied by a volume rendering of the nc82 channel shown in panel A (using the SurfaceGen and VolTex modules, respectively, of Amira). Orientation in panel C refers to the body axis (Haverkamp and Smid, 2014). Lettering as in panel B.

$p < 0.001$), but not in slope (L: 0.260, C: 0.245, S: 0.244; $F_{2,444} = 0.670$, $p = 0.512$). Similar results were found for wasps of generations 26 and 40 (see Figure S1). This shows that wasps of the L, C and S lines differ in head width independent

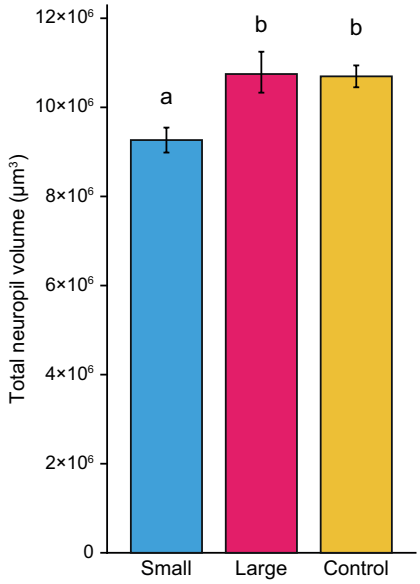

Figure 4. Absolute volumes of the total neuropil. Bars depict mean volume ± SE in μm^3, n = 9 for each selection regime. Letters indicate significant differences between selection regimes based on post-hoc pairwise comparisons ($\alpha = 0.05$).

of the body size effects due to selection. The effect on head-body size ratio is, therefore, not caused by allometric brain scaling resulting from the difference in body size between the lines. Body lengths, head widths and ratios between head width and body length for all generations are shown in Table S1.

Brain morphology

In the analysis of neuropil composition, 3 out of 12 brains from each replicate line were analysed, resulting in datasets for 9 brains per selection regime (Figure 3). First, we analysed the absolute volume of the neuropil in the selected lines. Neuropil volume differed between selection regimes (Figure 4; $F_{2,24} = 6.062$, $p = 0.007$). A TukeyHSD post-hoc test revealed that wasps of the S lines were smaller ($9.27 \times 10^6 \pm 0.28 \times 10^6$ μm^3, M ± SE) than wasps of the C lines ($10.70 \times 10^6 \pm 0.25 \times 10^6$ μm^3, $p = 0.018$) and the L lines ($10.75 \times 10^6 \pm 0.46 \times 10^6$ μm^3, $p = 0.014$). There was no difference between the C and L lines ($p = 0.994$). On average, the total neuropil of the L lines was 16% larger than in the S lines.

We further analysed the brains by comparing relative volumes of 11 neuropil regions, determined as percentages of the total neuropil volume (Figure 5). The only neuropil region that showed a significant effect of selection regime was the antennal lobe ($\chi^2_2 = 19.237$, $p < 0.001$). Post-hoc comparison revealed that the relative neuropil volume was higher in the L lines (12.08 ± 0.16 %, mean ± SE) compared to the C (11.29 ± 0.08 %, $\chi^2_1 = 14.0360$, $p < 0.001$) and the S (11.27 ± 0.20 %, $\chi^2_1 = 14.8094$, $p < 0.001$) lines. There were no differences between the control and small lines ($\chi^2_1 = 0.0104$, $p = 0.918$). Relative volumes and statistical comparisons of other neuropils are presented in Table S3.

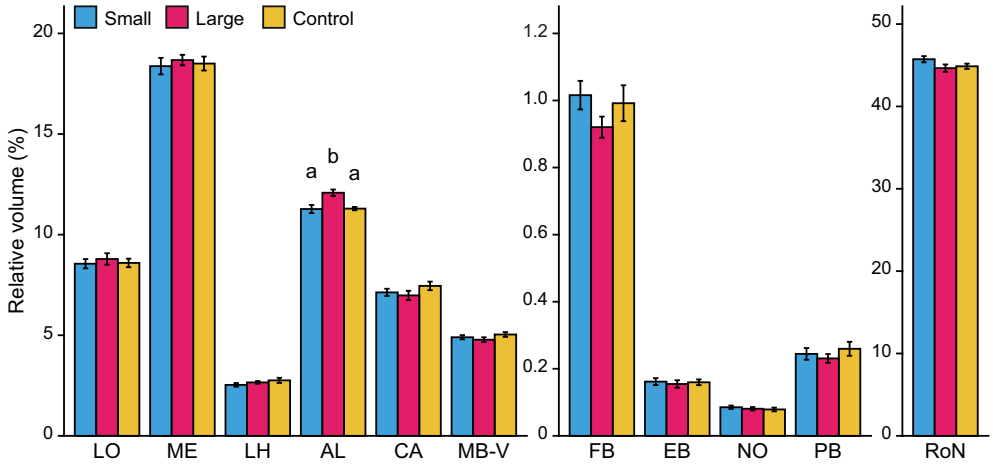

Figure 5. Relative volumes (mean ± SE) of the neuropils defined in Figure 3 (n = 9) for each selection regime. Y-axes have been split to better visualize differences between selection regimes for relatively smaller neuropils. Effects of selection regimes was first tested with a LMM, with Holm-Bonferroni correction for multiple comparisons (m = 11 neuropil regions). Letters indicate significant differences between selection lines based on post-hoc pairwise comparisons; unmarked bars indicate no significant effect was found for these neuropils.

Memory retention

Memory retention was analysed in 2502 wasps of the L line, 2759 wasps of the S line and 2883 wasps of the C line. Memory retention 1 day after conditioning was analysed in 12 reciprocal groups of each replicate line, resulting in 36 reciprocal groups per selection regime. Due to mortality this number decreased over the subsequent days, resulting in a final 23 reciprocal groups per selection regime at 3 days after conditioning, and 20 reciprocal groups at 5 days after conditioning.

Figure 6 shows memory retention (expressed as performance index, PI) levels for the different lines. There was significant memory retention ($\chi^2_1 = 62.238$, $p < 0.001$), and this retention decreased over time ($\chi^2_2 = 20.349$, $p < 0.001$). There was an overall difference in memory retention between the different selection regimes ($\chi^2_2 = 10.971$, $p = 0.004$). Memory retention did not differ between S and L ($\chi^2_1 = 0.066$, $p = 0.796$), but both lines differ in memory retention levels from C (L: $\chi^2_1 = 9.002$, $p = 0.003$; S: $\chi^2_1 = 7.884$, $p = 0.005$). The selected lines maintained memory up to 3 days after conditioning, and the C lines maintained memory up to 1 day after conditioning. However, there were no significant differences in decrease of memory retention level over time between the different lines ($\chi^2_4 = 2.794$, $p = 0.593$). There was no difference in response rate between wasps of the different lines ($\chi^2_2 = 1.054$, $p = 0.591$).

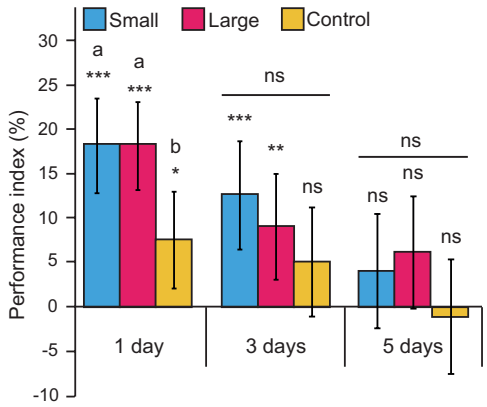

Figure 6. Memory retention over time for selection and control lines. Performance index (PI ± SE) shows difference in percentage of preference between reciprocally trained groups. Asterisks indicate significant memory retention (χ^2 pairwise comparisons of GLMM response); * $p < 0.05$; ** $p < 0.01$; *** $p < 0.001$; ns not significant; letters indicate significant differences between selection lines.

Longevity

Longevity (Figure 7) was affected by selection regime ($F_{2,1074} = 50.433$, $p < 0.001$), experience of a conditioning trial ($F_{1,1074} = 76.400$, $p < 0.001$) and the interaction between selection regime and conditioning ($F_{2,1074} = 7.435$, $p < 0.001$). Longevity was lower in L than in S (Tukey HSD $p < 0.001$; Table S2) and C (Tukey HSD $p < 0.001$). There was no difference in longevity between S and C (Tukey HSD $p = 0.924$).

Experience of a conditioning trial resulted in decreased longevity compared to naive wasps in L (Tukey HSD $p < 0.001$) and C (Tukey HSD $p < 0.001$), but not in S lines (Tukey HSD $p = 0.404$).

Discussion

Our bidirectional selection regime on *N. vitripennis* wasps resulted in a robust response in relative brain size that was not sensitive to relaxation for several generations, with on average 6.4% difference in head-body size ratio between wasps of the L and S lines. Total neuropil volume was 16% larger in wasps of the L lines than in wasps of the S lines. The response to selection, expressed as realized heritability, was lower in our study than in previous artificial selection experiments in guppies (i.e. 0.07 in our study and 0.48 for guppies; Kotrschal et al., 2013). The regulation of relative brain size may be more complex in *N. vitripennis* than in guppies, where a change in the expression of a single gene determines relative brain size (Chen et al., 2015). The slow, but substantial selection response indicates that there is heritable genetic variation in brain size in *N. vitripennis*, but that there are constraining factors that limit the response to artificial selection. These constraints may be particularly strong due to the small size of the wasps, which causes metabolic and cognitive trade-offs to have a large impact on the functioning of their miniaturized brains. The high metabolic costs of brain tissue (Aiello and Wheeler, 1995) may limit the development of relatively larger brains, while cognitive or behavioural costs may limit the formation of relatively

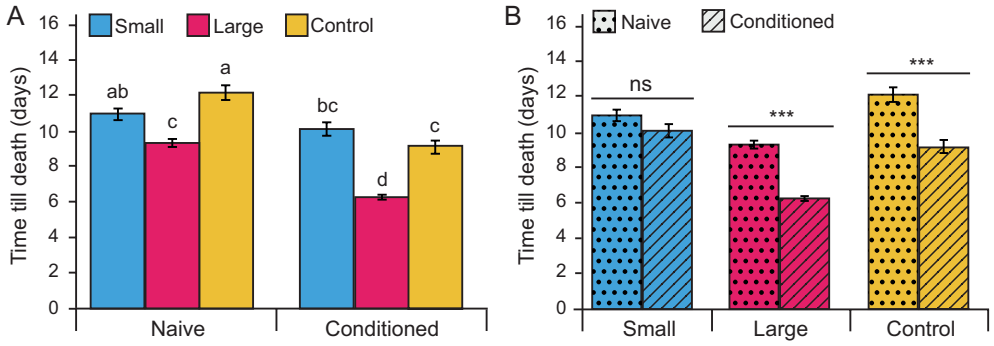

Figure 7. Survival of selection lines (mean ± SE), using a starting population of 180 wasps per group (60 per replicate line), with and without experiencing a single olfactory conditioning procedure. **(A)** Wasps with a relatively large brain have lower longevity than wasps with relatively small brains. Longevity is not improved by having a relatively small brain compared to the control lines. **(B)** A single olfactory conditioning experience affects longevity of wasps with a relatively large brain, but not of wasps with a relatively small brain. Asterisks and letters indicate significant differences between the groups based on Tukey HSD (see SI Table S2); *** $p < 0.001$; ns not significant.

smaller brains. Hence, relative brain size may be constrained by energetic costs on the upper limit and by functional requirements on the lower limit. Our study revealed such a cost of having large brains on longevity (Figure 7A), but no functional benefits for olfactory memory performance (Figure 6).

Deviation from Haller's rule

Our selection regime resulted in wasps of the S lines having on average larger body lengths than those of the L lines. Since Haller's rule predicts that larger wasps have relatively smaller brains, this could suggest that differences in head-body ratio reflect allometric brain scaling due to phenotypic plasticity in body size, such as we experimentally induced in a previous study (Groothuis and Smid, 2017). This could occur, for instance, if our selection regime resulted in wasps of the L lines laying more eggs in similar sized hosts than wasps of the S lines, resulting in smaller wasps. However, a brain-body size regression would then result in wasps of the S and L and C lines to be on the same regression line, with wasps of the S and L lines constituting the large and small individuals respectively. Figure 2 shows that this is not the case; the three lines differed in intercept, with L above C, and C above S. Moreover, wasps of the S lines, with larger body size, had not only relatively but also absolutely smaller brains than wasps of the L lines. Therefore, allometric brain scaling cannot explain the difference in head-body size ratio and brain volume between the wasps of the S

and L lines. Instead, grade shifts appear to have occurred. Such grade shifts are elevation displacements that illustrate a difference in the level of encephalization at similar body sizes between different groups (Striedter, 2005; Eberhard and Wcislo, 2011).

Our finding bears comparison with a recent analysis of brain scaling in 40 cichlid species (Tsuboi et al., 2016). Plotting both the inter- and intraspecific allometric brain-body size relationships, showed that the variation in intraspecific intercepts, rather than in the slopes, explained variation in relative brain size across species within a family (Tsuboi et al., 2016). Thus, the variation in relative brain size between these cichlid species was explained by overall differences in encephalization level, and not by species-specific variation in brain-body size scaling dynamics. Our results support this view, since our selection regime resulted in wasps of the L lines that had an absolutely larger brain size while having a smaller body size than wasps of the S lines. These differences in overall level of brain encephalization indicate that there was genetic variation in encephalization level in the starting (HVRx) population. This type of genetic variation may underlie evolution of differences in relative brain size.

Brain morphology

Our neuropil analysis (Figure 5) shows that our selection regime only affected the relative volume of the antennal lobe, which was larger in the L lines than in the S and C lines. These results are different from our previous work on body size effects on brain scaling and brain morphology in *N. vitripennis*, where we found differences in several neuropils, but not the AL (Groothuis and Smid, 2017). However, in that previous study we induced phenotypic plasticity in brain and body size, using varying degrees of scramble competition in an isogenic line. Genetic variation in brain size and phenotypic plasticity in brain size therefore appear to have different effects on neuropil composition, which implies that different mechanisms may be involved in regulating neuropil plasticity. Moreover, the difference in absolute neuropil volumes was much larger in our previous study addressing phenotypic plasticity: approximately 152% (Groothuis and Smid, 2017) in contrast to 16% in the present study (Figure 4).

These results suggest that the antennal lobe may have a fixed relative volume under scramble competition but a variable relative volume when genetic variation is present, whereas the opposite is the case for the other neuropils. For example, in both bumblebees and honeybees (which, in the same colony, have limited genetic variation, but 2 – 3 fold variation in brain volume), relative AL

volume does not vary over the size range of these species (Mares et al., 2005). Such constant scaling of AL volume was confirmed for honeybees in a later study (Gronenberg and Couvillon, 2010). By contrast, scramble competition in an isogenic strain of *T. evanescens* resulted in relatively smaller AL glomeruli in smaller brains (Chapter 3). Thus, the relation between relative neuropil volume, body size and genetic background deserves further study.

Memory retention

Our study shows that relative brain size does not affect memory performance. Wasps of the L and S lines showed similar levels and duration of memory retention. In contrast, a positive effect of larger brains on memory retention levels was recorded in our previous study on phenotypic plasticity in absolute brain size in *N. vitripennis* (Chapter 6). Furthermore, a study on guppies recorded higher memory retention levels in guppies that were selected for relatively larger brains (Kotrschal et al., 2013). Though other measures of brain size were used, thus hampering a comparison between guppies and wasps, the 16% difference in neuropil volume between *N. vitripennis* wasps of the L and S lines in our study exceeds the 9% difference in brain weight recorded in guppies. Hence, the similarity in olfactory memory performance of our selected *N. vitripennis* lines was surprising, but in line with our findings on relative neuropil volumes, as described below.

The mushroom bodies are important structures in the insect brain that are involved in learning and memory formation (Perry and Barron, 2012). Indeed, our previous study on phenotypic plasticity in body size shows that wasps with brains that are larger in absolute volume have higher memory retention levels (Chapter 6), and relatively larger mushroom bodies (Groothuis and Smid, 2017). In the current study, there was no difference in relative volumes of the mushroom bodies between the S, C and L lines (Figure 5), which is in line with the observed similarity in olfactory memory performance between wasps of the S and L lines. The combined results of the memory performance tests and neuropil analyses suggest that the costs and benefits of genetic changes in relative brain size may not be related to memory but to olfaction.

Our study also revealed a significantly higher level of memory retention abilities in the selected (S and L) than in the unselected C lines. Memory in the unselected C lines is, however, similar as in the original starting population HVRx (Figure S2). This indicates that our bidirectional selection regime resulted in increased memory retention abilities, whereas memory retention abilities remained

unchanged in the C lines. Our neuropil analysis suggests that this observed increase in both S and L lines does not have a basis in mushroom body volume, but potentially in other aspects of brain morphology not recorded in the present study.

Longevity

Our findings show that wasps with relatively larger brains live shorter than wasps with relatively small brains (Figure 7A). This illustrates the constitutive, global costs of brain tissue, in line with the theory that brain tissue is metabolically expensive (Aiello and Wheeler, 1995; Snell-Rood et al., 2009). Our results also show that C and L lines, but not the S lines, had lower longevity after an olfactory conditioning experience (Figure 7B). This suggests that memory formation is costly as well, but this cost did not become apparent in wasps with relatively smaller brains.

Memory formation can affect neuropil size and relative neuropil distribution. For instance, the relative volume of the mushroom bodies was found to increase with host-finding experience in the butterfly *Pieris rapae* (Snell-Rood et al., 2009). Such experience-dependent plasticity, in combination with the associated changes in metabolic costs, constitute the induced costs of learning (Snell-Rood et al., 2009). This could also underlie the learning-induced costs that were found in *Drosophila*, which live shorter after forming long-term memory (Mery and Kawecki, 2005) or when selected for improved aversion learning (Burger et al., 2008). That a conditioning experience did not affect longevity of wasps of the S lines in our study shows that learning-induced costs may be less severe in wasps with relatively small brains. The induced costs of learning may differ for wasps with differently sized brains, or with a different genetic background.

Conclusion

Our study shows for the first time the effects of artificial bidirectional selection on relative brain size in insects. We studied one of the smallest animals on Earth, the parasitic wasp *N. vitripennis*, which borders the limits of body and brain miniaturization. Due to its small size, *N. vitripennis* experiences particularly strong energetic and cognitive constraints that limit the variation in relative brain size. The variation in relative brain size is further limited by the unique brain-body size scaling relationship of *N. vitripennis*, with allometry in large individuals and isometry in the smallest individuals, which indicates that there is little phenotypic

plasticity in relative brain size. The limited selection response in our study indeed shows that the genetic variation in brain size is strongly constrained in this species. We have shown that small differences in relative brain size have large effects on longevity, indicating that strong energetic constraints act on relative brain size. The effect of relative brain size on relative antennal lobe volume indicates a specific adaptation in terms of olfaction. In the ongoing investigation of the question whether and how bigger brains are better (Chittka and Niven, 2009) we have provided a comprehensive and important dataset from the perspective of the smallest animal species studied in this regard, showing that bigger brains are not necessarily better, but certainly more costly.

Acknowledgements

We thank Bart Pannebakker and Gabriella Bukovinszkine Kiss (Laboratory of Genetics, Wageningen University) for providing the *Nasonia vitripennis* HVRx population and helpful discussion, and Marcel Dicke for commenting on drafts of this manuscript, and H. Schipper (Wageningen University, Experimental Zoology) for use of the confocal laser scanning microscope. This work was supported by NWO PE&RC Graduate Program grant 022.002.004 (to EW) and NWO Open Competition grant 820.01.012 (to HS and JG).

Supplementary Results

Table S1. Measured head and body size parameters for wasps of selected lines. Average body length and head width in μm (±SE) per generation in the selected lines.

	Body length			Head width		
Generation	Small	Large	Control	Small	Large	Control
0	1967 ± 10.2	1967 ± 10.2		668 ± 3.3	668 ± 3.3	
1	2426 ± 7.5	2350 ± 11.0		773 ± 2.1	776 ± 3.1	
2	2240 ± 10.1	2297 ± 12.2		740 ± 2.6	738 ± 3.4	
3	2230 ± 10.2	2280 ± 10.1		734 ± 3.5	756 ± 2.9	
4	2315 ± 9.6	2323 ± 9.8		746 ± 2.7	748 ± 2.7	
5	2271 ± 10.9	2245 ± 10.3		725 ± 3.2	732 ± 3.0	
6	2299 ± 14.6	2298 ± 12.3		734 ± 4.7	749 ± 3.6	
7	2272 ± 11.3	2317 ± 11.1		726 ± 3.3	746 ± 3.2	
8	2239 ± 12.6	2256 ± 10.7		729 ± 3.6	735 ± 3.2	
9	2208 ± 7.8	2230 ± 8.8		719 ± 2.4	727 ± 2.7	
10	2341 ± 8.4	2234 ± 13.6		741 ± 2.4	731 ± 3.9	
11	2281 ± 9.0	2293 ± 10.0		725 ± 2.5	750 ± 2.7	
12	2313 ± 12.9	2293 ± 12.0		724 ± 3.3	752 ± 3.4	
13	2284 ± 11.8	2321 ± 9.2		725 ± 3.3	752 ± 2.4	
14	2398 ± 6.9	2281 ± 10.8		751 ± 2.0	748 ± 2.9	
15	2388 ± 7.7	2385 ± 8.4		747 ± 1.8	764 ± 2.1	
16	2378 ± 10.1	2258 ± 10.6		737 ± 2.6	746 ± 3.0	
17	2293 ± 11.4	2264 ± 9.2		727 ± 3.4	740 ± 2.9	
18	2345 ± 10.9	2237 ± 9.7		736 ± 2.9	747 ± 2.9	
19	2299 ± 10.2	2226 ± 14.5		721 ± 2.6	731 ± 4.2	
20	2367 ± 8.7	2253 ± 10.3		737 ± 2.4	749 ± 2.6	
21	2279 ± 9.5	2289 ± 10.4		719 ± 2.5	742 ± 2.9	
22	2312 ± 8.6	2267 ± 9.9		724 ± 2.5	755 ± 2.9	
23	2331 ± 10.8	2194 ± 14.3		727 ± 2.9	724 ± 4.3	
24	2320 ± 11.0	2240 ± 14.9		722 ± 3.1	738 ± 4.6	
25	2383 ± 8.2	2236 ± 12.5	2347 ± 9.1	743 ± 2.6	732 ± 3.8	753 ± 2.6
26	2341 ± 10.2	2252 ± 10.6	2266 ± 13.3	728 ± 2.9	745 ± 3.1	725 ± 4.1
27	2341 ± 12.0	2286 ± 10.4	2384 ± 9.7	733 ± 3.3	751 ± 3.2	763 ± 3.0
28	2329 ± 9.2	2220 ± 12.6	2218 ± 11.2	718 ± 2.4	733 ± 4.0	719 ± 3.2
30	2289 ± 12.7	2108 ± 16.2	2237 ± 11.6	709 ± 3.4	702 ± 4.8	718 ± 3.5
33	2293 ± 8.3	2200 ± 11.7	2251 ± 10.3	720 ± 2.5	737 ± 3.3	731 ± 2.9
40	2244 ± 13.1	2172 ± 13.8	2238 ± 10.0	713 ± 4.0	732 ± 4.3	739 ± 3.1

Table S1. (cont.) Ratio between head width and body length (±SE) per generation in the selected lines. Final column shows the difference in average head-body ratio between the L and S lines (L-S) in percentages. N = 150 for each cell except generation 0, in which N = 300.

	Head - body ratio			
Generation	Small	Large	Control	Difference L-S (%)
0	0.3403 ± 0.0011	0.3403 ± 0.0011		
1	0.3186 ± 0.0005	0.3306 ± 0.0008		3.75
2	0.3307 ± 0.0010	0.3215 ± 0.0007		-2.78
3	0.3295 ± 0.0007	0.3317 ± 0.0008		0.68
4	0.3225 ± 0.0006	0.3221 ± 0.0007		-0.14
5	0.3194 ± 0.0006	0.3262 ± 0.0006		2.15
6	0.3195 ± 0.0007	0.3262 ± 0.0010		2.10
7	0.3196 ± 0.0007	0.3223 ± 0.0009		0.84
8	0.3259 ± 0.0007	0.3260 ± 0.0009		0.04
9	0.3257 ± 0.0007	0.3262 ± 0.0008		0.16
10	0.3166 ± 0.0007	0.3276 ± 0.0007		3.47
11	0.3180 ± 0.0006	0.3276 ± 0.0006		2.99
12	0.3134 ± 0.0007	0.3284 ± 0.0006		4.79
13	0.3177 ± 0.0007	0.3242 ± 0.0011		2.06
14	0.3132 ± 0.0007	0.3282 ± 0.0006		4.78
15	0.3131 ± 0.0007	0.3209 ± 0.0009		2.47
16	0.3104 ± 0.0008	0.3307 ± 0.0006		6.54
17	0.3169 ± 0.0007	0.3268 ± 0.0006		3.12
18	0.3143 ± 0.0007	0.3340 ± 0.0008		6.26
19	0.3140 ± 0.0006	0.3286 ± 0.0006		4.65
20	0.3115 ± 0.0006	0.3324 ± 0.0009		6.74
21	0.3153 ± 0.0007	0.3244 ± 0.0007		2.88
22	0.3133 ± 0.0005	0.3334 ± 0.0006		6.42
23	0.3122 ± 0.0007	0.3301 ± 0.0006		5.75
24	0.3115 ± 0.0007	0.3298 ± 0.0008		5.90
25	0.3118 ± 0.0006	0.3278 ± 0.0009	0.3208 ± 0.0006	5.14
26	0.3114 ± 0.0007	0.3310 ± 0.0006	0.3202 ± 0.0008	6.30
27	0.3134 ± 0.0007	0.3286 ± 0.0006	0.3199 ± 0.0006	4.86
28	0.3085 ± 0.0006	0.3302 ± 0.0006	0.3245 ± 0.0006	7.02
30	0.3100 ± 0.0007	0.3334 ± 0.0008	0.3209 ± 0.0006	7.55
33	0.3142 ± 0.0007	0.3352 ± 0.0007	0.3251 ± 0.0007	6.67
40	0.3180 ± 0.0009	0.3371 ± 0.0008	0.3305 ± 0.0009	6.03

Deviation from Haller's rule

Statistical analysis was performed on mean-centred body lengths (subtraction of mean body length of whole generation), whereas Figure S2 shows uncorrected body lengths and head widths (HW). Using mean-centred body lengths (sBL) for analysis ensured that differences in head-body ratio between the selected lines are reflected by differences in the intercept.

In generation 26, regression with mean-centred body length revealed significant differences in the intercept ($F_{2,444} = 48.523$, $p < 0.001$), but not in the slope ($F_{2,444} = 2.844$, $p = 0.059$). $R^2 = 0.805$. Large: HW = 0.273 × sBL + 757.123. Small: HW = 0.238 × sBL + 717.817. Control: HW = 0.273 × sBL + 733.394.

In generation 33, regression with mean-centred body length revealed significant differences in the intercept ($F_{2,444} = 36.466$, $p < 0.001$), but not in the slope ($F_{2,444} = 0.670$, $p = 0.512$). $R^2 = 0.784$. Large: HW = 0.260 × sBL + 749.048. Small: HW = 0.244 × sBL + 709.134. Control: HW = 0.245 × sBL + 730.396.

In generation 40, regression with mean-centred body length revealed significant differences in the intercept ($F_{2,444} = 60.432$, $p < 0.001$), but not in the slope ($F_{2,444} = 2.042$, $p = 0.131$). $R^2 = 0.809$. Large: HW = 0.292 × sBL + 745.181. Small: HW = 0.271 × sBL + 705.932. Control: HW = 0.258 × sBL + 734.108.

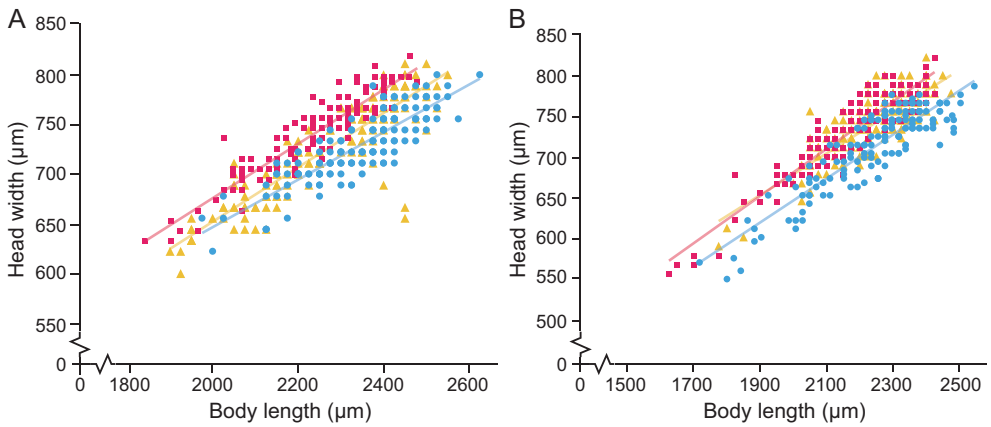

Figure S1. Head width and body length of wasps selected for relatively large (magenta squares) and small (blue circles) head-body ratio, and unselected control lines (yellow triangles). Measurements are shown for **(A)** generation 26 and **(B)** generation 40. Regression analysis was performed on mean-centred body lengths, because differences in head-body ratio can then be revealed by differences in the intercepts.

Memory retention levels

One day after conditioning, wasps from the S lines showed a mean PI (± SE) of 18.37 ± 5.39%, L of 18.36 ± 5.01% and C of 7.62 ± 5.51%. This memory retention was significant in all lines (S: $\chi^2_1 = 28.878$, $p < 0.001$; L: $\chi^2_1 = 34.082$, $p < 0.001$; C: $\chi^2_1 = 5.096$, $p = 0.024$). There was a significant difference in the level of memory retention between the selected and C lines 1 day after conditioning (S vs. C: $\chi^2_1 = 5.26$, $p = 0.022$; L vs. C: $\chi^2_1 = 7.84$, $p = 0.005$), but not between the S and L lines ($\chi^2_1 = 0.33$, $p = 0.567$). Three days after conditioning, wasps from the S lines showed a PI of 12.73 ± 6.17%, L of 9.14 ± 6.03% and C of 5.14 ± 6.22%. This memory retention was significant in the S and L lines (S: $\chi^2_1 = 13.935$, $p < 0.001$; L: $\chi^2_1 = 7.429$, $p = 0.006$), but not in C ($\chi^2_1 = 2.363$, $p = 0.124$). There were no significant differences in the level of memory retention between the lines 3 days after conditioning (S vs. C: $\chi^2_1 = 2.57$, $p = 0.109$; L vs. C: $\chi^2_1 = 0.82$, $p = 0.365$; S vs. L: $\chi^2_1 = 0.46$, $p = 0.498$). Five days after conditioning, S showed a PI of 4.10 ± 6.52%, L of 6.23 ± 6.40% and C of -1.09 ± 6.52%. None of this was significant memory retention (S: $\chi^2_1 = 1.20$, $p = 0.273$; L: $\chi^2_1 = 2.783$, $p = 0.095$; C: $\chi^2_1 = 0.084$, $p = 0.772$), and there were no differences in memory retention levels between the lines (S vs. C: $\chi^2_1 = 0.95$, $p = 0.329$; L vs. C: $\chi^2_1 = 1.96$, $p = 0.161$; S vs. L: $\chi^2_1 = 0.21$, $p = 0.649$).

Response rate was defined as the percentage of wasps that made a choice, out of the total amount of wasps that were inserted into the T-maze. There was no difference in response rate between wasps of the different lines ($\chi^2_2 = 1.054$, $p = 0.591$). Time after conditioning did affect response rate ($\chi^2_2 = 33.296$, $p < 0.001$), with higher response rates longer after conditioning (day 1 – 3: $\chi^2_1 = 11.363$, $p < 0.001$; day 3 – 5: $\chi^2_1 = 5.742$, $p = 0.017$; day 1 – 5: $\chi^2_1 = 31.834$, $p < 0.001$). The average response rate (±SE) was 72.53 ± 0.24% on day 1, 77.79 ± 0.19% on day 3 and 81.21 ± 0.27% on day 5. There was no significant effect of the interaction between the lines and time after conditioning ($\chi^2_4 = 1.302$, $p = 0.861$) on response rate.

Memory comparison with HVRx and AsymCx strains

We performed additional controls to compare memory performance of our selection and control lines to memory performance of the HVRx starting population and the AsymCx strain that we used in our previous study (Chapter 6). We therefore analysed memory retention of 2470 HVRx and 2179 AsymCx wasps following the same methodology as for our selection and control lines (Figure S4). There was significant memory retention (GLMM: conditioning $\chi^2_1 = 157.37$,

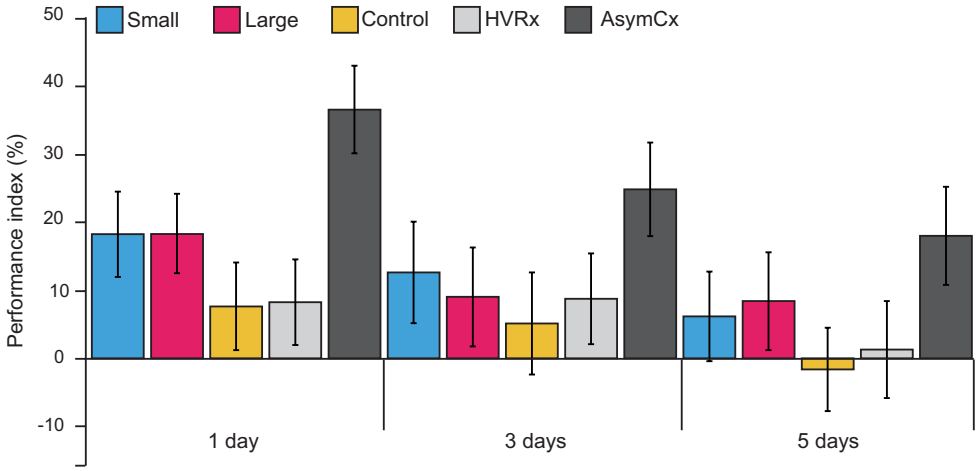

Figure S2. Memory retention over time for selection and control lines, and additional controls with the HVRx starting population and isogenic AsymCx line. Performance index (mean ± SE) shows difference in percentage of preference between reciprocally trained groups.

$p < 0.001$), and this retention decreased over time (GLMM: conditioning × time $\chi^2_2 = 32.59$, $p < 0.001$). There was an overall difference in memory retention between the different lines (GLMM: conditioning × line $\chi^2_4 = 67.64$, $p < 0.001$). Memory retention did not differ between S and L ($\chi^2_1 = 0.090$, $p = 0.767$), nor between C and HVRx. ($\chi^2_1 = 0.840$, $p = 0.359$). All other pairwise comparisons did yield significant differences (AsymCx – L: $\chi^2_1 = 18.46$, $p < 0.001$; AsymCx – C: $\chi^2_1 = 61.04$, $p < 0.001$; AsymCx – S: $\chi^2_1 = 44.81$, $p < 0.001$; AsymCx – HVRx: $\chi^2_1 = 22.23$, $p < 0.001$; L – C: $\chi^2_1 = 11.88$, $p < 0.001$; L – HVRx: $\chi^2_1 = 5.97$, $p = 0.015$; C – S: $\chi^2_1 = 10.64$, $p = 0.001$; HVRx – S: $\chi^2_1 = 4.95$, $p = 0.026$). Memory was maintained up to 3 days after conditioning in HVRx, and up to 5 days in AsymCx.

Longevity

Within the group of wasps that received a conditioning trial, mean longevity (± SE) was 10.11 ± 0.38 days in S, 6.28 ± 0.13 days in L and 9.17 ± 0.37 days in C. Within the group of naive wasps, mean longevity was 10.98 ± 0.32 days in S, 9.32 ± 0.22 days in L and 12.17 ± 0.42 days in C.

Table S2. All TukeyHSD comparisons of longevity in naive and conditioned wasps of the three lines. These values were used for Figure 7A.

		Naive			Conditioned		
		Small	Large	Control	Small	Large	Control
Naive	Small	-	-	-	-	-	-
	Large	$p = 0.004$	-	-	-	-	-
	Control	$p = 0.097$	$p < 0.001$	-	-	-	-
Conditioned	Small	$p = 0.404$	$p = 0.513$	$p < 0.001$	-	-	-
	Large	$p < 0.001$	$p < 0.001$	$p < 0.001$	$p < 0.001$	-	-
	Control	$p = 0.001$	$p = 0.999$	$p < 0.001$	$p = 0.304$	$p < 0.001$	-

Brain morphology

Table S3. Relative and absolute volumetric data on several neuropil regions in Small (S), Large (L), and Control (C) lines of selected *Nasonia vitripennis* wasps. Descriptives for all measurements are reported with n = 9 per selection regime.

	Line	**Relative volume** [1]					**Absolute volume** [2]				
		Statistics		Mean (%)	±	SE	Statistics		Mean (µm³)	±	SE
Total Neuropil	S			100			χ^2_2=8.0793 p = 0.0176	a	9.27 E+06	±	2.80 E+05
	L	N.S.		100				b	1.07 E+07	±	4.60 E+05
	C			100				b	1.07 E+07	±	2.46 E+05
Lobula	S			8.55	±	0.231			7.97 E+05	±	4.35 E+04
(Optic Lobe)	L	N.S.		8.79	±	0.285			9.47 E+05	±	5.41 E+04
	C			8.59	±	0.214			9.23 E+05	±	4.27 E+04
Medulla	S			18.37	±	0.411			1.71 E+06	±	8.57 E+04
(Optic Lobe)	L	N.S.		18.68	±	0.263			2.01 E+06	±	9.49 E+04
	C			18.50	±	0.346			1.99 E+06	±	8.29 E+04
Antennal Lobe	S	χ^2_2=19.237 p = 0.0007	a	11.27	±	0.205			1.04 E+06	±	2.18 E+04
	L		b	12.08	±	0.161			1.30 E+06	±	6.49 E+04
	C		a	11.29	±	0.082			1.21 E+06	±	2.48 E+04
Lateral Horn	S			2.53	±	0.092			2.35 E+05	±	1.17 E+04
	L	N.S.		2.66	±	0.067			2.86 E+05	±	1.50 E+04
	C			2.76	±	0.128			2.94 E+05	±	1.44 E+04
Lobes & Peduncle	S			4.90	±	0.105			4.53 E+05	±	1.35 E+04
(Mushroom Body)	L	N.S.		4.78	±	0.121			5.12 E+05	±	2.10 E+04
	C			5.04	±	0.118			5.37 E+05	±	1.12 E+04

Calyx	S		7.13 ± 0.180	6.59 E+05 ± 2.12 E+04
(Mushroom Body)	L	N.S.	6.98 ± 0.231	7.49 E+05 ± 3.64 E+04
	C		7.45 ± 0.212	7.95 E+05 ± 1.97 E+04
Fan-Shaped Body	S		1.02 ± 0.043	9.35 E+04 ± 3.06 E+03
(Central Complex)	L	N.S.	0.92 ± 0.031	9.94 E+04 ± 6.60 E+03
	C		0.99 ± 0.054	1.06 E+05 ± 4.70 E+03
Ellipsoid Body	S		0.16 ± 0.010	1.48 E+04 ± 7.78 E+02
(Central Complex)	L	N.S.	0.15 ± 0.011	1.67 E+04 ± 1.57 E+03
	C		0.16 ± 0.009	1.70 E+04 ± 7.46 E+02
Noduli	S		0.09 ± 0.005	7.86 E+03 ± 4.34 E+02
(Central Complex)	L	N.S.	0.08 ± 0.005	8.67 E+03 ± 6.33 E+02
	C		0.08 ± 0.006	8.37 E+03 ± 5.61 E+02
Protocerebral Bridge	S		0.24 ± 0.017	2.27 E+04 ± 1.87 E+03
(Central Complex)	L	N.S.	0.23 ± 0.013	2.48 E+04 ± 1.74 E+03
	C		0.26 ± 0.021	2.77 E+04 ± 2.15 E+03
Rest of neuropil	S		45.73 ± 0.376	4.23 E+06 ± 1.08 E+05
	L	N.S.	44.65 ± 0.446	4.79 E+06 ± 1.97 E+05
	C		44.87 ± 0.319	4.80 E+06 ± 9.06 E+04

[1]) Relative neuropil volumes were analysed with linear mixed model in R, followed by Holm-Bonferroni correction for multiple comparisons m=11 (LO,ME,AL,LH,MB-V,CA,FB,EB,NO,PB,RoN). Original p-value for the AL is $p < 0.003$. A post-hoc comparison (using the phia package) showed that the L line was different from S & C, with no difference between those. S↔L $p = 0.00012$, C↔L $p = 0.000179$, S↔C N.S. $p = 0.9188$.

[2]) Absolute neuropil volumes were only statistically analysed for the total neuropil volume. Selection regime had a significent effect on total neuropil volume, $\chi^2_2=8.0793$, $p = 0.0176$. Post-hoc pairwise comparisons revealed that S was different from L&C, with no difference between those. S↔C $p = 0.016$, S↔L $p = 0.012$, C↔L N.S. $p = 0.929$.

Chapter 8

General discussion

Introduction

The present thesis focussed on how evolutionary pressures on cognition and energetic costs shaped the characteristics of intraspecific brain-body size scaling in evolutionarily miniaturized parasitic wasps. I investigated which adaptations to neural morphology underlie intraspecific brain scaling, how these affect the cognitive performance of small and large wasps, and what the neural and cognitive consequences are of genetic variation in relative brain size. The results that are presented in my thesis reveal some intriguing solutions that enable parasitic wasps to cope with very small body sizes. These solutions include a brain-body size scaling strategy that is different in *Trichogramma evanescens* than in all other animal species studied so far, which is accompanied by an unexpected lack of cognitive consequences, and may be regulated by plasticity in the size rather than in the complexity of neural components. This general discussion will connect the findings of the previous chapters and elaborate on their implications.

Breaking Haller's rule

In Chapter 1, I explained how Haller's rule describes the general phenomenon of negative allometry in brain-body size scaling: small animals have relatively larger brains than large animals (Rensch, 1948; Rensch, 1956). Negative brain allometry may result from the combination of the positive correlation between brain size and brain performance, and the positive correlation between brain size and metabolic costs. These two factors constitute an energy-performance trade-off that constrains brain size through the level of brain performance that is required for adequate functioning, but also through the amount of energy that can be allocated to the development and maintenance of metabolically expensive brain tissue (Chapter 1). This energy-performance trade-off may be the most general force that acts on brain-body size scaling, drives evolution of brain size, and can be used to explain the consequences of variation in brain size.

Haller's rule holds in comparisons between species, i.e. evolutionary allometry, and between adults of the same species, i.e. static allometry (Chapter 1). In Chapters 1 and 2, I explained how evolutionary miniaturization processes could have restricted the size and complexity of the brains of the smallest insect species. Miniaturized insects may consequently have brains that are compromised compared to those of larger-bodied species. Intraspecific variation in body size, either through phenotypic plasticity or genetic variation, may cause some individuals within these evolutionarily miniaturized species to be even smaller. These smallest insects may not be able to reduce brain size proportionally to

the reduction in body size, because this would result in loss of vital aspects of brain performance. They may therefore need to heavily invest in brain tissue to maintain appropriate levels of cognition, which leads to strong negative allometry in brain-body size scaling.

Allometric brain scaling may be especially strong in evolutionarily miniaturized species when the smallest individuals of these species still require complex behaviour: their brains simply cannot be reduced too much without losing vital traits. I expected that this would be the case for *Trichogramma evanescens*. This miniaturized parasitic wasp is among the smallest insects on Earth, but still shows complex behavioural and cognitive traits. Even the smallest *T. evanescens* individuals hitch-hike on butterflies that are about to lay their eggs (Fatouros et al., 2005), can learn to remember odours and colours (Chapter 6) and can form long-term memory (Huigens et al., 2009; Kruidhof et al., 2012). The wasps need these cognitive abilities to find and parasitise their hosts. I therefore expected that the need to maintain these cognitive requirements would outbalance the need to reduce the energetic costs of brain tissue in the smallest individuals. This led to my hypothesis of very strong allometric brain scaling in *T. evanescens*, with a low scaling coefficient (Chapters 1 and 2).

The results of Chapter 2 were rather unexpected. The finding of an isometric scaling coefficient (Figure 1D) makes *T. evanescens* the first species known to escape from the predictions of Haller's rule. This brain-body size scaling strategy may be caused by the large relative brain size of *T. evanescens*, which constitutes on average 8.2% of body volume (Chapter 2). They therefore spend a large proportion of their energy on the development and maintenance of a large amount of brain tissue. The smallest *T. evanescens* may experience higher pressures to reduce energetic costs of brain tissue than to maintain brain performance, and consequently form smaller brains than expected from the predictions of Haller's rule.

Brain-body size scaling is more complex in the slightly larger parasitic wasp species *Nasonia vitripennis* (Groothuis and Smid, 2017). In this species, there is a diphasic brain-body size relationship with different allometric lines for small and large wasps (Figure 1E). Small *N. vitripennis* show isometry, whereas larger *N. vitripennis* show negative allometry. Due to this allometric brain scaling in large *N. vitripennis*, small *N. vitripennis* do have relatively larger brains than large conspecifics, but their brains are smaller than predicted by Haller's rule. This again suggests that the wasps experience higher evolutionary pressures to reduce energy expenditure than to maintain brain performance, especially the smaller individuals.

Trichogramma evanescens | *Nasonia vitripennis*

Variation in brain size

A Scramble competition

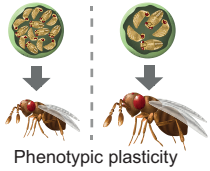

Phenotypic plasticity in brain and body size

B Scramble competition

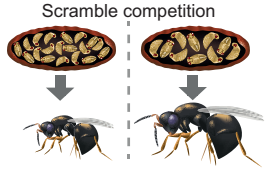

Phenotypic plasticity in brain and body size

C Artificial bidirectional selection

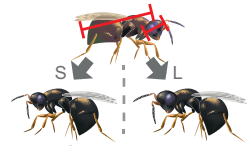

Genetic variation in relative brain size

Brain scaling

D Isometry (Chapter 2)

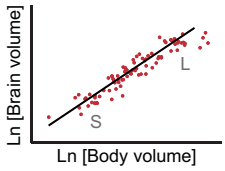

E Isometry-allometry (Groothuis and Smid, 2017)

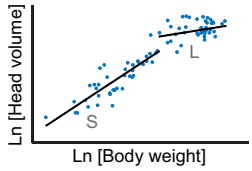

F Grade shift (Chapter 7)

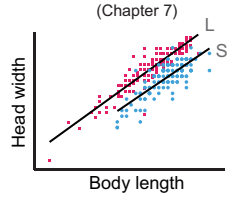

Memory performance

G

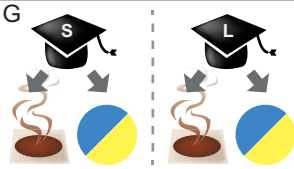

Equal olfactory memory performance
Equal visual memory performance
(Chapter 6)

H

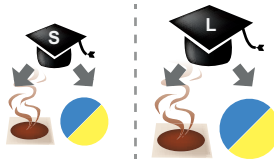

Small wasps: lower visual and olfactory memory performance
(Chapter 6)

I

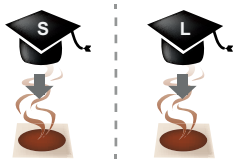

Equal olfactory memory performance
(Chapter 7)

Antennal lobe scaling

J Small wasps: relatively smaller antennal lobes

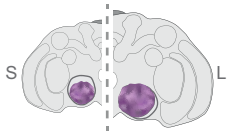

Equal number of glomeruli
(Chapter 3)

K Equal relative volume of antennal lobes

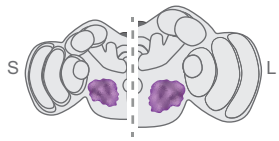

(Groothuis and Smid, 2017)

L Small-brained wasps: relatively smaller antennal lobes

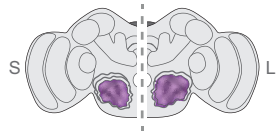

Equal relative volume other neuropils
(Chapter 7)

Neuron scaling

M Small wasps: smaller diameter of monoaminergic cell bodies

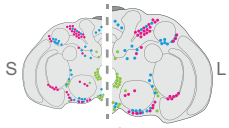

Equal number of monoaminergic neurons, similar to larger insects
(Chapters 4 & 5)

Neuropil scaling

N

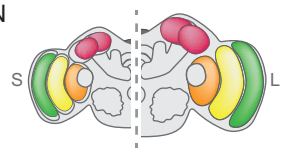

Small wasps: relatively smaller mushroom body calyx and optic lobes
(Groothuis and Smid, 2017)

Longevity

O

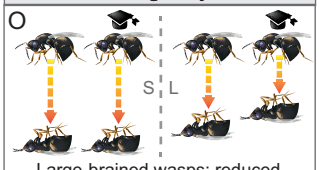

Large-brained wasps: reduced longevity, further reduction after memory formation
(Chapter 7)

◄ **Figure 1.** General overview of the characteristics of intraspecific brain scaling in *T. evanescens* and *N. vitripennis*. Variation in the level of scramble competition during larval development results in phenotypic plasticity in brain and body size in genetically identical wasps of the species *T. evanescens* **(A)** and *N. vitripennis* **(B)**. Artificial bidirectional selection on the ratio between body length and head width in a genetically diverse population of *N. vitripennis* gave rise to selection lines of wasps with relatively large and relatively small brains **(C)**. In both species, intraspecific brain-body size scaling deviates from the allometry that is predicted by Haller's rule. *Trichogramma evanescens* shows isometric brain-body size scaling **(D)**, and *N. vitripennis* shows diphasic brain scaling with isometry in small individuals and allometry in large individuals **(E)**. This deviation may be caused by energetic constraints caused by the high metabolic costs of brain tissue. The difference in relative brain size between large- and small-brained wasps of *N. vitripennis* selection lines **(F)** appears to be caused by a grade shift (elevation displacement on the brain-body size plot). Due to isometric and isometric – allometric brain scaling, small *T. evanescens* and *N. vitripennis* have brains that are smaller than is predicted by Haller's rule. Despite these small brains, small *T. evanescens* have similar visual and olfactory memory performance as large *T. evanescens* **(G)**. Small *N. vitripennis* do have reduced visual and olfactory memory performance compared to larger *N. vitripennis* **(H)**, whereas there was no effect of relative brain size on olfactory memory performance in this species **(I)**. The effect of phenotypic variation in brain size on the relative size of the antennal lobe differs between *T. evanescens* and *N. vitripennis*. In *T. evanescens*, small wasps have relatively smaller antennal lobes than large wasps **(J)**, whereas this is not the case for *N. vitripennis* **(K)**. Small and large *N. vitripennis* do differ in the relative size of some other neuropil areas, such as the optic lobes and mushroom body calyces **(N)**. Interestingly, *N. vitripennis* that were selected for relatively smaller brains do have relatively smaller antennal lobes than *N. vitripennis* that were selected for relatively larger brains **(L)**, whereas they do not differ in the relative size of other neuropil areas. Brain complexity, as quantified by the number of antennal lobe glomeruli **(J)** and monoaminergic neurons **(M)**, was equal for small and large *T. evanescens*. Wasps of this species even showed similar numbers of monoaminergic neurons as larger insects. The energetic costs of developing, maintaining and using a relatively large brain are illustrated by the reduced longevity of large-brained *N. vitripennis* compared to wasps with relatively small brains **(O)**. Longevity was even further reduced in large-brained wasps that had received a conditioning experience. Small-brained wasps did not show an effect of memory formation on longevity.

The deviation from Haller's rule results in "undersized" brains in the smallest *T. evanescens* and *N. vitripennis*, and these brains may be too small to maintain similar levels of cognitive, sensory and motor performance as in larger individuals. I therefore hypothesized that small *T. evanescens* and *N. vitripennis* would show reduced memory performance when compared to larger conspecifics. Due to the presence of allometric brain scaling in large *N. vitripennis*, I expected that the effect of body size on memory performance would be stronger in *T. evanescens* than in *N. vitripennis*. The results of Chapter 6 show the opposite. Small *T. evanescens* perform just as well in olfactory and visual memory retention

tests as their larger conspecifics (Figure 1G), whereas small *N. vitripennis* showed lower levels of olfactory and visual memory retention than larger conspecifics (Figure 1H). These results suggest that there are cognitive costs of being small in *N. vitripennis*, as expected from their isometric – allometric brain-body size scaling. In contrast, *T. evanescens* may be able to combine the best of the two extremes of brain-scaling: the smallest *T. evanescens* minimize energetic expenditure by scaling brain size isometrically, but they can also maintain memory performance (which should require strong allometric brain scaling).

Preparedness to develop small brains

Variation in body size was very large in *T. evanescens* and *N. vitripennis*. Body length ranged between 0.367 – 0.967 mm in *T. evanescens* and 1.375 – 2.825 mm in *N. vitripennis* (Chapter 6), while the use of isofemale strains ensured that the differently-sized conspecifics were genetically identical. This large size variation is therefore the result of phenotypic plasticity, as a result of variation in the level of induced scramble competition during larval development. The phenotypic response of a genotype to developmental conditions, such as the amount of available nutrition, is determined by genetically encoded developmental plasticity programmes (Lanet and Maurange, 2014). As a result, a single genotype has the potential to become a small or large adult, with the neural design that this requires (e.g. size, number and complexity of neural components and corresponding energy consumption). When there is genetic variation in developmental plasticity programmes, selective forces can act on the dynamics of brain-body size scaling, and optimize them to specific ecological circumstances. This can result in different brain-body size scaling rules, or in different consequences of brain-body size scaling on brain morphology and brain performance.

The difference between *T. evanescens* and *N. vitripennis* in the cognitive consequences of brain scaling suggests that their developmental plasticity programmes are adapted to a different balance between evolutionary pressures. Both species appear to experience strong selective pressures to minimize energy expenditure of brain tissue, which resulted in the evolution of isometric brain scaling in *T. evanescens* and small *N. vitripennis*. The two species experience additional evolutionary pressures to maintain cognitive abilities in the smallest brains. For *T. evanescens*, these pressures may have driven the evolution of neural pathways that support cognitive performance of even the smallest wasps. These wasps could still experience other trade-offs of isometric brain scaling, on which I elaborate below. The different effects of body size on memory performance between the two species could also indicate that small *T. evanescens* rely stronger

on learning abilities to find their hosts than small *N. vitripennis*, although memory retention levels cannot be directly compared between the two species. For *N. vitripennis*, it may be more adaptive to invest in other aspects of brain performance (e.g. maintenance of other neural pathways or functions), at the cost of memory retention.

As a result of the isometric component of diphasic brain scaling, there is little variation in relative brain size in genetically identical *N. vitripennis* (Groothuis and Smid, 2017). The genetic component of relative brain size may be similarly constrained. The work that is presented in Chapter 7 focusses on the questions of whether there is heritable genetic variation in relative brain size, and what the neural and cognitive consequences are of genetic variation in relative brain size. Artificial selection for increased and decreased relative brain size in *N. vitripennis* (Figure 1C) revealed that the selection response is slower, and realized heritability lower, than recorded for guppies in a similar experiment (Kotrschal et al., 2013). The slow selection response and low realized heritability suggest that variation in relative brain size is indeed strongly limited in *N. vitripennis*, possibly by strong energetic or cognitive constraints. Despite my aim to keep body size constant and focus solely on changes in relative brain size, the selection regime did also affect body size of the selected lines. This resulted in wasps with relatively larger brains also having a smaller body than wasps that were selected for relatively smaller brains. The size range of wasps that the selection regime yielded was within the size range of wasps that showed allometric brain scaling in the study of Groothuis and Smid (2017, Figure 1E). The difference in body size between the selected lines could therefore directly have caused differences in relative brain size through allometric brain scaling. However, Chapter 7 also reveals that the selected lines had different brain-body size regression lines, which had the same slope but different intercepts (Figure 1F). This suggests that the differences in relative brain size occurred through grade shifts, while the strength of brain-body size scaling remained constant between the selected lines. Additional volumetric brain and body size measurements are required for a large range of body sizes within both selected lines to establish if this is indeed the case.

The selection experiments showed that *N. vitripennis* with relatively large brains have reduced longevity, which was even further reduced after a learning experience (Figure 1O). This indicates that having and using relatively large brains is energetically costly. However, *N. vitripennis* with relatively large brains did not have improved olfactory memory retention abilities compared to *N. vitripennis* with relatively small brains (Chapter 7, Figure 1I). This indicates that genetic variation in relative brain size does not have cognitive consequences for

N. vitripennis. These results are in interesting contrast with the results of Chapter 6, which showed that phenotypic plasticity in body and brain size does affect memory retention strength in *N. vitripennis*. The combination of these results suggests that memory retention abilities may have evolved to be optimized in *N. vitripennis* with relatively small brains, but not in *N. vitripennis* with small body sizes.

How to cope with being small

In Chapter 1, I explained how the small size and number of neurons in small animals can affect their brain performance, and cause a "dilemma" that involved three not mutually exclusive strategies to cope with the costs of being small (Eberhard and Wcislo, 2011). These strategies are (1) size limitation, i.e. compromised behavioural and cognitive abilities in small animals, (2) economy of design, i.e. more efficient neural architecture that allows maintained cognitive performance in small animals, and (3) oversized brain, i.e. small animals having a relatively larger brain to maintain neural performance and neural architecture. This framework was originally developed for evolutionary body size miniaturization (Eberhard and Wcislo, 2011), but I argued that the same strategies can also underlie phenotypic plasticity in body size (Chapter 1).

The results on reduced memory retention levels in small *N. vitripennis* (Chapter 6) suggest that this species mostly applies the strategy of compromised brain performance at small sizes. It is more difficult to establish whether the wasps apply the other two strategies as well. As mentioned above, these wasps show diphasic brain-body size scaling with isometry in small wasps and allometry in large wasps (Groothuis and Smid, 2017). Due to the allometric component of this brain-scaling strategy, small wasps have relatively larger brains than large wasps. These brains are, however, smaller than expected from the predictions of Haller's rule due to the isometric component of diphasic brain-body size scaling. Hence, depending on the comparison that is made, small individuals can be argued to have both oversized and undersized brains. The work of Groothuis and Smid (2017) shows that small and large *N. vitripennis* differ in brain morphology. Many neuropil areas are smaller in relative size at small body sizes (Figure 1N), whereas others are maintained or even increase in relative volume. This indicates that specific neuropils are selectively maintained in small *N. vitripennis*, at the cost of other neuropils. Genetic variation in relative brain size does not have this effect on neuropil composition in *N. vitripennis* (Chapter 7). All neuropil areas are similar in relative size in *N. vitripennis* with relatively small and relatively large brains, with the exception of the antennal lobe (Figure

1L). Interestingly, the antennal lobe was among the neuropil areas that were not affected by phenotypic plasticity in body size (Groothuis and Smid, 2017; Figure 1K). This contrasting effect indicates that different mechanisms may underlie the development of neuropil areas, which cause relative neuropil volumes to be mostly genetically fixed, but variable under phenotypic plasticity in body size, whereas the opposite occurs for relative antennal lobe volume. This could suggest that a certain level of economized brain design evolved, although further research needs to establish if neural complexity is maintained in small *N. vitripennis*.

Trichogramma evanescens appears to cope differently with being small than *N. vitripennis*. Isometric brain scaling results in the same relative brain size in small and large *T. evanescens* (Chapter 2). Hence, *T. evanescens* do not apply the strategy that involves the formation of an oversized brain at small body sizes. The similarities in memory retention abilities in small and large *T. evanescens* (Chapter 6) indicate that *T. evanescens* also do not apply the strategy of compromised brain performance at small sizes. Instead, economized brain design may have evolved in this species. This would involve specific adaptations in the brain of *T. evanescens* that facilitate isometric brain scaling without affecting cognitive performance of small individuals. The present thesis discloses an exploration of such adaptations on neuropil level in the antennal lobe (Chapter 3), and on the level of monoaminergic neurons (Chapter 5). Similar results were found on both of these levels. Small and large wasps have equal numbers of glomeruli inside the antennal lobe (Figure 1J), and equal numbers of monoaminergic neurons in their brain (Figure 1M). There is, however, a difference in the size of these neural components. Small wasps have smaller glomeruli, both in absolute volume and relative to total brain volume. The monoaminergic cell bodies of small wasps are also smaller in diameter than those of large wasps. There may be similar levels of maintained neural complexity in other neural systems or neuropil areas, which may cause similar levels of neural functioning. The data presented in Chapters 3 and 5 suggest that isometric brain scaling in *T. evanescens* is facilitated by plasticity in the size, but not the complexity, of neural components. This may be the economy-of-design mechanism that underlies isometric brain scaling and simultaneously maintains the cognitive abilities of the smallest brains (Chapter 6), allowing even the smallest wasps to find suitable hosts.

The art of being small

The evolutionary forces and developmental programmes that underlie small body sizes may put strict limits on brain size and metabolic rate. For evolutionarily

miniaturized insects with a very limited number of neurons and a strict energy balance, it may be an especially challenging task to develop and maintain the ecologically required level of behavioural and cognitive performance. The work that is presented in this thesis reveals an interesting solution to this challenge of being extremely small. The data suggest that the smallest *T. evanescens* maintain neural complexity and cognitive performance while forming brains that are smaller, and therefore energetically cheaper, than would be possible in the situation that is described by Haller's rule. The strategy of maintaining neural complexity and brain performance under isometric brain scaling may be the "trick" that enables extremely small body sizes, which may form the art of being small.

However, isometric brain scaling not only causes brains sizes that are smaller than predicted by Haller's rule in small wasps, but also brain sizes that are larger than predicted by Haller's rule in large wasps. For small wasps, developing such small brains may be a solution to save energy. For large wasps, developing brains that are larger than predicted by Haller's rule has high energetic costs. This suggests that having a very large brain must be beneficial for large wasps, and that these benefits outweigh the associated energetic costs. Hence, there must be costs of having a small brain and benefits of having a large brain under isometric brain scaling that my research has not yet revealed for *T. evanescens*. These costs and benefits appear not to be associated with memory retention (Chapter 6), olfaction (Chapter 3) or performance of monoaminergic neurons (Chapter 5).

The costs and benefits of isometric brain scaling may relate to neural modifications at differ levels than those that are presented in this thesis. For example, small and large wasps may differ in the number of neuronal cell bodies other than those that produce octopamine, dopamine or serotonin. Having fewer neurons could reduce neural functioning in small wasps, because neural pathways may be modified or removed. It would be especially interesting to compare total numbers of neuronal cell bodies in the brains of small and large *T. evanescens*. Neural cell counts have been made for mammalian brains with an isotropic fractionator, which homogenizes brain tissue into a suspension of neural nuclei that can be fluorescently stained, visualized and counted (Herculano-Houzel and Lent, 2005). This method could be adapted to the smaller size of neural cell bodies in insects, and subsequently used to compare numbers of cell bodies and glial cells in the brains of small and large conspecific wasps of the isofemale strains of *T. evanescens* and *N. vitripennis*.

Furthermore, differences in neural complexity between small and large *T. evanescens* may occur at the level of individual synapses. Absolute and relative volume of

the glomeruli in the antennal lobe are smaller in the brains of small *T. evanescens* when compared to larger conspecifics (Chapter 3). Glomeruli contain the many synaptic connections between olfactory neurons, interneurons and projection neurons (Davis, 2004). The smaller size of glomeruli in small wasps may relate to a smaller number of synapses, which could negatively affect the further processing of olfactory information. Similar reductions in number of synapses may occur in other neural networks, which may reduce the computational abilities of small brains (Niven and Farris, 2012).

Finally, there may also be costs of isometric brain scaling that arise from having very small neurons. Small *T. evanescens* have significantly smaller monoaminergic cell bodies than large *T. evanescens* (Chapter 5). Having such small cell bodies can be costly, because there is little space available for cytoplasm and cell organelles (Niven, 2016). As a result, the number of mitochondria may be lower, which reduces the available energy for neural activity. The nucleus may also be smaller, due to a reduction of genome size or increased chromatin compaction (Gregory, 2001; Polilov, 2015). This may negatively affect transcriptional dynamics and protein synthesis. The functioning and maintenance of neurons may therefore be compromised in wasps with small cell bodies. This could underlie the reduced longevity of small wasps compared to larger conspecifics, which has been observed for several species of the genus *Trichogramma*, including *T. evanescens* (Waage and Ming, 1984; Bai et al., 1992; Pavlik, 1993; Olson and Andow, 1998; Kuhlmann and Mills, 1999).

More severe reductions of cell body size may require the lysis of nuclei. This formation of anucleated neurons is shown by *Megaphragma mymaripenne*, a trichogrammatid wasp that is more strongly miniaturized than *T. evanescens* (Polilov, 2012). Approximately 95% of neural nuclei in the brain of *M. mymaripenne* lyse during the final pupal stage, resulting in adults with only ~215 nucleated neurons in the brain. This strategy must have severe costs for neural functioning, because the lysed nuclei are incapable of transcription. How this affects the level of cognitive and behavioural complexity of this species, and its host-finding success, is unfortunately unknown. The low number of nucleated neurons may relate to the relatively short longevity of this species: honey-fed *M. mymaripenne* survive for five days at 25ºC (Bernardo and Viggiani, 2000) whereas e.g. *Trichogramma minutum* survive for 25 days at 25ºC (Yu et al., 1984). The number of nucleated neurons has been estimated to be around 37,000 in small adult *T. evanescens* (Polilov, 2012), and anucleated neurons have not been observed in this species (Makarova and Polilov, 2013). This suggests that *T. evanescens* applies a more subtle brain miniaturization strategy than *M. mymaripenne*, which enables

T. evanescens to maintain neural and cognitive complexity, but could prevent further miniaturization of brain size. Future studies should reveal if the neural modifications that are outlined above occur in *T. evanescens*, and what their consequences are for brain performance or fitness.

Conclusion

Evolutionarily miniaturized parasitic wasps experience strong selective pressures on brain size. These force them to reduce the energy expenditure of their brain, while cognitive abilities need to be maintained to find suitable hosts. In this thesis, I have revealed how these evolutionary pressures on cognition and energetic costs shaped the characteristics of intraspecific brain-body size scaling. The two species that were the focus of this thesis show distinctly different brain scaling strategies, with different neural backgrounds and cognitive consequences, possibly because they experienced a different balance between the energetic and cognitive constraints of brain size. *Trichogramma evanescens* is the first species to show isometric brain-body size scaling, and *N. vitripennis* is the first species to show diphasic brain-body size scaling with isometry in small individuals and allometry in large individuals.

For *N. vitripennis*, two separate developmental programmes regulate brain-body size scaling: one that involves allometric brain scaling and one that involves isometric brain scaling. Energetic constraints may have been so strong that, under scramble competition, the smallest body sizes can only be achieved through isometric brain scaling. The lower memory retention levels in these small *N. vitripennis* compared to larger conspecifics suggest that it is more adaptive for small wasps to invest in other aspects of brain performance, at the cost of memory retention abilities. Relative brain size is constrained in these genetically identical *N. vitripennis*, due to the isometric component of diphasic brain scaling. The genetic component of relative brain size is also very constrained in *N. vitripennis*, as was shown by the slow response of bidirectional selection on relative brain size. The energetic constraints of brain tissue are revealed by the reduced longevity of wasps with relatively larger brains, and the further reduction of longevity after these wasps have used their brains to form memory. Surprisingly, genetic variation in relative brain size does not affect memory retention abilities, which contrasts the effects of phenotypic plasticity in body size on memory retention. This contrast suggests that memory retention abilities may have evolved to be optimized in *N. vitripennis* with relatively small brains, but not in *N. vitripennis* with small body sizes.

For *T. evanescens*, the energetic constraints of brain tissue must also be very strong to have resulted in isometric brain-body size scaling. Nonetheless, small and large individuals of this species showed unexpectedly similar memory retention levels. This suggests that *T. evanescens* also experienced strong evolutionary pressures to maintain cognitive performance, despite the limited brain size. The maintained memory retention abilities could be caused by maintained neural complexity, as isometric brain scaling appears to be facilitated by plasticity in size rather than in complexity of neural components in *T. evanescens*. However, isometric brain scaling can still be costly for the smallest individuals through reduction in size and complexity of neurons and processing pathways, which larger wasps avoid by investing more in brain tissue.

To conclude, my thesis revealed some intricate solutions that the smallest animals apply to meet the challenges of maintaining adequate brain performance with a very limited brain size. Evading Haller's rule may allow evolutionarily miniaturized species to achieve smaller brain and body sizes by avoiding the excessive energetic costs of maintaining a relatively larger brain. Through some unexpected neural solutions, the most miniaturized insects are able to maintain cognitive performance in an extremely small brain. This may form the art of being small.

References

Adams MD, Celniker SE, Holt RA, Evans CA, Gocayne JD, Amanatides PG, Scherer SE, Li PW, Hoskins RA, Galle RF, George RA, Lewis SE, Richards S, Ashburner M, Henderson SN, Sutton GG, Wortman JR, Yandell MD, Zhang Q, Chen LX, Brandon RC, Rogers Y-HC, Blazej RG, Champe M, Pfeiffer BD, Wan KH, Doyle C, Baxter EG, Helt G, Nelson CR, Gabor GL, Miklos, Abril JF, Agbayani A, An H-J, Andrews-Pfannkoch C, Baldwin D, Ballew RM, Basu A, Baxendale J, Bayraktaroglu L, Beasley EM, Beeson KY, Benos PV, Berman BP, Bhandari D, Bolshakov S, Borkova D, Botchan MR, Bouck J, Brokstein P, Brottier P, Burtis KC, Busam DA, Butler H, Cadieu E, Center A, Chandra I, Cherry JM, Cawley S, Dahlke C, Davenport LB, Davies P, Pablos Bd, Delcher A, Deng Z, Mays AD, Dew I, Dietz SM, Dodson K, Doup LE, Downes M, Dugan-Rocha S, Dunkov BC, Dunn P, Durbin KJ, Evangelista CC, Ferraz C, Ferriera S, Fleischmann W, Fosler C, Gabrielian AE, Garg NS, Gelbart WM, Glasser K, Glodek A, Gong F, Gorrell JH, Gu Z, Guan P, Harris M, Harris NL, Harvey D, Heiman TJ, Hernandez JR, Houck J, Hostin D, Houston KA, Howland TJ, Wei M-H, Ibegwam C, Jalali M, Kalush F, Karpen GH, Ke Z, Kennison JA, Ketchum KA, Kimmel BE, Kodira CD, Kraft C, Kravitz S, Kulp D, Lai Z, Lasko P, Lei Y, Levitsky AA, Li J, Li Z, Liang Y, Lin X, Liu X, Mattei B, McIntosh TC, McLeod MP, McPherson D, Merkulov G, Milshina NV, Mobarry C, Morris J, Moshrefi A, Mount SM, Moy M, Murphy B, Murphy L, Muzny DM, Nelson DL, Nelson DR, Nelson KA, Nixon K, Nusskern DR, Pacleb JM, Palazzolo M, Pittman GS, Pan S, Pollard J, Puri V, Reese MG, Reinert K, Remington K, Saunders RDC, Scheeler F, Shen H, Shue BC, Sidén-Kiamos I, Simpson M, Skupski MP, Smith T, Spier E, Spradling AC, Stapleton M, Strong R, Sun E, Svirskas R, Tector C, Turner R, Venter E, Wang AH, Wang X, Wang Z-Y, Wassarman DA, Weinstock GM, Weissenbach J, Williams SM, Woodage T, Worley KC, Wu D, Yang S, Yao QA, Ye J, Yeh R-F, Zaveri JS, Zhan M, Zhang G, Zhao Q, Zheng L, Zheng XH, Zhong FN, Zhong W, Zhou X, Zhu S, Zhu X, Smith HO, Gibbs RA, Myers EW, Rubin GM, Venter JC. 2000. The Genome Sequence of *Drosophila melanogaster*. Science 287(5461):2185-2195.

Aiello LC, Wheeler P. 1995. The expensive-tissue hypothesis - the brain and the digestive system in human and primate evolution. Curr Anthropol 36(2):199-221.

Amornsak W, Cribb B, Gordh G. 1998. External morphology of antennal sensilla of *Trichogramma australicum* Girault (Hymenoptera: Trichogrammatidae). Int J Insect Morphol Embryol 27(2):67-82.

Anderson ML. 2010. Neural reuse: A fundamental organizational principle of the brain. Behav Brain Sci 33(4):245-266.

Ardila-Garcia AM, Umphrey GJ, Gregory TR. 2010. An expansion of the genome size dataset for the insect order Hymenoptera, with a first test of parasitism and eusociality as possible constraints. Insect Mol Biol 19(3):337-346.

Arnold G, Masson C, Budharugsa S. 1985. Comparative study of the antennal lobes and their afferent pathway in the worker bee and the drone (*Apis mellifera*). Cell Tissue Res 242(3):593-605.

Aso Y, Herb A, Ogueta M, Siwanowicz I, Templier T, Friedrich AB, Ito K, Scholz H, Tanimoto H. 2012. Three dopamine pathways induce aversive odor memories with different stability. PLoS Genet 8(7):e1002768.

Aso Y, Siwanowicz I, Bracker L, Ito K, Kitamoto T, Tanimoto H. 2010. Specific dopaminergic neurons for the formation of labile aversive memory. Curr Biol 20(16):1445-1451.

Bai B, Luck RF, Forster L, Stephens B, Janssen JAM. 1992. The effect of host size on quality attributes of the egg parasitoid, *Trichogramma pretiosum*. Entomol Exp Appl 64(1):37-48.

Bates D, Maechler M, Bolker B, Walker S. 2014. lme4: Linear mixed-effects models using Eigen and S4. R package version 1.1-7.

Bennett DM, Hoffmann AA. 1998. Effects of size and fluctuating asymmetry on field fitness of the parasitoid *Trichogramma carverae* (Hymenoptera : Trichogrammatidae). J Anim Ecol 67(4):580-591.

Bernardo U, Viggiani G. 2000. Biological data on *Megaphragma amalphitanum* Viggiani and *Megaphragma mymaripenne* Timberlake (Hymenoptera: Trichogrammatidae), egg-parasitoids of *Heliothrips haemorrhoidalis* (Thysanoptera: Thripidae) in southern Italy. Boll Lab Entomol Agrar Filippo Silvestri 58:77-85.

Beutel RG, Pohl H, Hunefeld F. 2005. Strepsipteran brains and effects of miniaturization (Insecta). Arthropod Struct Dev 34(3):301-313.

Bleeker MA, Smid HM, Van Aelst AC, Van Loon JJA, Vet LEM. 2004. Antennal sensilla of two parasitoid wasps: a comparative scanning electron microscopy study. Microsc Res Tech 63(5):266-273.

Bleeker MAK, Van der Zee B, Smid HM. 2006. Octopamine-like immunoreactivity in the brain and suboesophageal ganglion of two parasitic wasps, *Cotesia glomerata* and *Cotesia rubecula*. Anim Biol 56(2):247-257.

Blenau W, Thamm M. 2011. Distribution of serotonin (5-HT) and its receptors in the insect brain with focus on the mushroom bodies: lessons from *Drosophila melanogaster* and *Apis mellifera*. Arthropod Struct Dev 40(5):381-394.

Bloch G, Simon T, Robinson EG, Hefetz A. 2000. Brain biogenic amines and reproductive dominance in bumble bees (*Bombus terrestris*). J Comp Physiol

A 186(3):261-268.
Boddy AM, McGowen MR, Sherwood CC, Grossman LI, Goodman M, Wildman DE. 2012. Comparative analysis of encephalization in mammals reveals relaxed constraints on anthropoid primate and cetacean brain scaling. J Evol Biol 25(5):981-994.
Brandt R, Rohlfing T, Rybak J, Krofczik S, Maye A, Westerhoff M, Hege HC, Menzel R. 2005. Three-dimensional average-shape atlas of the honeybee brain and its applications. J Comp Neurol 492(1):1-19.
Budnik V, White K. 1988. Catecholamine-containing neurons in *Drosophila melanogaster*: distribution and development. J Comp Neurol 268(3):400-413.
Burger JM, Kolss M, Pont J, Kawecki TJ. 2008. Learning ability and longevity: a symmetrical evolutionary trade-off in *Drosophila*. Evolution 62(6):1294-1304.
Burke CJ, Huetteroth W, Owald D, Perisse E, Krashes MJ, Das G, Gohl D, Silies M, Certel S, Waddell S. 2012. Layered reward signalling through octopamine and dopamine in *Drosophila*. Nature 492(7429):433-437.
Burns JG, Saravanan A, Rodd FH. 2009. Rearing environment affects the brain size of guppies: lab-reared guppies have smaller brains than wild-caught guppies. Ethology 115(2):122-133.
Busch S, Selcho M, Ito K, Tanimoto H. 2009. A map of octopaminergic neurons in the *Drosophila* brain. J Comp Neurol 513(6):643-667.
Campi KL, Krubitzer L. 2010. Comparative studies of diurnal and nocturnal rodents: differences in lifestyle result in alterations in cortical field size and number. J Comp Neurol 518(22):4491-4512.
Cardona A, Saalfeld S, Schindelin J, Arganda-Carreras I, Preibisch S, Longair M, Tomancak P, Hartenstein V, Douglas RJ. 2012. TrakEM2 software for neural circuit reconstruction. PLoS One 7(6).
Chen Y-C, Harrison PW, Kotrschal A, Kolm N, Mank JE, Panula P. 2015. Expression change in Angiopoietin-1 underlies change in relative brain size in fish. Proc R Soc Lond B Biol Sci 282(1810).
Cheverud JM. 1982. Relationships among ontogenetic, static, and evolutionary allometry. Am J Phys Anthropol 59(2):139-149.
Chittka L, Niven J. 2009. Are bigger brains better? Curr Biol 19(21):R995-R1008.
Claridge-Chang A, Roorda RD, Vrontou E, Sjulson L, Li H, Hirsh J, Miesenbock G. 2009. Writing memories with light-addressable reinforcement circuitry. Cell 139(2):405-415.
Consoli FL, Kitajima EW, Parra JR. 1999. Sensilla on the antenna and ovipositor of the parasitic wasps *Trichogramma galloi* Zucchi and *T. pretiosum* Riley (Hym., Trichogrammatidae). Microsc Res Tech 45(4-5):313-324.
Couto A, Alenius M, Dickson BJ. 2005. Molecular, anatomical, and functional

organization of the *Drosophila* olfactory system. Curr Biol 15(17):1535-1547.
Cuvillier-Hot V, Lenoir A. 2006. Biogenic amine levels, reproduction and social dominance in the queenless ant *Streblognathus peetersi*. Naturwissenschaften 93(3):149-153.
Dacks AM, Christensen TA, Agricola HJ, Wollweber L, Hildebrand JG. 2005. Octopamine-immunoreactive neurons in the brain and subesophageal ganglion of the hawkmoth *Manduca sexta*. J Comp Neurol 488(3):255-268.
Dacks AM, Christensen TA, Hildebrand JG. 2006. Phylogeny of a serotonin-immunoreactive neuron in the primary olfactory center of the insect brain. J Comp Neurol 498(6):727-746.
Darling DC, Werren JH. 1990. Biosystematics of *Nasonia* (Hymenoptera: Pteromalidae): two new species reared from birds' nests in North America. Ann Entomol Soc Am 83(3):352-370.
Das P, Fadamiro HY. 2013. Species and sexual differences in antennal lobe architecture and glomerular organization in two parasitoids with different degree of host specificity, *Microplitis croceipes* and *Cotesia marginiventris*. Cell Tissue Res 352(2):227-235.
Davis RL. 2004. Olfactory learning. Neuron 44(1):31-48.
De Rosario-Martinez H. phia: post-hoc interaction analysis. R package version 0.1-5.
De Vos K. 2010. ImageJ Cell Counter plugin. Version 2010/12/07.
Dicke U, Roth G. 2016. Neuronal factors determining high intelligence. Philos Trans R Soc Lond B Biol Sci 371(1685):20150180.
Doyon J, Boivin G. 2005. The effect of development time on the fitness of female *Trichogramma evanescens*. J Insect Sci 5:4.
Dutton A, Bigler F. 1995. Flight activity assessment of the egg parasitoid *Trichogramma brassicae* (Hym: Trichogrammatidae) in laboratory and field conditions. Entomophaga 40(2):223-233.
Eberhard WG, Wcislo WT. 2011. Grade changes in brain–body allometry: morphological and behavioural correlates of brain size in miniature spiders, insects and other invertebrates. In: Casas J, ed. Spider Physiology and Behaviour. Vol 40: Academic Press. p 155-214.
Egset CK, Bolstad GH, Rosenqvist G, Endler JA, Pelabon C. 2011. Geographical variation in allometry in the guppy (*Poecilia reticulata*). J Evol Biol 24(12):2631-2638.
Faisal AA, Selen LPJ, Wolpert DM. 2008. Noise in the nervous system. Nat Rev Neurosci 9(4):292-303.
Faisal AA, White JA, Laughlin SB. 2005. Ion-channel noise places limits on the miniaturization of the brain's wiring. Curr Biol 15(12):1143-1149.

Falster DS, Warton DI, Wright IJ. 2006. SMATR: Standardised major axis tests and routines. Version 2.

Farris SM, Schulmeister S. 2011. Parasitoidism, not sociality, is associated with the evolution of elaborate mushroom bodies in the brains of hymenopteran insects. Proc Biol Sci 278(1707):940-951.

Fatouros NE, Broekgaarden C, Bukovinszkine'Kiss G, van Loon JJA, Mumm R, Huigens ME, Dicke M, Hilker M. 2008a. Male-derived butterfly anti-aphrodisiac mediates induced indirect plant defense. Proc Natl Acad Sci U S A 105(29):10033-10038.

Fatouros NE, Dicke M, Mumm R, Meiners T, Hilker M. 2008b. Foraging behavior of egg parasitoids exploiting chemical information. Behav Ecol 19(3):677-689.

Fatouros NE, Huigens ME, van Loon JJA, Dicke M, Hilker M. 2005. Chemical communication: butterfly anti-aphrodisiac lures parasitic wasps. Nature 433(7027):704.

Fatouros NE, Lucas-Barbosa D, Weldegergis BT, Pashalidou FG, van Loon JJA, Dicke M, Harvey JA, Gols R, Huigens ME. 2012. Plant volatiles induced by herbivore egg deposition affect insects of different trophic levels. PLoS One 7(8):e43607.

Fatouros NE, Pineda A, Huigens ME, Broekgaarden C, Shimwela MM, Figueroa Candia IA, Verbaarschot P, Bukovinszky T. 2014. Synergistic effects of direct and indirect defences on herbivore egg survival in a wild crucifer. Proc Biol Sci 281(1789):20141254.

Feener DH, Lighton JRB, Bartholomew GA. 1988. Curvilinear allometry, energetics and foraging ecology: a comparison of leaf-cutting ants and army ants. Funct Ecol 2(4):509-520.

Fischer S, Muller CH, Meyer-Rochow VB. 2011. How small can small be: the compound eye of the parasitoid wasp *Trichogramma evanescens* (Westwood, 1833) (Hymenoptera, Hexapoda), an insect of 0.3- to 0.4-mm total body size. Vis Neurosci 28(4):295-308.

Fox J, Weisberg, S. 2011. An {R} companion to applied regression. Thousand Oaks, CA: Sage.

Gao Q, Yuan B, Chess A. 2000. Convergent projections of *Drosophila* olfactory neurons to specific glomeruli in the antennal lobe. Nat Neurosci 3(8):780-785.

Gonda A, Herczeg G, Merila J. 2011. Population variation in brain size of nine-spined sticklebacks (*Pungitius pungitius*) - local adaptation or environmentally induced variation? BMC Evol Biol 11:75.

Grabe V, Strutz A, Baschwitz A, Hansson BS, Sachse S. 2015. Digital in vivo

3D atlas of the antennal lobe of *Drosophila melanogaster*. J Comp Neurol 523(3):530-544.
Grebennikov VV. 2008. How small you can go: Factors limiting body miniaturization in winged insects with a review of the pantropical genus *Discheramocephalus* and description of six new species of the smallest beetles (Pterygota: Coleoptera: Ptiliidae). Eur J Entomol 105(2):313-327.
Gregory TR. 2001. Coincidence, coevolution, or causation? DNA content, cell size, and the C-value enigma. Biol Rev 76(1):65-101.
Gronenberg W, Couvillon MJ. 2010. Brain composition and olfactory learning in honey bees. Neurobiol Learn Mem 93(3):435-443.
Groothuis J, Smid HM. 2017. *Nasonia* parasitic wasps escape from Haller's rule by diphasic, partially isometric brain-body size scaling and selective neuropil adaptations. Brain Behav Evol, *in press*.
Haller Av. 1757. Elementa physiologiae corporis humani. Auctore Alberto v. Haller. Lausannae: Sumptibus M. M. Bousquet et Sociorum.
Hammer M, Menzel R. 1995. Learning and memory in the honeybee. J Neurosci 15(3 Pt 1):1617-1630.
Hanken J, Wake DB. 1993. Miniaturization of body-size - organismal consequences and evolutionary significance. Annu Rev Ecol Syst 24:501-519.
Hansson BS, Anton S. 2000. Function and morphology of the antennal lobe: new developments. Annu Rev Entomol 45:203-231.
Harris JW, Woodring J. 1992. Effects of stress, age, season, and source colony on levels of octopamine, dopamine and serotonin in the honey-bee (*Apis mellifera* L) Brain. J Insect Physiol 38(1):29-35.
Harvey PH, Krebs JR. 1990. Comparing brains. Science 249(4965):140-146.
Haverkamp A, Smid HM. 2014. Octopamine-like immunoreactive neurons in the brain and subesophageal ganglion of the parasitic wasps *Nasonia vitripennis* and *N. giraulti*. Cell Tissue Res 358(2):313-329.
Heinbockel T, Shields VD, Reisenman CE. 2013. Glomerular interactions in olfactory processing channels of the antennal lobes. J Comp Physiol A Neuroethol Sens Neural Behav Physiol 199(11):929-946.
Herculano-Houzel S, Lent R. 2005. Isotropic fractionator: A simple, rapid method for the quantification of total cell and neuron numbers in the brain. J Neurosci 25(10):2518-2521.
Hoedjes KM, Kralemann LEM, van Vugt JJFA, Vet LEM, Smid HM. 2014a. Unravelling reward value: the effect of host value on memory retention in *Nasonia* parasitic wasps. Anim Behav 96:1-7.
Hoedjes KM, Kruidhof HM, Huigens ME, Dicke M, Vet LEM, Smid HM.

2011. Natural variation in learning rate and memory dynamics in parasitoid wasps: opportunities for converging ecology and neuroscience. Proc Biol Sci 278(1707):889-897.

Hoedjes KM, Smid HM. 2014. Natural variation in long-term memory formation among *Nasonia* parasitic wasp species. Behav Processes 105(0):40-45.

Hoedjes KM, Smid HM, Vet LEM, Werren JH. 2014b. Introgression study reveals two quantitative trait loci involved in interspecific variation in memory retention among *Nasonia* wasp species. Heredity 113(6):542-550.

Hoedjes KM, Steidle JL, Werren JH, Vet LEM, Smid HM. 2012. High-throughput olfactory conditioning and memory retention test show variation in *Nasonia* parasitic wasps. Genes Brain Behav 11(7):879-887.

Hölldobler B, Wilson EO. 2009. The superorganism: the beauty, elegance, and strangeness of insect societies. New York: Norton.

Holm S. 1979. A simple sequentially rejective multiple test procedure. Scand J Statist 6(2):65-70.

Hopwood D. 1967. Some aspects of fixation with glutaraldehyde. A biochemical and histochemical comparison of the effects of formaldehyde and glutaraldehyde fixation on various enzymes and glycogen, with a note on penetration of glutaraldehyde into liver. J Anat 101(Pt 1):83-92.

Hoyer SC, Liebig J, Rossler W. 2005. Biogenic amines in the ponerine ant *Harpegnathos saltator*: serotonin and dopamine immunoreactivity in the brain. Arthropod Struct Dev 34(4):429-440.

Huigens ME, de Almeida RP, Boons PA, Luck RF, Stouthamer R. 2004. Natural interspecific and intraspecific horizontal transfer of parthenogenesis-inducing *Wolbachia* in *Trichogramma* wasps. Proc Biol Sci 271(1538):509-515.

Huigens ME, de Swart E, Mumm R. 2011. Risk of egg parasitoid attraction depends on anti-aphrodisiac titre in the large cabbage white butterfly *Pieris brassicae*. J Chem Ecol 37(4):364-367.

Huigens ME, Luck RF, Klaassen RH, Maas MF, Timmermans MJ, Stouthamer R. 2000. Infectious parthenogenesis. Nature 405(6783):178-179.

Huigens ME, Pashalidou FG, Qian MH, Bukovinszky T, Smid HM, van Loon JJA, Dicke M, Fatouros NE. 2009. Hitch-hiking parasitic wasp learns to exploit butterfly antiaphrodisiac. Proc Natl Acad Sci U S A 106(3):820-825.

Huigens ME, Woelke JB, Pashalidou FG, Bukovinszky T, Smid HM, Fatouros NE. 2010. Chemical espionage on species-specific butterfly anti-aphrodisiacs by hitchhiking *Trichogramma* wasps. Behav Ecol 21(3):470-478.

Ignell R, Dekker T, Ghaninia M, Hansson BS. 2005. Neuronal architecture of the mosquito deutocerebrum. J Comp Neurol 493(2):207-240.

Isidoro NB, F Colazza, S Vinson, S B. 1996. Morphology of antennal gustatory

sensilla and glands in some parasitoid Hymenoptera with hypothesis on their role in sex and host recognition. J Hymenoptera Res 5.
Isler K, Christopher Kirk E, Miller JM, Albrecht GA, Gelvin BR, Martin RD. 2008. Endocranial volumes of primate species: scaling analyses using a comprehensive and reliable data set. J Hum Evol 55(6):967-978.
Ito K, Shinomiya K, Ito M, Armstrong J, Boyan G, Hartenstein V, Harzsch S, Heisenberg M, Homberg U, Jenett A, Keshishian H, Restifo LL, Rössler W, Simpson JH, Strausfeld NJ, Strauss R, Vosshall LB. 2014. A systematic nomenclature for the insect brain. Neuron 81(4):755-765.
Jacob S, Boivin G. 2005. Costs and benefits of polyandry in the egg parasitoid *Trichogramma evanescens* Westwood (Hymenoptera: Trichogrammatidae). Biol Control 32(2):311-318.
Johnston JS, Ross LD, Beani L, Hughes DP, Kathirithamby J. 2004. Tiny genomes and endoreduplication in Strepsiptera. Insect Mol Biol 13(6):581-585.
Kaas JH. 2000. Why is brain size so important: design problems and solutions as neocortex gets bigger or smaller. Brain Mind 1(1):7-23.
Keasar T, Ney-Nifle M, Mangel M. 2000. Evidence for learning of visual host-associated cues in the parasitoid wasp *Trichogramma thalense*. Isr J Zool 46(3):243-247.
Kelber C, Rossler W, Kleineidam CJ. 2010. Phenotypic plasticity in number of glomeruli and sensory innervation of the antennal lobe in leaf-cutting ant workers (*A. vollenweideri*). Dev Neurobiol 70(4):222-234.
Kelber C, Rossler W, Roces F, Kleineidam CJ. 2009. The antennal lobes of fungus-growing ants (*Attini*): neuroanatomical traits and evolutionary trends. Brain Behav Evol 73(4):273-284.
Kittel RJ, Wichmann C, Rasse TM, Fouquet W, Schmidt M, Schmid A, Wagh DA, Pawlu C, Kellner RR, Willig KI, Hell SW, Buchner E, Heckmann M, Sigrist SJ. 2006. Bruchpilot promotes active zone assembly, Ca^{2+} channel clustering, and vesicle release. Science 312(5776):1051-1054.
Knauthe P, Beutel RG, Hörnschemeyer T, Pohl H. 2016. Serial block-face scanning electron microscopy sheds new light on the head anatomy of an extremely miniaturized insect larva (Strepsiptera). Arthropod Systematics & Phylogeny.
Koon AC, Ashley J, Barria R, DasGupta S, Brain R, Waddell S, Alkema MJ, Budnik V. 2011. Autoregulatory and paracrine control of synaptic and behavioral plasticity by octopaminergic signaling. Nat Neurosci 14(2):190-199.
Kotrschal A, Buechel SD, Zala SM, Corral-Lopez A, Penn DJ, Kolm N. 2015a. Brain size affects female but not male survival under predation threat. Ecol

Lett 18(7):646-652.
Kotrschal A, Corral-Lopez A, Amcoff M, Kolm N. 2015b. A larger brain confers a benefit in a spatial mate search learning task in male guppies. Behav Ecol 26(2):527-532.
Kotrschal A, Corral-Lopez A, Zajitschek S, Immler S, Maklakov AA, Kolm N. 2015c. Positive genetic correlation between brain size and sexual traits in male guppies artificially selected for brain size. J Evol Biol 28(4):841-850.
Kotrschal A, Kolm N, Penn DJ. 2016. Selection for brain size impairs innate, but not adaptive immune responses. Proceedings of the Royal Society of London B: Biological Sciences 283(1826).
Kotrschal A, Lievens EJP, Dahlbom J, Bundsen A, Semenova S, Sundvik M, Maklakov AA, Winberg S, Panula P, Kolm N. 2014. Artificial selection on relative brain size reveals a positive genetic correlation between brain size and proactive personality in the guppy. Evolution 68(4):1139-1149.
Kotrschal A, Rogell B, Bundsen A, Svensson B, Zajitschek S, Brannstrom I, Immler S, Maklakov AA, Kolm N. 2013. Artificial selection on relative brain size in the guppy reveals costs and benefits of evolving a larger brain. Curr Biol 23(2):168-171.
Krashes MJ, DasGupta S, Vreede A, White B, Armstrong JD, Waddell S. 2009. A neural dircuit mechanism integrating motivational state with memory expression in *Drosophila*. Cell 139(2):416-427.
Kreissl S, Eichmuller S, Bicker G, Rapus J, Eckert M. 1994. Octopamine-like immunoreactivity in the brain and subesophageal ganglion of the honeybee. J Comp Neurol 348(4):583-595.
Kruidhof HM, Pashalidou FG, Fatouros NE, Figueroa IA, Vet LEM, Smid HM, Huigens ME. 2012. Reward value determines memory consolidation in parasitic wasps. PLoS One 7(8):e39615.
Kruska D. 1996. The effect of domestication on brain size and composition in the mink (*Mustela vison*). J Zool 239:645-661.
Kruska DC. 2005. On the evolutionary significance of encephalization in some eutherian mammals: effects of adaptive radiation, domestication, and feralization. Brain Behav Evol 65(2):73-108.
Kuebler LS, Kelber C, Kleineidam CJ. 2010. Distinct antennal lobe phenotypes in the leaf-cutting ant (*Atta vollenweideri*). J Comp Neurol 518(3):352-365.
Kuhlmann U, Mills NJ. 1999. Comparative analysis of the reproductive attributes of three commercially-produced *Trichogramma* species (Hymenoptera: Trichogrammatidae). Biocontrol Sci Technol 9(3):335-346.
Lanet E, Maurange C. 2014. Building a brain under nutritional restriction: insights on sparing and plasticity from *Drosophila* studies. Front Physiol 5:117.

Lenth RV. 2014. lsmeans: Least-Squares Means. R package version 2.11
Libersat F, Pflueger HJ. 2004. Monoamines and the orchestration of behavior. Bioscience 54(1):17-25.
Liu C, Placais PY, Yamagata N, Pfeiffer BD, Aso Y, Friedrich AB, Siwanowicz I, Rubin GM, Preat T, Tanimoto H. 2012. A subset of dopamine neurons signals reward for odour memory in *Drosophila*. Nature 488(7412):512-+.
Lucas C, Sokolowski MB. 2009. Molecular basis for changes in behavioral state in ant social behaviors. PNAS 106(15):6351-6356.
Luo L, Flanagan JG. 2007. Development of continuous and discrete neural maps. Neuron 56(2):284-300.
Makarova AA, Polilov AA. 2013. Peculiarities of the brain organization and fine structure in small insects related to miniaturization. 2. The smallest Hymenoptera (Mymaridae, Trichogrammatidae). Entomol Rev 93(6):714-724.
Mao Z, Davis RL. 2009. Eight different types of dopaminergic neurons innervate the *Drosophila* mushroom body neuropil: anatomical and physiological heterogeneity. Front Neural Circuits 3:5.
Mares S, Ash L, Gronenberg W. 2005. Brain allometry in bumblebee and honey bee workers. Brain Behav Evol 66(1):50-61.
Margulies C, Tully T, Dubnau J. 2005. Deconstructing memory in *Drosophila*. Curr Biol 15(17):R700-R713.
Martin RD. 1981. Relative brain size and basal metabolic rate in terrestrial vertebrates. Nature 293(5827):57-60.
McDougall SJ, Mills NJ. 1997. The influence of hosts, temperature and food sources on the longevity of *Trichogramma platneri*. Entomol Exp Appl 83(2):195-203.
Menzel R, Giurfa M. 2001. Cognitive architecture of a mini-brain: the honeybee. Trends Cogn Sci 5(2):62-71.
Mery F, Kawecki TJ. 2005. A cost of long-term memory in *Drosophila*. Science 308(5725):1148.
Monastirioti M. 1999. Biogenic amine systems in the fruit fly *Drosophila melanogaster*. Microsc Res Tech 45(2):106-121.
Monastirioti M, Linn CE, Jr., White K. 1996. Characterization of *Drosophila* tyramine beta-hydroxylase gene and isolation of mutant flies lacking octopamine. J Neurosci 16(12):3900-3911.
Nässel DR. 1988. Serotonin and serotonin-immunoreactive neurons in the nervous system of insects. Prog Neurobiol 30(1):1-85.
Nässel DR, Elekes K. 1992. Aminergic neurons in the brain of blowflies and *Drosophila*: dopamine- and tyrosine hydroxylase-immunoreactive neurons

and their relationship with putative histaminergie neurons. Cell Tissue Res 267.

Nässel DR, Meyer EP, Klemm N. 1985. Mapping and ultrastructure of serotonin-immunoreactive neurons in the optic lobes of three insect species. J Comp Neurol 232(2):190-204.

Navarrete A, van Schaik CP, Isler K. 2011. Energetics and the evolution of human brain size. Nature 480(7375):91-93.

Nishikawa M, Nishino H, Misaka Y, Kubota M, Tsuji E, Satoji Y, Ozaki M, Yokohari F. 2008. Sexual dimorphism in the antennal lobe of the ant *Camponotus japonicus*. Zoolog Sci 25(2):195-204.

Niven JE. 2016. Neuronal energy consumption: biophysics, efficiency and evolution. Curr Opin Neurobiol 41:129-135.

Niven JE, Chittka L. 2010. Reuse of identified neurons in multiple neural circuits. Behav Brain Sci 33(4):285.

Niven JE, Farris SM. 2012. Miniaturization of nervous systems and neurons. Curr Biol 22(9):R323-329.

Niven JE, Laughlin SB. 2008. Energy limitation as a selective pressure on the evolution of sensory systems. J Exp Biol 211(Pt 11):1792-1804.

Oliai SE, King BH. 2000. Associative learning in response to color in the parasitoid wasp *Nasonia vitripennis* (Hymenoptera: Pteromalidae). J Insect Behav 13(1):55-69.

Olson DM, Andow DA. 1993. Antennal sensilla of female *Trichogramma nubilale* (Ertle and Davis) (Hymenoptera, Trichogrammatidae) and comparisons with other parasitic Hymenoptera. Int J Insect Morphol 22(5):507-520.

Olson DM, Andow DA. 1998. Larval crowding and adult nutrition effects on longevity and fecundity of female *Trichogramma nubilale* Ertle & Davis (Hymenoptera: Trichogrammatidae). Environ Entomol 27(2):508-514.

Pagel MD, Harvey PH. 1989. Taxonomic differences in the scaling of brain on body weight among mammals. Science 244(4912):1589-1593.

Parnas M, Lin AC, Huetteroth W, Miesenbock G. 2013. Odor discrimination in *Drosophila*: from neural population codes to behavior. Neuron 79(5):932-944.

Pashalidou FG, Huigens ME, Dicke M, Fatouros NE. 2010. The use of oviposition-induced plant cues by *Trichogramma* egg parasitoids. Ecol Entomol 35(6):748-753.

Paulk A, Sean Millard S, Van Swinderen B. 2013. Vision in *Drosophila*: Seeing the world through a model's eyes. Annu Rev Entomol. Vol 58. p 313-332.

Pavlik J. 1993. The size of the female and quality assessment of mass-reared *Trichogramma* Spp. Entomol Exp Appl 66(2):171-177.

Payne TL, Moeck HA, Willson CD, Coulson RN, Humphreys WJ. 1973. Bark

beetle olfaction — II. Antennal morphology of sixteen species of Scolytidae (Coleoptera). Int J Insect Morphol Embryol 2(3):177-192.
Perge JA, Niven JE, Mugnaini E, Balasubramanian V, Sterling P. 2012. Why do axons differ in caliber? J Neurosci 32(2):626-638.
Perry CJ, Barron AB. 2012. Neural mechanisms of reward in insects. Annu Rev Entomol.
Peters RS. 2010. Host range and offspring quantities in natural populations of *Nasonia vitripennis* (Walker, 1836) (Hymenoptera: Chalcidoidea: Pteromalidae). J Hymenoptera Res 19(1):128-138.
Polilov AA. 2005. Anatomy of the feather-winged beetles *Acrotrichis montandoni* and *Ptilium myrmecophilum* (Coleoptera, Ptiliidae). Zoologichesky Zhurnal 84(2):181-189.
Polilov AA. 2008. Anatomy of the smallest coleoptera, featherwing beetles of the tribe Nanosellini (Coleoptera, Ptiliidae), and limits of insect miniaturization. Entomol Rev 88(1):26-33.
Polilov AA. 2012. The smallest insects evolve anucleate neurons. Arthropod Struct Dev 41(1):29-34.
Polilov AA. 2015. Small is beautiful: features of the smallest insects and limits to miniaturization. Annu Rev Entomol 60(1):103-121.
Polilov AA. 2016. Features of the structure of hymenoptera associated with miniaturization: 2. Anatomy of *Trichogramma evanescens* (Hymenoptera, Trichogrammatidae). Entomol Rev 96(4):419-431.
Polilov AA, Beutel RG. 2009. Miniaturisation effects in larvae and adults of *Mikado* sp (Coleoptera: Ptiliidae), one of the smallest free-living insects. Arthropod Struct Dev 38(3):247-270.
Pompanon F, DeSchepper B, Mourer Y, Fouillet P, Bouletreau M. 1997. Evidence for a substrate-borne sex pheromone in the parasitoid wasp *Trichogramma brassicae*. J Chem Ecol 23(5):1349-1360.
Preibisch S, Saalfeld S, Tomancak P. 2009. Globally optimal stitching of tiled 3D microscopic image acquisitions. Bioinformatics 25(11):1463-1465.
Quesada R, Triana E, Vargas G, Douglass JK, Seid MA, Niven JE, Eberhard WG, Wcislo WT. 2011. The allometry of CNS size and consequences of miniaturization in orb-weaving and cleptoparasitic spiders. Arthropod Struct Dev 40(6):521-529.
Ramirez-Esquivel F, Zeil J, Narendra A. 2014. The antennal sensory array of the nocturnal bull ant *Myrmecia pyriformis*. Arthropod Struct Dev 43(6):543-558.
Rehder V, Bicker G, Hammer M. 1987. Serotonin-immunoreactive neurons in the antennal lobes and suboesophageal ganglion of the honeybee. Cell Tissue Res 247(1):59-66.

Rensch B. 1948. Histological changes correlated with evolutionary changes of body size. Evolution 2(3):218-230.

Rensch B. 1956. Increase of learning capability with increase of brain-size. Am Nat 90(851):81-95.

Rivara C-B, Sherwood CC, Bouras C, Hof PR. 2003. Stereologic characterization and spatial distribution patterns of Betz cells in the human primary motor cortex. Anat Rec A Discov Mol Cell Evol Biol 270A(2):137-151.

Rivero A, West SA. 2002. The physiological costs of being small in a parasitic wasp. Evol Ecol Res 4(3):407-420.

Riveros AJ, Gronenberg W. 2010a. Brain allometry and neural plasticity in the bumblebee *Bombus occidentalis*. Brain Behav Evol 75(2):138-148.

Riveros AJ, Gronenberg W. 2010b. Sensory allometry, foraging task specialization and resource exploitation in honeybees. Behav Ecol Sociobiol 64(6):955-966.

Robertson HM, Wanner KW. 2006. The chemoreceptor superfamily in the honey bee, *Apis mellifera*: Expansion of the odorant, but not gustatory, receptor family. Genome Res 16(11):1395-1403.

Roeder T. 1994. Biogenic amines and their receptors in insects. Comp Biochem Phys C 107(1):1-12.

Roeder T. 2005. Tyramine and octopamine: ruling behavior and metabolism. Annu Rev Entomol 50:447-477.

Roth G, Dicke U. 2005. Evolution of the brain and intelligence. Trends Cogn Sci 9(5):250-257.

Ruschioni S, Romani R, Riolo P, Isidoro N. 2012. Morphology and distribution of antennal multiporous gustatory sensilla related to host recognition in some *Trichogramma* spp. Bull Insectol 65(2):171-176.

Salt G. 1940. Experimental studies in insect parasitism. VII. The effects of different hosts on the parasite *Trichogramma evanescens* West. (Hym. Chalcidoidea). Proc R Entomol Soc Lond Ser A Gen Entomol 15(10-12):81-95.

Sane SP. 2016. Neurobiology and biomechanics of flight in miniature insects. Curr Opin Neurobiol 41:158-166.

Schafer S, Rehder V. 1989. Dopamine-like immunoreactivity in the brain and suboesophageal ganglion of the honeybee. J Comp Neurol 280(1):43-58.

Schindelin J, Arganda-Carreras I, Frise E, Kaynig V, Longair M, Pietzsch T, Preibisch S, Rueden C, Saalfeld S, Schmid B, Tinevez JY, White DJ, Hartenstein V, Eliceiri K, Tomancak P, Cardona A. 2012. Fiji: an open-source platform for biological-image analysis. Nat Methods 9(7):676-682.

Schmidt JM, Smith JJB. 1985. Host volume measurement by the parasitoid wasp *Trichogramma minutum*: The roles of curvature and surface area. Entomol Exp Appl 39(3):213-221.

Schmidt JM, Smith JJB. 1987. The measurement of exposed host volume by the parasitoid wasp *Trichogramma minutum* and the effects of wasp size. Can J Zool 65(12):2837-2845.

Schroter U, Malun D, Menzel R. 2007. Innervation pattern of suboesophageal ventral unpaired median neurones in the honeybee brain. Cell Tissue Res 327(3):647-667.

Schurmann D, Sommer C, Schinko APB, Greschista M, Smid H, Steidle JLM. 2012. Demonstration of long-term memory in the parasitic wasp *Nasonia vitripennis*. Entomol Exp Appl 143(2):199-206.

Schürmann FW, Elekes K, Geffard M. 1989. Dopamine-like immunoreactivity in the bee brain. Cell Tissue Res 256(2):399-410.

Schürmann FW, Klemm N. 1984. Serotonin-immunoreactive neurons in the brain of the honeybee. J Comp Neurol 225(4):570-580.

Seid MA, Castillo A, Wcislo WT. 2011. The allometry of brain miniaturization in ants. Brain Behav Evol 77(1):5-13.

Seid MA, Goode K, Li C, Traniello JF. 2008. Age- and subcaste-related patterns of serotonergic immunoreactivity in the optic lobes of the ant *Pheidole dentata*. Dev Neurobiol 68(11):1325-1333.

Seidel C, Bicker G. 1996. The developmental expression of serotonin-immunoreactivity in the brain of the pupal honeybee. Tissue Cell 28(6):663-672.

Shanbhag SR, Müller B, Steinbrecht RA. 1999. Atlas of olfactory organs of *Drosophila melanogaster*: 1. Types, external organization, innervation and distribution of olfactory sensilla. Int J Insect Morphol Embryol 28(4):377-397.

Shingleton AW, Frankino WA, Flatt T, Nijhout HF, Emlen DJ. 2007. Size and shape: the developmental regulation of static allometry in insects. Bioessays 29(6):536-548.

Sinakevitch I, Niwa M, Strausfeld NJ. 2005. Octopamine-like immunoreactivity in the honey bee and cockroach: comparable organization in the brain and subesophageal ganglion. J Comp Neurol 488(3):233-254.

Sinakevitch I, Strausfeld NJ. 2006. Comparison of octopamine-like immunoreactivity in the brains of the fruit fly and blow fly. J Comp Neurol 494(3):460-475.

Sitaraman D, Zars M, LaFerriere H, Chen YC, Sable-Smith A, Kitamoto T, Rottinghaus GE, Zars T. 2008. Serotonin is necessary for place memory in *Drosophila*. Proc Natl Acad Sci U S A 105(14):5579-5584.

Smid HM, Bleeker MAK, van Loon JJA, Vet LEM. 2003. Three-dimensional organization of the glomeruli in the antennal lobe of the parasitoid wasps

Cotesia glomerata and *C. rubecula*. Cell Tissue Res 312(2):237-248.

Smid HM, Vet LEM. 2016. The complexity of learning, memory and neural processes in an evolutionary ecological context. Curr Opin Insect Sci 15:61-69.

Smid HM, Wang G, Bukovinszky T, Steidle JL, Bleeker MA, van Loon JJA, Vet LEM. 2007. Species-specific acquisition and consolidation of long-term memory in parasitic wasps. Proc Biol Sci 274(1617):1539-1546.

Snell-Rood EC, Papaj DR, Gronenberg W. 2009. Brain size: a global or induced cost of learning? Brain Behav Evol 73(2):111-128.

Spaethe J, Brockmann A, Halbig C, Tautz J. 2007. Size determines antennal sensitivity and behavioral threshold to odors in bumblebee workers. Naturwissenschaften 94(9):733-739.

Srinivasan MV. 2010. Honey bees as a model for vision, perception, and cognition. Annu Rev Entomol 55:267-284.

Stieb SM, Kelber C, Wehner R, Rossler W. 2011. Antennal-lobe organization in desert ants of the genus *Cataglyphis*. Brain Behav Evol 77(3):136-146.

Strausfeld NJ. 1976. Atlas of an Insect Brain: Springer Berlin Heidelberg.

Striedter GF. 2005. Principles of brain evolution. Sunderland, Massachusetts USA: Sinauer Associates, Inc.

Strutz A, Soelter J, Baschwitz A, Farhan A, Grabe V, Rybak J, Knaden M, Schmuker M, Hansson BS, Sachse S. 2014. Decoding odor quality and intensity in the *Drosophila* brain. Elife 3:e04147.

Stuermer IW, Plotz K, Leybold A, Zinke O, Kalberlah O, Samjaa R, Scheich H. 2003. Intraspecific allometric comparison of laboratory gerbils with Mongolian gerbils trapped in the wild indicates domestication in *Meriones unguiculatus* (Milne-Edwards, 1867) (Rodentia: Gerbillinae). Zool Anz 242(3):249-266.

Suzuki Y, Tsuji H, Sasakawa M. 1984. Sex allocation and effects of superparasitism on secondary sex ratios in the gregarious parasitoid, *Trichogramma chilonis* (Hymenoptera: Trichogrammatidae). Anim Behav 32(2):478-484.

Tammaru T, Esperk T. 2007. Growth allometry of immature insects: larvae do not grow exponentially. Funct Ecol 21(6):1099-1105.

Tsuboi M, Kotrschal A, Hayward A, Buechel SD, Zidar J, Løvlie H, Kolm N. 2016. Evolution of brain–body allometry in Lake Tanganyika cichlids. Evolution 70(7):1559-1568.

van de Zande L, Ferber S, de Haan A, Beukeboom LW, van Heerwaarden J, Pannebakker BA. 2014. Development of a *Nasonia vitripennis* outbred laboratory population for genetic analysis. Mol Ecol Resour 14(3):578-587.

van Wijk M, Wadman WJ, Sabelis MW. 2006. Morphology of the olfactory

system in the predatory mite *Phytoseiulus persimilis*. Exp Appl Acarol 40(3-4):217-229.
Voegelé J, Cals-Usciati J, Pihan JP, Daumal J. 1975. Structure de l'antenne femelle des trichogrammes. Entomophaga 20(2):161-169.
Vosshall LB, Stocker RF. 2007. Molecular architecture of smell and taste in *Drosophila*. Annu Rev Neurosci 30(1):505-533.
Vosshall LB, Wong AM, Axel R. 2000. An olfactory sensory map in the fly brain. Cell 102(2):147-159.
Waage JK, Ming N. 1984. The reproductive strategy of a parasitic wasp: I. Optimal progeny and sex allocation in *Trichogramma evanescens*. J Anim Ecol 53(2):401-415.
Waddell S. 2013. Reinforcement signalling in *Drosophila*; dopamine does it all after all. Curr Opin Neurobiol 23(3):324-329.
Wagh DA, Rasse TM, Asan E, Hofbauer A, Schwenkert I, Durrbeck H, Buchner S, Dabauvalle MC, Schmidt M, Qin G, Wichmann C, Kittel R, Sigrist SJ, Buchner E. 2006. Bruchpilot, a protein with homology to ELKS/CAST, is required for structural integrity and function of synaptic active zones in *Drosophila*. Neuron 49(6):833-844.
Walsh B, Lynch M. 2009. Least squares analysis of short-term selection experiments. In: Evolution and selection of quantitative traits, *in press*. p 241.
Warton DI, Duursma RA, Falster DS, Taskinen S. 2012. Smatr 3- an R package for estimation and inference about allometric lines. Methods Ecol Evol 3(2):257-259.
Warton DI, Wright IJ, Falster DS, Westoby M. 2006. Bivariate line-fitting methods for allometry. Biol Rev Camb Philos Soc 81(2):259-291.
Wehner R, Fukushi T, Isler K. 2007. On being small: brain allometry in ants. Brain Behav Evol 69(3):220-228.
Wendt B, Homberg U. 1992. Immunocytochemistry of Dopamine in the brain of the locust *Schistocerca gregaria*. J Comp Neurol 321(3):387-403.
Werren JH, Loehlin DW. 2009. The parasitoid wasp *Nasonia*: an emerging model system with haploid male genetics. Cold Spring Harbor protocols 2009(10):pdb.emo134-pdb.emo134.
Werren JH, Richards S, Desjardins CA, Niehuis O, Gadau J, Colbourne JK. 2010. Functional and evolutionary insights from the genomes of three parasitoid *Nasonia* species (vol 327, pg 343, 2010). Science 327(5973):1577-1577.
Whitfield JB. 2003. Phylogenetic insights into the evolution of parasitism in Hymenoptera. Adv Parasitol. Vol Volume 54: Academic Press. p 69-100.
Wu CL, Shih MF, Lee PT, Chiang AS. 2013. An octopamine-mushroom body circuit modulates the formation of anesthesia-resistant memory in *Drosophila*.

Curr Biol 23(23):2346-54.

Yamamoto S, Seto ES. 2014. Dopamine dynamics and signaling in *Drosophila*: an overview of genes, drugs and behavioral paradigms. Exp Anim 63(2):107-119.

Yu DSK, Hagley EAC, Laing JE. 1984. Biology of *Trichogramma minutum* Riley collected from apples in Southern Ontario. Environ Entomol 13(5):1324-1329.

Zhang K, Guo JZ, Peng Y, Xi W, Guo A. 2007. Dopamine-mushroom body circuit regulates saliency-based decision-making in *Drosophila*. Science 316(5833):1901-1904.

Zhang S, Zhang Z, Kong X, Wang H, Zhou G, Yu J. 2012. External morphology of *Trichogramma dendrolimi* Matsumura (hymenoptera: Trichogrammatidae) organ and ultrastructure of the sensilla. Microsc Res Tech 75(11):1513-1521.

Zube C, Kleineidam CJ, Kirschner S, Neef J, Rossler W. 2008. Organization of the olfactory pathway and odor processing in the antennal lobe of the ant *Camponotus floridanus*. J Comp Neurol 506(3):425-441.


R

Summary

Haller's rule

Small animals have relatively larger brains than large animals. This brain-body size scaling relationship is known as Haller's rule, and is described by a power law function that shows negative allometry. Small animals may need to form relatively larger brains to maintain similar levels of brain performance as large animals. The high metabolic costs of brain tissue simultaneously force animals to restrict brain size to the smallest size that can support adequate functioning. Haller's rule holds in comparisons between adults of the same species, i.e. static allometry, and in comparisons between species, i.e. evolutionary allometry. As a result of evolutionary allometry, small-bodied species have relatively larger brains than species with larger body sizes. The smallest animals therefore spend an exceptionally large proportion of energy on the development and maintenance of energetically expensive brain tissue. These small animals may experience the energetic constraints of brain tissue as a very strong evolutionary pressure.

Brain-body size scaling in miniaturized insects

The strong selective pressures that force the smallest insects to minimize energy expenditure and optimize brain performance may have shaped the characteristics of static brain allometry. The aim of this thesis was to find out how such evolutionary pressures shaped brain-scaling characteristics in miniaturized parasitic wasps, and what the neural and cognitive consequences are. One of the smallest animals on Earth is the parasitic wasp *Trichogramma evanescens*. These wasps parasitise and develop inside the eggs of butterflies and moths. These host eggs can be very small, which restricts body size and brain size of developing wasps. Adult body size of *T. evanescens* depends on the size of their host and the number of parasitoid larvae that develop inside the same host and compete for resources. Such scramble competition results in large phenotypic plasticity in body size that ranges between 0.3 and 0.9 mm, even between genetically identical sister wasps. Despite these small sizes, *T. evanescens* wasps show complex cognitive traits, such as hitch-hiking behaviour, associative learning, and long-term memory formation. Even the smallest *T. evanescens* need these traits to locate and exploit their hosts. This should require a relatively large and energetically expensive brain in the smallest *T. evanescens*, as predicted by Haller's rule.

Isometric brain scaling

In Chapter 2, I studied if *T. evanescens* scale their brains in a way that optimizes performance (at energetic costs) or minimizes energy expenditure (at cognitive costs). I induced a large variation in body size of genetically identical sister wasps, thereby excluding genetic variation in relative brain size. Brain and body volume were determined using tissue clearing procedures, confocal laser scanning microscopy and three-dimensional modelling software. Standardized major axis regression analyses showed that *T. evanescens* scale brain size isometrically to body size, thereby identifying the first species that forms an exception to Haller's rule. Relative brain volume is on average 8.2% of body volume in this species. This large relative brain size may represent a high energetic burden, and a further increase in relative brain size may be too costly for the smallest *T. evanescens*. Isometric brain scaling may be a brain-scaling strategy that is applied by miniaturized insect species to avoid the excessive energetic costs of relatively large brain, thereby achieving smaller brain and body sizes than would be possible under allometric brain scaling.

Flexibility in the morphology of the olfactory system

Isometric brain scaling implies that small individuals form smaller brains than are predicted by Haller's rule, and large individuals form larger brains than are predicted by Haller's rule. This indicates that there is a large flexibility in brain morphology of genetically identical *T. evanescens*. I studied this in the antennal lobes and antennal sensilla of the olfactory system, and on the level of individual neurons. In Chapter 3, I studied the olfactory system. Confocal laser scanning microscopy revealed that small and large wasps have a similar number of functional units (i.e. glomeruli) in their antennal lobes. These glomeruli are, however, smaller in both absolute and relative volume in the brains of small wasps. Scanning electron microscopy revealed that small and large wasps have similarly sized olfactory sensilla on their antennae, and similar numbers of most types of olfactory sensilla. There is a difference in the number of gustatory sensilla on the final antennal segment of small and large wasps. These results suggest that the complexity of the olfactory system is maintained between small and large wasps. Hence, isometric brain scaling may not require plasticity in the complexity, but rather in the size, of the olfactory system. Even the smallest *T. evanescens* may need to maintain olfactory precision in their search for suitable hosts.

Flexibility in size and number of monoaminergic neurons

To study the flexibility in brain morphology at the level of single neurons, I focussed on monoaminergic neurons that express serotonin, octopamine or dopamine. I used immunofluorescence stainings in combination with confocal laser scanning microscopy to reveal the clusters of cell bodies and the projections of these monoaminergic neurons in *T. evanescens*. Chapter 4 provides the first description of the distribution, projection patterns and number of monoaminergic neurons in this species. The brains of *T. evanescens* appear to contain comparable numbers of monoaminergic neurons as the brains of much larger insects (e.g. honeybees, fruit flies and *N. vitripennis*), despite the large differences in brain size between *T. evanescens* and these species. Clusters of serotonergic neurons appear to be especially conserved in neuron numbers, whereas there are more differences in the number of dopaminergic and octopaminergic neurons between *T. evanescens* and larger insects. These results suggest that some modifications to monoaminergic neurons were required during the evolutionary process of brain miniaturization in the species *T. evanescens*, although overall complexity is largely maintained. In Chapter 5, I compared the number and size of these monoaminergic neurons between small and large *T. evanescens*. I found that differently-sized wasps had the same number of serotonergic, octopaminergic and dopaminergic neurons in their brains. Small and large wasps did differ in the diameter of these neurons. The maintained numbers of antennal-lobe glomeruli and monoaminergic cell bodies could imply that isometric brain scaling is facilitated by plasticity in the size of neural components, rather than in their numbers.

Cognitive consequences of brain scaling

Through maintained neural complexity, isometric brain scaling could cause brain performance to be similarly maintained in even the smallest *T. evanescens*. In Chapter 6, I quantified the effect of brain scaling on cognition by comparing memory retention abilities between small and large genetically identical sister wasps, both for *T. evanescens* and for the larger parasitic wasp *Nasonia vitripennis*. *Nasonia vitripennis* are parasitic wasps of fly pupae, and show similar levels of phenotypic plasticity in body size as *T. evanescens*. Brain-body size scaling is diphasic in *N. vitripennis*, with isometry in small individuals and negative allometry in large individuals. The brain-scaling strategies of *T. evanescens* and *N. vitripennis* both cause brains that are smaller than predicted by Haller's rule in small wasps, and may be too small to maintain cognitive abilities. For both species, I compared visual and olfactory memory retention between small and large conspecifics. In *N. vitripennis*, small individuals had lower memory retention levels than large

individuals. This indicates that being small has cognitive costs in this species, which may relate to the undersized brains in small wasps. In contrast, isometric brain scaling does not affect memory retention in *T. evanescens*. This may be enabled by the maintained neural complexity that was described above, although brain properties different from memory performance (and outside the scope of this thesis) could still be affected by isometric brain scaling. Evolutionary pressures appear to have differentially shaped static brain scaling in *T. evanescens* and in *N. vitripennis*, resulting in different cognitive consequences. Both species experience strong energetic constraints, as indicated by their escape from Haller's rule. The selection pressures on maintained memory retention abilities could be especially strong in small *T. evanescens*, whereas it is more adaptive for small *N. vitripennis* to invest in other aspects of brain performance.

Potential costs of brain isometry

Although isometric brain scaling does not affect memory retention in *T. evanescens*, there should be costs of developing undersized brains for small *T. evanescens*, which large conspecifics avoid by forming brains that are larger (and energetically more expensive) than predicted by Haller's rule. To achieve the smallest brain sizes, isometric brain scaling may require costly reductions of neuronal cell body size. These modifications may compromise neural functioning and long-term maintenance of brain tissue, and reduce longevity of small wasps. Larger wasps can, to some extent, avoid these costs by being able to invest more in energetically expensive brain tissue and forming larger brains than are predicted by Haller's rule. Whether isometric brain scaling affects cell body volume through modifications to cytoplasm volume (thereby affecting energy generation by mitochondria) or to nucleus volume (thereby affecting transcriptional dynamics), and how these affect brain performance and fitness, should be addressed in future studies.

Genetic variation in relative brain size

Apart from an inbred homozygous strain, there is also a genetically variable population available for *N. vitripennis*, which allowed me to study how the genetic component of brain size (which I excluded in the experiments described above by using inbred, isofemale strains) affects neuropil composition, memory retention, and longevity. In Chapter 7, I created selection lines of *N. vitripennis* that genetically differ in relative brain size using an artificial bidirectional selection regime. This selection regime caused a robust change in relative brain

size, although the response to selection was slow. This indicates that there is heritable genetic variation in relative brain size, but that there are strong constraints (possibly energetic or cognitive constraints) that limit this variation. There was an average 16% difference in total neuropil volume between wasps with relatively small and relatively large brains. This difference in brain volume only affected the relative volume of the antennal lobes, which were relatively smaller in wasps with relatively smaller brains, whereas all other neuropil areas were similar in relative volume. Interestingly, there was no effect of relative brain size on olfactory memory retention abilities. Having a relatively larger brain did result in reduced longevity, indicating that brain tissue is energetically costly. A learning experience further reduced longevity in these wasps with relatively large brains, indicating that memory formation is also a more costly process than for wasps with smaller brains. The results of these experiments show that relatively large brains are costly, but not more beneficial for olfactory memory retention. These results sharply contrast the above-described effects of phenotypic plasticity in brain and body size in *N. vitripennis*. There may be different underlying mechanisms that regulate the consequences of plastic and genetic variation in brain size. As a result, memory retention abilities may have evolved to be optimized in *N. vitripennis* with relatively small brains, but not in *N. vitripennis* with small body sizes.

Conclusion

In conclusion, the work that is presented in this thesis reveals how the smallest animals face the challenge to maintain ecologically required levels of cognitive performance, while being limited by small numbers of neurons and a restricted energy balance. In the parasitic wasp *N. vitripennis*, developing into a small adult has cognitive costs, and relative brain size is strongly constrained. The extremely small parasitic wasp *T. evanescens* shows isometric brain scaling, which may have evolved to enable brains that are smaller, and therefore energetically cheaper, than would be possible in the situation that is described by Haller's rule. This brain-scaling strategy appears to be facilitated by plasticity in the size of neural components, rather than in their number or structural complexity. Maintaining neural complexity may the underlying mechanism that maintains the cognitive abilities of the smallest brains. The smallest brain and body sizes may be enabled by this strategy of maintaining neural complexity and brain performance under isometric brain scaling, possibly at the cost of reduced longevity as a consequence of their small neuronal cell bodies. This strategy could form the art of being small.


S

Curriculum vitae
and
list of publications

Publications

Emma van der Woude, Hans M. Smid, Lars Chittka, Martinus E. Huigens. 2013. Breaking Haller's rule: brain-body size isometry in a minute parasitic wasp. Brain, Behavior and Evolution 81(2):86-92.

Emma van der Woude, Hans M. Smid. 2016. How to escape from Haller's rule: olfactory system complexity in small and large *Trichogramma evanescens* parasitic wasps. Journal of Comparative Neurology 524(9):1876-1891.

Emma van der Woude, Hans M. Smid. 2017. Maximized complexity in miniaturized brains: morphology and distribution of octopaminergic, dopaminergic and serotonergic neurons in *Trichogramma evanescens* parasitic wasps. Cell and Tissue Research, 369(3), 477-496.

Emma van der Woude, Hans M. Smid. 2017. Effects of isometric brain-body size scaling on the complexity of monoaminergic neuron networks in a minute parasitic wasp. Brain, Behavior and Evolution 89(3):185-194.

Emma van der Woude, Martinus E. Huigens, Hans M. Smid. Differential effects of brain scaling on memory performance in parasitic wasps. *Submitted.*

Emma van der Woude*, Jitte Groothuis*, Hans M. Smid. No gains for bigger brains: Functional and neuroanatomical consequences of artificial selection on relative brain size in a parasitic wasp. *Submitted.*

* These authors contributed equally to this work.

About the author

Emma van der Woude was born on the 9th of November, 1988 in Oud-Beijerland, the Netherlands. Her deep interest in the *how* and *why* of life drove her to a BSc study in Biology at Wageningen University in September 2007. She combined a major in Ecology and Biodiversity with a minor in Infectious Diseases and Health, and graduated cum laude in September 2010.

Interested in how the smallest brains work, she continued her studies with a major MSc thesis at the Laboratory of Entomology of Wageningen University & Research. She quantified brain size in relation to body size in tiny *Trichogramma* wasps. This work was awarded with the WUF-KLV Thesis Prize 2011. The results are published in Brain, Behavior and Evolution, for which Emma received the PE&RC Publication Award 2014 (2nd prize).

For her MSc research internship, Emma decided to go to the USA for a joint project at the University of California, Riverside and the University of Hawaii at Manoa, Honolulu. She mapped parasitism rates of parasitic wasps in butterfly populations on the Hawaiian island Oahu, and performed molecular analyses and behavioural experiments on the Hawaiian samples in Riverside, California. She received the Uyttenboogaart-Eliasen MSc Thesis Award 2012 for this work.

During the final phase of her MSc study Emma participated in the PE&RC Research Master programme, which offered the opportunity to compete for a PhD grant. Emma wrote a research proposal to continue her work on the morphology and functioning of the smallest brains in *Trichogramma* wasps. This proposal was awarded with a personal grant for a 4-year research project. She started with this PhD in September 2012, the day after obtaining her MSc degree. The PhD thesis you are now holding in your hands presents the results of this project.

Emma enjoys drawing and graphic design. She started designing the cover of this PhD thesis only halfway through the 4-year project, and received the PE&RC Thesis Cover Award 2016 for it. She is currently working as software engineer for Keylane in Utrecht, the Netherlands.

PE&RC Training and Education Statement

With the training and education activities listed below the PhD candidate has complied with the requirements set by the C.T. de Wit Graduate School for Production Ecology and Resource Conservation (PE&RC) which comprises of a minimum total of 32 ECTS (= 22 weeks of activities).

Review of literature (4.5 ECTS)

- How brain size affects cognition: insights from the smallest minds (2012)

Writing of project proposal (4.5 ECTS)

- The art of being small: cognitive ecology of minute parasitic wasp (2012)

Post-graduate courses (3.1 ECTS)

- Entomology excursion to Swiss universities: Neuchâtel, Lausanne and Basel (2013)
- Linear models; PE&RC (2014)
- Generalized linear models; PE&RC (2014)
- Mixed linear models; PE&RC (2014)

Invited review of (unpublished) journal manuscript (1 ECTS)

- Proc Roy Soc B: evolution of brain size and brain morphology (2014)

Competence strengthening / skills courses (4.3 ECTS)

- Techniques for writing and presenting a scientific paper; WGS (2014)
- Communication with the media and general public; WGS (2014)
- Adobe Indesign; WUR Library (2015)
- Ethics and philosophy in life sciences; WGS (2015)

PE&RC Annual meetings, seminars and PE&RC weekend (2.4 ECTS)

- PE&RC Weekend (2013)
- PE&RC Day (2013, 2015, 2016)
- PE&RC Last year's weekend (2016)

Discussion groups, local seminars, other scientific meetings (8.6 ECTS)

- NEV Entomologendag; oral presentation;
  Ede, the Netherlands (2012)
- Wageningen Evolution and Ecology Seminars (WEES);
  Wageningen, the Netherlands (2013-2016)
- Brains & Behaviour discussion group;
  WUR, VU and NIOO (2013-2016)
- 2nd Wageningen PhD symposium; oral presentation;
  Wageningen, the Netherlands (2015)

International symposia, workshops and conferences (6.3 ECTS)

- International *Nasonia* meeting; oral presentation;
  Wageningen, the Netherlands (2013)
- Netherlands-Japan parasitoid meeting; poster presentation;
  Wageningen, the Netherlands (2014)
- 12th International Congress of Neuroethology; poster presentation;
  Montevideo, Uruguay (2016)

Lecturing / supervision of practicals / tutorials (8.4 ECTS)

- Behavioural ecology (2013-2015)
- Ecological aspects of bio-interactions (2013-2016)
- Ecophysiology (2014-2015)

Supervision of MSc students

- Effects of body size on learning and memory in *Trichogramma evanescens*

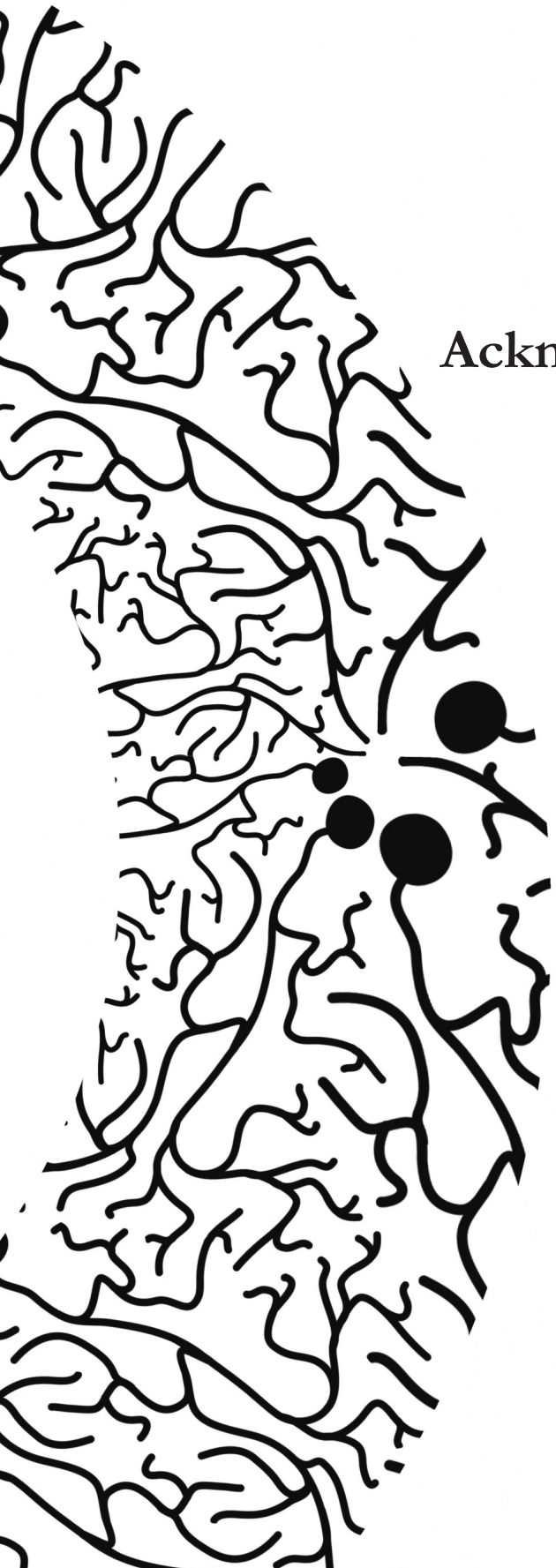

Acknowledgements

My final pages are dedicated to all the people that made these years of hard work worthwhile. So let's start with… Hans! You are the best supervisor any PhD student can wish for. You always gave me unlimited support and the freedom to focus on the topics that I found most interesting. No matter how busy you were, you would always make time to help me out. Looking back, I realise that I wouldn't be the scientist, or even the person, that I am today if had never met you. Your influence ranged from the crazy idea to dissect *Trichogramma* brains (did you even believe it was possible, at that time?) to the suggestion of making some figures to illustrate my work (going through this book you may notice that I probably liked that a bit too much). Under your guidance I had my very first beer (too shy to say I didn't like it), which gradually evolved into please-can-we-go-for-a-beer moments (realising that alcohol does help with the difficult bits of a PhD). The last year was tough, for you even more than for me. I greatly admire you for continuing your work as a supervisor, and I hope it didn't cost you too much. Your continued devotion saved me a great delay in finishing my PhD, and I am deeply grateful for that. Oh, and I may have accidentally promised to run a marathon with you on your 80th birthday. Let's forget that.

Then my dear paranymphs. Jitte! I really enjoyed having you as my geeky colleague. You taught me loads of neuro stuff, probably way more than you realise. I had a lot of fun acting as your assistant during the weird photography sessions in the lab, dropping tiny wasps on needles, pins and matches in front of your huge camera (the lucky shot of Figure 1C in Chapter 6 is my favourite picture ever). Our conference trip to Uruguay was something I will never forget: apart from the mountains of meat, the endless rain, the deserted towns, and the horrible sunburn we got right before representing the Dutch entomological society, I vividly remember how much fun it was to be on the other side of the world with you and Hans.

Jessica! You were still a MSc student when I started my PhD, but your work was essential for a very important part of this thesis. You developed the very first *Trichogramma* olfactory T-maze, and without it I wouldn't have been able to measure their learning abilities. It's great that this work helped you to get your very own PhD project, and that you still spend your time training wasps and measuring memory. Such a pity that they're the wrong species… Thank you for being my paranymph!

Ties! You deserve my sincere gratitude for starting all of this. It was your MSc thesis project that I signed up for, and that resulted not only in Chapter 2, but in this entire book. It was also you who first introduced me to the cutest wasps on this planet. I remember how surprised you were that the size of *Trichogramma*

didn't scare me away, while I was actually relieved that they were almost invisible (because insects are scary and disgusting). Your open, kind and inviting nature made me feel right at home at Ento. I also want to thank you for sending me on an MSc internship project to Hawaii and California, which turned out to be the best time of my life (so far).

Marcel! You are a truly admirable scientist and I am proud to have worked in your department. You have an almost supernatural ability to find the smallest typo in the longest list of references. Thank you for 'spoiling' so many evenings and weekends with your fast revisions and feedback, which usually came hours, days or even weeks before I expected to hear from you. But I mostly want to thank you for the opportunities you gave me: the 5 minutes of fame I got on the famous pop-stage Paradiso in Amsterdam, and the live interview on Radio 1.

Then the people of our wonderful Brains & Behaviour team: Katja, Joke, Maartje, Michel and Louise, thank you for all the fruitful discussions we had over the years (both during the actual meetings, and during the drinks that usually followed them). And my dear students: Lucía, Clara, Alexandra and Lisa, believe me when I say that supervising you taught me as much as I (hopefully) taught you. Thank you for your hard work!

To the Amazing Ento family: thank you for all the fun and *gezelligheid*! You are a crazy collection of passionate, creative and totally mad scientists, and I loved learning with you and from you. Thank you for all the beers, labuitjes, drinks, parties, dinners, breaks, cakes, chocolate, and for understanding the importance of social activities. Special thanks to my desk mates: Jeltje, Tobias, Karol, Nina, for keeping an eye on the birds and window washers with me. I heard our magpie Kareltje is doing very well. Keiko and Shuhang, I really enjoyed teaching you Dutch during our lunch meetings (ui, ui, uitje!) and learning Chinese during our mah-jong games (yî, èr, sân!). Jeltje, Anneke and Camille, thank you for organizing the PhD trip! It was great to race through Germany and Switzerland in the Emmamobile, and it certainly made me a better driver (despite the awesome rear view parking camera).

Lieve meiden van Retro 2.0: Sanne, Kelly en Arina, wie had gedacht dat de vrienden die het verst weg wonen en die ik het minst vaak zie, degenen zouden zijn die ik het vaakst zou spreken? Wespen zijn vies, spinnen zijn eng en mieren moeten dood. In mijn academische droomwereldje waren jullie altijd mijn contact met planeet aarde. Bedankt voor het gezellige geneuzel, de logeerpartijtjes en de verre vakanties naar Thailand, Macedonië en (niet minder exotisch) Friesland, Groningen en Limburg.

En dan team AnJetEl: Anne, Mariët en Ellen, bedankt voor de high tea's, de dagjes weg en de bizarre sluipwespgerelateerde Sinterklaassurprises. Zonder jullie was ik niet naar IJsland, Dubai en Trondheim gegaan, en al helemaal niet op vakantie naar de Efteling… Ellen, nu ik dit schrijf besef ik dat ik jou van al mijn vrienden het langst ken. Het is een eer (en nog steeds een beetje gek) om na 20 jaar vriendschap mijn carrière te vervolgen als jouw collega.

Loes, hoeveel honderden kilometer hebben wij inmiddels afgewandeld? Dat lijkt me iets wat we nog wel honderd jaar kunnen volhouden, dus laten we dat vooral doen. Bedankt voor alle gezellige dagjes sjokken, chocola eten, films kijken en natuurlijk dat toffe tripje naar Oostenrijk! Arisca en Anne, jullie ook bedankt voor alle gezellige avondjes met eten, spelletjes, honden, katten en de Mol.

Aan de Stitch 'n Bitch meiden: Anneke, Jenny, Jeltje en Marjolein, bedankt voor al die keren dat we naaimachines het land door sleepten… en uiteindelijk voornamelijk zaten te kletsen. Ik ben inmiddels wel twee kussenslopen én een berg lapjes rijker die er zonder jullie nooit zouden zijn geweest!

Daan, bedankt dat je mijn lieve stoere broer bent! De autoritjes van Oud-Beijerland naar Nijmegen zijn misschien wel de beste broer-zus momenten uit ons leven, met die dramatische natte dagen in dat tentje in Zeeland op nummer twee (misschien moeten we toch maar eens gaan duiken, nu we dat zouden moeten kunnen?).

En dan tot slot… Pap, mam, jullie simpelweg bedankt voor alles. Jullie leerden me dat plezier belangrijker is dan hoge cijfers, en dat je hart volgen meer geluk brengt dan puur rationele keuzes. Jullie hebben me mijn hele leven lang gesteund en geholpen, en me altijd het stabiele, veilige 'thuisthuis' geboden waar ik opgroeide en nog steeds graag naar terugkeer. Zonder jullie had ik dit nooit bereikt.

The research described in this thesis was financially supported by the Netherlands Organisation for Scientific Research (NWO PE&RC Graduate Program grant 022.002.004).

Layout and cover design by the author.

Printed by GVO drukkers & vormgevers, Ede, the Netherlands.